HUMAN MONOCLONAL ANTIBODY FRAGMENTS THAT NEUTRALIZE BIO-FUNCTIONS OF SURFACE EXPOSED PROTEINS OF TYPE A INFLUENZA VIRUSES

TIPPAWAN PISSAWONG

A THESIS SUBMITTED IN PARTIAL FULFILLMENT OF THE REQUIREMENTS FOR THE DEGREE OF DOCTOR OF PHILOSOPHY (IMMUNOLOGY) FACULTY OF GRADUATE STUDIES MAHIDOL UNIVERSITY 2013

Copyright © by Mahidol University

COPYRIGHT OF MAHIDOL UNIVERSITY

Thesis
entitled

HUMAN MONOCLONAL ANTIBODY FRAGMENTS THAT NEUTRALIZE BIO-FUNCTIONS OF SURFACE EXPOSED PROTEINS OF TYPE A INFLUENZA VIRUSES

Tippawan Pissawong
.....
Miss Tippawan Pissawong
Candidate

.....
Prof. Wanpen Chaicumpa,
D.V.M. (Hons.), Ph.D. (Microbiology)
Major Advisor

.....
Assoc. Prof. Taweesak Songserm,
D.V.M., Ph.D. (Veterinary Pathology)
Co-advisor

.....
Assist. Prof. Potjanee Srimanote,
Ph.D. (Molecular Microbiology)
Co-advisor

Santi M
.....
Mr. Santi Maneewatchararangsri,
Ph.D. (Biomedical Sciences)
Co-advisor

B. Mahaisavariya
.....
Prof. Banchong Mahaisavariya,
M.D., Dip Thai Board of Orthopedics
Dean
Faculty of Graduate Studies
Mahidol University

K Pattanapanyasat
.....
Prof. Kovit Pattanapanyasat,
Ph.D. (Hematology)
Program Director
Doctor of Philosophy Program in
Immunology
Faculty of Medicine, Siriraj Hospital
Mahidol University

Copyright by Mahidol University

Thesis
entitled

HUMAN MONOCLONAL ANTIBODY FRAGMENTS THAT NEUTRALIZE BIO-FUNCTIONS OF SURFACE EXPOSED PROTEINS OF TYPE A INFLUENZA VIRUSES

was submitted to the Faculty of Graduate Studies, Mahidol University
for the degree of Doctor of Philosophy (Immunology)
on
June 13, 2013

Tippawan Pissawong
.....
Miss Tippawan Pissawong
Candidate

P. Lekcharoensuk
.....
Assoc. Prof. Porntippa Lekcharoensuk,
D.V.M., Ph.D. (Veterinary Microbiology)
Chair

.....
Assoc. Prof. Taweesak Songserm,
D.V.M., Ph.D. (Veterinary Pathology)

.....
Prof. Wanpen Chaicumpa,
D.V.M. (Hons.), Ph.D. (Microbiology)
Member

.....
Assist. Prof. Potjanee Srimanote,
Ph.D. (Molecular Microbiology)
Member

Santi M.
.....
Mr. Santi Maneewatchararangsri,
Ph.D. (Biomedical Sciences)
Member

B. Mahaisavariya
.....
Prof. Banchong Mahaisavariya,
M.D., Dip Thai Board of Orthopedics
Dean
Faculty of Graduate Studies
Mahidol University

Udom K.
.....
Clin. Prof. Udom Kachintorn,
M.D.
Dean
Faculty of Medicine, Siriraj Hospital
Mahidol University

Copyright by Mahidol University

ACKNOWLEDGMENTS

For all successful completion of this work and invaluable experiences I gained during my Ph.D. tenure, I would like to express my deepest gratitude and appreciation to the persons whom I am indebted:

To Prof. Dr. Wanpen Chaicumpa, my major thesis supervisor and dedicated teacher for her valuable teaching, comments, kindness, encouragement and supports in many ways. Without her virtues, this study would not have been accomplished.

To my co-advisors; Dr. Santi Maneewatchararangsri, Asst. Prof. Dr. Potjanee Srimanote, and Assoc. Prof. Dr. Taweesak Songserm for their encouragements, kindness and valuable suggestions. Without their guidance and persistent help this dissertation would not have been possible.

Thanks to all members of Prof. Wanpen's laboratory for their invaluable helps, understanding and encouragement.

Special thanks to experimental animals that devote their life for the experiment

Sincerely thank you for technical supports and facilities to: Department of Parasitology and the Office for Research and Development, Faculty of Medicine, Siriraj Hospital, Mahidol University; Department of Veterinary Pathology, Kasetsart University, Kum-paeng-sean Campus; Faculty of Allied Health Sciences, Thammasat University; The nanotechnology Center (NANOTEC), NSTDA for providing the Discovery Studio 2.5 package and Center of Excellent for Antibody Research, Faculty of Tropical Medicine, Mahidol University for fluorescence microscopy.

Thanks and gratitude are due to the Thailand Research fund (DPG5380001) and the Office of Higher Education Commission (RG and NRU project) for the financial supports.

Finally, great appreciation is expressed to my mother and father who always stand by me with love and forever supports.

Tippawan Pissawong

Copyright by Mahidol University

HUMAN MONOCLONAL ANTIBODY FRAGMENTS THAT NEUTRALIZE BIO-FUNCTIONS OF SURFACE EXPOSED PROTEINS OF TYPE A INFLUENZA VIRUSES

TIPPAWAN PISSAWONG 5136954 SIIM/D

Ph.D. (IMMUNOLOGY)

THESIS ADVISORY COMMITTEE: WANPEN CHAICUMPA, D.V.M. (Hons.), Ph.D.; TAWEESAK SONGSERM, D.V.M., Ph.D.; POTJANEE SRIMANOTE, Ph.D.; SANTI MANEEWATCHARARANGSRI, Ph.D.

ABSTRACT

The surface proteins of the influenza A virus, namely hemagglutinin (HA), neuraminidase (NA), and matrix protein-2 (M2) are surface exposed and thus are vulnerable targets for neutralizing antibodies. HA is the most abundant protein on the viral surface and the virus uses this protein as a ligand for host cell receptor binding and subsequent cellular entry by receptor mediated endocytosis. In the acidic endosome, a conformational change in the cleavage-active HA molecule induces fusion of the HA to the host endosomal membrane, allowing the exit of the viral RNPs into the host cytoplasm and subsequent nuclear import for replication. NA is a sialidase enzyme that cleaves the NeuAcα2,3Gal or NeuAcα2,6Gal on new virions and releases them from the infected cell. The M2 protein forms a homotetramer which is a highly selective channel for H^+ influx into the intra-endosomal virion causing a dissociation of matrix protein-1 (M1) from the viral RNPs, allowing entry of the latter into the host cytosol. In the late stage of viral replication, M2 prevents acid-induced conformational change of newly synthesized hemagglutinin molecules that are cleaved in the trans-Golgi network. M2 functions also in inhibition of autophagy in infected cells causing accumulation of autophagosomes (macroautophagosome) to help the survival of the influenza virus in the infected cell. In addition, HA, NA, and M2 proteins also work together in viral assembly and budding. HA and NA help the M2 amphipathic helix in causing membrane curvature at the neck of the budding virion leading to membrane scission and virus release. As such, antibodies that interfere with HA, NA, and M2 functions have high potential as sole or adjunct therapeutic agents for influenza.

In this study, fully human monoclonal single chain antibody variable fragments (HuScFv) specific to HA, NA, and M2 of the influenza A virus were generated by using phage display technology. Influenza viruses adsorbed on the human erythrocyte ghosts were used as a phage biopanning antigen for selecting phage clones that dispalyed HuScFv from a human ScFv phage display library. The HuScFv specific to HA, NA and/or M2 derived from *huscfv*-phagemid transformed *E. coli* clones can be classified into 4 groups: HuScFv that bound to HA, NA, and M2 (clones no. 2, 10, 26, and 54); HuScFv that bound to HA and NA (clone no. 53); HuScFv that bound to M2 (clones no. 15 and 51); and HuScFv that bound to HA (clone no. 99). HuScFv from four selected clones which had different antigenic specificities and amino acid sequences particularly at their complementarity determining regions (CDRs), *i.e.*, clones no. 26, 51, 53, and 99, were tested for their efficacies in interfering with the influenza virus replication cycle in mammalian cell cultures. The results of the plaque assay revealed that the HuScFv of all clones could reduce the numbers of influenza virus foci in the HuScFv treated-infected cells.

Phage clones displaying HuScFv that bound specifically to full length recombinant M2 (rM2) were also selected from the human ScFv phage display library. Four *huscfv*-phagemid transformed *E. coli* clones, *i.e.*, no. 2, 19, 23 and 27, expressed HuScFv that bound not only to the rM2 but also to native M2 (nM2) in influenza virus infected cell homogenates and inside the cells. The HuScFv2, 19, 23, and 27 which had different amino acid sequences in immunoglobulin frameworks and CDRs could similarly reduce the amounts of viruses both in the culture supernatants and inside the cells infected with adamantane sensitive and resistant A/H5N1 strains belonging to different clades. A phage mimotope (peptide) search and multiple alignments revealed that conformational epitopes of HuScFv2 located at the residues important for ion channel activity, anti-autophagy, and M1 binding. Epitopic residues of HuScFv19 located at the M2 amphipathic helix and cytoplasmic tail important for anti-autophagy, virus assembly, morphogenesis, and release. The epitope of HuScFv23 involved residues important for the M2 activities similar to HuScFv2 and also amphipathic helix residues for viral budding and release. For the HuScFv27 epitope, it spanned ectodomain, ion channel, and anti-autophagy residues. The results of computerized homology modeling and molecular docking conformed to the epitope identification by phages. M2 epitopes bound by HuScFv2, 19, 23, and 27 are conserved across influenza A subtypes and human pathogenic clades of H5N1, indicating that the HuScFv have anti-influenza A activity.

Although molecular mechanisms of the HA-, NA-, and/or M2-specific-HuScFv(s) in interfering with the influenza virus replication cycle await experimental validations, these small antibody fragments which are fully human proteins have high potential for developing further as safe, novel, and mutation tolerable anti-influenza agents, especially against drug resistant variants.

KEY WORDS: INFLUENZA A VIRUSES/ HEMAGGLUTININ (HA)/ NEURAMINIDASE (NA) / MATRIX PROTEIN-2 (M2) / HUMAN SCFV/ PHAGE DISPLAY / MIMOTOPE / HOMOLOGY MODELING AND MOLECULAR DOCKING

216 pages

แอนติบอดีสายเดี่ยวมนุษย์แบบโมโนโคนาลที่สามารถลบล้างฤทธิ์การทำงานของโปรตีนที่อยู่บริเวณผิวของไวรัสไข้หวัดใหญ่//ไวรัสไข้หวัดใหญ่นก ชนิด เอ
HUMAN MONOCLONAL ANTIBODY FRAGMENTS THAT NEUTRALIZE BIO-FUNCTIONS OF SURFACE EXPOSED PROTEINS OF TYPE A INFLUENZA VIRUSES

ทิพวรรณ พิศวง 5136954 SIIM/D

ปร.ด. วิทยาภูมิคุ้มกัน

คณะกรรมการที่ปรึกษาวิทยานิพนธ์: วันเพ็ญ ชัยคำภา , D.V.M. (Hons.), Ph.D., ทวีศักดิ์ ส่งเสริม, D.V.M., Ph.D., พจนีย์ศรีมาโนชญ์, Ph.D., สันติ มณีวัชระรังษี, Ph.D.

บทคัดย่อ

โปรตีนที่ผิวของไวรัสไข้หวัดใหญ่/นกชนิดเอชื่อว่าฮีแมกกลูตินิน (เอชเอ), นิวรามินิเดส (เอ็นเอ) และแมทริกซ์สอง (เอ็มสอง) เป็นโปรตีนที่ผิวของไวรัสซึ่งง่ายต่อการเป็นเป้าหมายของแอนติบอดีที่จะทำการลบล้างฤทธิ์ โดยที่โปรตีนเอชเอนั้นมีมากที่สุดบนผิวของไวรัสและไวรัสใช้โปรตีนนี้เพื่อเป็นแกนสำหรับจับกับตัวรับซึ่งอยู่บนผิวของโฮสท์เซลล์ เพื่อใช้ในการเข้าสู่เซลล์เป้าหมายโดยขบวนการเอ็นโดไซโตสิส และในถุงเอ็นโดโซมนั้นเองจะเกิดการเปลี่ยนแปลงของโมเลกุลเอชเอเพื่อให้เกิดการรวมกันของผิวไวรัสและผิวโฮสท์เซลล์เพื่อทำการปลดปล่อยสารพันธุกรรมของไวรัสเข้าสู่ไซโตพลาสซึมของโฮสท์เซลล์เพื่อทำการจำลองสารพันธุกรรมใหม่ของอนุภาคไวรัสตัวลูกต่อไป ส่วนโปรตีนเอ็นเอนั้นมีคุณสมบัติเป็นเอ็นไซม์เซียลิซิเดสที่ใช้ในการตัดพันธะ (NeuAcα2,3Gal หรือ NeuAcα2,6Gal) ที่เชื่อมระหว่างโฮสท์และอนุภาคไวรัสตัวใหม่ เพื่อทำการปล่อยอนุภาคไวรัสตัวลูกออกจากเซลล์ที่ติดเชื้อนั้น ในขณะที่โปรตีนเอ็มสองจะรวมตัวเป็นเททราเมอร์ซึ่งทำตัวเป็นช่องที่ใช้ตรวจจับโปรตอนเข้ามาในอนุภาคไวรัสขณะที่อยู่ในถุงเอ็นโดโซมเพื่อใช้ในการแยกกันของโปรตีนเอ็มหนึ่งและสารพันธุกรรมไวรัสออกจากกัน เพื่อที่สารพันธุกรรมของไวรัสนั้นจะเข้าสู่ไซโตพลาสซึมของโฮสท์เซลล์ต่อไป และในขั้นท้ายของการจำลองอนุภาคไวรัสใหม่นั้น โปรตีนเอ็มสองมีส่วนช่วยในการป้องกันการเปลี่ยนแปลงรูปร่างของโปรตีนเอชเอที่สังเคราะห์ใหม่ขณะที่อยู่ในทรานซ์กอนจิเน็ตเวิร์ค โปรตีนเอ็มสองยังมีหน้าที่ในการขับยั้งกระบวนการออโตฟาจิในเซลล์ติดเชื้อโดยการทำให้เกิดการสะสมตัวของถุงฟาโกโซม (แม็กโครออโตฟาโกโซม) เพื่อ ช่วยในการอยู่รอดของไวรัสในเซลล์ที่ติดเชื้อ นอกจากนี้โปรตีนเอชเอ, เอ็นเอ และเอ็มสองยังทำงานร่วมกันในขณะการจำลองอนุภาคใหม่และการปลดปล่อยจากเซลล์ที่ติดเชื้อ โดยที่โปรตีนเอชเอและเอ็มสองช่วยกับโปรตีนเอ็มสองส่วนแอมฟิพาติกเฮลิกซ์ในการทำให้ผิวแมมเบรนของโฮสท์เซลล์เกิดการโค้งงอเพื่อให้ง่ายต่อการตัดอนุภาคไวรัสตัวใหม่ออกจากโอสท์เซลล์และปล่อยออกสู่ภายนอก จากเหตุผลดังกล่าวนี้เองแอนติบอดีที่สามารถรบกวนการทำงานของโปรตีนเอชเอ, เอ็นเอ และเอ็มสองจึ งน่าจะมีประสิทธิภาพสูงในการนำไปใช้ในการรักษาหรือเป็นตัวช่วยยาในการรักษาโรคไข้หวัดใหญ่/นก

ในการศึกษาครั้งนี้ แอนติบอดีสายเดี่ยวของมนุษย์แบบโมโลคนาลที่จำเพาะกับโปรตีนเอชเอ, เอ็นเอ และเอ็มสองของไวรัสไข้หวัดใหญ่/นกถูกผลิตขึ้นโดยใช้เทคโนโลยีฟาจดิสเพลย์ โดยที่อนุภาคไวรัสไข้หวัดใหญ่ที่ถูกตรึงบนผิวของเม็ดเลือดแดงที่ไม่มีฮีโมโกลบิลจะถูกใช้เป็นเป้าหมายสำหรับการคัดเลือกโคลนฟาจที่มีแอนติบอดีสายเดี่ยวแสดงอยู่บนผิวจากคลังฟาจแอนติบอดีสายเดี่ยวของมนุษย์ ซึ่งแอนติบอดีสายเดี่ยวที่จำเพาะกับโปรตีนเอชเอ, เอ็นเอ และหรือเอ็มสองจะได้รับจากอีโคไลโคลนที่บรรจุฟาจมิดที่มียีนแอนติบอดีสายเดี่ยวอยู่ และสามารถแบ่งแอนติบอดีสายเดี่ยวที่ได้รับออกเป็นสี่กลุ่มดังนี้ แอนติบอดีสายเดี่ยวที่จำเพาะกับโปรตีนเอชเอ, เอ็นเอ และเอ็มสองจำนวน ๔ โคลน (โคลนเลขที่ ๒, ๑๐, ๒๖ และ ๕๔) แอนติบอดีสายเดี่ยวที่จำเพาะกับโปรตีนเอชเอและเอ็นเอจำนวน ๑ โคลน (โคลนเลขที่ ๕๓) แอนติบอดีสายเดี่ยวที่จำเพาะกับโปรตีนเอ็มสองจำนวน ๒ โคลน (โคลนเลขที่ ๑๕ และ ๕๑) และ แอนติบอดีสายเดี่ยวที่จำเพาะกับโปรตีนเอชเอจำนวน ๑ โคลน (โคลนเลขที่ ๕๙) โดยที่แอนติบอดีสายเดี่ยวจำนวน ๔ โคลน (โคลนเลขที่ ๒๖, ๕๑, ๕๓ และ ๕๙) ซึ่งจำเพาะกับโปรตีนเป้าหมายที่แตกต่างกัน และยังมีลำดับกรดอะมิโนที่แตกต่างกันโดยเฉพาะบริเวณซีดีอาร์ ถูกนำมาทดสอบความสามารถในการรบกวนกระบวนการจำลองอนุภาคไวรัสในเซลล์ที่เลี้ยงในหลอดทดลอง ซึ่งผลจำนวนเซลล์ที่ติดเชื้อ (ไวรัสโฟไซ) เผยให้เห็นว่าทุกโคลนของแอนติบอดีสายเดี่ยวสามารถลดจำนวนไวรัสโฟไซได้ในเซลล์ติดเชื้อที่ได้รับแอนติบอดีสายเดี่ยว

ฟาจโคลนที่ดิสเพลย์แอนติบอดีสายเดี่ยวมนุษย์ที่จับจำเพาะกับตัวเต็มของโปรตีนรีคอมบิแนนท์เอ็มสอง (อาร์เอ็มสอง) ยังถูกคัดเลือกจากคลังฟาจแอนติบอดีสายเดี่ยวของมนุษย์อีกด้วย อีโคไลโคลนที่บรรจุฟาจมิดที่มียีนแอนติบอดีสายเดี่ยวอยู่จำนวน ๔ โคลนดังนี้ โคลนเลขที่ ๒, ๑๕, ๒๓ และ ๒๗ สามารถจับได้กับโปรตีนอาร์เอ็มสอง และ เนทีฟโปรตีนเอ็มสองที่ได้จากเซลล์โฮโมจีเนทของเซลล์ที่ติดเชื้อไวรัสไข้หวัดใหญ่ และที่อยู่ภายในเซลล์ แอนติบอดีสายเดี่ยว๒, ๑๕, ๒๓ และ ๒๗ ซึ่งมีลำดับกรดอะมิโนที่แตกต่างกันในส่วนอิมมูโนโกบลูลินเฟรมเวิร์คและซีดีอาร์ สามารถลดจำนวนไวรัสได้ทั้งในส่วนอาหารเลี้ยงเซลล์และภายในเซลล์ที่ติดเชื้อกับไวรัสไข้หวัดใหญ่/นก ซัปทัยป์ เอช๕เอ็น๑ ที่ดื้อและไม่ดื้อยา ซึ่งแตกต่างกันตามเคลดที่อยู่ การหาฟาจมิโมโทป (เปปไทด์) และการทำการเปรียบเทียบลำดับกรดอะมิโนที่จะเป็นอิพิโทปบนโปรตีนเอ็มสอง เผยให้เห็นว่า แอนติบอดีสายเดี่ยว๒ จับบริเวณที่ทำหน้าที่เป็นอิออนชาเนล, แอนติออโตฟาจิ และบริเวณที่ใช้จับกับโปรตีนเอ็มหนึ่ง แอนติบอดีสายเดี่ยว๑๕ จับบริเวณแอมฟิพาติกเฮลิกซ์ และไซโตพลาสมิคของโปรตีนเอ็มสองที่สำคัญต่อการเป็นแอนติออโตฟาจิ และการประกอบและปลดปล่อยอนุภาคไวรัสใหม่ แอนติบอดีสายเดี่ยว๒๓ จับบริเวณที่สำคัญต่อการเป็นอิออนชาเนลคล้ายกับแอนติบอดีสายเดี่ยว๒ แต่ยังสามารถจับส่วน แอมฟิพาติกเฮลิกซ์ที่สำคัญต่อการปลดปล่อยอนุภาคไวรัสใหม่อีกด้วย ในขณะที่แอนติบอดีสายเดี่ยว๒๗ จะจับส่วนเอ็กซ์โตโดเมน, อิออนชาเนล และส่วนที่จะเป็นแอนติออโตฟาจิ นอกจากนี้ผลของโฮโมโลจีเดลลิ่งและโมเลกุลาร์ด็อกซ์กิ้งยังสนับสนุนผลอิพิโทปที่ได้จากฟาจอีกด้วย ซึ่งอิพิโทปบนเอ็มสองที่จับโดยแอนติบอดีสายเดี่ยว๒, ๑๕, ๒๓ และ ๒๗ มีลักษณะที่อนุรักษ์ในระหว่างซัปทัยป์ของไวรัสไข้หวัดใหญ่/นก และ ไวรัสไข้หวัดนกซัปทัยป์ เอช๕เอ็น๑ ที่ติดเชื้อในมนุษย์ จากผลตรงนี้สามารถบอกเป็นนัยได้ว่าแอนติบอดีสายเดี่ยวสามารถใช้เป็นสารต่อต้านไวรัสไข้หวัดใหญ่/นกได้ในวงกว้าง

ถึงแม้ว่ากลไกการทำงานของด้านโมเลกุลาร์ของแอนติบอดีสายเดี่ยวที่จำเพาะกับโปรตีนเอชเอ, เอ็นเอ และหรือเอ็มสอง ที่ใช้ในการรบกวนการจำลองอนุภาคใหม่ของไวรัสไข้หวัดใหญ่/นกยังรอคอยการทดลองที่จะมาประเมินผล แต่แอนติบอดีสายเดี่ยวโมเลกุลเล็กเหล่านี้ที่ผลิตจากมนุษย์ก็มีประสิทธิภาพสูงพอที่จะพัฒนาต่อไปเป็นสารที่ใช้ในการต้านไวรัสไข้หวัดใหญ่ที่ปลอดภัย และทนต่อการเปลี่ยนแปลงกรดอะมิโนของโปรตีนเป้าหมายในไวรัสสายพันธุ์ที่ดื้อต่อยา

CONTENTS

Copyright by Mahidol University

CONTENTS (cont.)

Copyright by Mahidol University

CONTENTS (cont.)

Copyright by Mahidol University

CONTENTS (cont.)

Copyright by Mahidol University

CONTENTS (cont.)

Copyright by Mahidol University

CONTENTS (cont.)

Copyright by Mahidol University

CONTENTS (cont.)

Copyright© by Mahidol University

CONTENTS (cont.)

Copyright by Mahidol University

CONTENTS (cont.)

Copyright by Mahidol University

CONTENTS (cont.)

Copyright by Mahidol University

CONTENTS (cont.)

Copyright by Mahidol University

CONTENTS (cont.)

Copyright by Mahidol University

LIST OF TABLES

Copyright by Mahidol University

LIST OF FIGURES

Copyright by Mahidol University

LIST OF FIGURES (cont.)

Copyright by Mahidol University

LIST OF FIGURES (cont.)

Copyright by Mahidol University

LIST OF FIGURES (cont.)

Copyright by Mahidol University

LIST OF FIGURES (cont.)

Copyright by Mahidol University

LIST OF FIGURES (cont.)

Copyright by Mahidol University

LIST OF ABBREVIATIONS

Abbreviation or symbol	Term
%	Percent
×*g*	Specific gravity
°C	Degree Celsius
-OH	Hydroxyl group
A	Absorbance
Å	Ångström
µg	Microgram
µl	Microliter
3D	Three-dimension
A or Ala	Alanine
ABTS	2,2´-azino-bis (3-ethylbenzthiazoline-6-sulphonic acid)
AP	Alkaline phosphatase
BCIP/NBT	Alternative reading frame protein 5-bromo-4-chloro-3-indolyl phosphate / nitro blue tetrazolium
bp	Base pairs
BSA	Bovine serum albumin
CI	Constant domain I of heavy chain
CII	Constant domain II of heavy chain
CBB	Coomassie Brilliant Blue G-250
cDNA	Complementary deoxy-nucleic acid
CDRs	Complementarity determining regions
CL	Constant domain of light chain
CFU	Colony forming unit (s)
CRM1	Exportin I protein

Copyright by Mahidol University

LIST OF ABBREVIATIONS (cont.)

Abbreviation or symbol	Term
cRNA	Complimentary RNA
D or Asp	Aspartic acid
DAPI	4´, 6-diamidino-2-phenylindole
DEPC	Diethylpyrocarbonate
DNA	Deoxyribonucleic acid
DMEM	Dulbecco's Modified Eagle's Medium
DW	Distilled water
E. coli	*Escherichia coli*
EDTA	Ethylenediaminetetraacetic acid
e.g.	*Exempli gratia*
ELISA	Enzyme limked-immunosorbent assay
ER	Endoplasmic Reticulum
etc.	*Et cetera*
F or Phe	Phenylalanine
Fab	Monovalent antigen binding fragment
$F(ab)'_2$	bivalent antigen binding fragment
FBS	Fetal Bovine Serum
Fc	Fragment, crystalizable
FR	Framework
g	Gram
G or Gly	Glycine
Gal	Galactose
H or His	Histidine
H^+	Proton
HA	Hemagglutinin
HAMA	Human antibody to mouse antibody
HAU	Hemagglutinination unit

Copyright by Mahidol University

LIST OF ABBREVIATIONS (cont.)

Abbreviation or symbol	Term
HI	Hemagglutination inhibition
hRBC	Human red blood cell
HRP	Horse radish per oxidase
HuScFvIgG	Human single chain antibody
i.e.	*Id est*
IgG	Immunoglobulin G
IMGT	The international ImMunoGeneTics information system for immunoglobulins or antibodies
IPTG	Isopropyl-1-thiol-β-D-galactopyranoside
kb	Kilo bases
kDa	Kilo Daltons
L or Leu	Leucine
LC-MS/MS	Liquid chromatography and tandem mass spectrometry
M	Molar
M1	Matrix protein 1
M2	Matrix protein 2
M2e	Extracellular domain of Matrix protein 2
MAHA	Mouse Anti-Human Antibody
MAb	Monoclonal antibody
MDCK	Madin-Darby Canine Kidney Cells
Mg	Milligram (s)

Copyright by Mahidol University

LIST OF ABBREVIATIONS (cont.)

Abbreviation or symbol	Term
min	Minute (s)
ml	Milliliter (s)
mM	Millimolar
mPAb	Mouse polyclonal antibody
Mr	Relative molecular mass
MOI	Multiplicity of infection
mRNA	Messenger ribonucleic acid
N or Asn	Asparagine
NA or N	neuraminidase
NC	Nitro cellulose membrane
NeuAc	N-Acetylneuraminic acid or sialic acid
NEP	Nuclear export protein
ng	Nanogram (s)
Ni-NTA	Nickel-nitrilotriacetic acid
NP	Nucleoprotein
NS	Non-structural protein
nt	Nucleotide
OD	Optical density
PA	Acidic polymerase protein
PB	Basic polymerase protein
PAb	Polyclonal antibody
PBS	Phosphate buffer saline
PBS-T	Phosphate buffer saline with Tween-20
PCR	Polymerase chain reaction
PEG	Polyethylene glycol Restriction fragment length polymorphism

Copyright by Mahidol University

LIST OF ABBREVIATIONS (cont.)

Abbreviation or symbol	Term
qPCR	Real time RT-PCR
R or Arg	Arginine
RBC	Red blood cell
RFLP	Restriction fragment length polymorphism
RNA	Ribonucleic acid
rpm	Round per minute
RT-PCR	Reverse transcriptase polymerase chain reaction
S or Ser	Serine
ScFv	Single chain antibody
SD	Standard deviation
SDS	Sodium dodecyl sulfate
SDS-PAGE	Sodium dodecyl sulfate-poly acrylamide gel electrophoresis
Sec	Second (s)
SPF	specific pathogen-free
Taq	*Thermusaquaticus*
TBS	Tris buffered saline
TBS-T	Tris buffered saline with tween-20
TCID 50	median tissue culture infective dose
Tm	Time of mobile phase
UDW	Ultrapure distilled water
UV	Ultraviolet
W or Trp	Tryptophan
WHO	World Health Organization
V or val	Valine

Copyright by Mahidol University

LIST OF ABBREVIATION (cont.)

Abbreviation or symbol	Term
vh/VH	Variable region (sequence/segment) of immunoglobulin heavy chain gene/protein sequence of conventional antibody
v_hh/V_HH	Variable region (sequence/segment) of immunoglobulin heavy chain gene/protein sequence of heavy-chain antibody
VL	Variable region (sequence/segment) of immunoglobulin light chain
vRNP	viral ribonucleoprotein

Copyright by Mahidol University

CHAPTER I
INTRODUCTION

Influenza viruses are enveloped, negative-sense, single stranded-RNA viruses belonging to the family *Orthomyxoviridae*. They are divided into three types: A, B, and C, based on the host range and preference, epidemiological pattern and severity of symptoms. The type A viruses have the widest host range and cause disease of the most severity. They are subdivided into 16 antigenic hemagglutinin (H or HA) subtypes (H1-H16) and 9 antigenic neuraminidase (N or NA) subtypes (N1-N9). Virion of the type A may have any of the H and N subtypes, such as H1N1, H2N2, H3N2, H5N1, H7N9, *etc*. The type A influenza viruses are causative agents of an acute respiratory contagious disease, named influenza or flu, in avian and mammal species including humans, tigers, leopards, cats and dogs. Pattern of human influenza viruses may be sporadic, annual/seasonal epidemic or occasional pandemic. The disease severity varies, depending upon the host age and background immunity and the virus virulence, from acute febrile illness to bacterially superimposed pneumonitis which is highly fatal. Until the presence, the world population has experienced several influenza A pandemics including Spanish flu caused by subtype H1N1 in 1918, H2N2 Asian flu in 1957, H3N2 Hong Kong flu in 1968, and the more recent H1N1-2009 pandemic in 2009. Nowadays, the newly emerged H1N1-2009 influenza virus has replaced the old seasonal H1N1 strain in seasonal epidemics throughout the world. For the avian influenza, there have been outbreaks of A/H5N1 in 1997 to 2011. Recently in 2012-2013, the A/H7N9 has killed not only poultry but also many infected human. Humans infected with avian influenza tend to develop severe pneumonia with high fatality rate. Fortunately there has been no evidence, as yet, of human to human transmission of the A/H7N9 avian influenza.

Current influenza vaccines for human use are trivalent consisting of type A H1N1 and H3N2 strains and an influenza B strain. The vaccine is given *via* either parenteral or mucosal route. The World Health Organization (WHO) recommended

that the H1N1 for vaccines since 2010 must be H1N1-2009 or the antigenically related strain. There are limitations in both production and use of the current seasonal flu vaccines. The vaccine viruses are propagated in specific pathogen-free (SPF) embryonated eggs which not only the supply is limited, but also the vaccines are contra-indicated for people who are allergic to egg proteins. The vaccines are strain/subtype specific. The vaccine strains must match antigenically with the circulating/infecting influenza viruses in order to confer adequate protection. As such, viruses in the vaccines have to be changed almost annually due to antigenic variation of the circulating influenza viruses from year to year (which are different strains for the northern and southern hemispheres). Besides, immunity elicited by the vaccines is rather short-lived and frequent vaccination is required to induce and sustain the protective immunity level. The vaccines confer low protective rates in elderly, small children and immune-compromised individuals.

There have been only two pharmacologic drug families used for influenza treatment. One family is ion channel blockers and another is neuraminidase inhibitors. Both drugs must be given to the infected subjects during the early phase of the infection in order to expect satisfactory therapeutic efficiency. Influenza virus mutants that resist the anti-viral activities of the drugs have emerged continuously, leading to increment of influenza treatment failure. There is a need of novel therapeutic agents for influenza especially the regimens that have a broad spectrum and can tolerate the virus antigenic variations.

Influenza A virus has eight genomic RNA segments which encodes 11 functionally different proteins. Among the 11 proteins, hemagglutinin (HA), neuraminidase (NA), and ion channel protein or matrix protein-2 (M2) are surface exposed. Thus, these three proteins are vulnerable targets of neutralizing antibodies. Recent studies have shown that membrane of cells infected with influenza virus had increased permeability (Gonzalez and Carraso, 2003; Wang *et al*., 2011). Therefore, small anti-viral agents including antibodies such as single chain variable antibody fragments (ScFv) or single domain antibodies (nanobody/VH/V_HH) specific to intracellular influenza proteins could traverse the cell membrane during infection and interfere with the bio-functions of the targets which would eventually thwart the virus replication. The HA encoded by the fourth RNA segment, the most abundant proteins

Copyright by Mahidol University

on the influenza viral surface, is the virus ligand for host cell receptor binding and subsequent cellular entry by receptor mediated endocytosis. In the acidic endosome, a conformational change in the cleavage-active HA molecule induces HA-mediated host endosomal membrane fusion allowing the exit of the viral ribonucleoprotein (vRNP) (that has been released from the matrix protein-1 because of the ion channel activity of M2) into the host cytosol (the process called virus uncoating). Thus, the HA is an important target of neutralizing antibodies for prevention of the virus binding to cell surface receptor and inhibition of uncoating by the low pH mediated-conformational change in the HA molecule. The influenza virus NA is a sialicidase enzyme encoded by the sixth RNA segment. NA cleaves the NeuAcα2,3Gal or NeuAcα2,6Gal on new virions and release them from the infected cell. Thus, NA protein is another target of neutralizing antibodies which obstruct the virus release and spread. Recently, there has been evidence showing that the NA participates in cellular entry of the influenza virus. Thus, antibodies that neutralize NA function should reduce also the virus entry to cells (Su *et al*., 2009). Influenza virus M2 protein forms homotetramer on the virus particles and acts as a channel for influx of H^+ into the intra-endosomal virion causing a dissociation of the matrix protein-1 (M1) from the vRNPs allowing the latter to enter the host cytosol and subsequent nuclear import for replication. Moreover, M2 prevents acid-induced conformational change of the newly synthesized hemagglutinin molecules that are cleaved in trans-Golgi network. The M2 protein also functions in inhibition of fusion of autophagosomes to lysosomes in the influenza infected cells causing accumulation of the autophagosomes (macroautophagosome) for helping survival of influenza virus in infected cell. Besides, amphipathic helix of the M2 molecule also helps in altering membrane curvature at the neck of the budding virion, thus facilitating the membrane scission and the virus release. Hence, neutralizing antibodies specific to M2 should interfere with many steps of the influenza viral replication cycle. In addition, the HA, NA, and M2 proteins also work together in viral assembly and budding (Rossman and Lamb, 2011). From the above mentioned rationales, antibodies that inhibit functions of HA, NA and M2 should have high potential as therapeutic agents for influenza especially caused by drug resistant virus variants.

Copyright by Mahidol University

Legacy of influenza treatment annotated in the literature have shown that passive administration of specific antibody to influenza virus is highly effective for human influenza therapy and intervention of morbidity. For examples, passive transfer of the serum of the H5N1 convalescing subject could rescue readily the H5N1 infected recipient who was already refractory to the neuraminidase inhibitor (oseltamivir) (Zhou *et al*., 2007). Nevertheless, the supply of the human immune serum to a particular influenza virus subtype is limited and the medical practice is unethical. Mouse monoclonal antibody specific to ectodomain of M2 was found to accelerate the lung viral clearance following a sublethal influenza A virus infection in mice (Treanor *et al*., 1990). However, mouse antibodies are highly immunogenic in human and they are inappropriate for human use because of the adverse reaction subsequent to the human anti-mouse antibody (HAMA) response.

In this study, fully human single chain monoclonal antibody fragments (HuScFv) that bound specifically to- and interfere with- the biological functions of surface exposed proteins of influenza A virus, namely HuScFv to HA, NA and M2, were generated by using an established human ScFv phage display library as a biological tool. Focused was made on the therapeutic efficacies of the antibodies specific to M2 protein. The M2 specific HuScFv were characterized and evaluated: 1) *in vitro* by immunological assays for testing specific their specific binding to recombinant and native M2 across types and subtypes of influenza viruses, 2) *ex vivo* in the infected cell cultures to determine antibody efficacies in interfering with the replication cycles of both drug sensitive and resistant virus variants, and 3) *in silico* by homology modeling and molecular docking for determining interface binding and interactive residues of the antibodies with the targets in order to reveal the molecular mechanisms of the effective HuScFv. Experimental designs, the results thereof and discussion on the results form the basis of this thesis.

Copyright by Mahidol University

CHAPTER II
OBJECTIVES

ULTIMATE OBJECTIVE

To produce human single chain variable antibody fragment (HuScFv) that bind specifically to- and interfere with- the bio-functions of influenza virus surface exposed proteins, *i.e.*, hemagglutinin, neuraminidase and matrix protein-2 for using as a sole or adjunctive therapeutic agents of human influenza

SPECIFIC OBJECTIVES

1. To select phage clones that display HuScFv specific to native HA, NA and M2 of influenza A virus and to establish *Escherichia coli* transformants carrying the *huscfv*-phagemids that can express the recombinant HuScFv
2. To select phage clones that display HuScFv specific to recombinant M2 of influenza A virus and to establish *Escherichia coli* transformants carrying the *huscfv*-phagemids that can express the recombinant HuScFv
3. To characterize binding specificities of the bacterially derived-HuScFv to recombinant and/or native HA, NA and M2
4. To determine the ability of the HuScFv in neutralizing influenza A virus infectivity *ex vivo*
5. To identify epitopes on the target proteins that bound by the HuScFv
6. To test ability of the specific HuScFv in inhibition of the bio-functions of their respective antigens

Copyright by Mahidol University

CHAPTER III
LITERATURE REVIEW

3.1 Influenza viruses

3.1.1 General description of influenza viruses

Influenza viruses cause sporadic and recurrent seasonal epidemics of varying severity, as well as occasional global pandemics during which acute febrile respiratory disease occurs explosively in all age groups. The viruses are enveloped, negative-sense, single stranded-RNA viruses belonging to the family *Orthomyxoviridae* (Lamb and Krug, 2001). The influenza viruses are classified into three types: A, B, C, depended on the host range and preference, epidemiological patterns, and symptom severity. Type A has the widest host range including human, mammals and avian and infection of the influenza A virus in animal can cause high mortality (Webster, 1998). Both types B and C have human preference that cause mild symptoms compared to the type A viruses. All three types of the influenza viruses share similar physical structure. They have 7-8 gene segments encoding 10-11 proteins of diverse biological functions (types A and B viruses have 8 gene segments while type C virus has 7 segments and lacks the segment encoding neuraminidase) (Lamb and Krug, 2001).

3.1.2 Transmission

Both avian influenza A viruses such as A/H5N1 and A/H7N9 and human influenza viruses such as A/H1N1 and A/H3N2 can cause human infections. Human infections result from direct contact with influenza viruses which are shaded from infected animal or person (direct transmission), inhalation of the aerosols produced by an infected animal or person through coughing, sneezing or spitting (airborne transmission), or contact with contaminated surfaces (hand-to-eye, hand-to-nose, or hand-to-mouth transmission; fomites) (Brankston *et al*., 2004; Tellier, 2006).

Copyright by Mahidol University

Shedding of the influenza virus starts at the day before symptoms appear and viruses are released for approximately 5 to 7 days. People who contract influenza are most infective between the second and third days after infection (Carrat *et al*., 2006). The amount of virus shed appears to correlate with fever; higher amounts of virus shed when temperatures are highest. Children are much more infectious than adults and shed virus from just before they develop symptoms until two weeks after infection (Carrat *et al*., 2006; Mitamura and Sugaya, 2006).

3.1.3 Pathogenesis in human

The viral hemagglutinin protein (HA) of influenza virus is responsible for determining which species a virus strain can infect and where in the human respiratory tract a strain of influenza will bind (Nicholl *et al*., 2008). In mild and non-virulent viruses such as human influenza and low-pathogenic avian influenza, the structure of the HA can be cleaved only by proteases found in the throat and upper lungs while in highly virulent strains such as H5N1, the HA binds to receptors that are mostly found deep in the lungs (van Riel *et al*., 2006) and it is cleaved by a wide variety of proteases that cause the virus spreading throughout the body (Korteweg and Gu, 2008). This difference in the site of infection may be part of the reasons why the H5N1 strain causes severe viral pneumonia in the lungs, but is not easily transmitted by people coughing and sneezing (Shinya *et al*., 2006; van Riel *et al*., 2007). **Figure 3.1** shows different sites and outcomes of H1N1 *versus* H5N1 influenza virus infection.

The incubation period of influenza infection may be typically two to four days or up to eight day after exposure (Yuen *et al*., 1998; Chotpitayasunondh *et al*., 2004). Common symptoms of the flu such as fever, headaches and fatigue are the result of the huge amounts of proinflammatory cytokines and chemokines (such as interferon or tumor necrosis factor) produced from influenza-infected cells (Eccles, 2005; Schmitz *et al*., 2005). In contrast to the rhinovirus that causes the common cold, influenza does cause tissue damage; so the symptoms are not entirely due to the inflammatory response (Winther *et al*., 1998). The massive immune response might produce a life-threatening “cytokine storm” cause unusual lethality of both the H5N1 and H7N9 avian influenza (Cheung *et al*., 2002; Gao *et al*., 2013) and the pandemic

Copyright © by Mahidol University

strains (Kobasa *et al*., 2007; Kach *et al*., 2006; Fowlkes *et al*., 2012). However, another possibility is that these large amounts of cytokines are just a result of the massive levels of viral replication produced by these strains and the immune response does not itself contribute to the disease (Beigel and Bray, 2008).

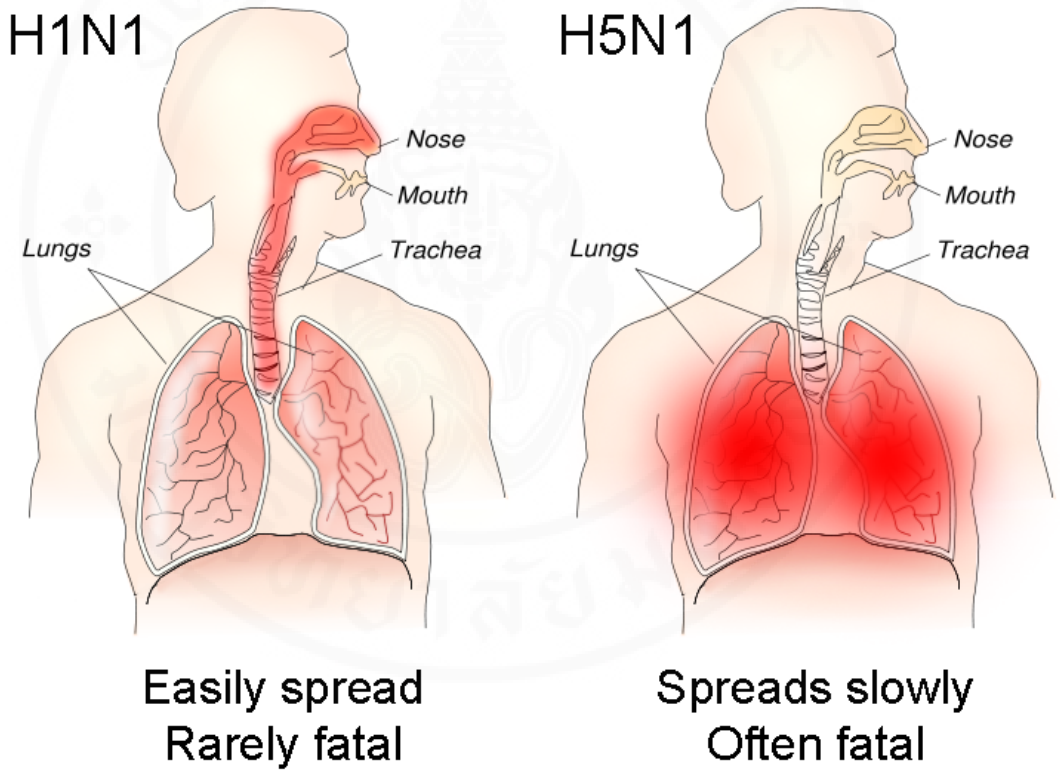

Figure 3.1 Different sites and outcomes of H1N1 *versus* H5N1 influenza virus infection

Source: http://en.wikipedia.org/wiki/Influenza

(Accessed on 31 May 2013)

Copyright by Mahidol University

3.1.4 Antigenic variation

The epidemiological success of influenza viruses is contributed mostly by two types of their antigenic variation that composed of antigenic drift and antigenic shift. The two mechanisms are described below.

3.1.4.1 RNA mutation (antigenic drift)

The antigenic drift (**Figure 3.2**) occurs in both influenza A and B viruses because of their low fidelity RNA polymerases, *i.e.*, lack proof-reading mechanisms to correct base-pairing mistakes during RNA replication resulting in genetic mutation during the influenza virus replication process. The estimated replication error rate is 1 per 10^{3}-10^{4} nucleotides (Matrosovich *et al*., 2004) and results in single amino acid substitutions (mutations) in viral proteins. In addition, the environment in the host cells especially from immune pressure causes also the antigenic drift by forcing influenza viruses to undergo antigenic change in order to escape the host immunity. The amino acid changes in the HA and NA proteins cause inability of the antibody to the previous infecting strains to neutralize the subsequently mutated virus (Bush *et al*., 1999; Plotkin and Dushoff, 2003). Thus, the composition of the vaccine needs to be adapted to match the circulating variants which usually are different in northern and southern hemispheres almost every year (Webster *et al.*, 1982; CDC, 2009).

3.1.4.2 RNA segment re-assortment (antigenic shift)

The occurrence of devastating worldwide pandemics is based on an abrupt change in the subtypes of HA and NA (**Figure 3.3**). This antigenic change comes from the genetic re-assortment among two different influenza A subtypes that happened to be replicated in the same host cell. Antigenic shift is responsible for worldwide pandemics. For example, pandemic 2009-H1N1 emerged from re-assortment of: 1) NA and M gene segments of the Eurasian swine genetic lineage, originally derived from an avian influenza virus and thought to have entered the Eurasian swine population in 1979; 2) HA, NP, and NS gene segments of the classical swine lineage, thought to have entered swine around 1918; 3) PB2 and PA gene segments of the swine triple reassortant lineage, originally from avian origin and entered swine in North America around 1998; and 4) PB1 gene segment which was seeded in swine from humans at the time of the North America swine triple re-

Copyright by Mahidol University

assortment event (**Figure 3.4**). From the above information, swine is considered as incubator for such new subtype recombination since they have receptors for both human and avian influenza viruses (Scholtissek *et al*., 1998).

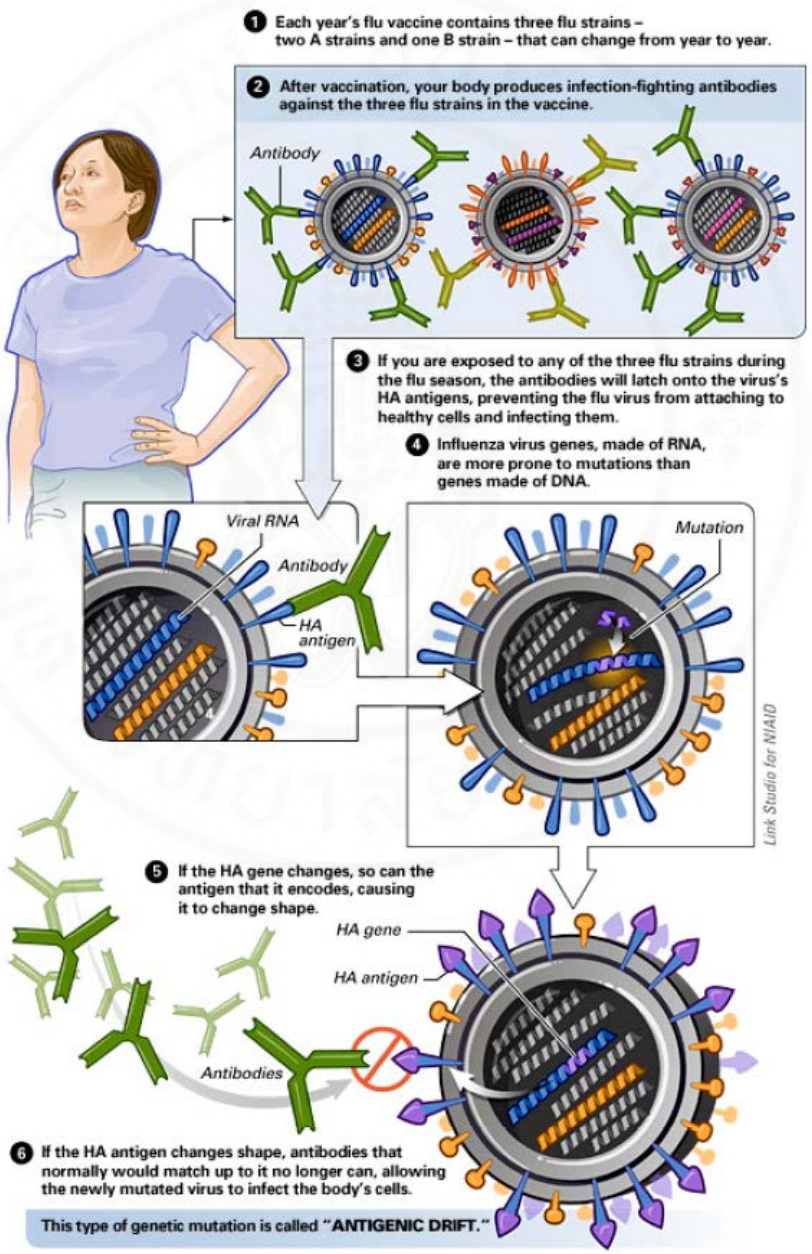

Figure 3.2 Schematic diagram of the antigenic drift of the influenza virus
Source: Kamps BS and Reyes-Teran G: www.InfluenzaReport.com
(Accessed on 20 January 2012)

Copyright by Mahidol University

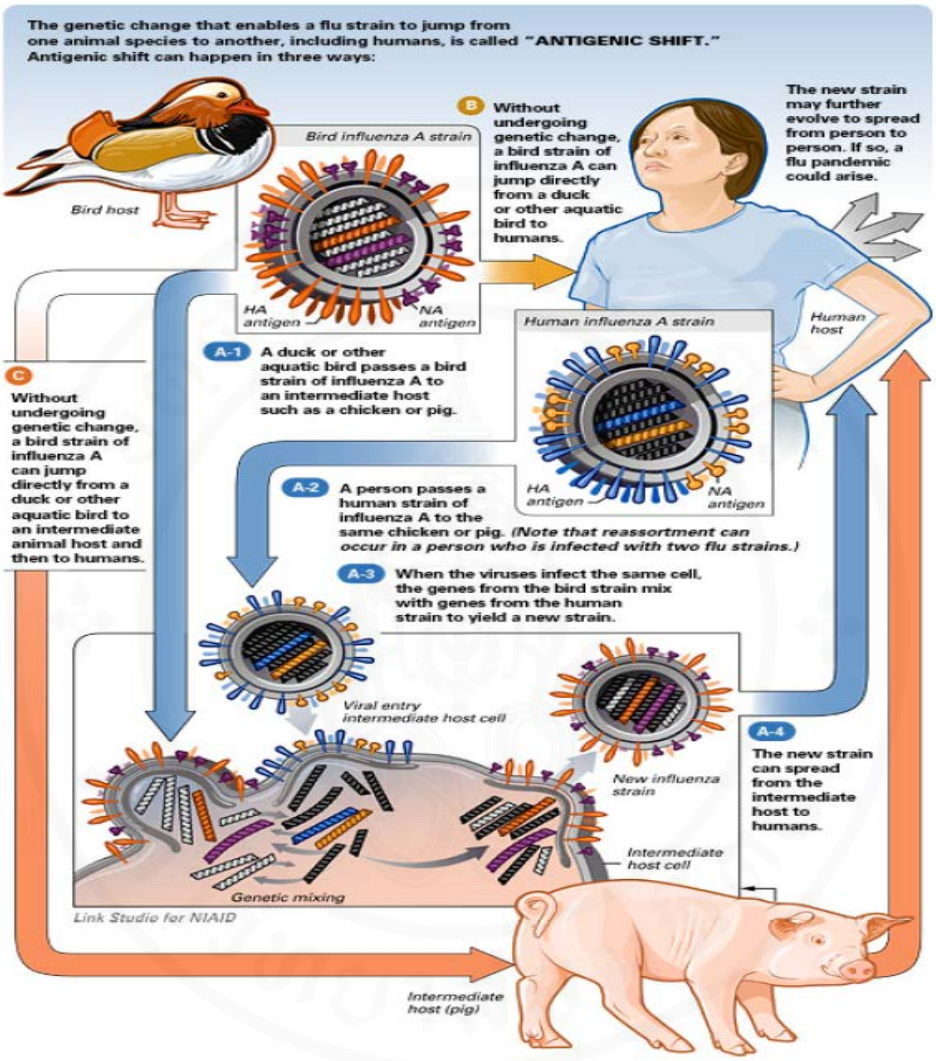

Figure 3.3 Schematic diagram of the antigenic shift of the influenza virus

Source: Kamps BS and Reyes-Teran G: www.InfluenzaReport.com

(Accessed on 20 January 2012)

Copyright by Mahidol University

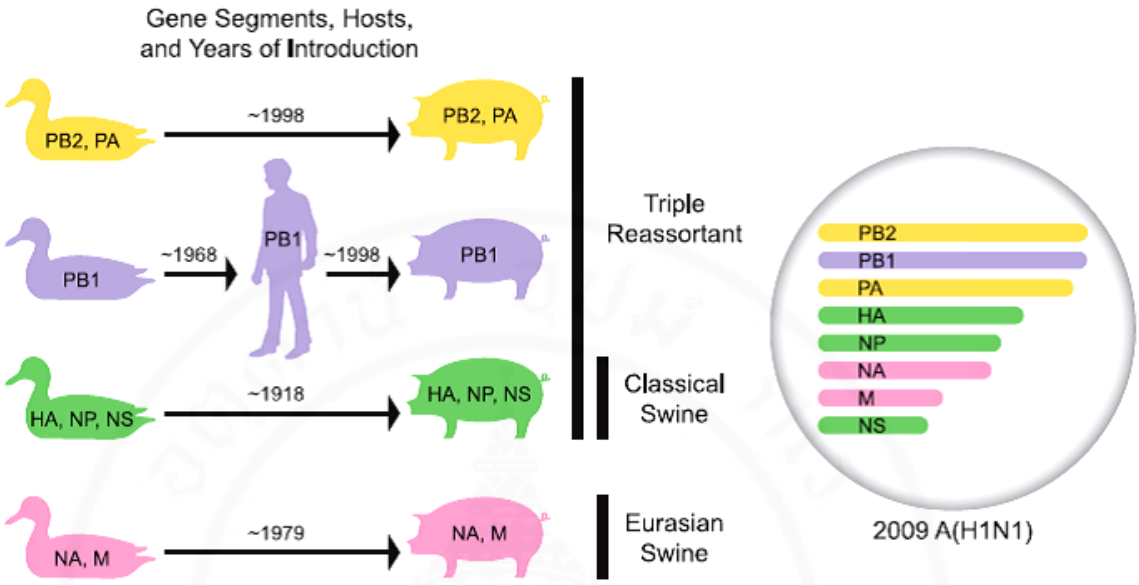

Figure 3.4 Schematic diagram of host and lineage origins for the gene segments of the 2009 A (H1N1) virus

Source: Garten *et al*, 2009.

3.1.5 Epidemiology of influenza

3.1.5.1 Seasonal variations

In Thailand (southern hemisphere), the incidence of seasonal influenza (**Figure 3.5**) normally starts in the hot season (April) and continues to increase until the beginning of the rainy season in May to August, then decrease in the dry season from November to March (Yuthao *et al*., 2008). In addition, the emerging of pandemic 2009-H1N1 has substituted season influenza H1N1 since 2009 and is also starting to resist both ion channel blocker and neuraminidase inhibitor drugs (Sheu *et al*., 2011).

Copyright by Mahidol University

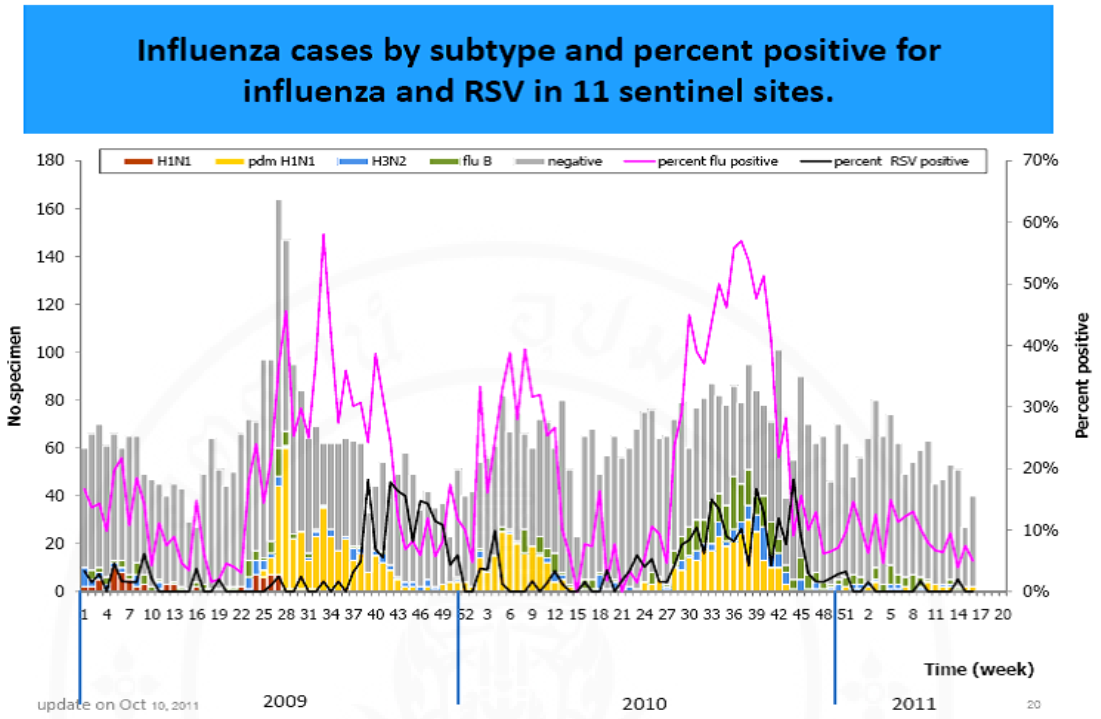

Figure 3.5 Incidence of influenza in Thailand (updated on Oct 10th, 2011)
Source: Department of Disease Control, Ministry of Public Health, Thailand

3.1.5.2 Epidemic and pandemic spread

Influenza occurs in distinct outbreaks of varying extent every year while an influenza pandemic is a rare but recurrent event. Historical influenza pandemics were caused by new influenza viruses that have adapted from avian and/or pig to humans. Four pandemics that occurred in the past included: “Spanish influenza (H1N1)” in 1918, “Asian influenza (H2N2)” in 1957, “Hong Kong influenza (H3N2)” in 1986, and “pandemic 2009-H1N1” in 2009. The A/H5N1 and A/H7N9 is newly emerged and highly pathogenic avian influenza virus. Since these strains have started to spread, most of infected people died after infection (Cheung *et al*., 2002; Gao *et al*., 2013). These pandemics killed millions of people worldwide and the unavailability of effective anti-viral drugs at the time. Therefore finding of new anti-influenza agents that are safe and tolerable to the virus mutations is needed.

Copyright by Mahidol University

3.2 Influenza A virus

3.2.1 Morphology of influenza A virus

Influenza A virus particles are pleomorphic with spherical or filamentous morphology, or mixture of both (**Figure 3.6**). They are envelope viruses which have 7-8 gene segments encoding 10-11 proteins. The known and proposed functions of the influenza virus-encoded proteins are listed in **Table 3.1**. The envelope of each influenza A virus derived from the host plasma membrane containing both cholesterol-enriched lipid rafts and non-raft lipids (Scheiffele *et al*., 1999; Zang *et al*., 2000; Nayak *et al*., 2009). The envelope membrane has three viral proteins, *i.e.* hemagglutinin (HA), neuraminidase (NA) and ion-channel protein (M2), deposit on it. HA is the most abundant envelope protein at approximately 80 percent, followed by NA, which makes up around 17 percent of the viral envelope proteins. M2 is a minor component of the envelope, with only 16 to 20 molecules per virion. HA and NA are associated exclusively with the lipid rafts in the viral lipid membrane, whereas M2 is not (Samji, 2009). Under the viral envelope, there is underlined matrix 1 protein (M1) that serves as a docking site of vRNAs during influenza virus assembly. Inside the viral envelope are 8 helical vRNP segments; each contains: nucleoprotein (NP) which protects the viral RNA (vRNA) and three polymerase proteins, *i.e.*, basic polymerase protein-1 (PB1), basic polymerase protein-2 (PB2) and acidic polymerase protein (PA), which form the viral RNA polymerase (transcriptase) complex. The small amounts of a nuclear export protein (NEP or NS2) are also found in the particle. Some strains of influenza A virus have PB1 gene that contains a second open reading frame that can produce a second protein called PB1-F2. The PB1-F2 is believed to be an important determinant of virulence because it suppresses immune response by inducing apoptosis of CD8 T-cells and alveolar macrophages and prolongs viral polymerase activity upon interaction with PB1 in nucleus of infected epithelial cells (Chen *et al*., 2001, Mazur *et al*., 2008; Mitzner *et al*., 2009).

Copyright by Mahidol University

A

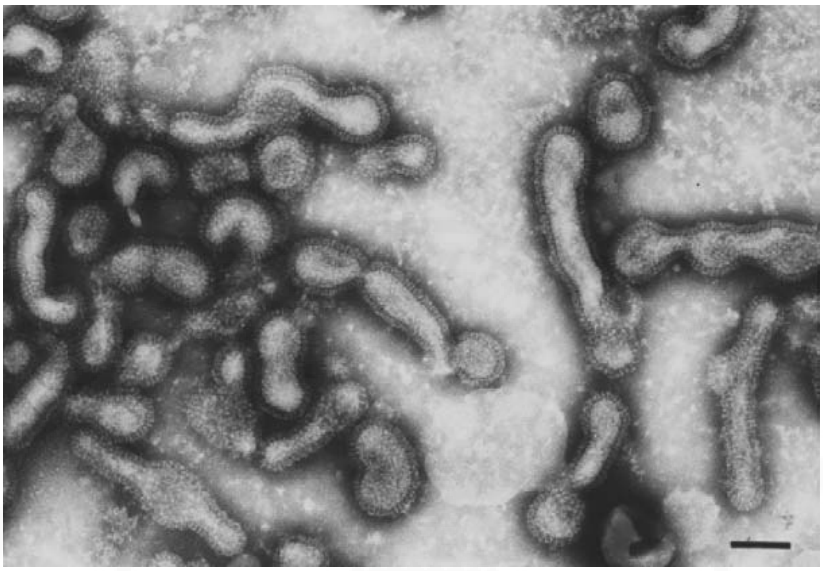

B

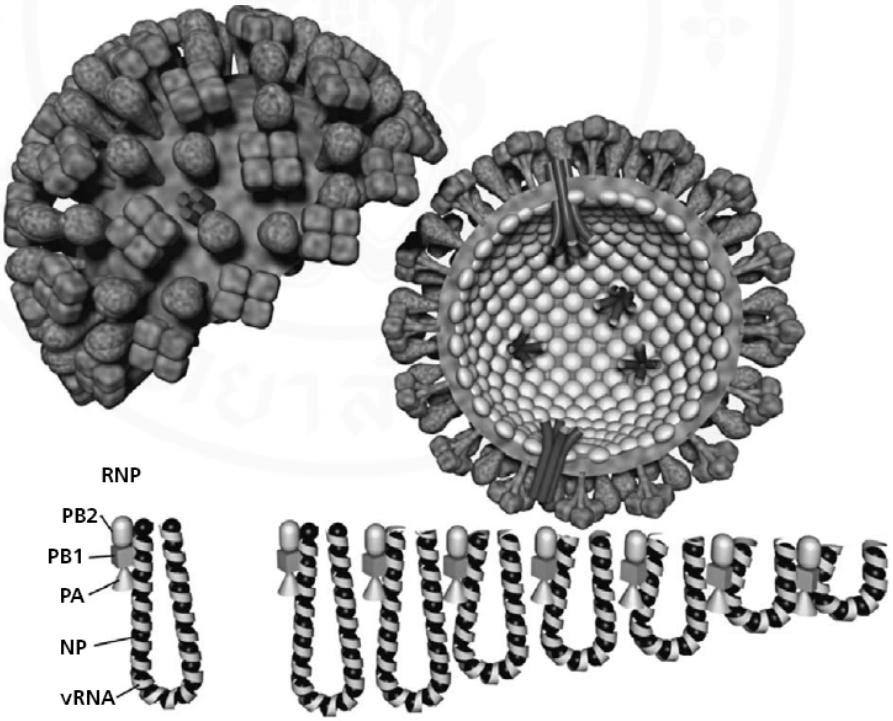

Figure 3.6 Influenza A virus particle

A, Appearance of pleomorphic influenza virus particles under electron microscopy

B, Schematic diagram showing the eight segmented RNA genome and vRNP complex of influenza virus

Source: Cox *et al*., 2010

Copyright by Mahidol University

Table 3.1 Influenza A virus genome RNA and protein coding assignments (Adapted from Cox *et al*., 2010)

RNA segment	Nucleotides[(a)]	Encoded polypeptide	Amino acids	Molecular weight (kDa)	Carbohydrates	Approximate copy no. per virion	Functions
1	2,341	PB2	759	87	-	30-60	Component of RNA transcriptase complex; host-cell capped mRNA recognition and binding
2	2,341	PB1	757	96	-	30-60	Component of RNA transcriptase complex; RNA-dependent RNA polymerase activity; capped mRNA endonuclease activity
		PB1-F2[(b)]	87	10.5	-	2,650	Induction of apoptosis of CD8 T-cells and alveolar macrophages; prolongs viral polymerase activity in infected epithelial cells

a) The lengths of the HA and NA genes differ among strains
b) Not encode by all influenza A viruses; NA, not applicable

Copyright by Mahidol University

Table 3.1 Influenza A virus genome RNA and protein coding assignments (Adapted from Cox *et al*., 2010) (cont.)

RNA segment	Nucleotides[(a)]	Encoded polypeptide	Amino acids	Molecular weight (kDa)	Carbohydrates	Approximate copy no. per virion	Functions
3	2,233	PA	716	85	-	30-60	Component of RNA transcriptase complex; required for replication; active in viral RNA synthesis
4	1,778	HA	566	63	+	500	Surface trimer glycoprotein cleaved into HA1 and HA2; major antigenic determinant; functions in virus binding to cell surface receptors and fusion; lipid raft association of HA is essential for viral replication
5	1,565	NP	498	56	-	1,000	Associated with RNA segments to form ribonucleoprotein (vRNPs)

a) The lengths of the HA and NA genes differ among strains

Copyright by Mahidol University

Table 3.1 Influenza A virus genome RNA and protein coding assignments (Adapted from Cox *et al*., 2010) (cont.)

RNA segment	Nucleotides[(a)]	Encoded polypeptide	Amino acids	Molecular weight (kDa)	Carbohydrates	Approximate copy no. per virion	Functions
6	1,413	NA	454	60	+	100	Surface tetramer glycoprotein; neuraminidase activity; function in viral release; function in enhancement of HA mediated cell-cell fusion and virus entry
7	1,027	M1	252	27	-	3,000	Major protein of virion; interacting with vRNPs and NEP; viral uncoating, assembly and budding
		M2	97	14	-	20-60	Coded by spliced mRNA; ion channel activity; target of adamantanes. The M2 cytoplasmic tail and amphipathic helix domain may play role in viral assembly and budding; macroautophagy formation

a) The lengths of the HA and NA genes differ among strains

Copyright by Mahidol University

Table 3.1 Influenza A virus genome RNA and protein coding assignments (Adapted from Cox *et al*., 2010) (cont.)

RNA segment	Nucleotides[(a)]	Encoded polypeptide	Amino acids	Molecular weight (kDa)	Carbohydrates	Approximate copy no. per virion	Functions
8	890	NS1	230	26	-	NA	Non-structural protein; inhibits mRNA transport from nucleus; interferon antagonist; important for evasion of host immunity
		NS2 (NEP)	121	14	-	130-200	Coded from spliced mRNA; viral nuclear export protein

a) The lengths of the HA and NA genes differ among strains

Copyright by Mahidol University

3.2.2 Replication cycle of an influenza virus (Figure 3.7)

The trafficking and processing steps that occur in infected cells with influenza virus play a crucial role in the outcome of the infection. These steps are targets for vaccines, anti-viral drugs and therapeutic antibodies.

3.2.2.1 Entry to the host cells (from attachment to uncoating)

Influenza A virus infects cell through binding of the viral surface glycoprotein HA to the sialic acid receptors on the host cell surface. Human influenza viruses recognize the α(2,6) linkage of the receptor, while avian influenza viruses recognize the α(2,3) linkages. Both receptors appear in pig which explains the importance of the animal as a good mixing vessel for avian and human influenza viruses, consequently producing dangerous pathogenic viruses (Roger *et al*., 1983; Skehel *et al*., 1982). Upon binding to the host cell sialic acid residues, receptor-mediated endocytosis occurs *via* clathrin-dependent and dependent-mechanism (Rust *et al*., 2004), then the virus enters the host endosome. The low pH of the late endosome triggers a conformational change in the cleavage-active HA molecule (Skehel *et al*., 1982) that leads to fusion of the viral and the endosomal membranes. The low pH also triggers the flow of protons into the virus *via* the M2 ion channel. Opening the M2 ion channels acidifies the viral M1 protein for dissociating the vRNPs into the host cell cytoplasm (Pinto *et al*., 1992).

3.2.2.2 Import the vRNPs into the nucleus

Influenza viral transcription and replication occurs in the nucleus after the vRNPs enter the nucleus. The vRNPs are imported to the nucleus by nuclear localization signals (NLSs) on NP protein and all three polymerase proteins (Whittaker *et al*., 2000). The NLSs can bind to the cellular nuclear import machinery *via* the CRM1-dependent pathway mediating vRNP entering into the nucleus (Boulo *et al*., 2007).

3.2.2.3 Viral transcription and translation

In the host nucleus, the influenza viral polymerase initiates viral mRNA synthesis with 5'capped RNA fragments cleaved from host pre-mRNAs. The PB2 subunit binds the 5'cap of host pre-mRNAs (Ulmanen *et al*., 1981) and the endonuclease domain in PB1 subunit cleaves the pre-mRNA 10-13 nucleotides downstream from the cap (Plotch *et al*., 1981). Viral mRNA transcription is

subsequently initiated from the cleaved 3’ end of the capped-RNA segment (Plotch *et al*., 1981; Hagen *et al*., 1994). Then viral mRNAs are transported to the cytoplasm for translation into viral proteins. The surface proteins HA, NA and M2 are processed in the endoplasmic reticulum (ER), glycosylated HA and NA in the Golgi apparatus and transported to the cell membrane. At the same time, the NS1 protein of influenza A virus plays a role in suppressing the production of host mRNAs by inhibiting the 3’end processing of host pre-mRNA (Nemeroff *et al*., 1998; Shimizu *et al*., 1998), consequently blocking the production of host mRNAs, including interferon-β mRNAs. Unlike host pre-mRNAs, the viral mRNAs do not require 3’ end processing by the host cell machinery. Hence, the viral mRNAs are transported to the cytoplasm, while the host mRNA synthesis is predominantly blocked. In addition, the viral polymerase unprimed replication of vRNAs in step of negative-sense stranded vRNA transcription to complimentary RNA (cRNA), and using the cRNA as template to amplify negative-sense stranded vRNA for incorporating into new virion. The nucleoproteins are also required for these two steps of replication and are deposited on the cRNA and vRNA during RNA synthesis (Newcomb *et al*., 2009). The vRNPs are subsequently transported to the cytoplasm, mediated by a M1-NEP complex that is bound to the vRNPs.

3.2.2.4 Export the vRNPs from the nucleus

Following virus replication in the nucleus, the initial event for virus assembly is the export of the newly formed vRNPs out of the nucleus through the nuclear pores into the cytoplasm with the help of M1 and nuclear export protein (NEP) (O’Neill *et al*., 1998; Neumann *et al*., 2000) *via* the CRM1-dependent pathway.

3.2.2.5 Virion morphogenesis and budding at the host cell plasma membrane

Budding of new virions occurs at the apical side of polarized cells (Nayak *et al*., 2009) where the HA, NA and M2 are transported to this apical plasmid membrane. In brief, the HA and NA are targeted to lipid rafts, causing the clustering of HA and NA that leads to deform of the host cell membrane and initiates the virus budding event. Then M1 binds to the cytoplasmic tails of HA and NA where it can polymerize and forms the interior structure of the emerging virion. The HA and NA bound M1 serves as a docking site for recruitment of the vRNPs which can

Copyright by Mahidol University

mediate the recruitment of M2 to the site of virus budding. Thereafter, the M2 initially stabilizes the site of budding and helps in the polymerization of the matrix protein (M1) and the formation of filamentous virions (Rossman *et al.*, 2011).

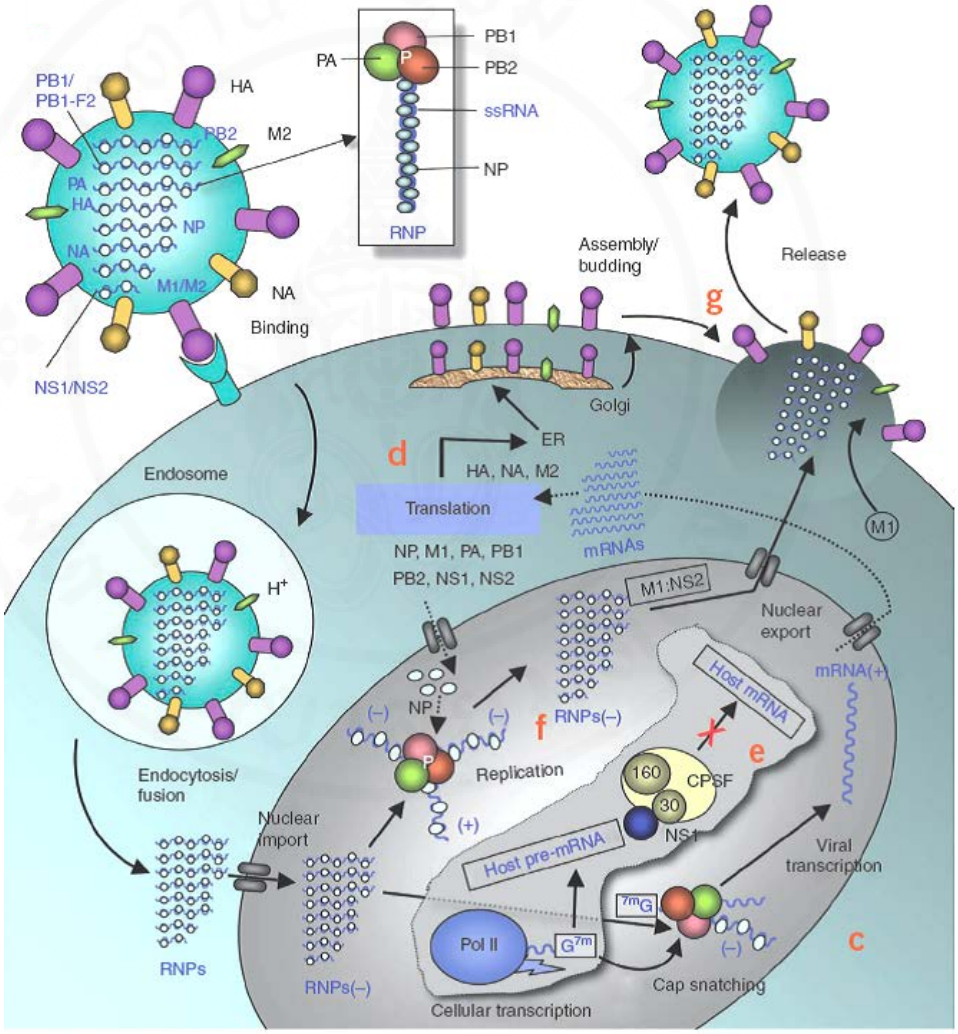

Figure 3.7 Schematic diagram of the influenza A virus life cycle
Source: Das K *et al.*, 2010

Copyright by Mahidol University

3.3 Surface proteins of influenza A virus

This thesis research focused has been made on three surface proteins of influenza virus, namely hemagglutinin (HA), neuraminidase (NA) and matrix-2 (M2) because they are vulnerable targets of anti-influenza agents. Detail attributes of these proteins are described:

3.3.1 Hemagglutinin (HA)

HA is the most abundant glycoprotein on the influenza viral surface. It is encoded by the fourth RNA segment which is the largest genomic segment of the virus. The HA forms homotrimer at the viral surface (**Figure 3.8**) and has functions in attachment and subsequent penetration of the virus into the host cell. Antigenicity of HA or H is subtype-specific and divided into 16 subtypes, H1-H16. Full length HA (called HA0) is folded into two distinct structural domains, *i.e*., globular head (HA1) and a fibrous stalk (HA2). The HA1 contains receptor-binding site which is surrounded by highly variable antigenic loop structures. The HA1 C-terminus contains cleavage site. The HA0 is cleaved at this site by proteases into HA1 and HA2. In virulent H5 and H7 avian influenza viruses, the cleavage site contains multiple basic amino acids which are the cutting site of intracellularly ubiquitous endogenous protease. The non-avian influenza A and non-influenza A viruses lack these multiple basic amino acids and HA0 cutting is done by extracellular proteases including tryptase, Clara and plasmin that are found in the host respiratory epithelial cells. The receptor binding specificity differs among influenza viruses. The avian viruses prefer the NeuAc α2,3 Gal linkage while human and classic H1N1 swine influenza viruses bind to the NeuAc α2,6 Gal linkage on the cell surface sialyl-oligosaccharides. After binding of the HA1 to the host cell receptor, the virus particle is endocytosed. Low pH in the late endosome induces a conformational change in the cleavage-active HA molecule and triggers HA-mediated membrane fusion by inserting a 38 residue fusion peptide in N-terminal of HA2 into the endosomal membrane. The HA2 of influenza A viruses is highly conserved (Sui *et al*., 2009) and plays important role in the HA-mediated membrane fusion **Figure 3.9**. Moreover, HA also has additional bio-activity in viral budding by serving as a docking site for the recruitment of the viral RNPs at cytoplasmic tail of the HA (Calder *et al.*, 2010).

Copyright by Mahidol University

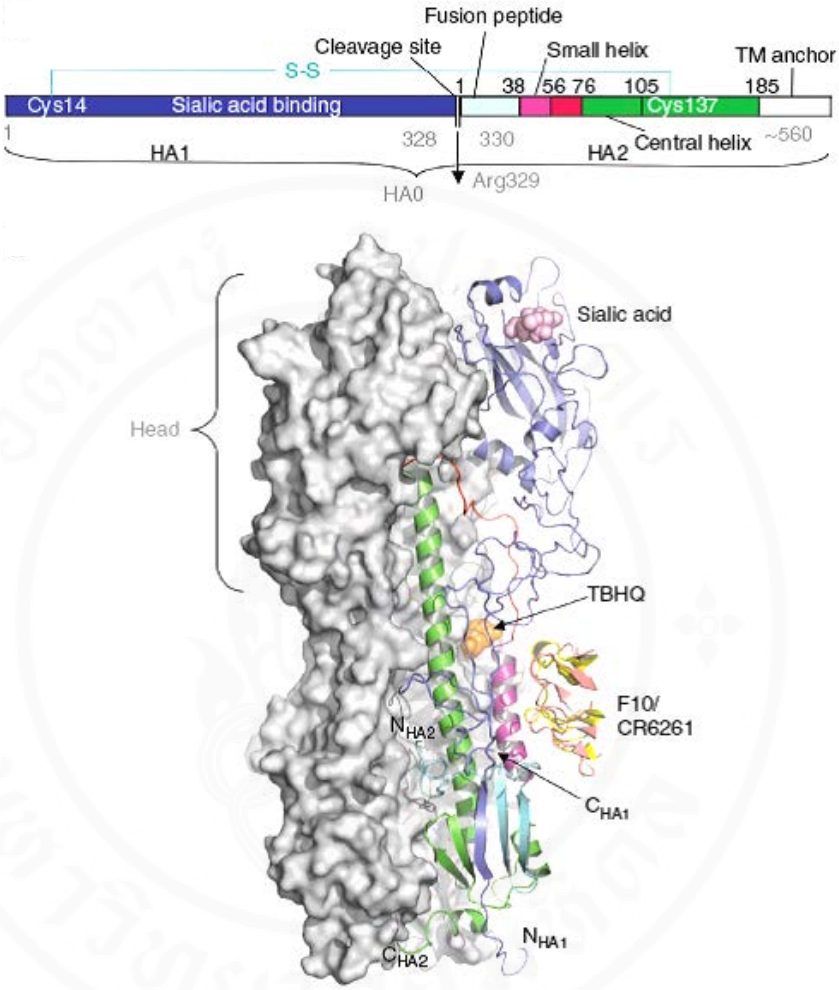

Figure 3.8 Schematic diagram of a hemagglutinin molecule of an influenza virus
Source: Das *et al*., 2010

Copyright by Mahidol University

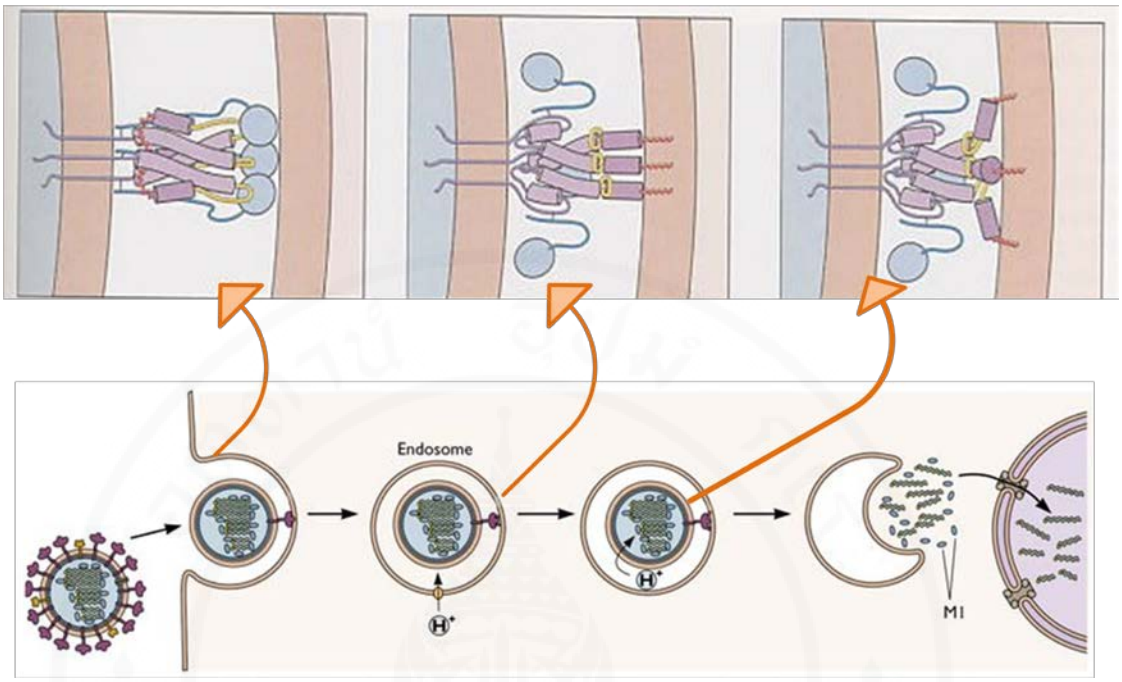

Figure 3.9 Hemagglutinin functions during influenza virus entry. The viral spike or fusion protein (HA), recognizes the host cell (*via* binding to sialic acid) and enters the endosome of the cell, where low pH triggers a conformational change in HA to expose the viral fusion peptide which inserts into the host cell membrane to initiate the process of membrane fusion and the delivery of the viral genome into the cytoplasm.
Source: Modified from Carr and Kim, 1994

3.3.2 Neuraminidase (NA)

NA is one of the two major glycoproteins on the influenza viral surface. It is encoded by the sixth segment of the influenza vRNA genome. NA protein forms homotetramer on the viral envelope. The tetrameric NA protein (**Figure 3.10**) is a type II glycoprotein (N-terminus is inside and C-terminus is outside the virion) (Air and Laver, 1989). NA composes of three major parts: box-shaped head, stalk, and cytoplasmic tail. The box-shaped head comprises four co-planar and roughly spherical subunits with the enzymatic activity at the center. NA is subdivided into 9 antigenic subtypes (N1-N9). The enzyme active-site forms a large pocket on the distal surface which is strictly conserved in all NA subtypes, and its function is the cleavage of the α-ketosidic linkage between a terminal sialic acid and adjacent sugar residues (Lenz *et*

Copyright by Mahidol University

al., 1987). Removal of sialic acid residues by the NA promotes both entry and release of influenza virus from infected cells (**Figure 3.11**). The NA has additional role in host range restriction because the avian NA (N3-N9) specific to substrate NeuAc α2,3 Gal but human NA (N1 and N2) specific to substrate NeuAc α2,6 Gal (Hinshaw *et al*., 1983). The stalk region is attached centrally to head and it is flexible in length and sequence. NA cytoplasmic region is highly conserved among all NA subtypes of influenza A viruses (Blok and Air, 1982). This region is important for incorporation of the NA into the virion but is not essential for virus replication (Bilsel *et al*., 1993; Garcia-Sastre and Palese, 1995). Recent study of the NA activity in influenza A virus life cycle showed that the NA protein of influenza A virus is not only required for virion release and spread but also plays a critical role in virion infectivity and HA-mediated membrane fusion (Su *et al*., 2009).

Copyright by Mahidol University

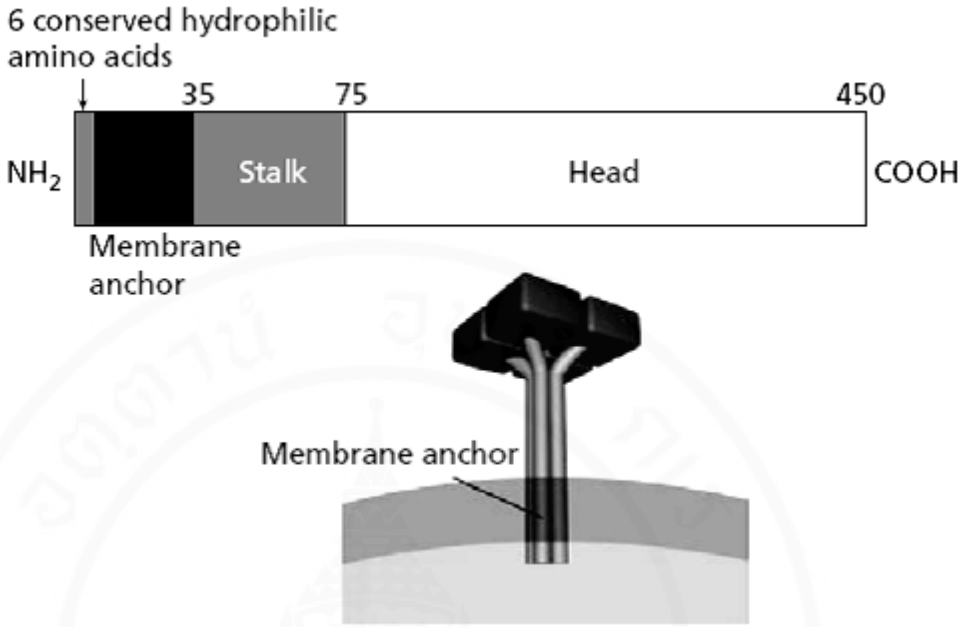

Figure 3.10 Schematic diagram of a neuraminidase molecule of influenza virus
Source: Cox *et al*., 2010

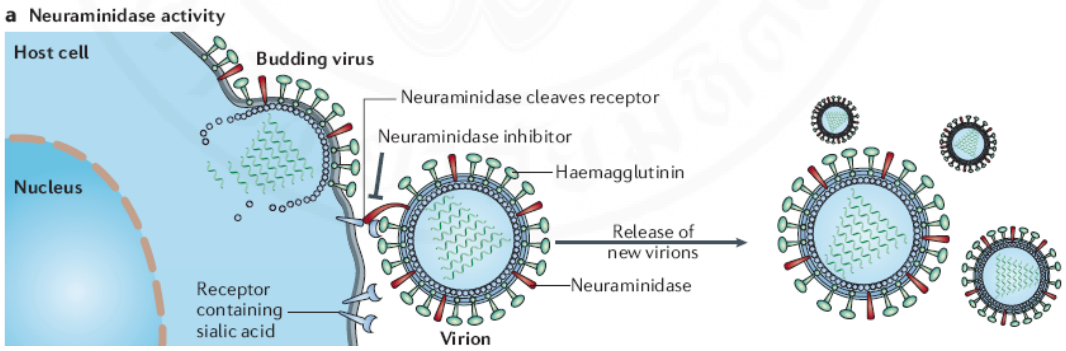

Figure 3.11 Mechanism of action of neuraminidase. This figure shows the action of neuraminidase in cleavage of sialic acid residues from hemagglutinin and promoting viral release.
Source: Moscona, 2005

Copyright by Mahidol University

3.3.3 Matrix-2 (M2)

The seventh RNA segment of influenza virus genome is bicistronic and encodes two functionally different proteins, M1 and M2. M2 protein has 97 amino acids that share 8 amino-terminal residues with M1 and followed by 88 residues in a +1 reading frame by being translated from a spliced mRNA (nt 1-26 at 5' end and nt 715-982 at 3' end) (Krung and Lamp, 1996). The M2 protein evolves slowly when compared to HA and NA (Ito *et al.*, 1991) and is also relatively conserved among the influenza A viruses. M2 protein is type III transmembrane protein (single pass-transmembrane protein that N-terminus is outside and the transmembrane domain is located close to the N-terminus of the protein and functions as an anchor) of a class IA viroporin family (Nieva *et al.*, 2012). The M2 molecule forms homotetramer by two disulfide bond linkage of cysteine residues in order to acts as selective ion channel on viral membrane (**Figure 3.12**). Each M2 molecule comprises different domains: N-terminal ectodomain (M2e; 25 residues; 1-25), transmembrane domain (21 residues; 26-46), amphipathic helix (16 residues; 47-62) and C-terminal (35 residues; 63-97) (Schnell *et al.*, 2008; Rossman and Lamb, 2011). Large numbers of M2 homotetrameric molecules are present on infected cell surface with ratio approximately two M2 molecules per one HA trimer on CV-1 cells (Lamb *et al*., 1985), but appear only few (about 23-60 molecules) on the virion (Zebedee *et al*., 1988). At the early phase of infection, the M2 protein functions as a pH-activated ion channel that allows protons to enter the virion during uncoating for dissociating vRNPs from M1 and releasing them to cytoplasm for further replication in nucleus (Helenius, 1992). The ion channel is regulated by His-37 as sensor and Trp-41 as gate. In the late phase of infection, M2 also functions as ion channel for prevention of acid-induced conformational changes of intracellularly cleaved HA (H5 and H7) in trans-Golgi network of newly synthesize HA (Sugrue *et al*., 1990) (**Figure 3.13**). Recently, M2 was found to block fusion of autophagosomes to lysosomes and inhibit autophagy causing accumulation of the autophagosomes (formation of macroautophagosome) which compromised virus infected cell survival (Gannage *et al*., 2009) (**Figure 3.14**). Moreover, M2 plays an important role in virus morphogenesis and assembly by acting as cofactor in virus budding where it interacts with M1 to determine virus morphology- spherical or filamentous (Lamb and Rossman, 2011). After that, M2

amphipathic helix alters membrane curvature at the neck of the budding virion causing membrane scission and the virus release (Lamb and Rossman, 2011) (**Figure 3.15**). Because of highly conserved in amino acid sequence and the multiple pivotal functions in the influenza virus infectious cycle, M2 has been an attractive target of anti-influenza agents. Previous studies on M2 were focused on the extracellular domain of M2 (M2e) and the transmembrane helices which forms ion channel have been interested. For examples, M2e was used as a component of a broad-spectrum anti-influenza vaccine and M2e-specific monoclonal antibody to mice accelerated the lung viral clearance following a sublethal influenza A virus infection (Treanor *et al*., 1990). Single domain antibody (V_HH) blocked the M2 ion channel activity and neutralized influenza virus infection in mice (Wei *et al*., 2011). Emerging of drug resistant viruses render a failure of adamantane drug family which block M2 ion channel in treatment of influenza (Sheu *et al*., 2011).

Copyright by Mahidol University

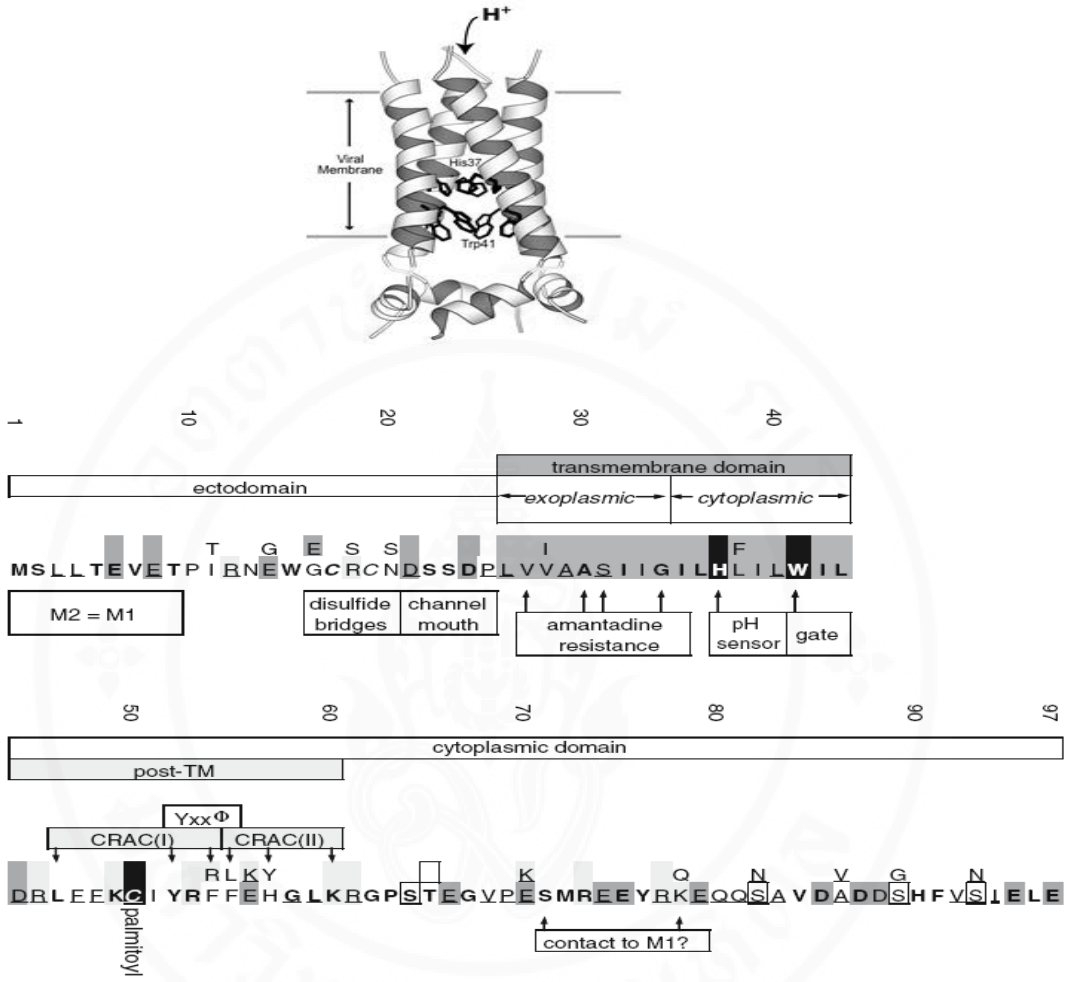

Figure 3.12 Schematic diagram of an M2 molecule of influenza virus

Source: *Viral Membrane Proteins: Structure, Function, and Drug Design*, edited by Wolfgang Fischer. Kluwer Academic / Plenum Publishers, New York, 2005.

Copyright by Mahidol University

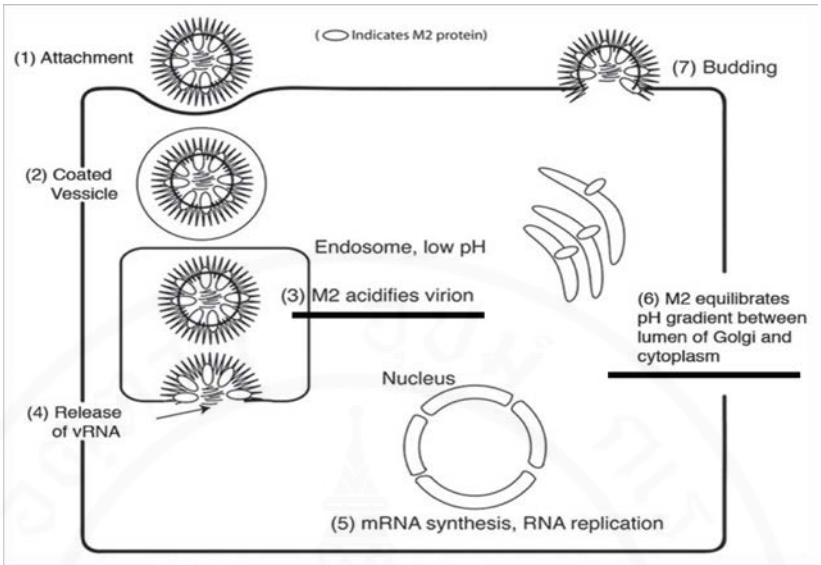

Figure 3.13 M2 protein acts as an ion channel for proton influx into the intra-endosomal virion for dissociating vRNPs from M1 and release them to cytoplasm and prevention of acid-induced conformational changes of intracellularly cleaved HA of H5 and H7 in trans-Golgi network of newly synthesize HA

Source: Kelly *et al.*, 2003

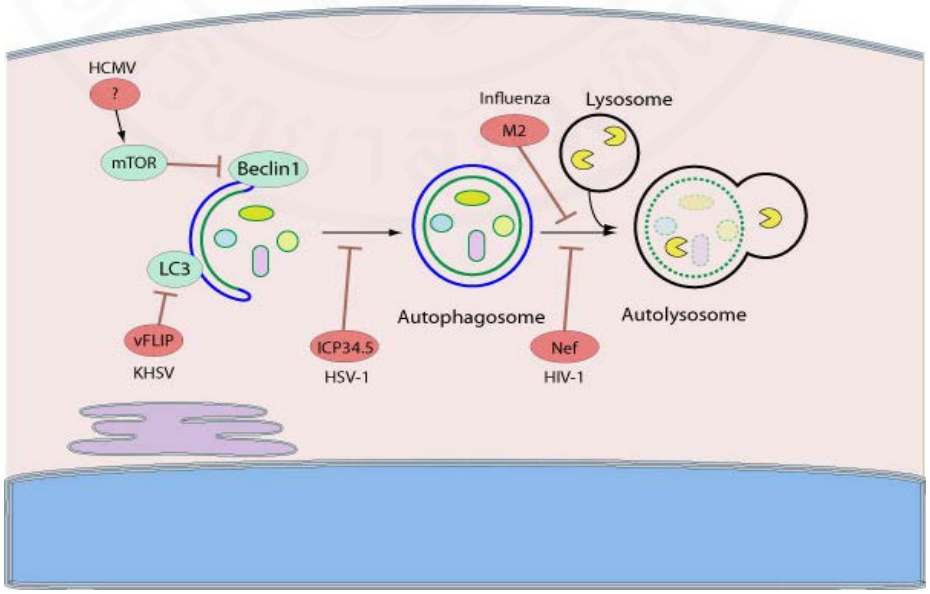

Figure 3.14 M2 function in blocking autophagosome maturation by preventing fusion with the lysosome.

Source: Gannage *et al.*, 2009

Copyright by Mahidol University

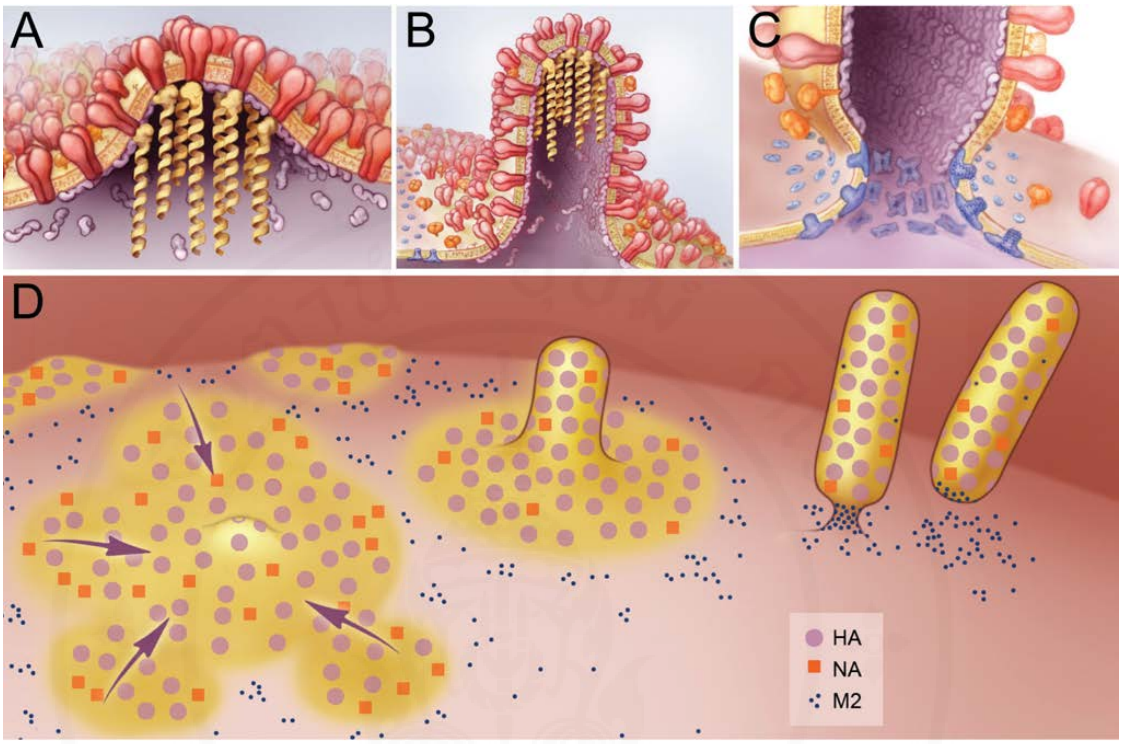

Figure 3.15 Model of influenza virus budding. **A**, The initiation of virus budding caused by clustering of HA (shown in red) and NA (shown in orange) in lipid raft domains. M1 (shown in purple) is seen binding to the cytoplasmic tails of HA and NA and serves as a docking site for the vRNPs (shown in yellow). **B**, Elongation of the budding virion caused by polymerization of the M1 protein, resulting in a polarized localization of the vRNPs. M2 (shown in blue) is recruited to the periphery of the budding virus though interactions with M1. **C**, Membrane scission caused by the insertion of the M2 amphipathic helix at the lipid phase boundary, altering membrane curvature at the neck of the budding virus and leading to release of the budding virus. **D**, Overview of the budding of influenza viruses, showing the coalescence of HA and NA containing lipid rafts (shown in yellow), the formation of a filamentous virion and membrane scission caused by M2 clustered at the neck of the budding virus.

Source: Lamb and Rossman, 2011

Copyright by Mahidol University

3.4 Vaccines against influenza

Current influenza vaccines for human use are divided into two main types. The first type contains either inactivated (killed) whole virus-, split product- or subunit-vaccines. The second type is live-attenuated vaccine for intranasal administration. All vaccines are still produced by growing viruses in allantoic sacs of embryonated chicken eggs. Several strategies have to be used in the vaccine production line, *e.g*., to get as high as possible the virus yield and purity (elimination of as much as possible the egg proteins). The seasonal influenza vaccines are trivalent containing antigen from each three strains selected for that particular year. Two vaccine strains are type A -H1N1 and -H3N2, and one influenza B strain. The vaccines are protective only against the naturally occurring outbreaks of the year and do not cross-protect against pandemic from unexpected new strain and subtype.

3.5 Drug therapy of influenza virus infection

Presently, there are two families of anti-influenza drugs: the adamantanes and the neuraminidase inhibitors (Fiore *et al*., 2011). These drugs must be taken at the early phase of infection for high therapeutic effectiveness (Jefferson *et al*., 2012). Influenza viruses that resist both families of the anti-viral drugs have emerged continuously and cause influenza treatment failure (Sheu *et al*., 2011).

3.5.1 The adamantanes

The adamantanes (amantadine and rimantadine) are the first family of pharmacologic agents for treatment of influenza. They are effective in interfering replication cycle of all subtypes of influenza A viruses but not type B viruses (van Voris and Newell, 1992; Hayden, 1996). Both drugs are effective when given within 48 hours of the disease onset. Besides, they cause central nervous system involved side-effects. The antiviral activity of both of these compounds is mediated by blocking the ion channel activity of influenza A viruses. Amantadine obstructs the ion channel pore by binding to Ser^{31} and the surrounding Val^{27}, Ala^{30} and Gly^{34} of the M2 protein (Stouffer *et al*., 2008) while rimantadine binds to the gate at a lipid facing pocket of the channel formed by Trp^{41}, Ile^{42}, and Arg^{45} from one transmembrane helix and

Copyright by Mahidol University

Leu^{40}, Leu^{43}, and Asp^{44} of the nearby helix (Schnell and Chou, 2008). Resistance to the drugs has occurred in > 98% of transmissible A/H1N1, A/H3N2, A/H5N1 and A/H7N9 subtypes by mutations, most frequently S31N and less so V27A and L26F (Layne *et al*., 2009; Balgi *et al*., 2013; Hu *et al*., 2013). The mutations cause failure of ion channel blocking by amantadine and ineffective fitting of rimantadine into the channel pocket due to the weakness of the TM helix packing (Pielak *et al*., 2009). Several compounds that are potent inhibitors of V27A and L26F mutants have been produced and tested (Balannik *et al*., 2009). However, effective inhibitor of S31N mutant has not been found (Du *et al*., 2012).

3.5.2 The neuraminidase inhibitors

The neuraminidase inhibitors, *i.e.*, inhaled zanamivir (Relenza™) and oral oseltamivir (Tamivir™), block the enzymatic active site of the NA resulting in inhibition of release of influenza virus progeny from infected host cells. This process prevents infection of new host cells and consequently slowing down the spread of infection in the respiratory tract. The neuraminidase inhibitors are effective against both influenza A and B viruses (Hayden *et al*., 1999). Nevertheless, they must be administered as early as possible. When administered within two days of the illness onset to healthy adults, both drugs can reduce the duration of uncomplicated influenza A and B illness by approximately one day, compared with placebo (Hayden *et al*., 1999; Makela *et al*., 2000; Demichelli *et al*., 2000). Recently, a rise in resistance to the oseltamivir, due to the H275Y mutation (H274Y in N2 numbering) in the NA, was reported among seasonal influenza A (H1N1) viruses in 2007-2008 (Sheu *et al*., 2008; Lackenby *et al*., 2008). Prevalence of oseltamivir-resistant influenza A (H1N1) viruses increased to approximately 100% in many countries during 2008-2009 (Lackenby *et al*., 2008).

The evidence of drug resistance in influenza A viruses indicates that anti-viral drugs might be less useful than anticipated if resistant of influenza A viruses become more prevalent and the virus gains the ability to pass easily from person to person. The incidence of anti-viral drug resistance indicates that the strategy for the treatment of influenza should include additional/new pharmacological agents or the sole alternatives.

Copyright by Mahidol University

3.6 Antibody for treatment of influenza

3.6.1 Antibodies for neutralizing influenza virus infectivity

The antibody response is important for preventing influenza A virus infection and also help to resolve the infection. After being infected with influenza virus, antibodies are produced against many epitopes on multiple virus proteins. Some antibodies can block virus infection by a process that is called *"neutralization"*. The processes that antibodies neutralize viruses are shown in **Figure 3.16** (Lambert *et al*., 2010). First, some of neutralizing antibodies can interfere with virion binding to host cell receptor by attaching to- or sterically hinder of- HA1 in the parts that help in binding to receptor site. Second, some of them can bind to HA2 portion for inhibition of conformational change in HA that leads to inhibition of fusion of viral and endosomal membranes (prevent uncoating). Third, binding of antibodies to M2 may lead to prevention of disassociating of the vRNPs from M1. Forth, the antibodies specific to the virus surface exposed proteins can cause aggregation of virus particles that prevent of infection and/or spreading.

Recently studies have shown that during influenza virus infection, cellular membrane has increased permeability (Gonzalez and Carraso, 2003; Wang *et al*., 2010) allowing small anti-influenza agent including antibody fragments such as ScFv to become accessible to the intracellular targets. Thus, the antibodies may confer benefit to the host either as a sole therapeutic or adjunct anti-influenza agent.

3.6.2 Antibody therapy for influenza

Antibody has been used with success for influenza treatment. Examples are: the use of human blood product from patients recovering from Spanish flu for treatment of influenza in human (Luke *et al*., 2006). Convalescing plasma could rescue patient infected with drug escape H5N1 virus mutant (Zhou *et al*., 2007). The use of specific monoclonal antibody produced from immune B cells of immunized mice for treatment of influenza in mice (Smirnov *et al*., 2000; Renegar *et al*., 2004). The used of humanized and horse derived $F(ab)'_2$ fragments specific to H5N1 for treatment of infected mice (Hanson *et al*., 2006; Lu *et al*., 2006). Human monoclonal single chain antibodies (HuScFv) specific to HA of H5N1 virus could rescue mice

from lethal infections with homologous and heterologous H5N1 strains (Maneewatch *et al*., 2009). Using of single domain antibody (V_HH) blocked the M2 ion channel activity and neutralized influenza virus infection in mice (Wei *et al*., 2011). Passively transferred M2e-specific monoclonal antibody to mice caused acceleration of the lung viral clearance (Treanor *et al*., 1990). Antibody therapy is not only safe (when human or humanized antibodies are used) but also the antibodies are highly tolerable to mutation of the viral target than small molecule drugs (Kim and Toge, 2004).

Copyright by Mahidol University

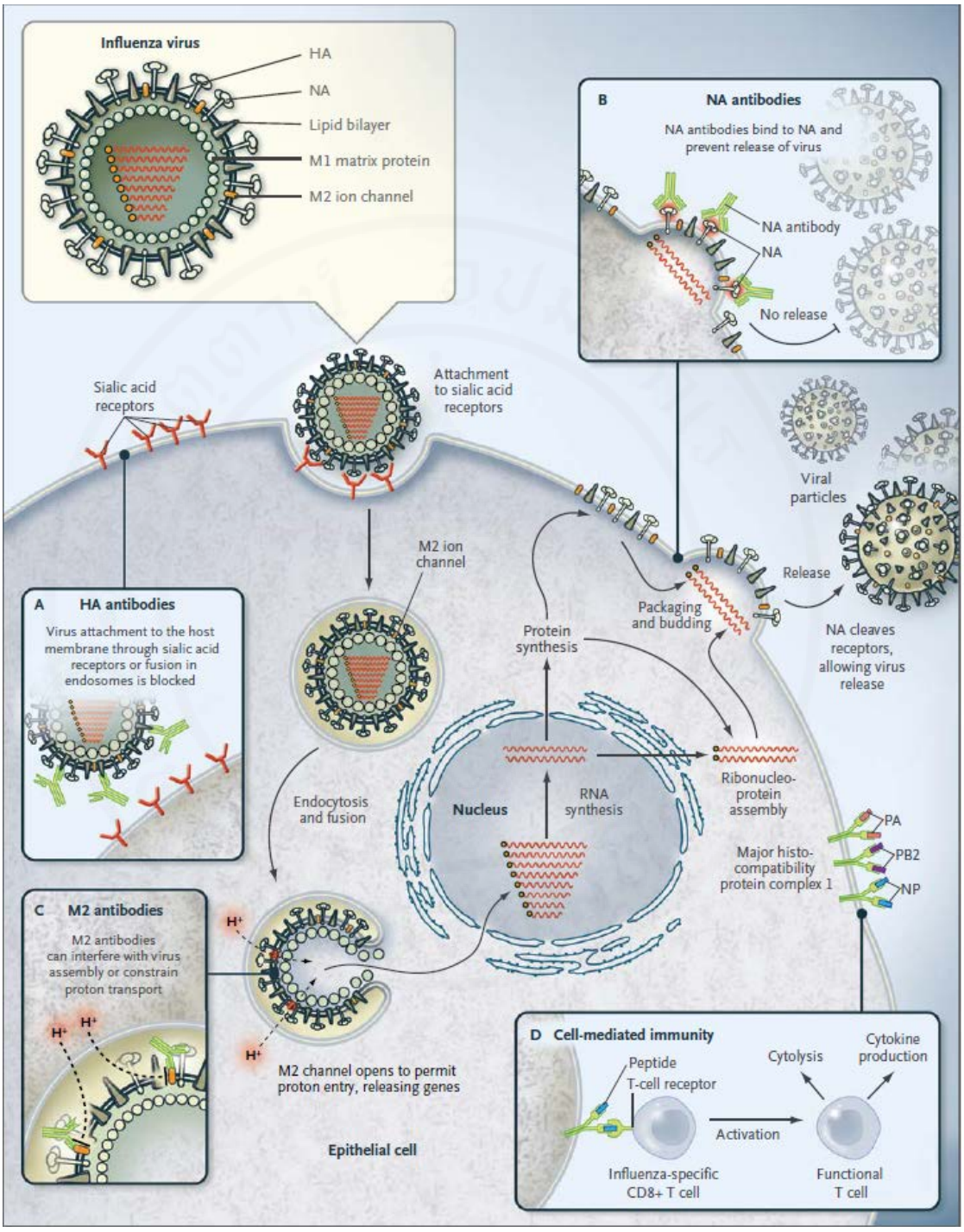

Figure 3.16 Structure and replication cycle of influenza A virus and neutralizing antibodies for influenza viruses (shown in block **A, B** and **C)**

Source: Linda *et al*., 2010

Copyright by Mahidol University

3.7 Therapeutic antibody

Antibody has been used for treatment and intervention of disease/infection since the early 1900s even before the discovery of the antibacterial activity of the first antibiotic, penicillin. Moreover, antibody has been used as novel therapeutic agents for treatment of cancer, autoimmune diseases, and inflammations for more than 30 years (Brekke and Sandlie, 2004). Because of their high affinity and specificity for binding to their antigenic targets which involve several contact residues, most antibodies can cope up with pathogens that resist the pharmacologic drug by means of their single or multiple point mutation(s) (David *et al*., 1996). Nowadays, antibody of various formats can be designed and produced by engineering of the molecule genetically to achieve the desired specificity. Fully-human or humanized-animal antibody molecules for use in human recipient can be produced readily *in vitro* without the prolonged *in vivo* immunization. **Figure 3.17** illustrates several formats of the human therapeutic antibodies.

3.7.1 Recombinant antibodies

Hybridoma technology invented by Kohler and Milstein in 1975 has been used for production of monoclonal antibody (MAb), usually of murine origin, for biological, bio-medical and therapeutic purposes. The MAb of the desired characteristics, *e.g.*, high specificity and affinity to the target antigen can be produced. However, immunotherapy using passively given mouse MAb to the human recipients has limitations. The mouse protein/antibody is foreign to the human immune system and human anti-mouse antibody (HAMA) is produced by the human recipient which causes adverse sequel such as anaphylaxis and serum sickness (Khazaeli *et al*., 1994). Therapeutic antibody with minimal or no immunogenicity is needed for human therapy. The first attempt to reduce the mouse MAb in human was to produce human-mouse chimeric monoclonal antibody by molecular linking the antigen-binding fragment (Fab) encoding gene from the mouse hybridoma to human fragment crystallizable (Fc) coding sequence; the engineered antibody is called chimeric antibody (Morrison *et al*., 1984). The chimeric antibody retains original specificity of the mouse antibody but the Fc-mediated functions, *e.g.*, complement fixation and opsonization, are attributable to the adjoined human Fc. However, the recombinant

Copyright by Mahidol University

chimeric antibody is still immunogenic in human because about half of the molecule remains murine. For further reduction of the mouse monoclonal antibody immunogenicity in human, the mouse single chain antibody fragments (ScFv) consisting of mouse VH-linker-VL was used in human therapy when the *in vivo* bio-functions of the Fc is not required. Nevertheless, ScFv still contains mouse immunoglobulin frameworks (FRs) which can induce human anti-mouse protein response. This obstacle was eliminated subsequently by replacing the mouse immunoglobulin frameworks (FRs) with the human immunoglobulin FRs by molecular grafting all of the mouse CDR sequences onto the most matched human FRs; the process which is called "Humanization" (Reichmann *et al*., 1988). In addition, fully human monoclonal antibody can be produced by several strategies nowadays such as by using transgenic animals that carry human immunoglobulin transgenes, Epstein-Barr virus transformed antigen specific B cells, and antibody display technology including cell, ribosomal or phage. For the human antibody phage display system, a collection of human immunoglobulin genes isolated from B lymphocytes of multiple donors can be cloned into display phagemid vector (called human antibody phage display library) (Kulkeaw *et al*., 2009). Fully human monoclonal antibody can be produced in any of the desired formats including full-size molecule (whole IgG), bivalent or monovalent antigen binding fragments [F(ab)'$_2$ or Fab], single-chain variable fragment (VH-linker-VL; ScFv) or single domain antibody molecules (VH/V_HH/VL) (Nelson and Reichert 2009; Thanongsaksrikul *et al*., 2010; Thueng-in *et al*., 2012).

Copyright by Mahidol University

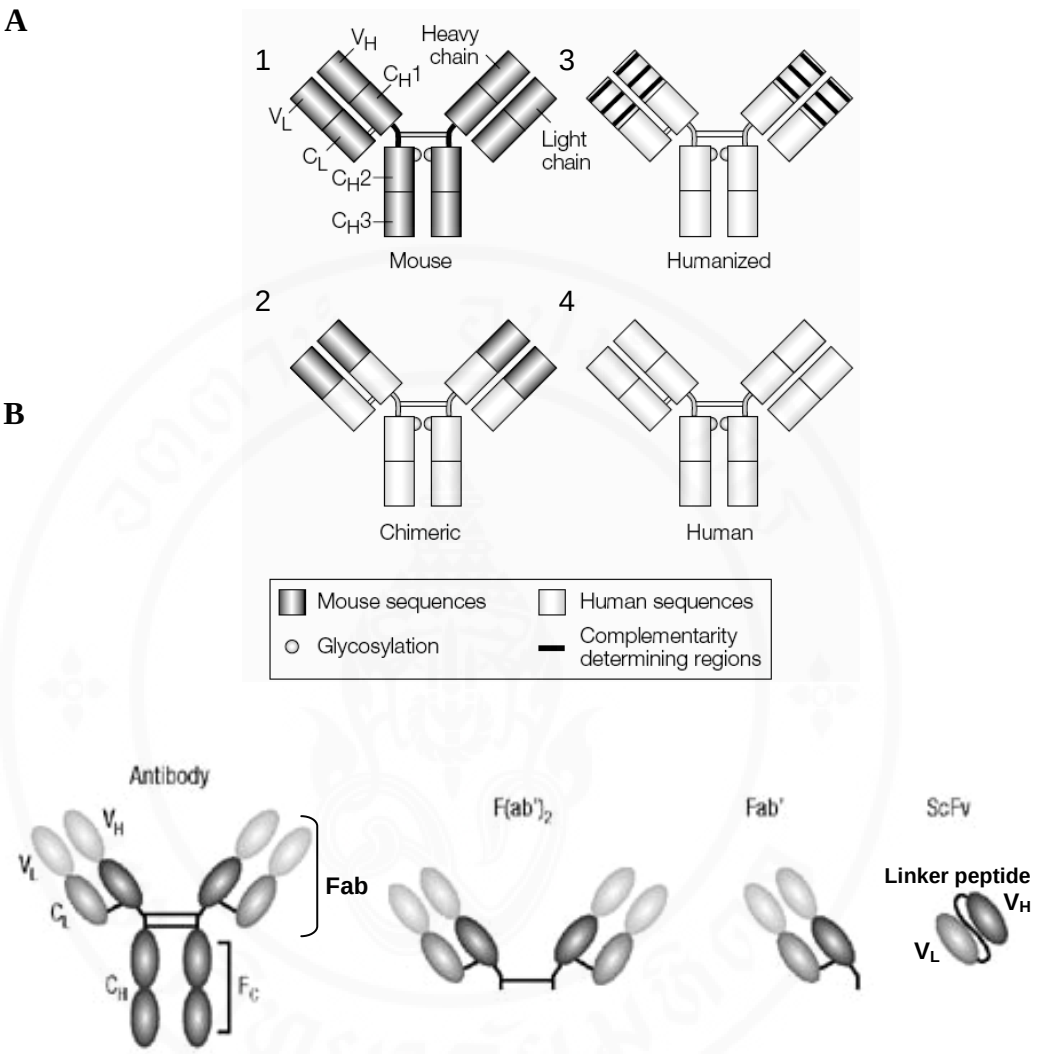

Figure 3.17 Schematic structures of monoclonal antibodies and antibody fragments.
A, Structures of full-size murine (panel 1), chimeric (panel 2), humanized- (panel 3), and human (panel 4) monoclonal antibodies
B, Structures of recombinant monoclonal antibody fragments. VL, variable domain of light chain; VH, variable domain of heavy-chain; CL, constant domain of light chain; C1, constant domain-I of heavy chain; CII, constant domain-I of heavy chain; Fab, antigen-binding fragment; Fc, fragment crystallisable; ScFv, single-chain variable fragment(s)
Source: www.nature.com
(Accessed on Jan 20th, 2012)

Copyright by Mahidol University

3.7.2 Phage display technology for antibody production (Figure 3.18)

A vast diversity of antibody gene repertoire which is generated by combinatorial immunoglobulin gene rearrangement made up to 10^{10} of antigen-binding site diversity (Goldsby *et al*., 2003). This antibody gene repertoire can be generated *in vitro* by cloning of the immunoglobulin genes from B cells of donors such as humans or animals with or without immunization, into bacteriophages (phages in short) to construct antibody phage display library (McCafferty *et al*., 1997). The antibody phage display technology allows convenient determination of direct interaction between displayed antibodies on the phage surface with their specific target molecules that mimics clonal selection process *in vivo* (Winter *et al*., 1994). In recombinant antibody phage display library, the antibody molecule is displayed on the surface of phages, usually filamentous phages such as M13. Antigen-specific phages can be selected from the library by "biopanning" process. The desired antigen that immobilized on a solid phase will trap the specific phages by association with the displayed antibody molecule while the unbound phages removed. These antigen-bound phages can be either subjected to further multiple rounds of biopanning in order to enrich high affinity binders or proceed to infecting bacteria host (Winter *et al*., 1994; Kulkeaw *et al*., 2009). After infecting appropriate bacteria, the soluble recombinant antibody molecules can be produced by the bacteria grown under appropriate induction condition.

Copyright by Mahidol University

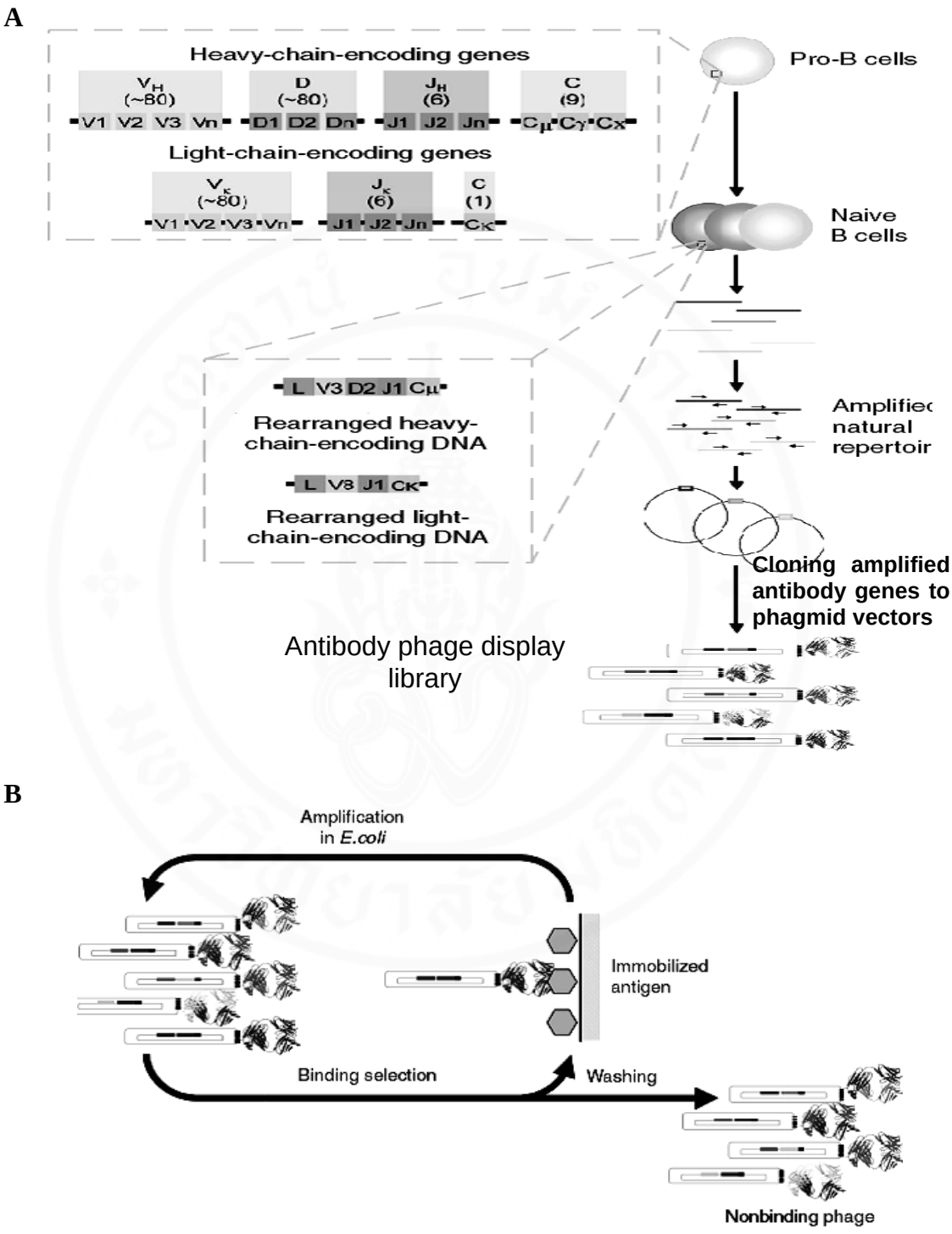

Figure 3.18 Schematic diagrams for construction of antibody phage display library **(A)** and selection of antigen specific phage by bio-panning **(B)**

Source: Sidhu and Fellouse, 2006

Copyright by Mahidol University

CHAPTER IV
MATERIAL AND METHODS

4.1 Influenza A viruses

The influenza viruses used in this study are listed in **Table 4.1**. They were propagated in 8-10 day old embryonated chicken eggs. The allantoic fluids containing living viruses were collected, pooled, filtrated through 0.2 µM membrane (Pall, Michigan, USA) and kept in small aliquots at -80 ºC. Virus titers were determined by hemagglutination (HA) assay against 1% erythrocytes according to WHO protocol. Optimal multiplicity of infection (MOI) was calculated from titration of 50% tissue culture infected dose (TCID50) which were performed in Mardin-Darby canine kidney (MDCK) cells grown at 37 ºC under 5% CO_2 atmosphere in viral growth medium [DMEM (Invitrogen, Michigan, USA) containing 2% FBS, 2 mM L-glutamine, penicillin (100 U/mL), streptomycin (100 µg/mL)] (Groves *et al*., 1973; Wang, 2011; Carrasco, 1978; WHO manual, 2002).

4.1.1 Hemagglutination (HA) assay

Hemagglutination unit [HAU; the smallest amount of the virus that gave 100% agglutination of the red blood cells (human group O red blood cells for human influenza viruses and goose/chicken red blood cells for avian influenza viruses; recommended by WHO manual, 2002)] of individual influenza A viruses were determined. Serial dilutions of individual virus preparations were prepared in V-bottom microtiter plate (Greiner Laboratories, Alphen, The Netherlands) (25 µl/well); control well was added with only 25 µl PBS, pH 7.4 (without virus). Then 50 µl of 1% red blood cells (RBC) in PBS were added to mix with the virus. The plate was kept at 25 ºC until the red blood cells in the control well (containing only red blood cells and PBS) set as a button at the well bottom. The hemagglutination titer of each virus preparation was determined. The HA titer was the highest dilution of the virus preparation that could agglutinated 100% of the RBC in the well and one HAU was

Copyright by Mahidol University

the smallest amount (highest dilution) of the virus which could agglutinate 100% of the RBC.

4.1.2 Tissue culture infected dose-50 (TCID 50) and multiplicity of infection (MOI)

Optimal multiplicity of infection (MOI) was calculated from titration of 50% tissue culture infected dose (TCID50) which were performed in MDCK cells before keeping the virus preparations in small aliquots at -80 ºC.

4.1.2.1 Preparation of MDCK cell monolayer

Monolayer of MDCK cells were established in DMEM supplemented with 10% FBS, 100 µg/ml streptomycin and 100 units/ml penicillin. The cells were grown at 37 ºC in a humidified 5% CO_2 incubator.

4.1.2.2 Infection of MDCK cell monolayer with influenza A virus

MDCK cell monolayer at 80% confluent growth were prepared as described in **section 4.1.2.1** in 96-well tissue culture plates (Costar®, New York, USA). Cells were rinse twice with plain DMEM before added with 100 µl of undiluted or tenfold serial dilutions in plain DMEM of individual influenza viruses (for human influenza virus, TPCK-trypsin solution at 2 µg/ml final concentration was added in all media for cleaving hemagglutinin in order to help the virus infection) and the cellular entry was allowed at 37 ºC for 1 hour for avian influenza viruses and 2 hours for human influenza viruses. Cells incubated with DMEM instead of the virus were used as non-infected control. The supernatant was removed and 150 µl of viral growth medium were added. Cells were grown further at 37 ºC in humidified 5% CO_2 incubator for 24 hours.

4.1.2.3 Plaque (foci) formation assay for determination of $TCID_{50}$ and MOI of viruses

Infected cells in each tissue culture well from **section 4.1.2.2** were washed with PBS, fixed with cold absolute methanol at 25 ºC for 1 hour, washed again, and permeabilized by using 0.3% Triton X-100 in PBS for 20 minutes. The cells were blocked by incubating with 3% FBS at 25 ºC for 1 hour. After washing, mouse polyclonal antibody (PAb) to recombinant NP protein (1:1,000) from **section**

4.4 was added and incubated at 25 ºC for 1 hour. Goat anti-mouse-alkaline phosphatase (AP) conjugate (Southern biotech, Alabama, USA) (1:3,000) was added, incubated at 25 °C for 1 hour and the cells were equilibrated in 0.15 M Tris–HCl, pH 9.6, at 25 °C for 15 minutes before adding with BCIP/NBT substrate (KPL, Maryland, USA) for color development. When the purple foci appeared under inverted light microscope, the reaction was stopped by rinsing with distilled water. The foci in the MDCK cell monolayer were observed and counted under an inverted light microscope.

The $TCID_{50}$ was calculated from the plaque numbers by the Reed-Muench method (Reed and Muench, 1938) and MOI was calculated from $TCID_{50}$ by multiple with 0.69 (Carrasco, 1978; WHO, 2002).

Copyright by Mahidol University

Table 4.1 List of influenza viruses used in the study

Nomenclature	Subtype	Clade	Host	HA reciprocal titer	Reference/ accession number
A/duck/Thailand/144/2005*	H5N1	1	Duck	nd	Songserm *et al*., 2006
A/dog/Thailand-Suphanburi/KU-08/2004*	H5N1	1	Dog	256	DQ530170-7
A/chicken/Thailand/NP-172/2006**	H5N1	2.3.4	Chicken	32	DQ999872-3
A/Thailand/CU-H106/2009	H1N1 (pdm)		Human	128	GQ866928
A/Thailand/CU41/2006	H1N1 (seasonal)		Human	64	EU021246.1

nd, not determined; pdm, pandemic H1N1/2009 strain; *, adamantine resistance; **, adamantane sensitive (Pissawong *et al*., 2013)

4.2 Production and purification of recombinant H1 (HA0, HA1, and HA2), NA, M2 and NP proteins

4.2.1 Production and purification of recombinant H1 (HA0, HA1 and HA2)

4.2.1.1 Viral RNA extraction

Viral RNA was extracted from living influenza A/Thailand/CU41/2006 (H1N1) freshly collected from infected MDCK cells by using QIAamp MinElute Virus Spin kit (Qiagen, Hilden, Germany) according to the manufacturer's instruction in biosafety cabinet class II.

4.2.1.2 Synthesis of cDNA of influenza virus *h1*

The viral RNA was reverse-transcribed to cDNA by RevertAid^{TM} first strand cDNA synthesis kit (Thermo scientific, Massachusetts, USA) according to the manufacturer's instruction using Uni 12 primer (**Table 4.2**). Composition of the reaction mixture is shown below.

Ingredient	Volume (µl)
5x Reaction buffer	4.0
2.5 mM each dNTP mix	2.0
10mM Uni 12 primer	2.0
RevertAid^{TM} H minus M-MuLV reverse transcriptase (200 units/µl)	2.0
Viral RNA	10.0
Total	**20.0**

The cDNA was used as templates for amplification of HA0-, HA1- and HA2-coding sequences by conventional PCR.

4.2.1.3 Amplification of HA0-, HA1- and HA2-coding sequences

Copyright by Mahidol University

The nucleotide primers for PCR amplification of cDNA of H1-coding sequence (*ha0*, *ha1*, and *ha2*) were designed from the full length H1 gene

sequence deposited in the GenBank database (accession no. EU021246.1). Primer sequences for amplifications of the *ha0*, *ha1*, and *ha2* are shown in **Table 4.2**. For the cloning purpose, the *Bam*HI (ggatcc) and *Hin*dIII (aagctt) restricted sequences were included at the 5' ends of the forward and reverse primer sequences, respectively, to facilitate subsequent DNA cloning.

Table 4.2 List of oligonucleotide primers used for amplification of influenza virus gene segments

Target gene segment	**Primer sequences (Reference)**
Viral RNA gene segments	Uni 12: 5'-agcaaaagcagg-3' (Hoffmann *et al*., 2001)
ha0	*ha1F*: 5'-aaggatccgacacaatatgtataggc-3'
	ha2R: 5' aagcttgatgcatattctacactgc-3'
ha1	*ha1F*: 5'-aaggatccgacacaatatgtataggc-3'
	ha1R: 5'-aaaagctttctggattgaatggatgg-3'
ha2	*ha2F*: 5'-ggatccggtttgtttggagccattgc-3'
	ha2R: 5'-aagcttgatgcatattctacactgc-3'

The HA0-, HA1- and HA2-coding DNA sequences were amplified by the polymerase chain reaction (PCR) using cDNA from **section 4.2.1.2** as the template and the primers from **Table 4.2**. The PCR amplicons were verified by 1% gel agarose electrophoresis and ethidium bromide staining.

Copyright by Mahidol University

Ingredients	**Volume** (µl)
10x PCR buffer (High fidelity)	1.25
25 mM $MgCl_2$	0.75
2 mM each dNTP	1.00
0.2 µM Forward primer	0.50
0.2 µM Reverse primer	0.50
High fidelity enzyme (5 units/µl)	0.10
(Fermentas, California,USA)	
cDNA template	1.00
Sterile ultrapure distilled water (UDW)	7.40
Total	**12.5**

The thermal cycles were set as the following:

1. Initial denaturation	at 94 ºC for 10 minutes
2. Thirty cycles of :	
Denaturation	at 94 ºC for 1 minute
Annealing	at 60 ºC for 1 minute
Extension	at 72 ºC for 2 minutes
3. Final extension	at 72 ºC for 10 minutes

4.2.1.4 Verification of the nucleic acid preparations by agarose gel electrophoresis

The nucleic acid preparations, *e.g.*, PCR amplicons from **section 4.2.1.3**, were verified by using 1% agarose gel electrophoresis and ethidium bromide staining. For the electrophoresis, 1% agarose gel (USB, Ohio, USA) in TAE buffer (**Appendix A**) was prepared. Electrophoresis was carried out in a MINI-SUB®CELL CT apparatus (Bio-Rad, California, USA). Molten agarose was casted and allowed to polymerize in the gel casting apparatus at 25 ºC for 1 hour. Each sample was mixed with 10x loading buffer (**Appendix A**) to the final concentration of 1x loading buffer. TAE buffer (1x) was used as an electrode buffer. Electrophoresis was carried out at 100 Volts for about 30 minutes. The nucleic acid band(s) was/were visualized, after staining with ethidium bromide (0.5 µg/ml ethidium bromide in TAE

Copyright by Mahidol University

buffer) for 10-15 minutes, by using UV Transilluminator (BioDoc-It™ Imaging System, California, USA).

4.2.1.5 Ligation of cDNA of HA0-, HA1- and HA2-coding sequences into cloning vectors

The PCR amplicons containing 3' poly-A overhang were ligated into TOPO® vector (Invitrogen, Michigan, USA) using the ligation mixture as shown below. The mixture was kept at 4 ºC for 16 hours.

Ingredients	**Volume** (µl)
Vector pT257R/T (55 ng/µl)	1.0
5x ligation buffer	2.0
PCR amplicon	2.0
Sterile UDW	4.7
T4 DNA ligase (5 units/µl)	0.3
Total	**10**

4.2.1.6 Preparation of chemically competent *E. coli* cells

A single isolated colony of JM109 *E. coli* on LB agar plate (**Appendix B**) was inoculated into 5 ml of LB broth (**Appendix B**) and grown at 37 ºC with shaking at 250 rpm for 16 hours. One hundred microliters of the *E. coli* culture were inoculated into 10 ml of fresh LB broth and incubated at 37 ºC with shaking at 250 rpm until the optical density (OD) at A_{600nm} (OD_{600nm}) reach 0.5. The culture was kept in an ice-bath for 20 minutes then the bacterial cells were harvested by centrifugation at 4,000 ×*g*, 4 ºC for 15 minutes. The bacterial pellet was dissolved in 10 ml of ice-cold 0.1 M $MgCl_2$ (**Appendix C**), resuspended in 10 ml of ice-cold 0.1 M $CaCl_2$ and kept in the ice-bath for 1 hour before using in the transformation. Aliquots of the so-prepared competent cells were kept at -80 ºC for further use in 20% glycerol (**Appendix C**).

4.2.1.7 Transformation of the competent bacterial cells

One hundred microliters of the chemically competent JM109 *E. coli* from **section 4.2.1.6** were added to the tube containing 10 µl of the ligation mixture. After mixing, the tube was kept in ice for 20 minutes. Competent cells were

Copyright by Mahidol University

heated in a 42 ºC water-bath for 2 minutes then brought to ice for 2 minutes before adding 900 µl of LB broth. The tube was incubated at 37 ºC with shaking at 250 rpm for 30 minutes. One hundred microliters of the reaction mixture were spread onto LB-A agar plate (**Appendix B**); then the plate was incubated at 37 ºC overnight.

4.2.1.8 Screening of transformed JM109 *E. coli* clones

White colonies grown on the overnight selective agar plate (LB-A agar plate) were randomly picked and used directly as templates for detecting the presence of the recombinant *ha0*-, *ha1*- and *ha2*-plasmid by PCR using M13 universal primers which annealed to the vector. Replica plates were also prepared for each bacterial colony by streaking a small portion of each of the transformed bacterial colony onto LB-A agar plate. The oligonucleotide primers used in the PCR were the pUC/M13-forward primer: 5′-cgccagggttttcccagtcacgac-3′ and the pUC/M13-reverse primer: 5′-tcacacaggaaacagctatgact-3′. The PCR reaction mixture was:

Ingredients	**Volume** (µl)
10x PCR buffer with KCl	1.25
25 mM $MgCl_2$	0.75
2 mM each dNTP	1.00
0.1 µM pUC/M13-Forward primer	0.50
0.1 µM pUC/M13-Reverse primer	0.50
Taq polymerase enzyme (Fermentas, California, USA) (5 units/µl)	0.10
Small portion of colony	
Sterile UDW	8.40
Total	**12.5**

Copyright by Mahidol University

The thermal cycles were set as the following:

1.	Initial denaturation	at 94 ºC for 10 minutes
2.	Thirty cycles of :	
	Denaturation	at 94 ºC for 1 minute
	Annealing	at 54 ºC for 1 minute
	Extension	at 72 ºC for 2 minutes
3.	Final extension	at 72 ºC for 10 minutes

4.2.1.9 Preparation of recombinant *ha0*-, *ha1*- and *ha2*-plasmids

The positive *ha0*, *ha1* and *ha2* amplicon-transformed JM109 *E. coli* colonies were picked from the replica plates and inoculated individually into 3 ml of LB-A broth (**Appendix B**) and grown at 37 ºC with shaking overnight. The culture was centrifuged at 4,000 ×*g* for 5 minutes to pellet the bacterial cells. Plasmid DNAs were extracted from the cells by using QIAGEN plasmid mini kit (Qiagen, Hilden, Germany) according to the manufacturer's instruction. Concentration of each plasmid DNA was determined by measuring the OD_{260nm}.

4.2.1.10 Restriction endonuclease digestion of the recombinant *ha0*-, *ha1*- and *ha2*-plasmids

For subcloning of the recombinant *ha0*-, *ha1*- and *ha2*-plasmids into expression vector, *i.e.,* pQE30 for *ha0* and *ha1* and pET23a$^+$ for *ha2*, the recombinant plasmids extracted from the cloning vectors and the expression backbone plasmids (pQE30 and pET23a$^+$) were digested doubly to create sticky ends at both 3' and 5' termini. The extracted plasmid DNA digestion reaction mixture is shown below.

Copyright by Mahidol University

Ingredient	**Volume** (µl)
10x *Bam*HI buffer	2.0
*Bam*HI (10 units/µl)	1.0
*Hin*dIII (10 units/µl)	2.0
Plasmid DNA (1 µg/µl)	5.0
Sterile DW	10.0
Total	**20.0**

The mixture was incubated at 37 ºC for 5 hours and subjected to 1% agarose gel electrophoresis and ethidium bromide staining. The gel slices containing digested DNA fragments were collected and the DNA was extracted from the gel pieces by using NucleoSpin® Extract II (Macherey-Nagel, Düren, Geramany) according to the manufacturer's instruction. Finally, DNA was eluted from silica gel by adding sterile UDW. After centrifugation, the supernatant was collected.

4.2.1.11 Ligation of the HA0-, HA1- and HA2- coding sequences with the expression vectors and introduction of the recombinant vectors into competent host cells for protein expressions

The digest HA0-, HA1- and HA2-coding sequences and the expression vectors (pQE30 and pET23a$^+$) were ligated appropriately at 16 ºC for 16 hours in a reaction mixture as shown below:

Ingredient	**Volume (µl)**
10x Ligation buffer	1.0
Digested *ha0, ha1* or *ha2* (10 ng/µl)	6.0
Digested pQE30 (for *ha 0* and *ha1*) or pET23a$^+$ (for *ha2*), 50 ng/µl	2.0
T4 DNA ligase (New England Biolabs, Massachusetts, USA) (400 units/µl)	1.0
Total	**10.0**

Copyright by Mahidol University

The chemically competent BL21 (DE3) *E. coli* expression host was prepared as described for the competent JM109 *E. coli* in **section 4.2.1.6**. The

ligation mixture between digested *ha 0* and *ha1* and pQE30 was introduced into the competent M15 *E. coli* cells and the ligation mixture between digested *ha2* and pET23a$^+$ was introduced into the competent BL21 (DE3) *E. coli* by using a heat-shock method. The transformed bacteria were selected by using the LB-AK plate (**Appendix B**) for the rHA0-pQE30 and rHA1-pQE30 and LB-A plate for rHA2-pET23a$^+$as described in **section 4.2.1.7**. A fraction of the transformed *E. coli* colonies grown on the selective agar plate was screened for the presence of the recombinant *ha0*- and *ha1*-pQE30 and *ha2*-pET23a$^+$ by PCR using specific primers from **Table 4.2**. Each reaction mixture was used similarly as in **section 4.2.1.2**. Plasmid DNA of the *E. coli* clone carrying *ha0*, *ha1* and *ha2* gene inserts were extracted as described in **section 4.2.1.9** and subjected to DNA sequencing for verification. The nucleotide sequences were blasted against the sequences deposited in the NCBI database to determine degrees of identity between the cloned *ha0, ha1* and *ha2* sequences and the database sequences.

4.2.1.12 Production of recombinant rHA0, rHA1 and rHA2

Transformed M15 *E. coli* colonies carrying rHA0-pQE30 and rHA1-pQE30 were inoculated separately into 5 ml aliquots of LB-AK broth (**Appendix B**) while transformed BL21 (DE3) *E. coli* colonies carrying rHA2-pET23a$^+$ was inoculated into 5 ml aliquots of LB-A broth for making starter. The starters were incubated at 37 ºC with shaking at 250 rpm for 16 hours. Two Fresh LB-A or LB-AK broth culture (250 ml) was incubated with 2.5 ml of each starter and grown until the OD_{600nm} reached 0.4-0.5. IPTG (USB, Ohio, USA) was added to final concentration of 0.5 mM. The culture was incubated further for 4 hours. The bacterial cells were collected by centrifugation at 4,000 ×*g*, 25 ºC for 20 minutes. The cells (100 µg) were re-suspended in 1 ml of phosphate buffer saline, pH 7.4 (PBS) and subjected to sonication on ice-bath by using sonication machine (LABSONIC®P, Sartorius Stedim Biotech, France). Proteins in the supernatants (soluble protein) and sediments (inclusion body or insoluble protein) were separated by centrifugation. Protein preparations were equally (*v/v*) mixed with 6x reducing sample buffer and boiled for 5 minutes before subjecting to 12% SDS-PAGE and Western blot analysis (**section 4.3**)

For Western blot analysis, the nitrocellulose membrane (NC) (GE Healthcare, Buckinghamshire, UK) blotted with the 12% SDS-PAGE-separated

components was incubated with 5% skim milk in PBS at 25 ºC for 1 hour before washing with washing buffer (**Appendix F**). The blotted NC was incubated in a solution of mouse monoclonal anti-6xHis-tag antibody (Abcam®, Cambridge, UK) diluted 1:5,000 in the washing buffer. Goat anti-mouse immunoglobulin (IgG)-Alkaline phosphatase (AP) conjugate and BCIPT/NBT substrate were used for revealing bands of the recombinant proteins. Each NC was thoroughly rinsed with DW before air-drying.

4.2.1.13 Purification of recombinant HA0, HA1 and HA2

Bacterial cells (one gram of wet weight) were lysed by adding 10 ml of denaturing lysis buffer or buffer C (**Appendix D**). The preparation was sonicated on ice-bath for 5 minutes then it was centrifuged at 12,000 ×*g*, 4 ºC for 15 minutes. The supernatant was collected. Ni-NTA beads (1 ml) (Invitrogen™, Life Technologies, New York, USA) were pre-equilibrated with denaturing lysis buffer for 15 minutes. The pre-equilibrated Ni-NTA beads were mixed with the bacterial lysate and kept on rotating platform with gently agitation at 25 ºC for 2 hours. The beads were allowed to set by gravity in a polystyrene column and washed serially with 30 ml of a denaturing washing buffer (**Appendix D**) and 20 ml of denaturing lysis buffer. The Ni-NTA bead bound proteins were then eluted with gradient fractions of 50-300 mM imidazole solutions made in buffer C. Three ml fractions were collected (6 fractions; labeled E1-E6). Proteins in each fraction were analyzed by SDS-PAGE and Western blot analysis. The rHA0, rHA1 and rHA2 proteins were revealed by Coomassie Brilliant Blue G-250 (CBB) staining and Western blot analysis as described in **section 4.2.1.12**. Fractions containing purified HA0, HA1 or HA2 were pooled, refolded and dialyzed against PBS until molarity of the urea in each preparation was reduced to nil. The proteins were kept at -20 ºC until use.

4.2.2 Recombinant N-terminally truncated-NA protein (ΔrN-NA) protein of influenza A virus, subtype N1

The purified recombinant N-terminally truncated NA (subtype N1) protein (~44 kDa) in small aliquots at concentration 0.11 µg/µl in 20% glycerol in PBS was a kind gift from Assist. Prof. Dr. Potjanee Srimanote, Faculty of Allied Health Sciences, Thammasat University, Rangsit campus, Pathumthani, Thailand. In briefly, coding

sequences of 5' deleted *NA* (1,167 bp) was PCR amplified from A/duck/Thailand/144/2005 (H5N1) cDNA by using uni 12 primer (**Table 4.2**). The amplicon was cloned into protein expression vector and introduced into BL21 (DE3) *E. coli.* Selected transformed *E. coli* clones were grown in LB-A (**Appendix B**) until the OD_{600nm} reached 0.5. The *E. coli* cultures were induced with 1 mM IPTG to express the recombinant truncated NA. The bacterial lysates containing 6x-His-tagged-rNA were verified by 12% SDS-PAGE and Western blot analysis.

4.2.3 Production and purification of recombinant M2 and NP

4.2.3.1 Production of recombinant M2 and NP

Transformed BL21 (DE3) *E.coli* carrying rM2- and rNP-pET20b$^+$ were constructed by Dr. Kanyarat Thueng-in (Thueng-in *et al*, 2010). In briefly, coding sequences of NP (1,500 bp) and M2 (291 bp) were PCR amplified from A/duck/Thailand/144/2005 (H5N1) cDNA by using uni 12 primer (**Table 4.2**). Each amplicon was cloned into pET-20b$^+$ vector (Novagen, Darmstadt, Germany) and introduced into BL21 (DE3) *E. coli.* Selected transformed *E. coli* clones were grown in LB-A (**Appendix B**) until the OD_{600nm} reached 0.5. The *E. coli* cultures were induced with 0.5 mM IPTG to express the recombinant proteins. The bacterial lysates containing 6x-His-tagged-NP and –M2 were verified by 12% or 14% SDS-PAGE, Western blot analysis and LC-MS/MS.

4.2.3.2 Purification of recombinant-M2 and -NP

Purifications of recombinant M2 and NP were done similarly to recombinant protein purification in section 4.2.1.13. Besides, the rM2 protein was also purified under native condition by using Ni-NTA beads.The purified proteins were analyzed by SDS-PAGE and Western blot analysis. The rM2 and rNP (protein bands at ~ 17 and 60 kDa, respectively) were revealed by CBB staining and Western blotting by reacting the NC blots with mouse monoclonal anti-6xHis tag antibody, goat anti-mouse immunoglobulin-AP conjugate and substrate, respectively. Fractions containing purified rM2 or rNP were pooled, refolded and dialyzed against PBS, pH 7.4 until molarity of the urea in the preparations was reduced to nil. The protein preparations were kept at -20 ºC until use.

Copyright by Mahidol University

4.2.4 Protein quantification by Bradford reagent and/or NanoDrop Spectrophotometer

The microtiter plate protocol of Bio-Rad Protein Assay (Bio-Rad, USA) was followed for protein quantification. BSA was used as protein standard. Five dilutions of BSA were prepared: 0.05 to 0.5 mg/ml, which was a suitable linear range of the microtiter plate assay. Ten microliters of each diluted BSA solution and sample were added to individual wells of the microtiter plate (Corning®, New York, USA) in duplicate. Diluted dye reagent (200 µl) was added to each well and mixed. The mixtures were kept at 25 ºC for 5 minutes. OD_{595nm} of the colored content in each well was measured. A protein standard curve was constructed by plotting the BSA concentrations against the respective OD read-outs. The protein content of the unknown was calculated from the curve.

The NanoDrop ND-1000 Spectrophotometer (Thermo Scientific, Massachusetts, USA) was used also in protein quantification in the case of small amount and volume of the protein preparation. After measuring protein concentration by using the NanoDrop spectrophotometer, amount of the protein was multiplied with co-efficiency according to the type of protein recommended from the spectrophotometer.

4.3 Sodium dodecyl sulfate-polyacrylamide gel electrophoresis (SDS-PAGE) and Western blot analysis (WB)

4.3.1 SDS-PAGE

4.3.1.1 Preparation of the sample for loading into slab gel

Five parts of the protein sample was mixed with one part of the 6x sample buffer (**Appendix E**) and boiled for 5 minutes. After boiling, the mixture was loaded into slots of the stacking gel. Pre-stained SDS-PAGE broad range standard (Bio-Rad) or PageRuler™ pre-stained protein ladder (Fermentas, New York, USA) was included in at least one slot of each gel slab.

Copyright by Mahidol University

4.3.1.2 Sample separation

SDS-PAGE was performed by using the technique described by Laemmli (1970) with some modifications. In this study, a 4% acrylamide stacking gel (**Appendix E**) and 12% or 14% acrylamide separating gels (**Appendix E**) were used. The vertical slab gel (8.0 x 7.3 cm) was prepared using the casting apparatus (Minutei-PROTEAN®3 cell, Bio-Rad, California, USA) and electrophoresis was done in electrophoresis chamber at 20 mA per gel with an electric power supply (Model 3,000/300, Bio-Rad). At the end of the electrophoresis, the gel containing the separated proteins was either stained with CBB dye (**Appendix F**) for direct visualization of the separated components or subjected to Western blotting.

4.3.2 Staining of proteins in the polyacrylamide gel with Coomassie Brilliant Blue G-250 dye

Proteins in polyacrylamide gel were fixed by using freshly prepared fixing buffer (1% *o*-phosphoric acid and 20% methanol in DW) at 25 ºC for 1 hour. After fixing, the gel was immersed in a solution of freshly prepared dye [1% (*w/v*) Coomassie Brilliant G-250, 8% ammonium sulfate, 1% *o*-phosphoric acid and 20% methanol in DW] for 16 hours. The gel was removed from the dye solution, destained with destaining solution [Mixing of DW, methanol and acetic acid in ratio of 50/40/10 (*v/v/v*)] and kept in DW at 25 ºC. The proteins in the gel were visualized directly or photograph was taken. For long-term storage, the gel was dried on cellophane membrane and kept at 25 ºC.

4.3.3 Western blot analysis (WB)

The separated proteins on polyacrylamide gel were transblotted onto NC by using the Mini Trans-Blot® Electrophoresis Transfer Cell (Bio-Rad, California, USA). The protein containing polyacrylamide gel, NC, filter paper and filter pad were immersed with transfer buffer (**Appendix F**) at 25 ºC for 15 minutes then the protein from polyacrylamide gel were transferred to NC by the electric current at 100 volts for 70 minutes. The NC was blocked with 5% skim milk in PBS at 25 ºC with gently agitating for 1 hour. After washing three times with TBS-T (**Appendix F**), NC was reacted with mouse monoclonal anti-6xHis antibodies (1: 5,000 dilute in TBS-T) at 25

Copyright by Mahidol University

ºC with gently agitating for 1 hour. After washing, the NC was reacted with goat anti-mouse IgG-AP (1:5,000 dilution) at 25 ºC with gently agitating for 1 hour. The NC was thoroughly wash with washing buffer then rinsed with 0.15 M Tris-HCl, pH 9.6 before dipping in BCIP/NBT phosphatase substrate solution until the protein band(s) appeared. In finally, the NC was washed with DW and air-dried at 25 ºC.

4.4 Production of mouse polyclonal antibodies to recombinant H1, N1, M2 and NP

4.4.1 Animal immunization

For mouse immunization, Five hundred microliters of the recombinant H1, M2, or NP in PBS (1 µg/µl) from **section 4.2** was mixed individually with 250 µl of alum adjuvant (Pierce, Illinois, USA) with agitation on platform shaking at 25 ºC for 30 minutes. The mixture was injected intraperitoneally into ICR mice (100 µl per mouse). Two booster injections were given at 14-day intervals. The mice were bled one week following the second booster. The hyperimmune sera were designated mouse polyclonal anti-H1, -M2, and –NP (PAb-H1, PAb-M2, and PAb-NP).

The hyperimmune serum containing PAb to rN1 was a kind gift from Assist. Prof. Dr. Potjanee Srimanote.

All animal experiments were approved by Veterinary Science-Animal Care and Use Committee (FVS-AUCU), Faculty of Veterinary Medicine, Kasetsart University, Thailand (ID number ACKU 03455) (**Appendix J**).

4.4.2 Determination of binding specificity of PAb-H1, -M2, and –NP by indirect ELISA and Western blotting

Serum antibody titers against the homologous antigens were determined by indirect ELISA. Five-hundred nanograms of recombinant H1, M2, or NP from **section 4.2** in 100 µl of coating buffer (**Appendix G**) were added to each well of the ELISA plate and the plate were kept at 37 ºC for 16 hours. Unbound protein was washed out and the unoccupied sites in each well were blocked by adding 150 µl of

Copyright © by Mahidol University

3% BSA in PBS. After removing the blocking solution and washed, serially-diluted antibody preparation was added to the well and the plate was incubated in a humidified chamber at 37 ºC for 1 hour. After washing with PBST, goat anti-mouse IgG-HRP conjugate (1:3,000) was added and incubated for 1 hour. After washing, ABTS substrate was added and kept in the dark for 30 minutes. The OD at A_{405nm} of the content of each well was determined against a blank (wells filled with PBS instead of antibody). Pre-immunized mouse serum was tested and served as a baseline control of the PAbs.

Western blot analysis was used for determining antigenic specificities of the antibody preparation. Recombinant H1, M2, and NP were subjected to 14 or 12% SDS-PAGE. The separated components were electroblotted onto NC. After unoccupied sites on the NC were blocked with 5% skim milk in PBS and washed, the NC was incubated with the mouse immune sera. Goat anti-mouse IgG-AP conjugate and BCIP/NBT substrate was used for revealing the rH1, rM2, and rNP-antibody reactive bands at ~60, 17, and 60 kDa, respectively.

4.5 Selection of phage clones displaying human single chain variable fragment (HuScFv) that bound to native HA, NA and M2 on influenza virus particle and HuScFv that bound to the purified rM2

4.5.1 Human antibody phage display library

A human ScFv phage library was constructed by Dr. Kasem Kulkeaw in Professor Dr. Wanpen Chaicumpa's laboratory (Kulkeaw *et al*, 2009). Human immunoglobulin gene segments encoding for all families of human variable heavy (*vh*) and kappa variable light (*vκ*) chains were amplified from B lymphocytes of 60 Thai blood donors using degenerate primers. The amplified *vh* and *vκ* sequences were linked randomly *via* a polynucleotide linker into *scfv* sequences and the *scfv* repertoire was cloned into TG1 *E. coli*. After the phagemid transfecteion of *E. coli* and co-infecting the phagemid transformed TG1 *E. coli* with the helper phage (M13KO7), a large repertoire phage library (~6.5 x 10^{12} cfu/ml) displaying a ~2.6 x 10^{8} human

antibody diversity and ~85% of phages in the library contained human *scfv* sequences (*huscfv*) were obtained.

4.5.2 Selection of phage clones that bound to native H1, N1 and M2 of influenza A virus

4.5.2.1 Preparation of human group O red blood cell (hRBC) ghosts (Homma and Ohuchi, 1973)

Human group O RBC (hRBC) was collected by using an EDTA blood tube. One ml of the packed hRBC was washed with 9 ml of PBS, pH 7.4, three times. Then the packed hRBC was lyzed by mixing with 30 ml of 0.0004% acetic acid and kept in ice-batch (~1-3 ºC) for 60 minutes with stirring. The hRBC ghosts were than washed several times in a 0.001 M chilled acetate buffer (pH 5.0) by centrifugation at 1,000 ×*g* for 5 minutes until the supernatant was de-colored. The same washing procedure was performed by using chilled PBS and the hRBC ghosts were kept at 4 ºC for 16 hours. After the last wash, the hRBC ghosts were re-suspended in PBS at 20% *v/v* and kept at 4 ºC.

4.5.2.2 Preparation of the hRBC ghosts with the H1N1 viruses adsorbed on the surface

Influenza A virus [A/Thailand/CU-H106/2009 (H1N1/2009)] (250 µl of HA reciprocal titer 32) was mixed with equal volume of 4% hRBC ghost (*v/v*) in biosafety cabinet class II and kept on rotating platform at 25 ºC for 1 hour. The un-adsorbed viruses were removed by centrifugation a1 5,000 ×*g* at 25 ºC for 5 minutes. The virus adsorbed ghosts was washed and used as a panning antigen in selecting phage clones that displayed HuScFv to native surface proteins of the virus from a human antibody phage display library.

4.5.2.3 Single round phage bio-panning for selection of phage clones that displayed HuScFv specific to H1, N1 and M2 by using the influenza virus adsorbed hRBC ghosts as the panning antigen

4.5.2.3.1 Subtractive bio-panning with un-infected egg allantoic fluid

Copyright by Mahidol University

Two micrograms of allantoic fluid protein of un-infected egg in 100 µl of coating buffer (**Appendix G**) was added to an ELISA well

(Corning®, New York, USA) and incubated at 37 ºC for 16 hours. The unbound allantoic fluid proteins were removed by washing with PBST (**Appendix G**). The well was blocked with 200 µl of 3% BSA in PBS (**Appendix G**) at 25 ºC for 1 hour. After washing the well with PBST, 200 µl of the phage display library (2.2×10^{10} cfu/ml) from section 4.5.2.1 were added to the well, incubated at 25 ºC for 1 hour. The unbound phages were collected and the panning with the allantoic proteins was repeated two more times. After removing the phages that bound to the allantoic fluid proteins, the unbound phage library from the third panning round were collected for use in the next step.

4.5.2.3.2 Subtractive bio-panning with human red blood cell ghosts

The subtracted phage library from **section 4.5.2.3.1** was mixed with 200 µl of the 4% hRBC ghost (*v/v*) and incubated with rotation at 25 ºC for 1 hour. After centrifugation at 5,000 ×*g* for 5 minutes, the unbound phage library was collected and repeated this subtractive step two more times. After the third panning round, the unbound phage library was collected for use in the positive bio-panning with the H1N1 virus adsorbed on the hRBC ghosts.

4.5.2.3.3 Positive bio-panning of the subtracted phage library with the H1N1/2009 virus adsorbed on hRBC ghosts

The subtracted phage library from **section 4.5.2.3.2** was mixed with equal volume of the hRBC ghosts which the H1N1/2009 virus had been adsorbed on the surface from **section 4.5.2.2** and incubated with rotation at 25 ºC for 1 hour. After removing unbound phage by centrifugation at 5,000 ×*g* for 5 minutes, the pellet of phages that bound to the virus adsorbed on the hRBC ghosts was washed extensively with PBS to eliminate unbound phages. After washing, log phase grown HB2151 *E. coli* (200 µl) was added to the phage preparation, mixed thoroughly, and the phage transfection was allowed to occur at 37 ºC for 30 minutes. An aliquot of the transformed *E. coli* preparation was spread onto 2xYT-AG agar plate (**Appendix B**) and the plate was incubated at 37 ºC for 16 hour for screening of the phagemid transformed *E. coli*. The remaining portion of the phage transfected *E. coli* was kept properly in 20% sterile glycerol at -80 ºC.

Copyright by Mahidol University

4.5.3 Selection of phage clones that bound to the recombinant M2 protein with single round phage bio-panning

Purified rM2 protein was used as antigens in the bio-panning for selecting phage clones that display rM2 bound-HuScFv. One microgram of the rM2 in 100 µl of coating buffer (**Appendix G**) was added to a well of a microtiter plate (Corning®, NewYork, USA) and incubated at 37 ºC for 16 hours. The antigen coated well was washed with PBS-T and blocked with 3% BSA in PBS. HuScFv phage display library (100 µl) was added into the antigen coated well and kept at 25 ºC for 1 hour. After discarding the fluid, the well was washed thoroughly with PBST to remove unbound phages. Log phase grown HB2151 *E. coli* (200 µl) was added to the well containing rM2 bound-phages; the phage transfection was allowed to occur at 37 ºC for 15 minutes in humidified chamber. A small aliquot of the content in the well was spread onto 2xYT-AG agar plate (**Appendix B**) and the plate was incubated at 37 ºC for 16 hours for screening of the phagemid transformed *E. coli*. The remaining portion of the phage transfected *E. coli* was kept properly in 20% sterile glycerol at -80 ºC.

4.6 Screening of transformed HB2151 *E. coli* colonies carrying *huscfv*-phagemids by colony PCR

Amplicillin resistant colonies of HB2151 *E. coli* colonies grown on the selective 2xYT-AG agar plate were screened for *huscfv*-phagemid containing clones by using a direct colony PCR and the primers for the antibody coding genes. The PCR primers were *R1* (forward): 5'-ccatgattacgccaagcttt-3' and *R2* (reverse): 5'-gctagatttcaaaacagcagaaagg-3'. The transformed *E. coli* colonies were randomly picked for the PCR and also streak on 2xYT-AG agar for preparing replica plates. The PCR products were resolved on 1% agarose gel electrophoresis and stain with ethidium bromide. The *E. coli* clones giving *huscfv* amplicons with expected size of ~ 1,000 bp were selected and the *huscfv*-positive *E. coli* clones were stored as bacterial stocks in 20% sterile glycerol at -80 ºC for further use.

Copyright by Mahidol University

The direct colony PCR reaction mixture was prepared as the following:

Ingredients	**Volume** (µl)
10x PCR buffer with KCl	1.25
25 mM $MgCl_2$	0.75
2 mM each dNTP	1.00
0.1 µM, *R1*-Forward primer	0.50
0.1 µM, *R2*-Reverse primer	0.50
Taq polymerase enzyme (Fermentas) (5 units/µl)	0.10
Small portion of colony	
Sterile DW	8.40
Total	**12.5**

The thermal cycles were set as the following:

1. Initial denaturation	at 94 ºC for 10 minutes
2. Thirty cycles of :	
Denaturation	at 94 ºC for 1 minute
Annealing	at 55 ºC for 1 minute
Extension	at 72 ºC for 2 minutes
3. Final extension	at 72 ºC for 10 minutes

4.7 Screening of phagemid-transduced *E. coli* that could express soluble HuScFv

The bacterial transformants carrying the recombinant *huscfv*-phagemid vectors were screened further for their ability to express soluble HuScFv by Western blot analysis. From the replica plate, each selected HB2151 *E. coli* clone was grown in 2xYT-AG broth to prepare a starter culture. One hundred microliters of the starter culture were inoculated into 10 ml of 2xYT-AG broth and grown at 37 ºC with shaking at 250 rpm until the OD_{600nm} was 0.3-0.5. The culture was centrifuged at 3,000 ×*g* for 15 minutes and the 2xYT-AG broth was discarded. Ten ml of 2xYT-A broth was added to the bacterial cell pellet, mixed, and induced to express the HuScFv

Copyright© by Mahidol University

by adding IPTG to a final concentration of 0.5 mM. The culture was incubated at 37 ºC with shaking further for 5 hours. The bacterial cells were harvested by centrifugation at 3,000 ×*g*, 25 ºC for 15 minutes. The cells in the pellet were re-suspended with 500 µl of PBS. The bacterial cells were lysed by sonication and the homogenate was centrifuged at 12,000 ×*g*, 4 ºC for 15 minutes. The soluble antibody molecules in the bacterial lysate (supernatant) was detected by Western blot analysis using mouse monoclonal anti-E-Tag™ antibody (Abcam®, Cambridge, UK), goat-anti-mouse IgG-AP conjugate and BCIP/NBT substrate, respectively.

4.8 Antigen binding test

Indirect ELISA, Western blotting, and immunofluorescence assay were used for testing the binding of the selected soluble HuScFv derived from different recombinant phagemid transformed HB2151 *E. coli* clones to the recombinant HA (HA0, HA1, HA2), NA and M2 and native counterparts.

4.8.1 Indirect ELISA

One micrograms of the purified recombinant HA (HA0, HA1, and HA2), NA, M2, or BSA (irrelevant antigen control) in 100 µl of carbonate-bicarbonate buffer, pH 9.6 (**Appendix G**) were immobilized onto individual wells of an ELISA plate. After removing the excess antigens by washing, the antigen-coated wells were blocked with 3% BSA in PBS then the wells were incubated with 100 µl of individual HB2151 *E. coli* lysates which contained soluble HuScFv (from **section 4.7**). After washing, the amount of antigen-bound HuScFv in each well was detected using mouse monoclonal anti-E-Tag antibody, goat-anti-mouse immunoglobulin-horseradish peroxidase (HRP) conjugate and ABTS substrate, respectively. The OD_{405nm} of the content of each well was determined against a blank (wells filled with PBS instead of HuScFv containing *E. coli* lysate). A well added with lysate of normal HB2151 *E. coli* instead of HuScFv containing *E. coli* lysate served as background control. Polyclonal antibody specific to the antigens (HA, NA, and M2) served as positive control.

Copyright by Mahidol University

In addition, native antigens were used also in specificity binding test with individual HB2151 *E. coli* lysates containing the soluble HuScFv from bio-panning

with the influenza virus adsorbed hRBC ghosts. In briefly, 100 µl of the H1N1/2009 influenza virus adsorbed hRBC ghosts (from section 4.5.2.2) in 0.6 ml Eppendorf tube was blocked with 3% BSA in PBS and incubated with rotation at 25 ºC for 1 hour. After centrifugation at 5,000 ×*g* for 5 minutes, the influenza virus adsorbed hRBC ghosts was mixed with 100 µl of individual HB2151 *E. coli* lysates containing the soluble HuScFv and incubated with rotation at 25 ºC for 2 hours. After washing, the amount of antigen bound-HuScFv was detected using mouse monoclonal anti-E-Tag antibody, goat-anti-mouse IgG-HRP conjugate and ABTS substrate, respectively. The OD_{405nm} of the content of each well was determined against a blank (wells filled with PBS instead of HuScFv containing *E. coli* lysate). A well added with lysate of normal HB2151 *E. coli* instead of HuScFv containing *E. coli* lysate served as background control. Polyclonal antibody specific to the antigens (HA, NA, and M2) served as positive control.

4.8.2 Western blot analysis

The purified recombinant HA, NA, or M2 (~15 µg) was loaded into long slot 12% SDS-PAGE gel for rHA and rNA and 14% SDS-PAGE gel for rM2. The rHA, rNA, or rM2 was resolved by electrophoresis and transferred onto NC as described in **section 4.3.3**. The recombinant protein blotted NC was cut into several vertical strips which were probed individually with 1:2 diluted HuScFv lysates derived from different HB2151 *E. coli* clones. Lysate of normal HB2151 *E. coli* was used as negative control and polyclonal antibody specific to the antigens (HA, NA, and M2) served as positive controls. After 1 hour, the strips were washed with TBS-T, the bound antibody fragments on each strip were detected by mouse monoclonal anti-E-Tag antibody, goat-anti-mouse IgG-AP conjugate and a BCIP/NBT chromogenic substrate, respectively.

For native antigens, the MDCK cells infected with H1N1 or H5N1 viruses for 72 hours were harvested, washed and added with a volume of PBS. The cells were sonicated and the homogenates containing the viruses were collected after centrifugation at 12,000 ×*g*, 4 °C for 15 minutes. The viral homogenates were added individually with sample buffer and subjected to 12% SDS-PAGE. The separated components were blotted onto NC. The blotted NC was blocked and cut vertically into

strips. The strips were incubated appropriately with individual HuScFv preparations. Lysate of normal HB2151 *E. coli* was used as negative control, and polyclonal antibody specific to the antigen (HA, NA, and M2) (1:5,000 dilution) served as positive antibody control. The antigen-antibody reactive bands were revealed by using mouse monoclonal anti-E tag antibody, goat anti-mouse IgG-AP conjugate and BCIP/NBT chromogenic substrate.

4.8.3 Immunofluorescence assay

The selected HuScFv specific to M2 (**section 4.11**) and polyclonal antibody to rM2 (pAb-M2) were also tested by immunofluorescence assay for their binding to native M2 in MDCK cells infected with influenza A subtype H5N1of clades 1 and 2. Briefly, The MDCK monolayer on 12mm diameter cover slip in 24 well-tissue culture well were infected with H5N1 at MOI 1 and incubated in 5% CO_2 atmosphere, 37 °C for 1 hour to allow the virus entry. After extracellular viruses in each well were discarded, the cells were rinsed with plain DMEM, replenished with viral growth medium, and incubated in 5% CO_2 atmosphere, 37 °C further for 24 hours. Then the infected cells with H5N1 were washed with PBS, fixed with cold absolute methanol, and permeabilized with 1% Triton-X 100 in PBS for 20 minutes. After blocking with 3% FBS in PBS, the well was probed with HuScFv or pAb-M2 (1:3,000) at 25 ºC for 1 hour. The unbound materials were removed by washing with PBS. The cells were reacted with mouse monoclonal anti-6xHis tag antibody and incubated at 25 ºC for 1 hour. Then Alexa Fluor® 488-labeled chicken anti mouse Ig (Amersham Biosciences, Uppsala, Sweden) (1:1,000) were added and incubated at 25 ºC for 1 hour. The plate was then reacted with DAPI stain (Invitrogen, Oregon, USA) (1:3,000) at 25 ºC for 30 minutes. After extensively washed with PBS, glass cover slips were applied to the glass slide, mounted with a drop of 50% glycerol, and sealed with nail polish on microscopic glass slides. Fluorescence emission was visualized by using fluorescence microscopy with a 40x magnification objective lens.

Copyright by Mahidol University

4.9 Characterization of HA, NA, or M2-specific HuScFv

4.9.1 Restriction fragment length polymorphism (RFLP) of the *huscfv* sequences

Diversity of the DNA sequences coding for HuScFv that could bind to the HA, NA, and/or M2 were determined by restriction fragment length polymorphism (RFLP) technique as described previously (Shin *et al*., 2003; Thathaisong *et al*., 2008). The amplified *huscfv* products (from **section 4.6**) were digested with *Mva*I restriction endonuclease at 37 ºC for 5 hours. The *Mva*I digestion mixture is shown in the table below. The digested mixtures (5 µl) were mixed individually with 10x DNA loading dye **(Appendix A)** and resolved on 12% polyacrylamide gel containing 0.5% glycerol **(Appendix H)**. The electrophoresis was carried out in 0.5x TBE buffer **(Appendix H)** by applying 20 mA electric power per one slab gel**.** The resolved DNA bands were stained by ethidium bromide **(Appendix A)** and the RFLP DNA banding patterns were compared visually under UV illumination using BioDoc-It UV Transilluminator®.

*Mva*I digestion mixture:

Ingredient	**Volume** (µl)
UDW	17.4
10x Red buffer	2.5
*Mva*I restriction endonuclease (Fermentas) (10 units/µl)	0.1
huscfv amplicon	5.0
Total	**25.0**

Each reaction mixture was kept in a 37 ºC water-bath for 5 hours.

Copyright by Mahidol University

4.10 Identification of immunoglobulin frameworks (FR) and complementarity determining regions (CDRs) of the HuScFv

The *huscfv* sequences coded for HA, NA, and/or M2 specific-HuScFv from HuScFv clones in individual *E. coli* clones that gave positive binding to recombinant HA, NA, and M2 by using indirect ELISA and Western blotting were extracted the *huscfv*-pCANTAB5E plasmid by using Fast-n-easy plasmid mini prep kit (Jena Bioscience GmbH, Germany). The nucleotide sequences of the selected *huscfv* were determined by DNA sequencing (FirstBase Laboratories, Malaysia). The deduced amino acid sequences of nucleotide sequences of all clones were aligned with human VH and VL sequences of IMGT database. The immunoglobulin frameworks (FRs) and the complementarity determining regions (CDRs) of individual HuScFv were determined using the IMGT server (http://www.imgt.org/IMGT_vquest).

4.11 Large scale production and purification of specific HuScFv

4.11.1 Subcloning of HuScFv genes into pET vector

For large scale production of the HuScFv, the *huscfv* of selected *E. coli* clones were subcloned into pET vectors (pET23b$^+$ or pET32c$^+$) which had T7 promoter. The pET vector backbone (pET23b$^+$ or pET32c$^+$) and the selected *huscfv*-pCANTAB5E were digested doubly with restriction endonucleases (*Hin*dIII and *Not*I) (Fermentas, California, USA). The mixture was incubated at 37 ºC for 5 hours and subjected to 1% agarose gel electrophoresis and ethidium bromide staining. The digested pET vectors and *huscfv* amplicon were purified by using Agarose Gel extraction kit (Jena Bioscience GmbH, Germany). The composition of the digestion reaction was shown below.

Copyright by Mahidol University

Recombinant plasmid/*huscfv* digestion mixture:

Ingredient	**Volume** (µl)
UDW	11.0
10x Orange buffer	2.0
*Hin*dIII endonuclease enzyme (10 units/µl) (Fermentas)	1.5
*Not*I endonuclease enzyme (10 units/µl) (Fermentas)	0.5
The pET vector backbone and *huscfv*-pCANTAB5E	5.0
Total	**20.0**

The digested pET vector backbone and *huscfv* were ligated by using T4 DNA ligase enzyme (New England Biolabs, Massachusette, USA). The ligation mixture (see below) was incubated at 16 ºC for 16 hours.

Ligation mixture:

Ingredient	**Volume** (µl)
10x Buffer	1.5
Digested pET vector (1 µg/µl)	3.0
T4 DNA ligase (400 units/µl)	1.0
Digested *huscfv* amplicon	3.5
UDW	7.0
Total	15.0

4.11.2 Transformation of the recombinant plasmids

The recombinant pET plasmids (pET23b^{+} or pET32c^{+}) containing *huscfv* inserts were introduced into competent BL21 (DE3) by heat shock method as shown in section 4.2.1.11. After incubating the mixture for 30 minutes, individual preparations were spread on 2xYT-A selective agar **(Appendix B)** and incubated for 16 hours. Colonies of transformed *E. coli* were picked randomly and replica plates were made on 2xYT-A selective agar. The transformed *E. coli* BL21 (DE3) clones were screened for the presence of inserted *huscfv* by PCR using T7 promoter and terminator primers,

Copyright by Mahidol University

i.e., T7 promoter (forward) primer: 5'-taatacgactcactatagg-3' and T7 terminator (reverse) primer: 5'-gctagttattgctcagcgg-3'. The appropriateness of the *huscfv* insertions (~1,000 bp) in the plasmids were verified by DNA sequencing (as described in **section 4.9**). The size of *huscfv* amplicon including the flanking region of the plasmid vector sequence was ~1,000 bp. The *huscfv*-positive *E. coli* clones were screened further for their ability to express the 6xHis-tagged-antibody fusion HuScFv as described in **section 4.6**. The expressed 6xHis-tagged-HuScFv was detected by Western blot analysis using mouse monoclonal anti-6x His antibody, goat-anti-mouse IgG-AP conjugate and BCIP/NBT chromogenic substrate, respectively.

The direct colony PCR reaction mixture was prepared as the following:

Ingredient	**Volume** (µl)
UDW	9.4
10x PCR buffer with KCl	1.75
50 mM $MgCl_2$	0.75
2 mM each dNTP mix	0.5
T7 promoter-forward primer (10µM)	0.25
T7 terminator-reverse primer (10µM)	0.25
Taq polymerase enzyme (Fermentas) (5 units/µl)	0.1
Total	**12.5**

The thermal cycle program was set as the following:

1. Initial denaturation	at 94 ºC for 10 minutes
2. Thirty cycles of :	
Denaturation	at 94 ºC for 1 minute
Annealing	at 55 ºC for 1 minute
Extension	at 72 ºC for 2 minutes
3. Final extension	at 72 ºC for 10 minutes

Copyright by Mahidol University

4.11.3 Large scale expression of HuScFv

Large scale expression of His-tagged HuScFv (HuScFv-His) was done as described in **section 4.2.1.12**. Briefly, 2 liter sized-sterile glass flask was used for bacterial culture. Each flask was added with 250 ml of 2xYT-A broth (**Appendix B**), inoculated with 2.5 ml overnight culture (starter) of individual *E. coli* clones and grown until the OD_{600nm} reached 0.4-0.5. IPTG (USB, USA) was added to final concentration of 0.5 mM and the culture was incubated further for 4 hours. After harvesting the bacterial cells, an aliquot of the cells was used for checking HuScFv expression. The cells were homogenized and subjected to 12% SDS-PAGE and Western blot analysis using mouse monoclonal anti-6xHis tag antibody as described in **section 4.2.1.12**. HuScFv were then purified.

4.11.4 Purification and refolding of the 6xHis-tagged HuScFv

The HuScFv-His in *E. coli* homogenate were purified by using TALON^{TM} affinity resin (Clontech Laborstories, California, USA) under denaturing condition. The bacterial pellets were lysed by sonication at 30% amplitude, 0.5 cycles for 5 minutes in 1x denaturing extraction buffer (**Appendix D**) (one gram of pellet per 10 ml of buffer). The translucent homogenate was centrifuged at 12,000 ×*g*, 4 ºC for 20 minutes. The supernatant was transferred carefully to a clean tube without disturbing the cell debris. The TALON^{TM} affinity resin kept in 20% ethanol was re-suspended in TALON resin suspension buffer and 2 ml of the resin suspension were transferred to a clean tube (2 ml of the resin suspension made 1 ml volume of packed resin). The resin suspension was centrifuged at 700 ×*g*, 25 ºC for 3 minutes and the supernatant was discarded. Sterile water (20 ml) was added and mixed gently to wash the resin. The resin suspension was centrifuged and re-washed. The resin preparation after the last wash was added with 10 ml of 1x denaturing extraction buffer (**Appendix D**) and mixed gently to pre-equilibrate the resin. After spinning at 700 ×*g*, 25 ºC for 3 minutes, the supernatant was discarded. The bacterial homogenate was added to the resin tube and mixed gently on a rocking platform at 25 ºC for 2 hours to allow binding of the 6xHis-tagged HuScFv to the resin. The resin suspension was transferred to the gravity-flow column with an end-cap in place and allowed the resin to settle out of the suspension. The unbound fraction was allowed to flow through. The resin was

Copyright by Mahidol University

washed by adding 30 ml of 1x denaturing extraction buffer and allowed the buffer to drain out. The 6xHis-tagged protein bound to the resin was eluted by adding 10 ml of 1x denaturing elution buffer containing 500 mM imidazole (**Appendix D**) and kept as an eluted fraction. The resin was washed as above and kept in 20% ethanol for subsequent use. The purity of HuScFv-His preparation was analyzed by using 12% SDS-PAGE, CBB staining, and Western blotting as described in **section 4.2.1.12**. The purified HuScFv-His protein was refolded by adding gradually (drop-wise) PBS, at 4 ºC with stirring slowly. The refolding buffer was added until the concentration of urea decreased to nil. The HuScFv preparations were dialyzed against PBS at 4 ºC for 5 hours. Then, the preparation was centrifuged at 12,000 ×*g*, 4 ºC for 15 minutes to removed aggregates. The supernatants containing refolded 6xHis tagged-HuScFv were collected and analyzed again by 12% SDS-PAGE, CBB staining, and Western blotting. The concentration of each purified 6xHis tagged-HuScFv preparation was quantified by NanoDrop machine and multiplied with extinction coefficient scfv (ε = 1.4) (Layne, 1958; Stoscheck, 1990; Nielsen *et al*, 2000). The HuScFv(s) were kept appropriately at -20 ºC for subsequent use. Reactivity of the purified HuScFv to rM2 was re-verified by indirect ELISA and Western blot analysis using rM2 as the antigen and mouse monoclonal anti-6x-His antibody as the primary antibody for detecting the 6x-His tagged-HuScFv.

4.12 HuScFv mediated interference of virus replication cycle (Figure 4.1)

Three experimental designs for studying the HuScFv mediated interference of influenza virus replication cycle were performed:

Experimental design 1: influenza A viruses, subtype H1N1/2009 or subtype H5N1 (MOI 0.1) were mixed with purified HuScFv (400 ng, ~9.64 x 10^{12} molecules) from individual *E. coli* clones at 25 ºC for 2 hours before adding to MDCK cell monolayer in tissue culture wells (24-well tissue culture plates). Viruses exposed to rimantadine (0.8 µM, ~4.82 x 10^{17} molecules) and pAb-M2 (10 µg, ~4 x 10^{13} molecules) instead of the HuScFv were used as positive inhibition controls. The viruses in culture medium served as negative inhibition or infected cell control. The

plates were incubated in 5% CO_2 atmosphere at 37 °C for 1 hour to allow virus entry. Extracellular viruses in each well were discarded; the cells were rinsed with plain DMEM and replenished with viral growth medium. After incubation for 15 hours, the spent culture fluid of each well was collected and the cells were washed with plain DMEM and harvested. Quantitative real-time RT-PCR was used for enumeration of the viruses in the culture fluids and inside the cells. Plaque (foci) assay was also performed for comparing intracellular viruses among treatments. Three independent experiments were done.

Experimental design 2: influenza A viruses, subtype H1N1/2009 or subtype H5N1 (MOI 0.1) were allowed to infect the MDCK cells in 5% CO_2 atmosphere at 37 °C for 1 hour. After washing to remove extracellular viruses, purified HuScFv from individual *E. coli* clones, pAb-M2, and rimantadine in viral growth medium (at the same amounts that used in **experiment 1**) were added to individual well and incubated further for 15 hours. Then the spent culture fluid of each well and the cells were collected. Quantitative real-time RT-PCR and plaque (foci) assay were performed for comparing viruses among treatments.

Experimental design 3: influenza A viruses, subtype H1N1/2009 or subtype H5N1 (MOI 0.1) were mixed with purified HuScFv from individual *E. coli* clones, pAb-M2 and rimantadine (at the same amounts that used in **experiment 1**) at 25 ºC for 2 hours before adding to MDCK cell monolayer in tissue culture wells. The plates were incubated in 5% CO_2 atmosphere at 37 °C for 1 hour to allow virus entry. Extracellular viruses in each well were discarded; the cells were rinsed with plain DMEM and replenished with viral growth medium containing the purified HuScFv from individual *E. coli* clones, pAb-M2, and rimantadine, respectively. After incubation for 15 hours, the spent culture fluid of each well and the cells were collected. Quantitative real-time RT-PCR and plaque (foci) assay were performed for comparing viruses among treatments.

*For human influenza A virus infection (H1N1/2009), all three experimental designs were done in 96-well tissues culture plate, vaccinated/ convalescent human serum was used as positive inhibition control, and only plaque assay was performed for enumeration of the virus in the samples. Three independent experiments were done.

Copyright by Mahidol University

4.12.1 Plaque (foci) assay

Influenza virus plaques (foci) in the infected cells were revealed as described in section 4.1.2.3. Infected cells in each tissue culture well were washed with PBS, fixed with cold absolute methanol at 25 °C for 1 hour, washed again, and permeabilized by using 0.3% Triton X-100 in PBS for 20 minutes. The cells were blocked by incubating with 3% FBS at 25 °C, 1 hour. After washing, mouse PAb to rNP (1:3,000), goat anti-mouse-AP, and BCIP/NBT substrate were added, respectively, for color development. When the purple foci appeared under inverted microscope, the reaction was stopped by rinsing the cells with distilled water. The foci in the MDCK cell monolayer were observed and counted under a light inverted microscope.

4.12.2 Quantitative real-time RT-PCR (qPCR)

Viral RNA was extracted from 500 µl of each culture supernatant by using viral nucleic acid extraction kit II (Geneaid, New Taipei, Taiwan). The RNA was dissolved with 20 µl of DEPC-treated water. Total RNA was extracted from the virus infected cells by using total RNA purification kit (Jena Bioscience, Jena, Germany). The amount of total RNA in each preparation was measured by using NanoDrop ND-1000 Spectrophotometer and kept at -80 °C until use. In each qPCR reaction, either 2 µl of extracted RNA from the culture supernatant or 200 ng of total RNA from infected cells were subjected to viral RNA quantification using 1-step Brilliant II SYBR green qRT-PCR master mix kit (Agilent Technologies, California, USA). Each PCR master mix (12.5 µL) was prepared on ice with 2 × Brilliant II SYBR® Green QRT-PCR Master Mix, RT/RNase block enzyme, 200 nM of each primer specific to gene sequence coding for influenza A virus *M1*: forward 5'-cttctaaccgaggtcgaatcgta-3' and reverse 5'-tccatgagagcctcgagat-3', and RNA template. For total RNA from infected cell, amount of total RNA was normalized again with housekeeping gene: *actin* and each primer specific to *actin* gene coding sequence: forward 5'-gagcgggaaatcgtgcgtg-3' and reverse 5'-gaaggtagtttcgtggatg-3'. The qPCR was performed using Mx 3000PTM instrument (Stratagene, California, USA). The reaction mixture and the qPCR condition are shown below. A standard curve was constructed from Ct of ten-fold dilutions of the pET20b^{+} carrying gene sequence coding for M1

Copyright by Mahidol University

(ranged from 1000 to 1 ng or 2.07 x 10^{11} to 2.07 x 10^{8} copies). Ct of each sample was expressed as $\log_2$ of RNA copies calculated from the standard curve.

Real-time RT-PCR reaction mixture:

Ingredient	**Volume** (µl)
2x Brilliant II SYBR® Green QRT-PCR master mix	6.25
10 µM Forward primer: *M1* or *actin*	0.2
10 µM Reverse primer: *M1* or *actin*	0.2
RT/RNase block enzyme	0.1
RNA sample	x
UDW	5.75-x
Total	**12.5**

The thermal cycle program was set as the following:

1. Reverse transcription at 42 ºC for 1 hour
2. First denaturation at 95 ºC for 10 minutes
3. Denaturation at 95 ºC for 1 minute
4. Annealing at 58 ºC for 1 minute
5. Extension at 72 ºC for 1 minute
6. Repeat steps 2-4 for 40 cycles
7. Analysis the dissociation curve and melting temperature: 95 °C for 1 minute then ramped down to 55 °C (0.5 °C/s) for 45 seconds and ramped up to 95 °C

Copyright by Mahidol University

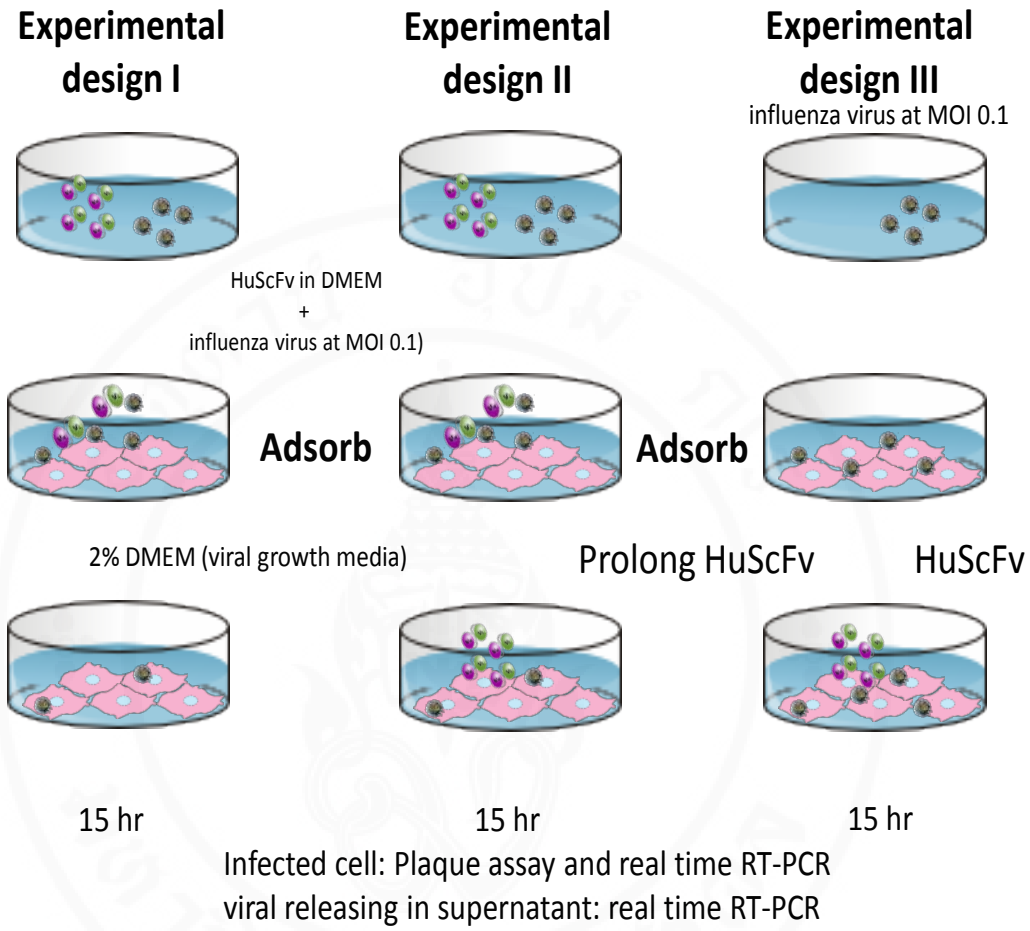

Figure 4.1 Three experimental designs for studying the HuScFv mediated interference of influenza virus replication cycle

Copyright by Mahidol University

4.13 Phage mimotope, HuScFv epitopes and validation of the phage mimotope

4.13.1 Determination of epitopes of the HuScFv by means of phage mimotope identification

The 12-mer peptides displayed on M13 phage [ph.D.-12^{TM} Phage Display Peptide Library Kit (New England BioLabs, Massachusetts, USA)] was used to identify phage mimotopes (peptides) of the rM2 specific-HuScFv. Each well of an ELISA plate was coated with 1 µg of individual HuScFv in 100 µl of PBS at 4 ºC for 16 hours. After washing the unbound protein with TBST, the coated wells were blocked with 3% BSA in TBS at 4 ºC for 1 hour. Peptide displaying phages (100 µl of diluted 1:100 in TBST which contained ~1.5 x 10^{11} pfu) was added to the HuScFv coated well. The plate was agitated gently on a rocking platform at 25 ºC for 1 hour. After extensive washing to remove unbound phages, HuScFv bound phages were eluted from the well surface by adding 100 µl of 0.2 M glycine-HCl, pH 2.2 (**Appendix I**) into the well and kept at 25 ºC for 10 minutes. The eluate was added to a tube containing 15 µl of 2 M Tris-base solution (**Appendix I**) to neutralize the pH of the phage suspension. The phages were amplified by infecting 20 ml of early log phage ER2738 *E. coli* (OD_{600nm}~0.3-0.4) at 37 ºC with shaking at 250 rpm for 4 hours. After removing the bacterial cells by centrifugation, the amplified phages in the supernatant were precipitated by adding 1/6 volume of PEG/NaCl (**Appendix I**) and the mixture was kept on ice at 4 ºC for 16 hours before centrifugation. The phages in the pellet were re-suspended in 0.1% TBST and used in the next round of bio-panning.

After three rounds of bio-panning, the eluted and neutralized phages from the last bio-panning round were diluted 1:1,000 with LB broth (**Appendix B**) and 10 µl of the diluted phage suspension were added to 200 µl of log phase ER2738 *E. coli* and the mixture was incubated at 25 ºC for 5 minutes. The mixture was then added to 3 ml of 45 ºC pre-warmed-top agarose and poured onto LB agar plate containing IPTG and X-gal. On the next day, phage titer was calculated from the number of blue plaques appeared on the agar plate.

Copyright by Mahidol University

The blue plaques of phages from the third round of bio-panning were individually picked and allowed to infect 5 ml of ER2738 *E. coli* for 6 hours. After removing bacterial cells, 1 ml of the phages was mixed with glycerol at final concentration 20% and kept at -80 ºC. The phage genome was extracted from the culture supernatant by using equal volume of phenol/chloroform. A volume of the upper phase (900 µl) of the extraction mixture was collected and 900 µl of absolute ethanol were added to precipitate the phage DNA. DNA pellet was washed by adding 500 µl of 70% ethanol and centrifuged. The preparation was air-dried before re-suspending in 50 µl of UDW. The DNA was subjected to 0.8% agarose gel electrophoresis, ethidium bromide staining and visualized by UV-transilluminator before DNA sequencing by using 96 sequencing primer (5'-gccctcatagttagcgtaacg-3') according to kit manual protocol. The DNA sequences were translated by using TRANSEQ program and the peptide sequences (phage mimotopes) were aligned with monomeric or tetrameric M2 linear sequences of drug sensitive and resistant A/H5N1 viruses (Accession numbers AY651385.1 for clade 1 and AB478035.1 for clade 2) by using CLUSTALW 2.0.5 multiple sequence alignments for identification of presumptive M2 residues bound by the HuScFv (epitopes).

4.13.2 ELISA inhibition for verification of the phage mimotopes

Phage clones displaying the mimotopes that bound to the HuScFv were tested in competitive ELISA for determining their capacity in blocking the binding HuScFv to rM2. Mimotopic phages were propagated in ER2738 *E. coli* and the titers of the amplified phages were determined according to manufacturer's instruction. Various amounts (10^4, 10^5 and 10^6 plaque forming units; pfu) of the phages (50 µl) were mixed individually with fixed amount of HuScFv (5 µg in 50 µl) and incubated at 37 °C for 1 hour. The HuScFv mixed with irrelevant phage mimotope [CF-6 (mimotope specific to Can f1): HIWWGPQPWMEP] served as background inhibition control and HuScFv in buffer were negative inhibition controls (maximum binding, 100%). After adding individual mixtures to the rM2 coated wells and incubated, all wells were washed and mouse monoclonal anti-E tag antibody, goat anti-mouse IgG-HRP conjugate and ABTS substrate were added, respectively, with washing between steps. OD_{405nm} of the content of each wells were determined against the background

Copyright© by Mahidol University

binding controls. The % ELISA inhibition was calculated: % ELISA inhibition = [(OD_{405nm} of maximum binding - OD_{405nm} of test) ÷ (OD_{405nm} maximum binding)].

4.14 Homology modeling and molecular docking to determine the regions and residues of tetrameric M2 ion channel bound by HuScFv

The selected HuScFv and M2 amino acid sequences were identified by using a Discovery studio (DS) database. Three dimensional (3D) structures of the sequences that provided maximum identities were used as templates for homology modeling. The modeled structures were validated by PROCHECK analysis. Complex structures between the modeled rM2 and HuScFv were predicted by using rigid bodies docking technique. The ZDOCK and RDOCK modules embedded on Discovery Studio program were used as tools for docking calculation and structural refinement, respectively. The modelled M2 was set as input receptor and the HuScFv as ligands. The dock complexes with the lowest RDOCK energy were determined for identification of the regions and residues of the tetrameric M2 ion channel interacting with the HuScFv.

4.15 Multiple alignments of M2 sequences of various subtypes and H5N1 clades causing human influenza infection

The M2 amino acid sequences of type A (AM2) influenza including H1N1, H3N2, H5N1 (clades 0, 1, 2 and 7 which infect humans), H7N3, H7N9 and H9N2 were retrieved from Influenza virus resource database available from the NCBI database (http://www.ncbi.nlm.nih.gov/protein). Multiple alignments were performed by using program MAFFT version 7. The alignments were verified following the algorithm of semi-homology. The verification concerned the possible genetic relationship between compared positions which were possible replacements by single transition/transversion.

Copyright by Mahidol University

4.16 Determination of hemagglutination inhibition (HI) activity of HA1-specific-HuScFv against 4HAU of H1N1/2009 virus

Hemagglutination inhibition assay (HI) was used for testing *in vitro* activity of the HA1 specific HuScFv in inhibiting the influenza virus binding to the host cell receptors. HuScFv derived from individual *E. coli* lysates were standardized based on the Western blot band intensities. Serial dilutions of the standardized HuScFv were prepared in wells of a microtiter plate (25 µl per well). Equal volumes of the virus containing 4 HAU were added to all wells and the plate was kept at 25 ºC for 1 hour. Vaccinated/convalescent human serum against was used as positive inhibition control. Fifty µl of the 1% group O hRBC in PBS was added to each well and the plate was kept untill 100% hemagglutination appeared in the hemagglutination positive control wells or well that contained only lysate of *E. coli* carrying only phagemid (no HuScFv), virus and hRBC. Wells that contained only the hRBC and PBS (without the virus; negative hemagglutination control) showed a button-like appearance at the well bottom. The HI titer is the highest dilution of HuScFv that caused complete inhibition of the 4 HAU of the virus.

4.17 Determination of ability of the M2 specific-HuScFv in inhibition of the bio-functions of their respective antigen

4.17.1 Determination of the ability of M2 specific-HuScFv in inhibiting influenza A virus forming macroautophagy (accumulation of autophagosomes) in infected cells

4.17.1.1 Protocal of neutralization [HuScFv mediated interference of macroautophagy (accumulation of autophagosomes) in influenza virus infected cells]

Influenza A viruses, subtype H5N1/NP172 (MOI 0.5) were allowed to infect the MDCK cells in 5% CO_2 atmosphere at 37 °C for 1 hour. After washing to remove extracellular viruses, the purified HuScFv from individual *E. coli* clones, pAb-M2, and rimantadine in viral growth medium were added to individual

Copyright © by Mahidol University

wells and incubated further in 5% CO_2 atmosphere at 37 °C for 24 hours. Then cells in each well were collected. The amounts of LC3-II mRNA were determined by using qPCR in comparison with positive virus infected cell control (MDCK cells infected with the viruses) and normal MDCK cells.

4.17.1.2 Detection of macroautophagosome formation with LC3-II mRNA by using qPCR

Total RNA was extracted from the virus infected cells by using total RNA purification kit (Jena Bioscience, Jena, Germany). The amount of total RNA in each preparation was measured by using NanoDrop ND-1000 Spectrophotometer and kept at -80 °C until use. In each qPCR reaction, 200 ng of total RNA of the infected cells/controls were subjected to viral RNA quantification using 1-step Brilliant II SYBR green qRT-PCR master mix kit (Agilent Technologies, California, USA). Each PCR master mix (12.5 µl) was prepared on ice with 2xBrilliant II SYBR® Green QRT-PCR Master Mix, RT/RNase block enzyme, 200 nM of each primer specific to gene sequence coding for *LC3-II*: forward 5'-gagaagcagcttcctgttctgg-3' and reverse 5'-gtgtccgttcaccaacagcaag-3', primer specific to gene sequence coding for influenza A virus *M1*: forward 5'-cttctaaccgaggtcgaatcgta-3' and reverse 5'-tccatgagagcctcgagat-3', and RNA template. For total RNA from infected cell, amount of total RNA was normalized again with house-keeping gene, *β-actin.* The primers specific to the β-actin gene coding sequence were: forward 5'-gagcgggaaatcgtgcgtg-3' and reverse 5'-gaaggtagtttcgtggatg-3'. The qPCR was performed using Mx 3000PTM instrument (Stratagene, California, USA). The reaction mixture and the qPCR condition are shown below:

Copyright by Mahidol University

Real-time RT-PCR reaction mixture:

Ingredient	**Volume** (µl)
Brilliant II SYBR® Green QRT-PCR master mix, 2x	6.25
Forward primer (10 µM): *LC3-II, M1* or *β-actin*	0.2
Reverse primer (10 µM): *LC3-II, M1* or *β-actin*	0.2
RT/RNase block enzyme	0.1
RNA sample	x
UDW	5.75-x
Total	**12.5**

The thermal cycle program was set as the following:

1. Reverse transcription at 42 ºC for 1 hour
2. First denaturation at 95 ºC for 10 minutes
3. Denaturation at 95 ºC for 1 minute
4. Annealing at 58 ºC for 1 minute
5. Extension at 72 ºC for 1 minute
6. Repeat steps 2-4 for 40 cycles
7. Analysis the dissociation curve and melting temperature: 95 °C for 1 min then ramped down to 55 °C (0.5 °C/s) for 45 seconds and ramped up to 95 °C

4.18 Statistical analysis

Means and standard deviations (SD) of $\log_2$ of M1 mRNA derived from triplicate cell culture wells of three independent experiments were used for comparison between tests and controls. *P* value < 0.05 of unpaired *t*-test was taken as significant difference by using SPSS program.

Copyright by Mahidol University

CHAPTER V
RESULTS

5.1 Production and purification of recombinant influenza proteins [HA (HA0, HA1 and HA2), NA, M2, and NP]

5.1.1 Results of molecular cloning of cDNA of HA0-, HA1- and HA2-coding sequences

The recombinant HA (rHA) was designed into 3 types (rHA0, rHA1 and rHA2) which depended on topology and functions of HA protein. The rHA0 or full length rHA consists of HA1 and HA2 divided by cleavage site of protease enzyme, and this rHA0 composes of amino acid residue 37 to 585 (548 residue) which deleted signal peptide sequences. The rHA1 is the globular head of HA protein containing receptor-binding site that composes of amino acid residue 37 to 401 (364 residue). The rHA2 is stem of the HA protein containing fusion peptide that is important for fusion with host cell membrane in virus uncoating and this rHA2 composes of amino acid residue 401 to 585 (184 residue). The schematic of recombinant HA (rHA0, rHA1 and rHA2) show in **Figure 5.1**.

5.1.1.1 Viral RNA extraction

Total RNA of influenza virus A/Thailand/CU41/2006 (H1N1) was extracted from supernatant of infected MDCK cells. The ratio of optical densities at A_{260nm} and A_{280nm} of the preparation was 2.14 implying high purity of the preparation.

5.1.1.2 Complementary DNA (cDNA) synthesis and amplification of cDNA of HA0-, HA1- and HA2-coding sequences

Copyright by Mahidol University

First strand cDNA was synthesized from the viral RNA by using Uni-12 primers. Then the cDNA was used as a template for amplification of cDNA of HA0-, HA1- and HA2- coding sequences by using HA specific primers set

from **Table 4.2** of **Chapter IV**. The $HA0_{37\text{-}585}$, $HA1_{37\text{-}401}$ and $HA2_{402\text{-}585}$ cDNA amplified products (1,644, 1,092 and 552 bp) are shown in **Figure 5.1.**

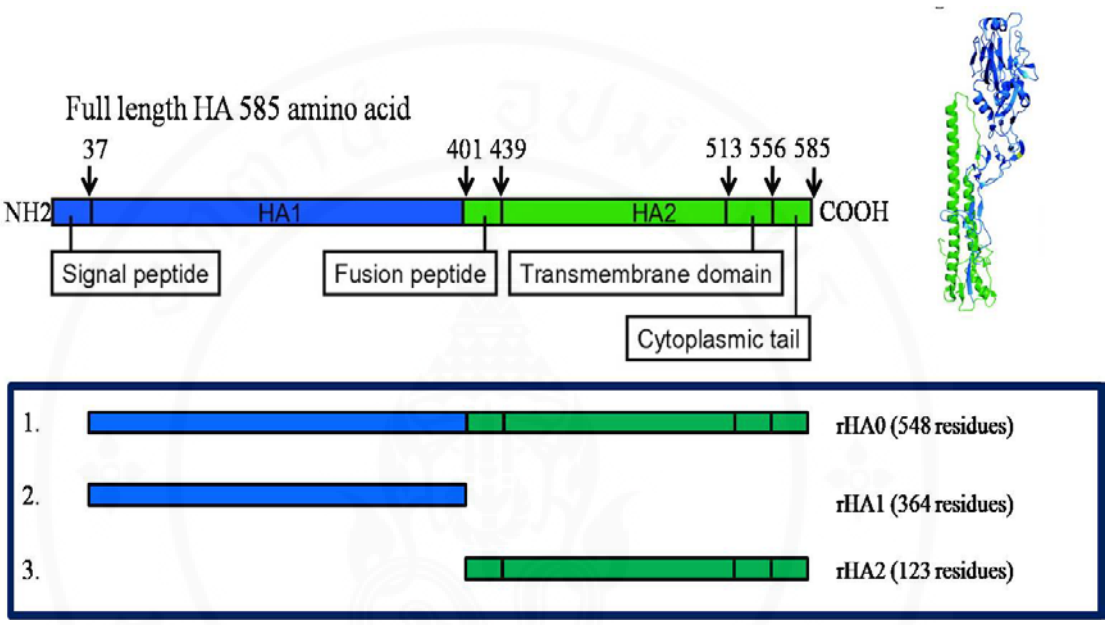

Figure 5.1 Schematic picture of the HA protein and the recombinant HA (rHA0, rHA1 and rHA2). The HA protein is divided into 2 parts (HA1 and HA2) depended on topology and their functions. The recombinant HA (rHA0, rHA1 and rHA2) show in blue box.

Copyright by Mahidol University

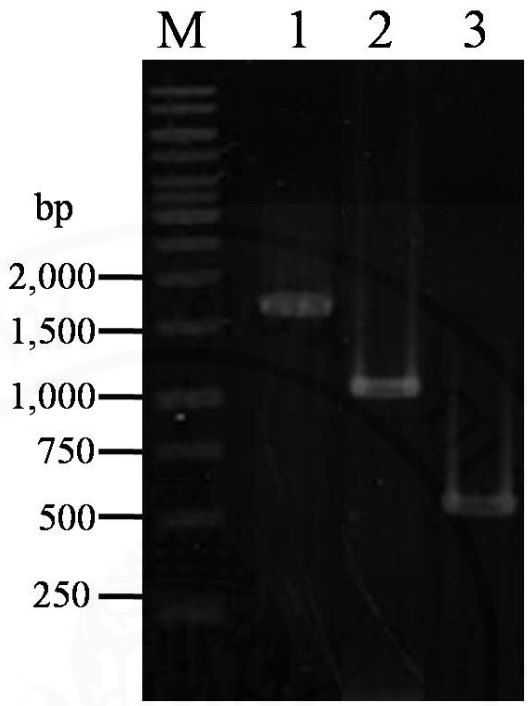

Figure 5.2 PCR amplicons of cDNA of HA0-, HA1- and HA2-coding sequences

Lane M, GeneRuler 1 kb DNA ladder

Lane 1, PCR amplicon of cDNA of HA0-coding sequence

Lane 2, PCR amplicon of cDNA of HA1-coding sequence

Lane 3, PCR amplicon of cDNA of HA2-coding sequence

Numbers at the left are DNA sizes in bp

Copyright by Mahidol University

5.1.1.3 Cloning of the HA0-, HA1- and HA2-coding sequences into cloning vector and introduction of the recombinant plasmids into competent *E. coli* (bacterial transformation)

HA0-, HA1- and HA2-coding sequences were separately ligated into TOPO® cloning vectors before introducing individual recombinant plasmids into the competent JM109 *E. coli*. Ten white colonies of the bacterial transformants that grown on each selective agar plates after incubation at 37 ºC overnight were randomly selected and used as the templates for amplification of the HA0-, HA1- and HA2-coding sequences. It was found that some colonies revealed amplicons of the *ha0, ha1* and *ha2* gene inserts seen as DNA bands at ~1,800, 1,200 and 600 bp (including franking region from M13 primer ~100 bp), respectively (**Figure 5.3**).

5.1.1.4 Extraction of the recombinant plasmids with the HA0, HA1 and HA2 gene inserts from the JM109 *E. coli* transformants and endonuclease digestions of the recombinant plasmids

Recombinant plasmids with the *ha0, ha1* and *ha2* gene inserts were extracted from the JM109 *E. coli* colonies of **section 4.2.1.11** by alkaline lysis method (lane 1-3 of **Figure 5.4**). After digesting doubly with *Bam*HI and *Hin*dIII, the cloning vectors were linearized as shown as an upper band (~2,500 bp) of **Figure 5.4**, while the band of HA0-, HA1- and HA2-coding sequences are as lower DNA bands at ~1,700, 1,100 and 500 bp, respectively (**lane 4, 5, and 6 of Figure 5.4**).

5.1.1.5 Cloning of the cut recombinant plasmids into expression vectors and introduction of the *HA0, HA1, HA2*-expression vectors into the competent *E. coli* (bacterial transformation)

The doubly digested HA0-, HA1- and HA2-coding sequences and expression plasmids (pQE30 and pET23a$^+$) previously cut with the same endonucleases were ligated, then the rHA0-pQE30 and rHA1-pQE30 are introduced into M15 *E. coli* and rHA2-pET23a$^+$ are introduced into BL21 (DE3) *E. coli*. The transformants grown on the selective agar plates were screened for the HA0, HA1 and HA2 gene sequences by PCR using specific primers. **Figure 5.5** shows the presence of gene amplicons at ~ 1,700, 1,100 and 500 bp from the selected transformant clones which are the expected sizes of the HA0, HA1 and HA2 gene amplicons, respectively.

Copyright by Mahidol University

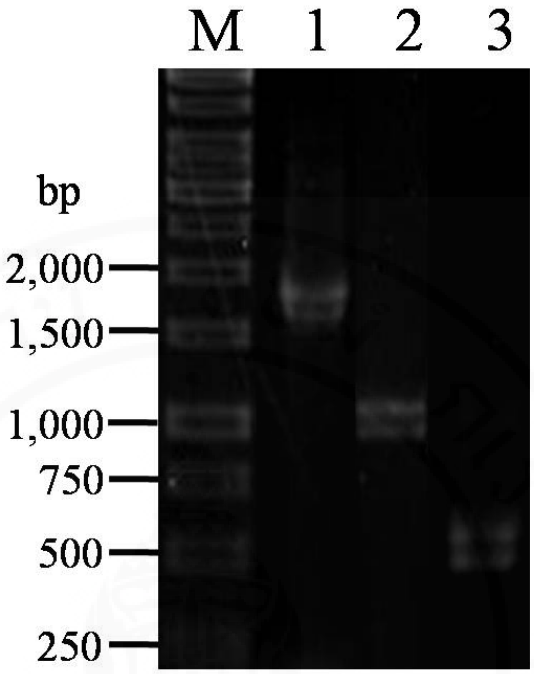

Figure 5.3 PCR amplicons of HA0-, HA1- and HA2-coding sequences (~1,800, 1,200 and 600 bp including franking region from M13 primer ~100 bp) in TOPO® vectors amplified from randomized colonies (Figure shows representatives of positive clones) of JM109 *E. coli* as DNA templates (lanes 1-3); implying that all of the three representative colonies carried the recombinant plasmids with HA0, HA1 and HA2 DNA inserts, respectively.

Lane M, GeneRuler 1 kb DNA ladder

Lane 1, PCR amplicon of HA0-coding sequence in TOPO® vector

Lane 2, PCR amplicon of HA1-coding sequence in TOPO® vector

Lane 3, PCR amplicon of HA2-coding sequence in TOPO® vector

Numbers at the left are DNA sizes in bp

Copyright by Mahidol University

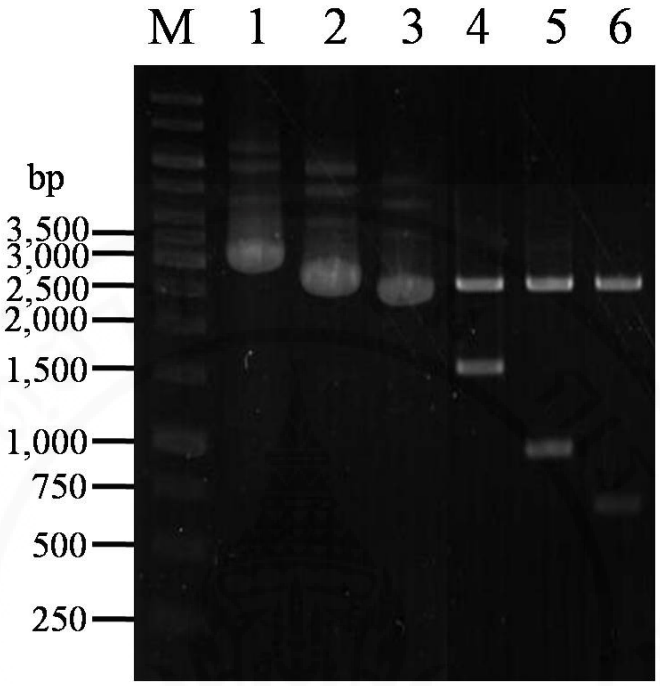

Figure 5.4 DNA patterns of cloning vectors harboring HA0-, HA1-, HA2-coding sequences extracted from JM109 *E. coli* transformants before and after restriction endonucleases digestion

Lane M, GeneRuler 1 kb DNA ladder

Lane 1, Recombinant plasmid DNA with HA0 gene insert

Lane 2, Recombinant plasmid DNA with HA1 gene insert

Lane 3, Recombinant plasmid DNA with HA2 gene insert

Lane 4, Recombinant plasmid DNA after *Bam*HI/*Hin*dIII restriction endonucleases digestion showing linearized vector (upper band) and HA0-coding sequence (lower band at ~1,700 bp)

Lane 5, Recombinant plasmid DNA after *Bam*HI/*Hin*dIII restriction endonucleases digestion showing linearized vector (upper band) and HA1-coding sequence (lower band at ~1,100 bp)

Lane 6, Recombinant plasmid DNA after *Bam*HI/*Hin*dIII restriction endonucleases digestion showing linearized vector (upper band) and HA2-coding sequence (lower band at ~500 bp)

Numbers at the left are DNA sizes in bp

Copyright© by Mahidol University

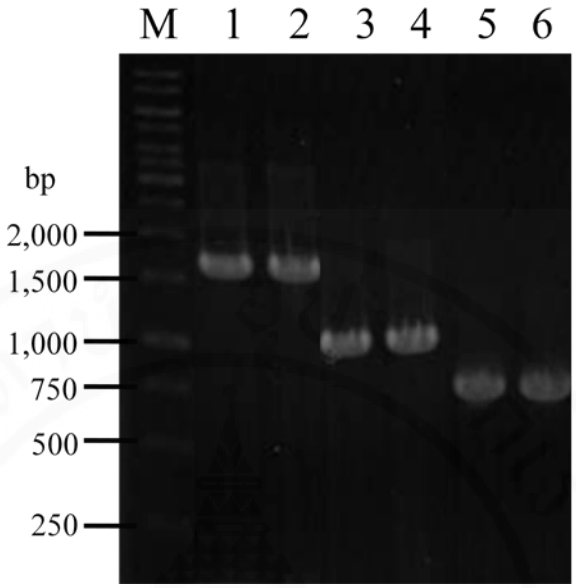

Figure 5.5 PCR amplicons of HA0-, HA1- and HA2-coding sequences in expression vectors (~1,700, 1,100 and 500 bp, respectively) from representative *E. coli* transformants

Lane M, GeneRuler 1 kb DNA ladder

Lane 1-2, Amplicons of HA0-coding sequences from two representative transformed M15 *E. coli* colonies

Lane 3-4, Amplicons of HA1-coding sequences from two representative transformed M15 *E. coli* colonies

Lane 5-6, Amplicons of HA2-coding sequences from two representative transformed BL21(DE3) *E. coli* colonies

Numbers at the left are DNA sizes in bp

Copyright by Mahidol University

For verification of amino acid sequences of the rHA0, rHA1 and rHA2, the recombinant plasmids were extracted and sequenced. The deduced amino acids which translated from nucleotide sequences were then aligned with the amino acid sequence coding for the influenza A virus HA from NCBI database. It was found that the cloned HA0, HA1 and HA2 deduced amino acids showed 100%, 99% and 100% identity, respectively, with the hemagglutinin amino acid sequence of influenza A virus [A/Thailand/CU41/2006 (H1N1) (accession number: ABS71664.1)] of the database which was used for preparing cDNA template for cloning (**Figures 5.6-5.8**).

Copyright by Mahidol University

A

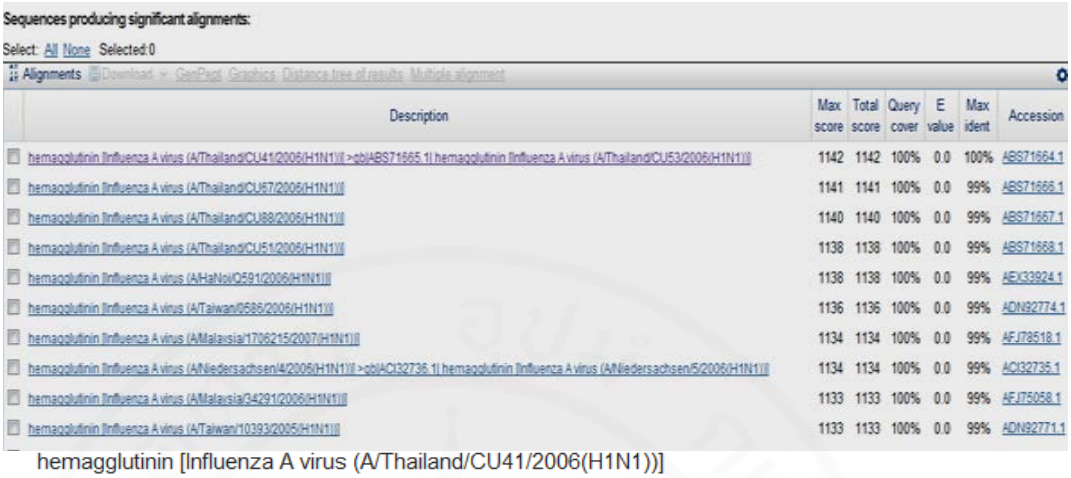

Sequences producing significant alignments:

Select: All None Selected: 0

Alignments Download GenPept Graphics Distance tree of results Multiple alignment

Description	Max score	Total score	Query cover	E value	Max ident	Accession
hemagglutinin [Influenza A virus (A/Thailand/CU41/2006/H1N1)] >gb|ABS71665.1| hemagglutinin [Influenza A virus (A/Thailand/CU53/2006/H1N1)]	1142	1142	100%	0.0	100%	ABS71664.1
hemagglutinin [Influenza A virus (A/Thailand/CU67/2006/H1N1)]	1141	1141	100%	0.0	99%	ABS71666.1
hemagglutinin [Influenza A virus (A/Thailand/CU88/2006/H1N1)]	1140	1140	100%	0.0	99%	ABS71667.1
hemagglutinin [Influenza A virus (A/Thailand/CU51/2006/H1N1)]	1138	1138	100%	0.0	99%	ABS71668.1
hemagglutinin [Influenza A virus (A/HaNoi/OF591/2006/H1N1)]	1138	1138	100%	0.0	99%	AEX33924.1
hemagglutinin [Influenza A virus (A/Taiwan/0586/2006/H1N1)]	1136	1136	100%	0.0	99%	ADN92774.1
hemagglutinin [Influenza A virus (A/Malaysia/1706215/2007/H1N1)]	1134	1134	100%	0.0	99%	AFJ78518.1
hemagglutinin [Influenza A virus (A/Niedersachsen/4/2006/H1N1)] >gb|ACI32736.1| hemagglutinin [Influenza A virus (A/Niedersachsen/5/2006/H1N1)]	1134	1134	100%	0.0	99%	ACI32735.1
hemagglutinin [Influenza A virus (A/Malaysia/34291/2006/H1N1)]	1133	1133	100%	0.0	99%	AFJ75058.1
hemagglutinin [Influenza A virus (A/Taiwan/10393/2005/H1N1)]	1133	1133	100%	0.0	99%	ADN92771.1

B

hemagglutinin [Influenza A virus (A/Thailand/CU41/2006(H1N1))]

Sequence ID: gb|ABS71664.1| Length: 565 Number of Matches: 1

See 1 more title(s)

Range 1: 18 to 565 GenPept Graphics Next Match Previous Match

Score	Expect	Method	Identities	Positives	Gaps
1142 bits(2955)	0.0	Compositional matrix adjust.	548/548(100%)	548/548(100%)	0/548(0%)

```
Query  1    DTICIGYHANNSTDTVDTVLEKNVTVTHSVNLLEDSHNGKLCLLKGIAPLQLGNCSVAGW  60
            DTICIGYHANNSTDTVDTVLEKNVTVTHSVNLLEDSHNGKLCLLKGIAPLQLGNCSVAGW
Sbjct  18   DTICIGYHANNSTDTVDTVLEKNVTVTHSVNLLEDSHNGKLCLLKGIAPLQLGNCSVAGW  77

Query  61   ILGNPECESLISRESWSYIVEKPSPENGTCYPGHFADYEELREQLSSVSSFERFEIFPKE  120
            ILGNPECESLISRESWSYIVEKPSPENGTCYPGHFADYEELREQLSSVSSFERFEIFPKE
Sbjct  78   ILGNPECESLISRESWSYIVEKPSPENGTCYPGHFADYEELREQLSSVSSFERFEIFPKE  137

Query  121  SSWPNHTATGVSASCSHNGESSFYKNLLWLTGKNGLYPNLSKSYANNKEKEVLVLWGVHH  180
            SSWPNHTATGVSASCSHNGESSFYKNLLWLTGKNGLYPNLSKSYANNKEKEVLVLWGVHH
Sbjct  138  SSWPNHTATGVSASCSHNGESSFYKNLLWLTGKNGLYPNLSKSYANNKEKEVLVLWGVHH  197

Query  181  PPNIGDQRALYHTENAYVSVVSSHYSRKFTPEIAKRPKVRDQEGRISYYWTLLEPGDTII  240
            PPNIGDQRALYHTENAYVSVVSSHYSRKFTPEIAKRPKVRDQEGRISYYWTLLEPGDTII
Sbjct  198  PPNIGDQRALYHTENAYVSVVSSHYSRKFTPEIAKRPKVRDQEGRISYYWTLLEPGDTII  257

Query  241  FEANGNLIAPRYAFALSRGFGSGIINSNAPMDECDAKCQTPQGAINSSLPFQNVHPVTIG  300
            FEANGNLIAPRYAFALSRGFGSGIINSNAPMDECDAKCQTPQGAINSSLPFQNVHPVTIG
Sbjct  258  FEANGNLIAPRYAFALSRGFGSGIINSNAPMDECDAKCQTPQGAINSSLPFQNVHPVTIG  317

Query  301  ECPKYVRSAKLRMVTGLRNIPSIQSRGLFGAIAGFIEGGWTGMVDGWYGYHHQNEQGSGY  360
            ECPKYVRSAKLRMVTGLRNIPSIQSRGLFGAIAGFIEGGWTGMVDGWYGYHHQNEQGSGY
Sbjct  318  ECPKYVRSAKLRMVTGLRNIPSIQSRGLFGAIAGFIEGGWTGMVDGWYGYHHQNEQGSGY  377

Query  361  AADQKSTQNAINGITNKVNSVIEKMNTQFTAVGKEFNKLERRMENLNKKVDDGFIDIWTY  420
            AADQKSTQNAINGITNKVNSVIEKMNTQFTAVGKEFNKLERRMENLNKKVDDGFIDIWTY
Sbjct  378  AADQKSTQNAINGITNKVNSVIEKMNTQFTAVGKEFNKLERRMENLNKKVDDGFIDIWTY  437

Query  421  NAELLVLLENERTLDFHDSNVKNLYEKVKSQLKNNAKEIGNGCFEFYHKCNDECMESVKN  480
            NAELLVLLENERTLDFHDSNVKNLYEKVKSQLKNNAKEIGNGCFEFYHKCNDECMESVKN
Sbjct  438  NAELLVLLENERTLDFHDSNVKNLYEKVKSQLKNNAKEIGNGCFEFYHKCNDECMESVKN  497

Query  481  GTYDYPKYSEESKLNREKIDGVKLESMGVYQILAIYSTVASSLVLLVSLGAISFWMCSNG  540
            GTYDYPKYSEESKLNREKIDGVKLESMGVYQILAIYSTVASSLVLLVSLGAISFWMCSNG
Sbjct  498  GTYDYPKYSEESKLNREKIDGVKLESMGVYQILAIYSTVASSLVLLVSLGAISFWMCSNG  557

Query  541  SLQCRICI  548
            SLQCRICI
Sbjct  558  SLQCRICI  565
```

Figure 5.6 Amino acid sequence which was deduced from the HA0-nucleotide sequence was subjected to BLASP search across HA0-coding sequence in the databases. (**A**), first ten amino acid sequences from NCBI database show that the rHA0 match with hemagglutinins of influenza A subtype H1N1. **(B),** the amino acid sequence of the cloned HA0 matched with 100% identity with the hemagglutinin of influenza A virus [A/Thailand/CU41/2006 (H1N1) (accession number: ABS71664.1)] of database which was used for preparing cDNA template for cloning of the HA0.

Copyright by Mahidol University

A

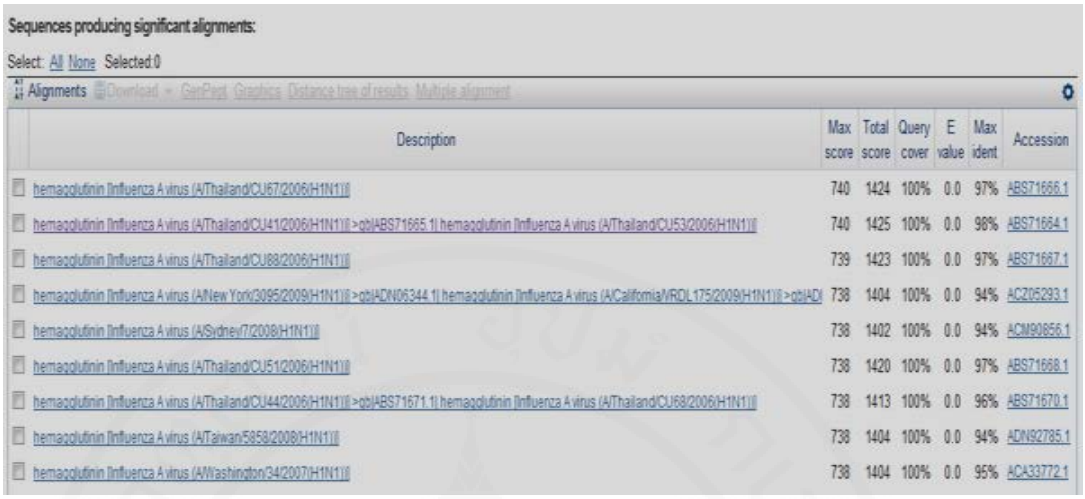

Sequences producing significant alignments:

Select: All None Selected 0

Alignments Download GenPept Graphics Distance tree of results Multiple alignment

Description	Max score	Total score	Query cover	E value	Max ident	Accession
hemagglutinin [Influenza A virus (A/Thailand/CU67/2006(H1N1)]	740	1424	100%	0.0	97%	ABS71666.1
hemagglutinin [Influenza A virus (A/Thailand/CU41/2006(H1N1)] >gb|ABS71665.1| hemagglutinin [Influenza A virus (A/Thailand/CU53/2006(H1N1)]	740	1425	100%	0.0	98%	ABS71664.1
hemagglutinin [Influenza A virus (A/Thailand/CU88/2006(H1N1)]	739	1423	100%	0.0	97%	ABS71667.1
hemagglutinin [Influenza A virus (A/New York/3095/2009(H1N1)] >gb|ADN06344.1| hemagglutinin [Influenza A virus (A/California/VRDL175/2009(H1N1)] >gb|ADI	738	1404	100%	0.0	94%	AC205293.1
hemagglutinin [Influenza A virus (A/Sydney/7/2008(H1N1)]	738	1402	100%	0.0	94%	ACM90856.1
hemagglutinin [Influenza A virus (A/Thailand/CU51/2006(H1N1)]	738	1420	100%	0.0	97%	ABS71668.1
hemagglutinin [Influenza A virus (A/Thailand/CU44/2006(H1N1)] >gb|ABS71671.1| hemagglutinin [Influenza A virus (A/Thailand/CU68/2006(H1N1)]	738	1413	100%	0.0	96%	ABS71670.1
hemagglutinin [Influenza A virus (A/Taiwan/5858/2008(H1N1)]	738	1404	100%	0.0	94%	ADN92785.1
hemagglutinin [Influenza A virus (A/Washington/34/2007(H1N1)]	738	1404	100%	0.0	95%	ACA33772.1

B

hemagglutinin [Influenza A virus (A/Thailand/CU41/2006(H1N1))]

Sequence ID: gb|ABS71664.1| Length: 565 Number of Matches: 1

▶ See 1 more title(s)

Range 1: 18 to 342 GenPept Graphics ▼ Next Match ▲ Previous Match

Score	Expect	Method	Identities	Positives	Gaps
677 bits(1748)	0.0	Compositional matrix adjust.	323/325(99%)	324/325(99%)	0/325(0%)

```
Query  1    DTICIGYHANNSTDTVDTVLEKNATVTHSVNLLEDSHNGKLCLLKGIAPLQLGNCSVAGW  60
            DTICIGYHANNSTDTVDTVLEKN TVTHSVNLLEDSHNGKLCLLKGIAPLQLGNCSVAGW
Sbjct  18   DTICIGYHANNSTDTVDTVLEKNVTVTHSVNLLEDSHNGKLCLLKGIAPLQLGNCSVAGW  77

Query  61   ILGNPECESLISRESWSYIVEKPSPENGTCYPGHFADYEELREQLSSVSSFERFEIFPKE  120
            ILGNPECESLISRESWSYIVEKPSPENGTCYPGHFADYEELREQLSSVSSFERFEIFPKE
Sbjct  78   ILGNPECESLISRESWSYIVEKPSPENGTCYPGHFADYEELREQLSSVSSFERFEIFPKE  137

Query  121  SSWPNHTATGVSASCSHNGESSFYKNLLWLTGKNGLYPNLSKSYANNKEKEVLVLWGVHH  180
            SSWPNHTATGVSASCSHNGESSFYKNLLWLTGKNGLYPNLSKSYANNKEKEVLVLWGVHH
Sbjct  138  SSWPNHTATGVSASCSHNGESSFYKNLLWLTGKNGLYPNLSKSYANNKEKEVLVLWGVHH  197

Query  181  PPNIGNQRALYHTENAYVSVVSSHYSRKFTPEIAKRPKVRDQEGRISYYWTLLEPGDTII  240
            PPNIG+QRALYHTENAYVSVVSSHYSRKFTPEIAKRPKVRDQEGRISYYWTLLEPGDTII
Sbjct  198  PPNIGDQRALYHTENAYVSVVSSHYSRKFTPEIAKRPKVRDQEGRISYYWTLLEPGDTII  257

Query  241  FEANGNLIAPRYAFALSRGFGSGIINSNAPMDECDAKCQTPQGAINSSLPFQNVHPVTIG  300
            FEANGNLIAPRYAFALSRGFGSGIINSNAPMDECDAKCQTPQGAINSSLPFQNVHPVTIG
Sbjct  258  FEANGNLIAPRYAFALSRGFGSGIINSNAPMDECDAKCQTPQGAINSSLPFQNVHPVTIG  317

Query  301  ECPKYVRSAKLRMVTGLRNIPSIQS  325
            ECPKYVRSAKLRMVTGLRNIPSIQS
Sbjct  318  ECPKYVRSAKLRMVTGLRNIPSIQS  342
```

Figure 5.7 Amino acid sequence deduced from the HA1-nucleotide sequence was subjected to BLASTP search across HA1-coding sequence in the NCBI databases. (**A**), first ten amino acid sequences from NCBI database show that the rHA1 match with hemagglutinins of influenza A subtype H1N1. (**B),** the sequence of the cloned HA1 sequence matched with 99% identity (with V24A and D186N substitutions) with the hemagglutinin of influenza A virus [A/Thailand/CU41/2006 (H1N1) (accession number: ABS71664.1)] of database which was used for preparing cDNA template for the HA1 cloning.

Copyright by Mahidol University

A

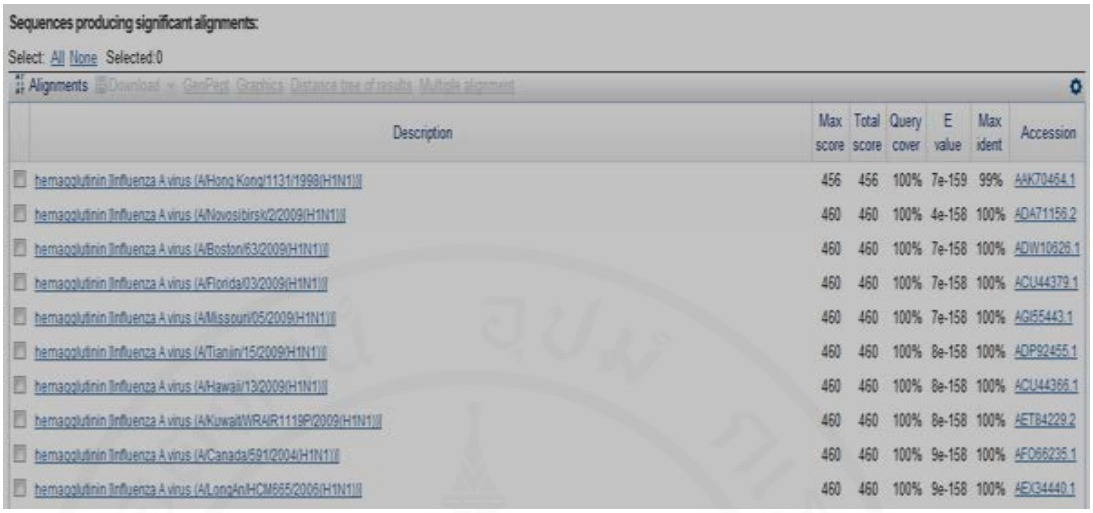

Sequences producing significant alignments:

Select: All None Selected:0

Alignments Download GenPept Graphics Distance tree of results Multiple alignment

Description	Max score	Total score	Query cover	E value	Max ident	Accession
hemagglutinin [Influenza A virus (A/Hong Kong/1131/1999(H1N1)]	456	456	100%	7e-159	99%	AAK70464.1
hemagglutinin [Influenza A virus (A/Novosibirsk/2/2009(H1N1)]	460	460	100%	4e-158	100%	ADA71156.2
hemagglutinin [Influenza A virus (A/Boston/63/2009(H1N1)]	460	460	100%	7e-158	100%	ADW10626.1
hemagglutinin [Influenza A virus (A/Florida/03/2009(H1N1)]	460	460	100%	7e-158	100%	ACU44379.1
hemagglutinin [Influenza A virus (A/Missouri/05/2009(H1N1)]	460	460	100%	7e-158	100%	AGI55443.1
hemagglutinin [Influenza A virus (A/Tianjin/15/2009(H1N1)]	460	460	100%	8e-158	100%	ADP92455.1
hemagglutinin [Influenza A virus (A/Hawaii/13/2009(H1N1)]	460	460	100%	8e-158	100%	ACU44366.1
hemagglutinin [Influenza A virus (A/Kuwait/WRAIR1119P/2009(H1N1)]	460	460	100%	8e-158	100%	AET84229.2
hemagglutinin [Influenza A virus (A/Canada/591/2004(H1N1)]	460	460	100%	9e-158	100%	AFO66235.1
hemagglutinin [Influenza A virus (A/LongAn/HCM665/2006(H1N1)]	460	460	100%	9e-158	100%	AEX34440.1

B

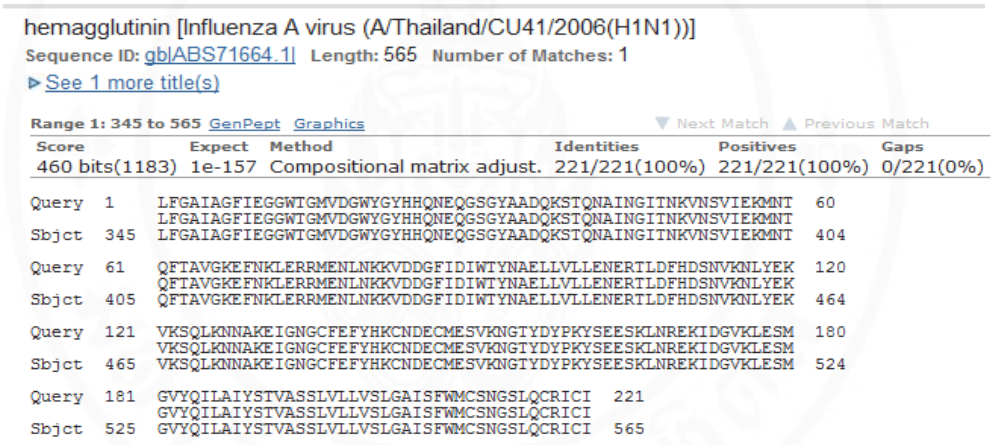

hemagglutinin [Influenza A virus (A/Thailand/CU41/2006(H1N1))]

Sequence ID: gb|ABS71664.1| Length: 565 Number of Matches: 1

See 1 more title(s)

Range 1: 345 to 565 GenPept Graphics Next Match Previous Match

Score	Expect	Method	Identities	Positives	Gaps
460 bits(1183)	1e-157	Compositional matrix adjust.	221/221(100%)	221/221(100%)	0/221(0%)

```
Query  1    LFGAIAGFIEGGWTGMVDGWYGYHHQNEQGSGYAADQKSTQNAINGITNKVNSVIEKMNT  60
            LFGAIAGFIEGGWTGMVDGWYGYHHQNEQGSGYAADQKSTQNAINGITNKVNSVIEKMNT
Sbjct  345  LFGAIAGFIEGGWTGMVDGWYGYHHQNEQGSGYAADQKSTQNAINGITNKVNSVIEKMNT  404

Query  61   QFTAVGKEFNKLERRMENLNKKVDDGFIDIWTYNAELLVLLENERTLDFHDSNVKNLYEK  120
            QFTAVGKEFNKLERRMENLNKKVDDGFIDIWTYNAELLVLLENERTLDFHDSNVKNLYEK
Sbjct  405  QFTAVGKEFNKLERRMENLNKKVDDGFIDIWTYNAELLVLLENERTLDFHDSNVKNLYEK  464

Query  121  VKSQLKNNAKEIGNGCFEFYHKCNDECMESVKNGTYDYPKYSEESKLNREKIDGVKLESM  180
            VKSQLKNNAKEIGNGCFEFYHKCNDECMESVKNGTYDYPKYSEESKLNREKIDGVKLESM
Sbjct  465  VKSQLKNNAKEIGNGCFEFYHKCNDECMESVKNGTYDYPKYSEESKLNREKIDGVKLESM  524

Query  181  GVYQILAIYSTVASSLVLLVSLGAISFWMCSNGSLQCRICI  221
            GVYQILAIYSTVASSLVLLVSLGAISFWMCSNGSLQCRICI
Sbjct  525  GVYQILAIYSTVASSLVLLVSLGAISFWMCSNGSLQCRICI  565
```

Figure 5.8 Amino acid sequences deduced from the HA2-nucleotide sequence was subjected to BLASTP search across HA2-coding sequence in the NCBI databases. (**A**), first ten amino acid sequences from NCBI database show that the rHA2 match with hemagglutinins of influenza A subtype H1N1. (**B),** the sequence of the cloned HA2 sequence matched with 100% identity with the hemagglutinin of influenza A virus [A/Thailand/CU41/2006 (H1N1) (accession number: ABS71664.1)] of database which was used for preparing cDNA template for HA2 cloning.

Copyright by Mahidol University

5.2 Production of recombinant HA (HA0, HA1, and HA2), NA, M2 and NP proteins

M15 *E. coli* clones carrying the recombinant expression plasmids with HA (HA0 and HA1) gene inserts and BL21 (DE3) *E. coli* clones carrying the recombinant expression plasmids with HA2, M2, or NP gene inserts were grown under optimal IPTG induction. The rHA0 and rHA1 with the 6xHis-tag at the N-termini (61 and 36 kDa) and the rHA2, rM2 and rNP proteins (24, 17, and 60 kDa, respectively) with the 6xHis-tag at the C-termini could be detected by Western blot analysis. **Figure 5.9** show only insoluble parts of the rHA0, rHA1, rHA2, rM2 and rNP, respectively which were detected by mouse monoclonal anti-6x-His antibody as the primary antibody for detecting the 6x-His tagged-HuScFv on Western blotting. The recombinant HA (HA0, HA1, and HA2), M2 and NP protein were successfully expressed by the respective transformed *E. coli* clones. The rNA protein (~44 kDa) with the 6xHis-tag at the C-terminus could be detected also by Western blot analysis as shown in **Figure 5.9**

5.3 Purification of the recombinant HA (HA0, HA1, and HA2), M2 and NP proteins

The recombinant HA (HA0, HA1, and HA2), M2 or NP proteins in the homogenate of transformed *E. coli* were affinity purified by using Ni-NTA resin under denaturing condition (solubilized in buffer containing 8 M urea). The resin-bound protein was eluted by using discontinuous gradients of imidazole. It was found that the recombinant proteins were present in some fractions after SDS-PAGE and CBB staining. **Figures 5.10A** to **5.14A** show rHA (rHA0, rHA1, and rHA2), rM2, and rNP protein, respectively). These were confirmed by immune-detection by using anti-6xHis-tag antibody as shown the reactive banes in **Figures 5.10B** to **5.14B**. The purified fractions containing the recombinant proteins were refolded and dialyzed against PBS until the molarity of the urea reduced to nil. The protein concentrations were measured and the preparations without glycerol preservation were kept at -20 ºC until use.

Copyright by Mahidol University

The rM2 was also purified from the soluble *E. coli* fraction by using Ni-NTA beads under native condition. The resin bound protein was eluted by using discontinuous gradients of imidazole. It was found that the recombinant protein was present in some fractions after detecting by using SDS-PAGE and CBB staining (**Figure 5.13C**) and Western blotting (**Figure 5.13D**). The purified protein was also dialyzed in PBS and protein concentration was measured and kept at -20 ºC until use.

Copyright by Mahidol University

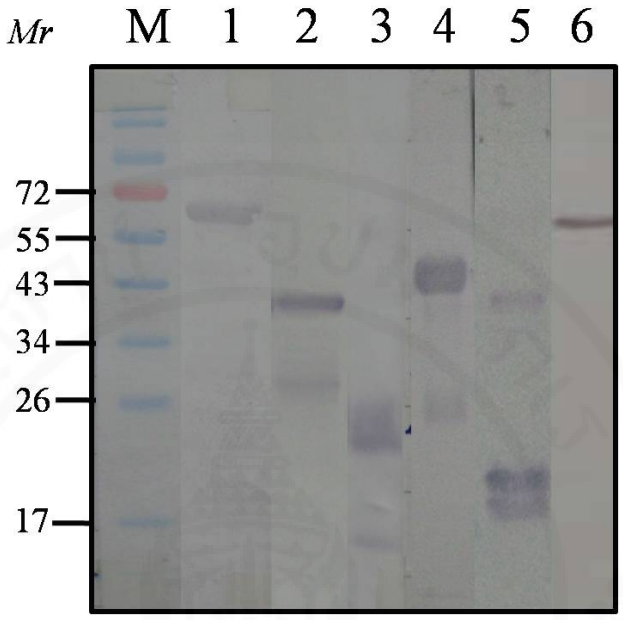

Figure 5.9 Patterns of HA (HA0, HA1, and HA2), NA, M2 and NP proteins in insoluble fractions of respective transformed *E. coli* clones.

Lanes M, Pre-stained broad range protein standard maker

Lane 1, Reactive band of recombinant HA0 (calculated 61 kDa)

Lane 2, Reactive band of recombinant HA1 (calculated 36 kDa)

Lane 3, Reactive band of recombinant HA2 (calculated 24 kDa)

Lane 4, Reactive band of recombinant NA (calculated 54 kDa)

Lane 5, Reactive bands of recombinant M2 [The lower band is mature rM2 (calculated 17 kDa); the upper band is rM2 linked which pelB1 leader peptide (calculated 21 kDa) of pET20b^{+} backbone and the uppermost band is suspected homodimeric rM2 (calculated 34 kDa)]

Lane 6, Reactive band of recombinant NP (calculated 60 kDa)

Copyright by Mahidol University

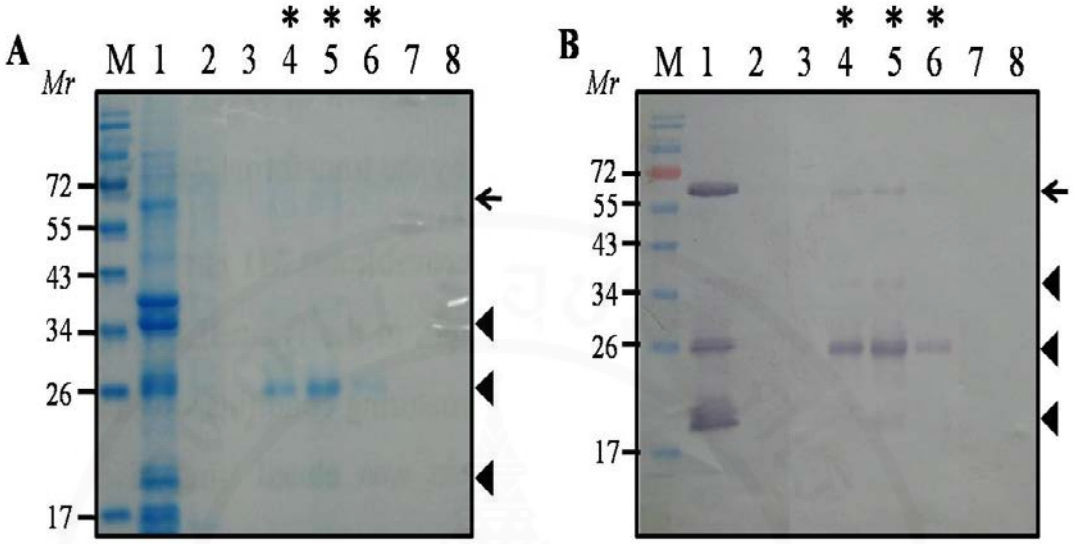

Figure 5.10 Results of recombinant HA0 purification by using Ni-NTA resin under denaturing condition

(**A**), SDS-PAGE-separated HA0 proteins in gel stained with CBB dye. (**B**), Western blot patterns of the SDS-PAGE-separated HA0 probed with anti-6xHis-tag antibody

Lane M, Pre-stained broad range protein standard marker

Lane 1, Homogenate of M15 *E. coli* harboring recombinant *ha0*-plasmids

Lane 2, Unbound *E. coli* protein fraction

Lanes 3-8, Eluted protein fraction no. 1-6
[50, 100, 150, 200, 200 and 250 mM of imidazole, respectively]

Arrows indicate the location of intact recombinant HA0 protein (61 kDa)

Arrow heads indicate degraded rHA0 at ~34, 26 and 20 kDa

* indicated positive eluted fractions containing rHA0

Numbers as the left of both blocks are relative molecular masses (*Mr*) of proteins

Copyright by Mahidol University

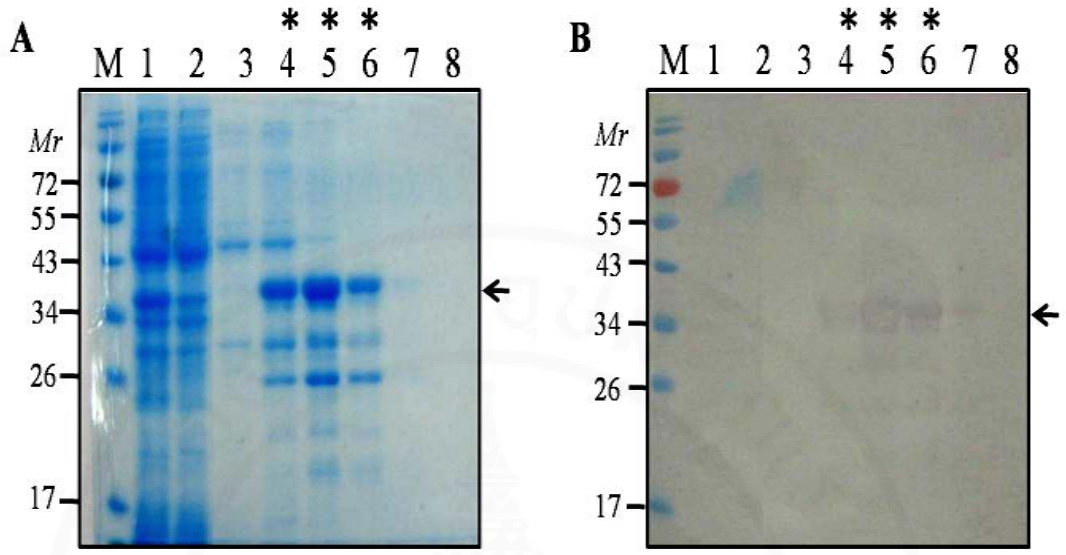

Figure 5.11 Results of recombinant HA1 purification by using Ni-NTA resin under denaturing condition

(**A**), SDS-PAGE-separated HA1 protein in gel stained with CBB dye. (**B**), Western blot patterns of the SDS-PAGE-separated HA1 protein probed with anti-6xHis-tag antibody.

Lane M, Pre-stained broad range protein standard marker

Lane 1, Homogenate of M15 *E. coli* harboring recombinant *ha1*-plasmids

Lane 2, Unbound *E. coli* protein fraction

Lanes 3-8, Eluted protein fraction no. 1-6
[50, 100, 150, 200, 200 and 250 mM of imidazole, respectively]

Arrows indicate the location of recombinant HA1 protein

* indicated positive eluted fractions containing rHA1

Numbers as the left of both blocks are relative molecular masses (*Mr*) of proteins

Copyright by Mahidol University

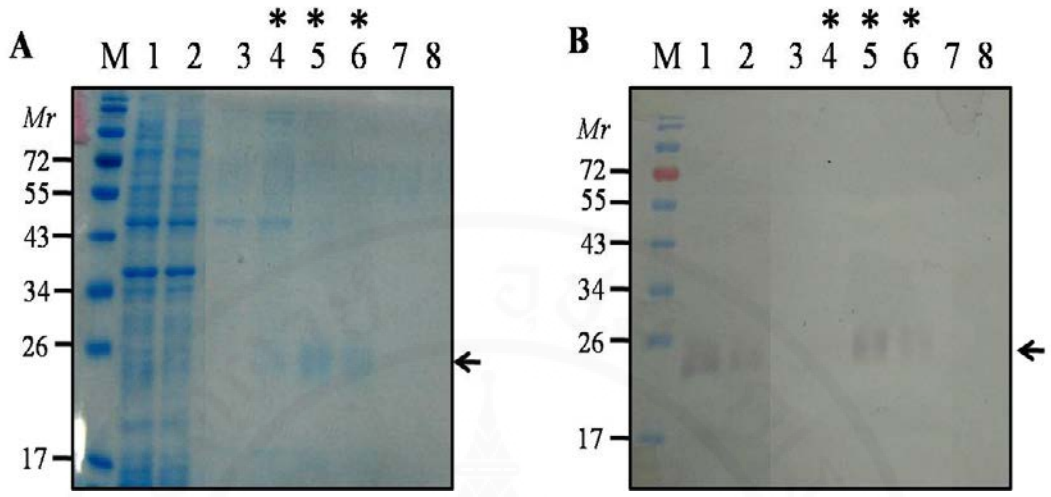

Figure 5.12 Results of recombinant HA2 purification by using Ni-NTA resin under denaturing condition.

(**A**), SDS-PAGE-separated HA2 proteins in gel stained with CBB dye. (**B**), Western blot patterns of the SDS-PAGE-separated HA2 protein probed with anti-6xHis-tag antibody.

Lane M, Pre-stained broad range protein standard marker

Lane 1, Homogenate of BL21 (DE3) *E. coli* harboring recombinant *ha2*-plasmids

Lane 2, Unbound *E. coli* protein fraction

Lanes 3-8, Eluted protein fraction no. 1-6
[50, 100, 150, 200, 200 and 250 mM of imidazole, respectively]

Arrows indicate the location of recombinant HA2 protein

* indicated positive eluted fractions containing rHA2

Numbers as the left of both blocks are relative molecular masses (*Mr*) of proteins

Copyright by Mahidol University

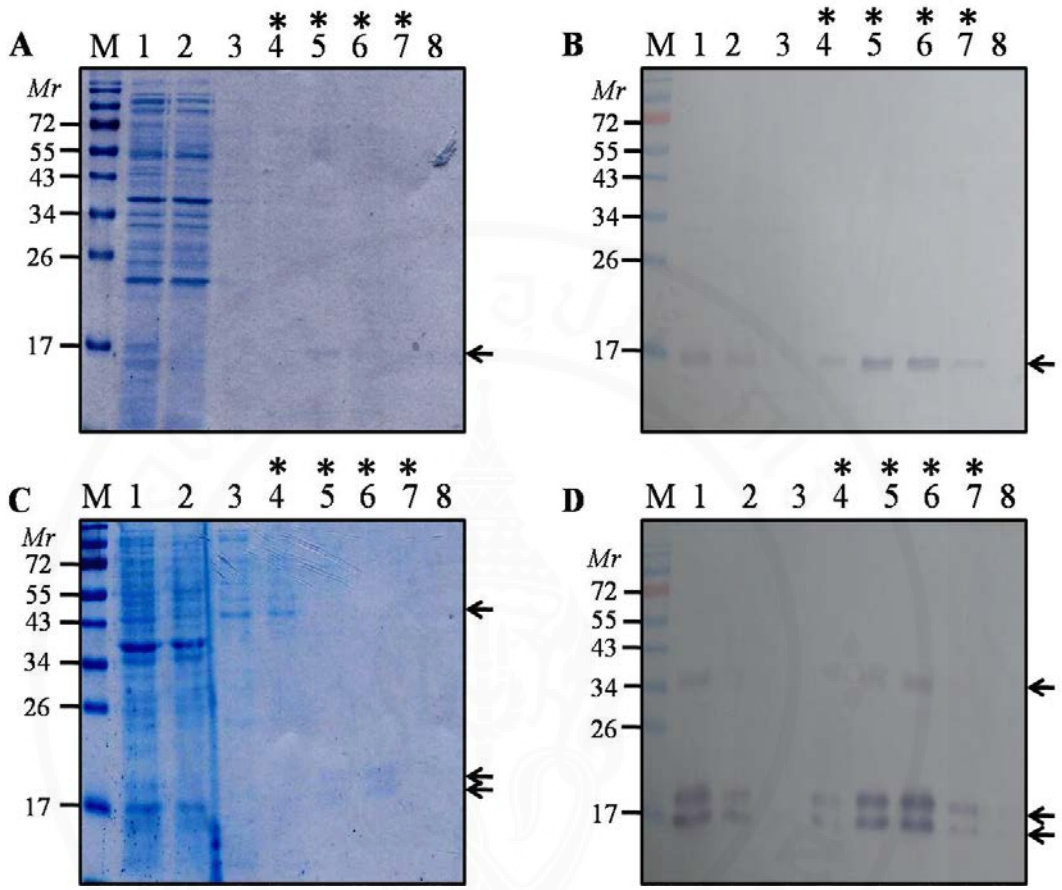

Figure 5.13 Results of recombinant M2 purification by using Ni-NTA resin.

(**A** and **B**), Soluble rM2 proteins were purified under native condition

(**C** and **D**), Insoluble rM2 proteins were purified under denaturing condition

(**A** and **C**), SDS-PAGE-separated M2 proteins in gel stained with CBB dye

(**B** and **D**), Western blot patterns of the SDS-PAGE-separated M2 proteins probed with anti-6xHis-tag antibody

Lane M, Pre-stained broad range protein standard marker

Lane 1, Homogenate of BL21 (DE3) *E. coli* harboring recombinant *M2*-plasmids

Lane 2, Unbound *E. coli* protein fraction

Lanes 3-8, Eluted protein fraction no. 1-6

[50, 100, 150, 200, 200 and 250 mM of imidazole, respectively]

Arrows indicate the location of recombinant M2 protein

* indicated positive eluted fractions containing rM2

Numbers as the left of all blocks are relative molecular masses (*Mr*) of proteins

Copyright by Mahidol University

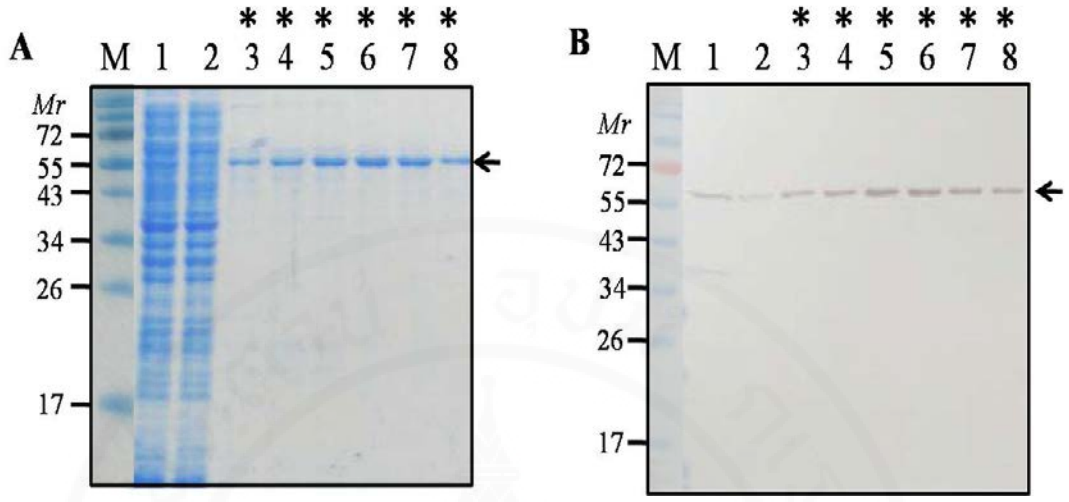

Figure 5.14 Results of recombinant NP purification by using Ni-NTA resin (**A**), SDS-PAGE-separated NP proteins in gel stained with CBB dye. (**B**), Western blot patterns of the SDS-PAGE-separated rNP probed with anti-6xHis-tag antibody.

Lane M, Pre-stained broad range protein standard marker

Lane 1, Homogenate of BL21 (DE3) *E. coli* harboring recombinant *NP*-plasmids

Lane 2, Unbound *E. coli* protein fraction

Lanes 3-8, Eluted protein fraction no. 1-6
[50, 100, 150, 200, 200 and 250 mM of imidazole, respectively]

Arrows indicate the location of recombinant NP protein

* indicated positive eluted fractions containing rNP

Numbers as the left of both blocks are relative molecular masses (*Mr*) of proteins

Copyright by Mahidol University

5.4 Production of mouse polyclonal antibodies to recombinant H1, N1, M2 and NP

All animal experiments were approved by Veterinary Science-Animal Care and Use Committee (FVS-AUCU), Faculty of Veterinary Medicine, Kasetsart University, Thailand. The certificate ID number of animal experiment is ACKU 03455 (**Appendix J**).

Four groups of five ICR mice each were prepared. They were immunized with the purified recombinant H1, N1, M2 or NP as described in **section 4.4** of **Chapter IV**. The individual immune mouse sera were tested by an indirect ELISA against the homologous antigens. The mouse sera showed the IgG ELISA titers equal to or higher than 1:12,800. The binding specificity of polyclonal antibodies against their respective recombinant H1, N1, M2 or NP was verified by using Western blotting (**Figure 5.15**). The purified recombinant proteins were used as target antigens and probed with their respective polyclonal antibodies. The mouse hyperimmune serum (the IgG ELISA titers equal to or higher than 1:12,800) to rNA was a kind gift from Assist. Prof. Dr. Potjanee Srimanote.

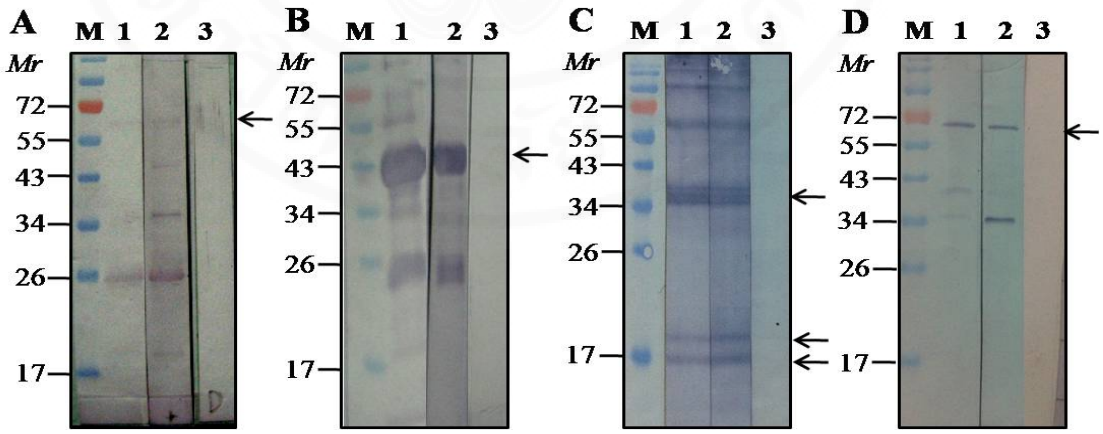

Figure 5.15 The binding specificity of polyclonal antibodies against their recombinant H1, N1, M2 or NP (**A**, **B**, **C**, and **D**, respectively)

Lane M, Pre-stained broad range protein standard marker

Lane 1, Recombinant protein probed with anti 6xHis tag antibody

Lane 2, Recombinant protein probed with respective polyclonal antibody

Lane 3, Recombinant protein probed with diluents control

Arrows indicate the location of intact recombinant H1, N1, M2 or NP protein

Copyright© by Mahidol University

5.5 Selection of phage clones harboring Human single chain antibody fragment gene (*huscfv*) and displaying the respective pIII-HuScFv that bound to the native HA, NA and M2 on influenza virus particle

5.5.1 Phages bio-panning with the native HA, NA and M2 on influenza virus particles adsorbed on human red blood cell ghosts

H1N1/2009 virus-adsorbed hRBC ghosts from **section 4.5.2.2** of **Chapter IV** were used as the target antigens in the phage bio-panning process (**section 4.5.2.3.3** of **Chapter IV**). After eluting the phages that bound to the target antigens on the hRBC ghost, the phages were allowed to infect the HB2151 *E. coli*. One hundred *E. coli* transformants were randomly selected from the selective agar plate. They were screened for the presence of *huscfv* by PCR using the phagemid specific pCANTAB-*R1* and pCANTAB-*R2* primers. Among the 100 screened colonies from bio-panning with H1N1/2009 virus-adsorbed hRBC ghosts, 34 clones (34%) revealed the *huscfv* amplicon at size ~1,000 bp (**Figure 5.16** show the representative clones (Lanes no. 3-6, 10, 11, and 15) that gave the *huscfv* amplicon at size ~1,000 bp).

5.5.2 Screening of the *huscfv*-phagemid transformed HB2151 *E. coli* clones that could produce soluble HuScFv

All of the 34 *huscfv*-positive HB2151 *E. coli* clones were grown under 0.5 mM IPTG induction and their cell lysates were analyzed for the presence of the soluble HuScFv by Western blot analysis (see method in **section 4.7** of **Chapter IV**) and 20 *E. coli* clones could express the soluble HuScFv which appeared as reactive bands at *Mr* ~26-35 kDa (**Figure 5.15**).

Copyright by Mahidol University

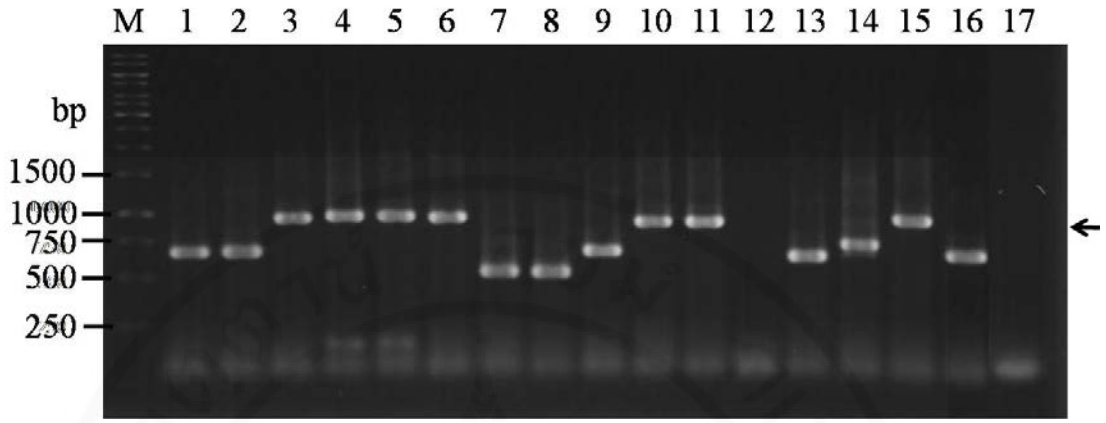

Figure 5.16 Amplicons of *huscfv* in representative phagemid transformed HB2151 *E. coli* clones

Lane M, GeneRuler 1 kb DNA ladder

Lanes 3-6, 10, 11 and 15 were positive for the *huscfv* in HB2151 *E. coli* Clones

Lane no. 12 was negative for the *huscfv* in HB2151 *E. coli* Clones (No insertion of *huscfv* in pCANTAB5E phagemid)

Arrows indicate the location of the expective *huscfv* amplicons (~1,000 bp)

Arrow head indicate the area of shorther PCR amplicons (~500- 750 bp) in lane no. 1-2, 7-9, 13, 14 and 16

Numbers at the left are DNA sizes in bp

Copyright by Mahidol University

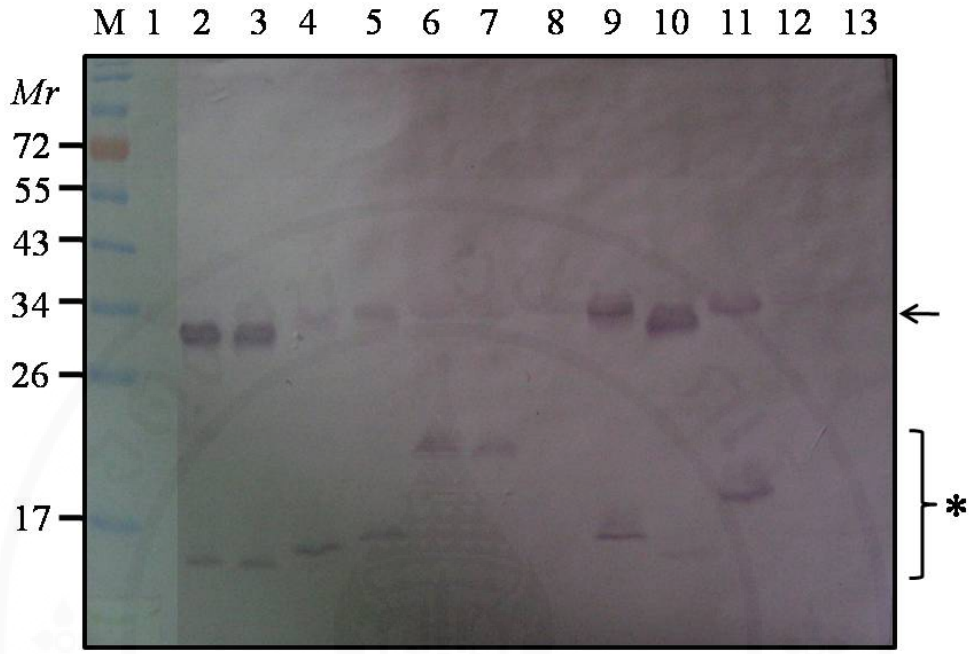

Figure 5.17 Western blot results for detection of HuScFv in lysates the representative *huscfv*-pCANTAB5E-transformed HB2151 *E. coli* colonies

Lane M, Pre-stained broad range protein standard

Lane 1, Lysate of HB2151 *E. coli* without *huscfv*-phagemid

Lanes 2, 3 and 9-11, HuScFv in lysates *huscfv*-phagemid transformed HB2151 *E. coli* clones (~26-35 kDa)

Arrows indicate the location of the expectd HuScFv protein

* indicate lower reactive bands of degraded products

Copyright by Mahidol University

5.6 Determination of the binding specificity of the HuScFv which selected from phage bio-panning with H1N1/2009 virus-adsorbed hRBC ghost

For determining binding activity specificity of HuScFv to the recombinant proteins (rHA0, rNA and rM2), cell lysates of the 20 transformed HB2151 *E. coli* clones that could express HuScFv from **section 5.5.2** were used in the indirect ELISA. BSA was used as an antigen control in the assay. Lysate of HB2151 *E. coli* without *huscfv*-phagemid and diluents were used as negative HuScFv control while the mPAb (**section 5.4**) was used as positive antibody controls. **Figures 5.18A-5.20A** show only 8 clones (clones no. 2, 10, 15, 26, 51, 53, 54 and 99) that gave positive results (significantly higher OD_{405nm} above lysate of HB2151 *E. coli* without HuScFv and more than 2x of the BSA control as a cut off criteria) in binding to recombinant proteins in indirect ELISA against rHA0, rNA1 and rM2, respectively. The OD_{405nm} of the positive control (mPAb) was high. Summary of binding activity and specificity of HuScFv against recombinant proteins by using indirect ELISA and Western blotting, respectively are shown in **Table 5.1**. In briefly, HuScFv of clones 2, 10, 26, 53, 54 and 99 bound to the rHA (**Figure 5.18A**), HuScFv of clones 2, 10, 26, 53 and 54 bound also to the rNA (**Figure 5.19A**), and HuScFv of clones 2, 10, 15, 26, 51 and 54 bound the rM2 (**Figure 5.20A**).

Copyright by Mahidol University

Table 5.1 Summary of the binding specificity of HuScFv against recombinant protein (HA0, NA and M2)

HuScFv clone no.	Recombinant protein					
	rHA0		rNA		rM2	
	Indirect ELISA	Western blotting	Indirect ELISA	Western blotting	Indirect ELISA	Western blotting
2	√	+	√	+	√	
10	√	+	√	+	√	
15					√	
26	√	+	√	+	√	
51					√	
53	√	+	√	+		
54	√	+	√	+	√	
99	√	+				

(√) positive binding by indirect ELISA against rHA0, rNA, or rM2

(+) positive binding by Western blotting against rHA0, rNA, or rM2

Binding specificity of the HuScFv to the recombinant proteins (rHA, rNA and rM2) were also determined by using Western blotting. The results of Western blotting show that all HuScFv that could bind to rHA0 (**Figure 5.18B**) and rNA (**Figure 5.97B)** in indirect ELISA also react to the recombinant target protein in Western blotting. However, the HuScFv that bound to rM2 in indirect ELISA could not bind to insoluble form rM2 protein on NC membrane (**Figure 5.20B**). Nevertheless, the HuScFv that gave positive results in binding to rM2 in indirect ELISA could bind to native M2 in homogenate of influenza A/H5N1 (**Figure 5.21A)** and A/H1N1(2009) (**Figure 5.21B**) infected MDCK cells.

Copyright by Mahidol University

From results of the determination of binding specificity to the target proteins by using indirect ELISA and Western blotting, the HuScFv could be divided according to their specific targets into 4 categories.

Table 5.2 Results of the determination of binding specificity to the target proteins by using indirect ELISA and Western blotting

Binding specificity	HuScFv clone no.
rHA0	99√
rM2 (Indirect ELISA) and nM2* (Western blotting)	15 and 51√
rHA0 and rNA	53√
rHA0, rNA, rM2 (Indirect ELISA) and nM2* (Western blotting)	2, 10, 26√ and 54

√ Selected for neutralization test and* lysate containing native M2 from A/H5N1 and A/H1N1 (2009)

From this summary, the HuScFv clone no. 26 (specific to HA, NA and M2), HuScFv clone no. 51 (specific to M2), HuScFv clone no. 53 (specific to HA and NA) and HuScFv of clone no. 99 (specific to HA) were selected for testing further in interfering with influenza virus replication cycle.

Copyright by Mahidol University

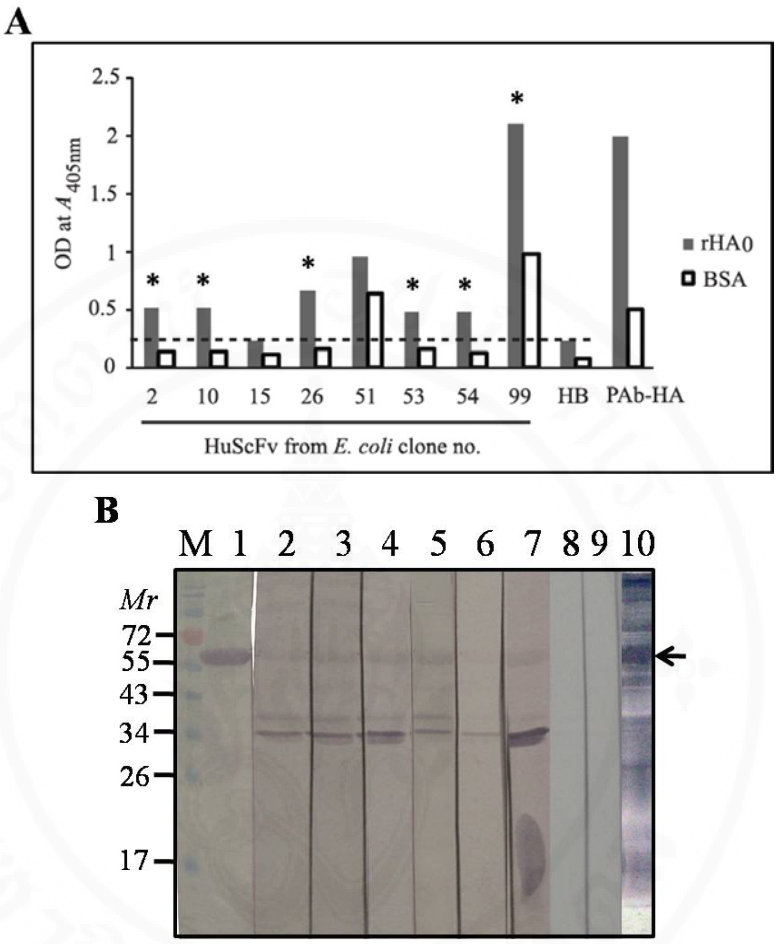

Figure 5.18 Results of indirect ELISA (**A**) and Western blotting (**B**) for determining the binding of HuScFv from eight *huscfv*-phagemid transformed-HB2151 *E. coli* clones to the rHA0.

In (**A**), * indicate positive binding and dash line indicate cut off criteria

In (**B**), Lane M, Pre-stained broad range protein standard marker

Lane 1, SDS-PAGE separated rHA0 probed with anti-6x His tag

Lanes 2-7, SDS-PAGE separated rHA0 probed with lysates containing HuScFv of clones no. 2, 10, 26, 53, 54 and 99, respectively

Lane 8, SDS-PAGE separated the probed with diluent control

Lane 9, SDS-PAGE separated rHA0 probed with lysate of HB2151 *E. coli* without HuScFv

Land 10, the rHA0 probed with mouse PAb-HA

Arrow indicates the location of intact recombinant HA0 protein (61 kDa)

Numbers as the left of the (**B**) block are relative molecular masses (*Mr*) of proteins

Copyright by Mahidol University

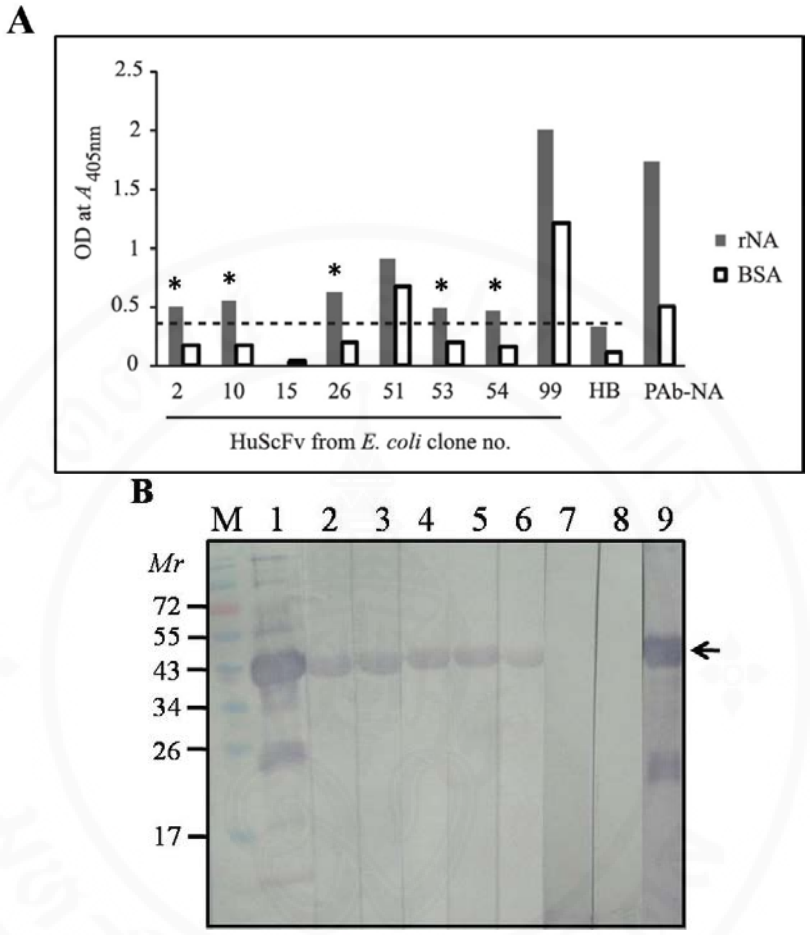

Figure 5.19 Results of indirect ELISA (**A**) and Western blotting (**B**) for determining the binding of HuScFv from eight *huscfv*-phagemid transformed-HB2151 *E. coli* clones to the rNA

In (**A**), * indicate positive binding and dash line indicate cut off criteria

In (**B**), Lane M, Pre-stained broad range protein standard marker

Lane 1, SDS-PAGE separated rNA probed with anti-6x His tag

Lanes 2-7, SDS-PAGE separated rNA probed with lysates containing HuScFv of clones no. 2, 10, 26, 53 and 54, respectively

Lane 8, SDS-PAGE separated rNA probed with diluent control

Lane 9, SDS-PAGE separated rNA probed with lysate of HB2151 *E. coli* without HuScFv

Land 10, SDS-PAGE separated rNA probed with mPAb to rNA

Arrow indicates the location of recombinant NA protein (54 kDa)

Numbers as the left of the (**B**) block are relative molecular masses (*Mr*) of Proteins

Copyright by Mahidol University

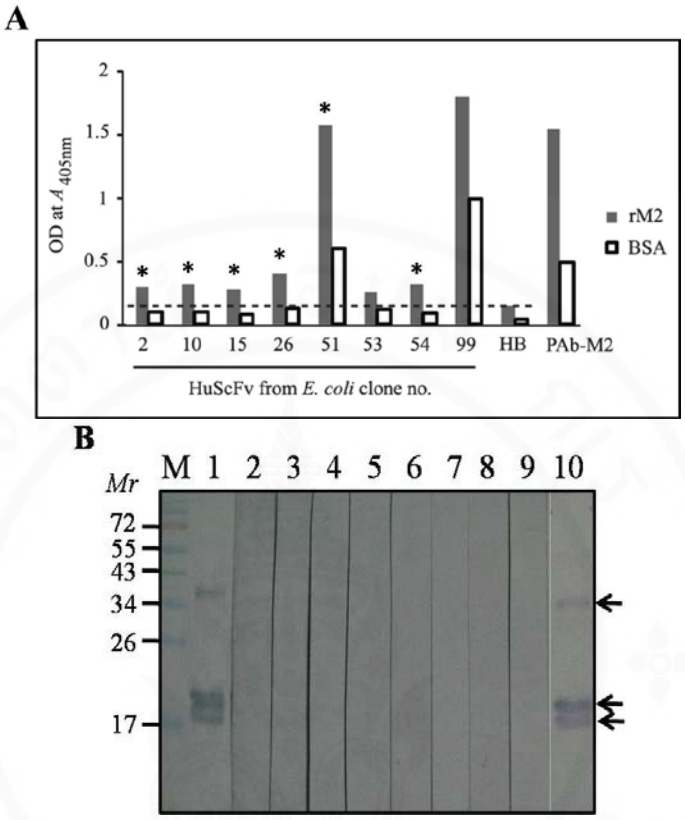

Figure 5.20 Results of indirect ELISA (**A**) and Western blotting (**B**) for determining the binding of HuScFv from eight *huscfv*-phagemid transformed-HB2151 *E. coli* clones to the rM2

In (**A**), * indicate positive binding and dash line indicate cut off criteria

In (**B**), Lane M, Pre-stained broad range protein standard marker

Lane 1, SDS-PAGE separated rM2 probed with anti-6x His tag

Lanes 2-7, SDS-PAGE separated rM2 probed with lysates containing HuScFv of clones no. 2, 10, 15, 26, 51 and 54, respectively

Lane 8, SDS-PAGE separated rM2 probed with diluent control

Lane 9, SDS-PAGE separated rM2 probed with lysate of HB2151 *E. coli* without HuScFv

Land 10, SDS-PAGE separated rM2 probed with mPAb to rM2 revealed dimeric rM2 (Upper arrow), immature rM2 with signal peptide (middle arrow) and monomeric rM2 (Lowest arrow)

Numbers as the left of the B block are relative molecular masses (*Mr*) of proteins

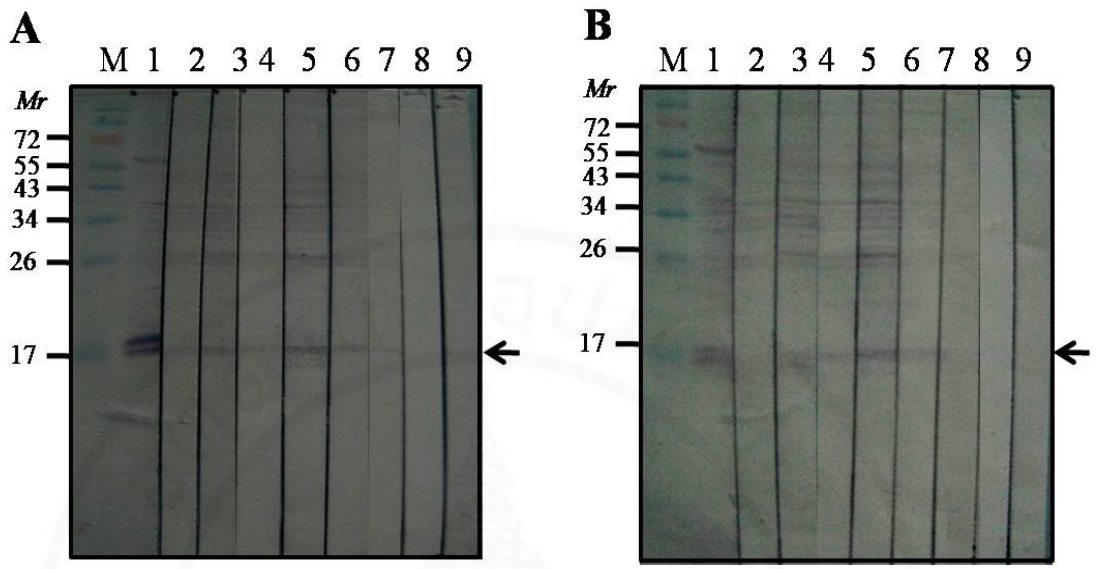

Figure 5.21 Western blot pattern of SDS-PAGE separated native M2 (nM2) in homogenate of MDCK cells infected cells with H5N1 (**A**) and homogenates of infected cells with H1N1/2009 (**B**) probed with HuScFv from huscfv-phagemid transformed E. coli clones that could bind to the rM2 in the indirect ELISA for determining the binding of HuScFv to native M2 protein

Lanes M of both A and B, Pre-stained broad range protein standard

Lanes 1 of both A and B, SDS-PAGE separated nM2 probed with mPAb to rM2

Lanes 2-7 of both A and B, SDS-PAGE separated rM2 probed with lysates containing HuScFv of clones no. 2, 10, 15, 26, 51 and 54, respectively

Lanes 8 of both A and B, SDS-PAGE separated rM2 probed with diluent control

Lanes 9 of both A and B, SDS-PAGE separated the rM2 probed with lysate of HB2151 *E. coli* without HuScFv

Arrows indicate the location of nM2 protein

Numbers as the left of both blocks are relative molecular masses (*Mr*) of proteins

Copyright by Mahidol University

5.7 Determination of the HA specific-HuScFv in inhibition of the hemagglutinin bio-function

5.7.1 Determination of the antigenic specificity of the HA-specific HuScFv to rHA1 or rHA2 by using indirect ELISA

HuScFv of *huscfv*-phagemid transformed *E. coli* clones that could bind to rHA0 of H1 were determined for binding specificity to rHA1 or rHA2 by using indirect ELISA before testing their ability in inhibiting the hemagglutinin bio-function. Cell lysates containing HA specific-HuScFv of clones no. 2, 10, 26, 53, 54 and 99 were used in the indirect ELISA using rHA1 or rHA2 as an antigen and BSA served as an antigen control. Lysate of HB2151 *E. coli* without HuScFv and diluents were used as negative controls while the mPAb to rHA were used as positive antibody control. **Figure 5.22A** shows that the HA specific-HuScFv of clones no. 2, 10, 26 and 54 gave OD_{405nm} value to rHA1 significantly higher than lysate of HB2151 *E. coli* alone and more than two times of the BSA control. HuScFv clone no. 53 and 99 gave significant OD_{405nm} to rHA2 (**Figure 5.22B**). The indirect ELISA results are summarized in **Table 5.3**.

The results indicated that HuScFv of clones no. 2, 10, 26 and 54 could bind to HA1 of the influenza virus HA. The HuScFv of these clones were tested for ability to inhibit hemagglutinin bio-function in the next experiment.

Table 5.3 Summary of antigenic specificities of HA specific-HuScFv

HuScFv clone no.	Recombinant protein	
	rHA1	rHA2
2	√	
10	√	
26	√	
53		√
54	√	
99		√

(√) positive binding by indirect ELISA against rHA1 or rHA2

Copyright by Mahidol University

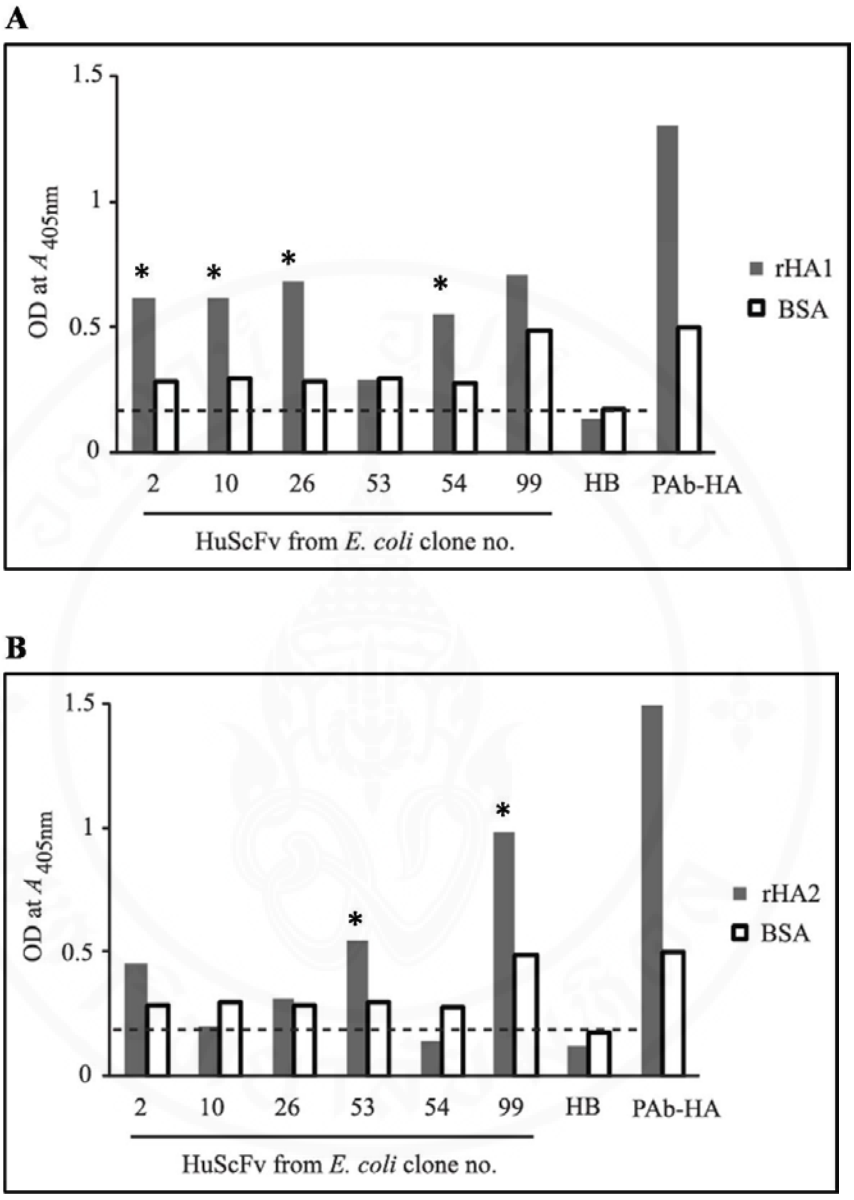

Figure 5.22 Results of indirect ELISA for determining the binding of HuScFv to the rHA1 (**A**) or rHA2 (**B**)

* indicate positive binding and dash line indicate cut off criteria

The results show that HuScFv of clones no. 2, 10, 26 and 54 gave significant OD_{405nm} against the rHA1 more than two times higher than to the BSA antigen control. HuScFv clones no. 53 and 99 gave OD_{405nm} to rHA2 more than two times higher than to BSA control. Lysate of HB2151 *E. coli* without HuScFv (HB) and mouse polyclonal antibody to HA (mPAb-HA) served as negative and positive controls, respectively.

5.7.2 Determination of hemagglutination inhibition (HI) of the HA1 specific-HuScFv

Hemagglutination inhibition assay (HI) was used for testing *in vitro* activity of the HA1 specific-HuScFv in inhibiting the hemagglutination activity of equal amount of HA1 specific-HuScFv in lysates of *E. coli* clones no. 2, 10, 26 and 54 were standardized based on the Western blot band intensities as determined spectrometrically. Serial two fold dilutions of the standardized HuScFv were mixed with equal volume of 4 HAU of H1N1/2009 virus. After adding 1% group O hRBC, the plate was kept until negative hemagglutination control showed a button-like appearance (see method in **Chapter 4.16**). The results in **Figure 5.23** show that HuScFv of clones no. 2, 10, 16 and 54 could inhibit the hemagglutination activity as shown in reciprocal titers of hemagglutination inhibition at 16, 16, 16 and 32, respectively. At equal amount of HuScFv, HA1 specific HuScFv clone no. 54 exhibit the highest reciprocal inhibition titer at 32 while the HB2151 lysate gave reciprocal inhibition titer at 4. The influenza vaccinated serum gave reciprocal inhibition titer at 64. Viral control (VC) could not inhibit hemagglutination while serum control (SC, which was the well added with undiluted lysate of *E. coli* containing HuscFv) could inhibit hemagglutination. These results indicated that HA1 specific-HuScFv could inhibit the hemagglutination activity of H1N1/2009 virus against hRBC.

Copyright by Mahidol University

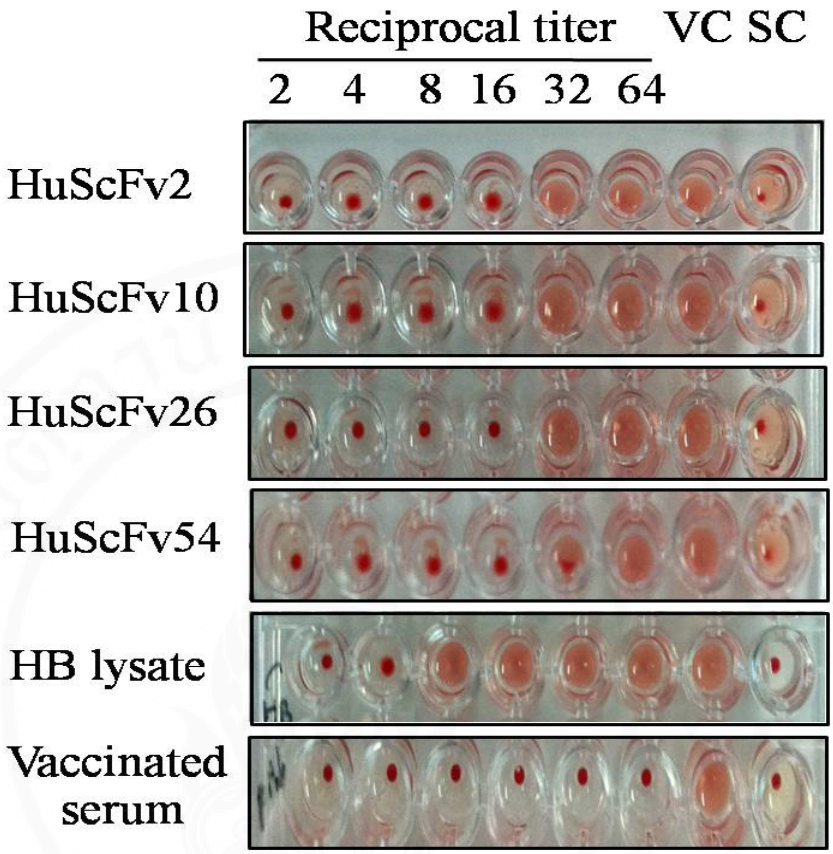

Figure 5.23 Result of hemagglutination inhibition assay (HI) for determination of HuScFv specific to HA1 in inhibiting the hemagglutination activity of H1N1/2009 virus against hRBC

Copyright by Mahidol University

5.8 Characterization of the HuScFv specific to rH1, rN1 and/or nM2 which derived from phage bio-panning with H1N1/2009 virus-adsorbed hRBC ghosts

From previous results, the HuScFv clone no. 26 (specific to rHA, rNA and nM2), HuScFv clone no. 51 (specific to nM2), HuScFv clone no. 53 (specific to rHA and rNA) and HuScFv of clone no. 99 (specific to rHA) were selected for characterization of the HuScFv before testing their interference on influenza virus replication cycle.

5.8.1 Restriction fragment length polymorphism (RFLP) of the huscfv sequences

The diversity of the DNA sequences coding for HuScFv of clones no. 26, 51, 53 and 99 were determined by *Mva*I restriction fragment length polymorphism (*Mva*I-RFLP) (Shin *et al*., 2003; Thathaisong *et al*., 2008). It was found that *huscfv* sequences of the 4 clones had different RFLP (DNA banding patterns) (**Figure 5.24**).

5.8.2 Identification of immunoglobulin frameworks (FRs) and complementarity determining regions (CDRs) of the HuScFv

The nucleotide sequences of the selected *huscfv* of clones no. 26, 51, 53 and 99) were sequenced. Multiple of the selected HuScFv amino acids were aligned by using ClustalW2 software available on http://www.ebi.ac.uk/Tool/services. The results of multiple alignment of the selected HuScFv are shown in **Figure 5.25**. The deduced amino acid sequences of all clones were shown to be complete; containing VH-linker-VL domains. The immunoglobulin frameworks (FRs) and complementarity determining regions (CDRs) of the deduced amino acids of *huscfv* sequences were predicted using the Immunogenetics Information System server (IMGT/V-QUEST).

Copyright by Mahidol University

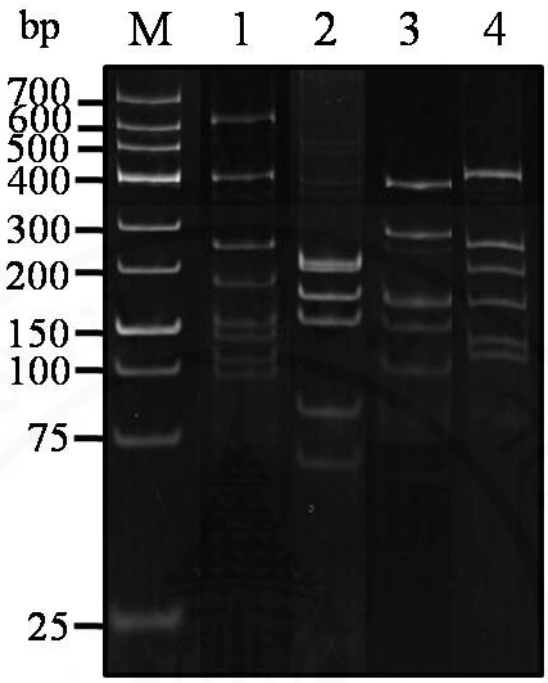

Figure 5.24 RFLP (DNA banding patterns) of *huscfv* sequences from HB2151 *E. coli* clones no. 26, 51, 53 and 99

Lane M, GeneRuler^{TM} low range DNA ladder

Lanes 1-4, RFLP (DNA banding patterns) of *huscfv* sequences from HB2151 *E. coli* clones no. 26, 51, 53 and 99, respectively

Numbers at the left are DNA sizes in bp

The *huscfv* sequences of the four clones revealed different DNA banding patterns.

Copyright by Mahidol University

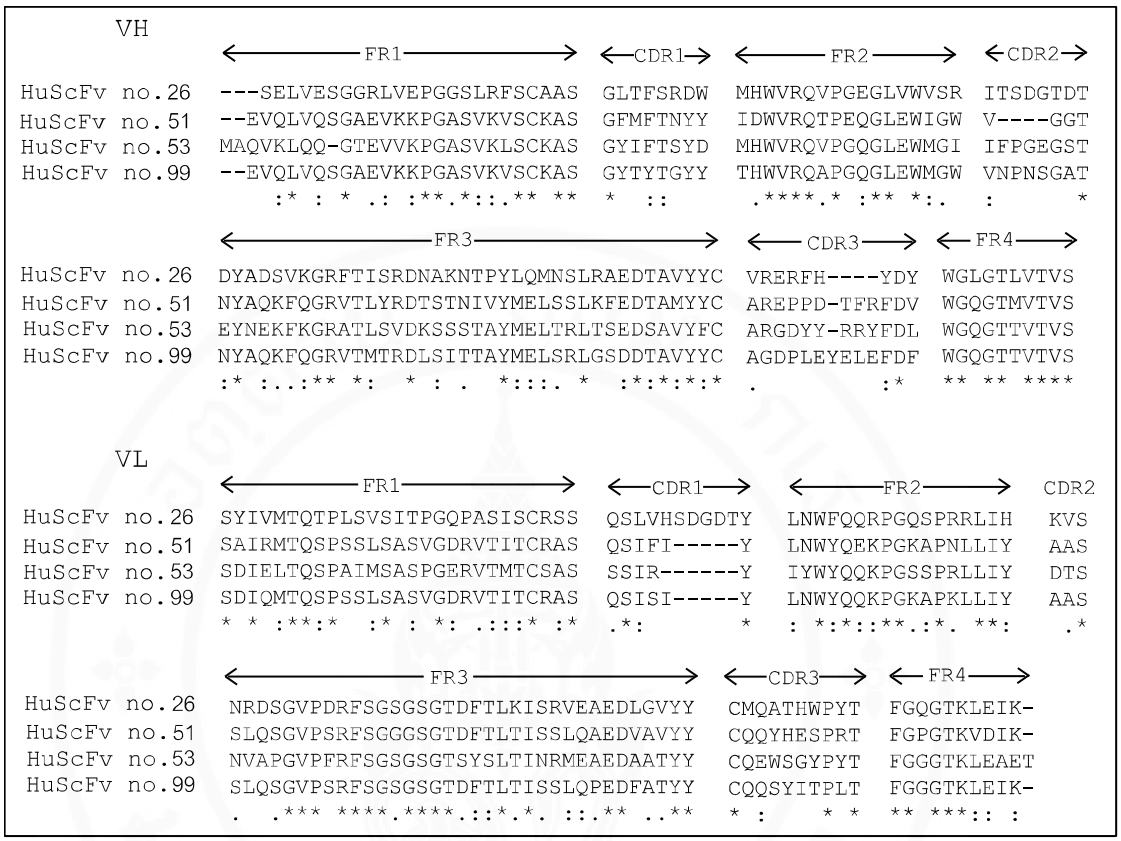

Figure 5.25 Immunoglobulin frameworks (FRs) and complementarity determining regions (CDRs) of heavy (VH) and light (VL) chains HuScFv sequence of clones no. 26, 51, 53 and 99. Three CDRs and four FRs of the HuScFv from the four HB2151 *E. coli* clones were determined by using the IMGT server. Multiple alignments of amino acid sequence diversities in CDRs of VH and VL of the four clones were verified by using ClustalW server.

* indicates identical amino acid

: indicates conservative amino acid substitution

. indicates a semiconservative amino acid substitution

Copyright by Mahidol University

5.9 Subcloning of HuScFv coding sequences into pET plasmid

5.9.1 Large scale expression of the selected HuScFv clones

The HuScFv coding sequences (*huscfv*) of clones no. 26, 51, 53 and 99 were subcloned from original pCANTAB5E phagemid into pET plasmid system to increase the yield of the recombinant antibody expression. Colony PCR was performed to screen the positive transformed BL21 (DE3) *E. coli* clones that carry the *huscfv* fragments with the expected size at ~1,000 bp (**Figure 5.26**).

The recombinant HuScFv 6xHis tag fusion proteins (HuScFv-6xHis) expressed by these clones were located predominantly in the insoluble parts of the *E. coli* homogenates. Large scale expression and purification of HuScFv-His by using TALON Metal Affinity resin under denaturing condition were performed. **Figure 5.27A** shows CBB stained purified HuScFv-6xHis from the respective transformed BL21 (DE3) clones after SDS-PAGE separation as well as their respective Western blot patterns (**Figure 5.27B**).

Copyright by Mahidol University

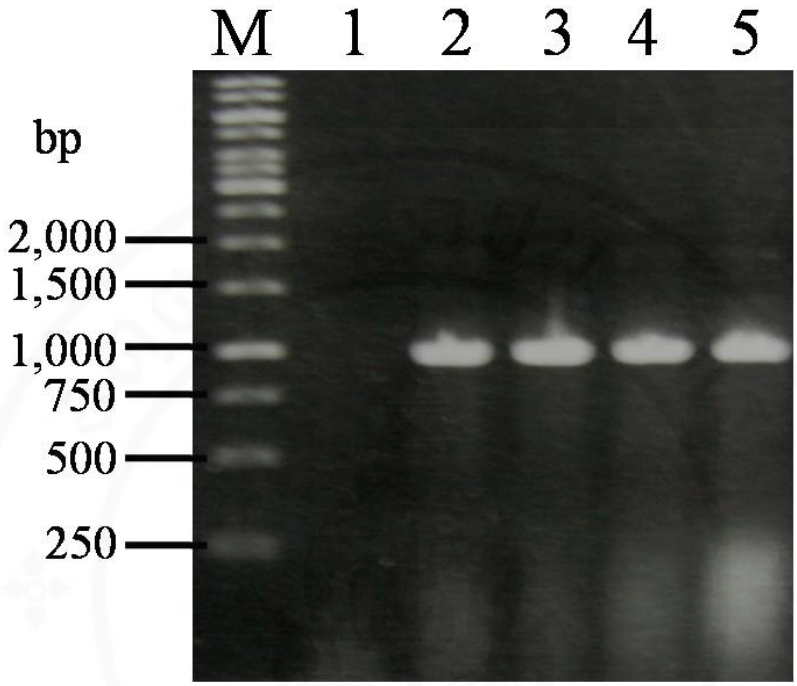

Figure 5.26 Results of PCR screening of transformed BL21 (DE3) *E. coli* colonies carrying *huscfv*-pET plasmid by using T7 primers and randomly selected *E. coli* colonies as DNA templates. Positive clones revealed the *huscfv* DNA amplicons at ~1,000 kb.

Lane M, GeneRuler^{TM} 1 kb DNA ladder

Lane 1, Negative control (no DNA template)

Lanes 2-5, DNA amplicons of HuScFv26, HuScFv51, HuScFv53 and HuScFv99 sequences, respectively.

Numbers at the left are DNA sizes in bp

Copyright by Mahidol University

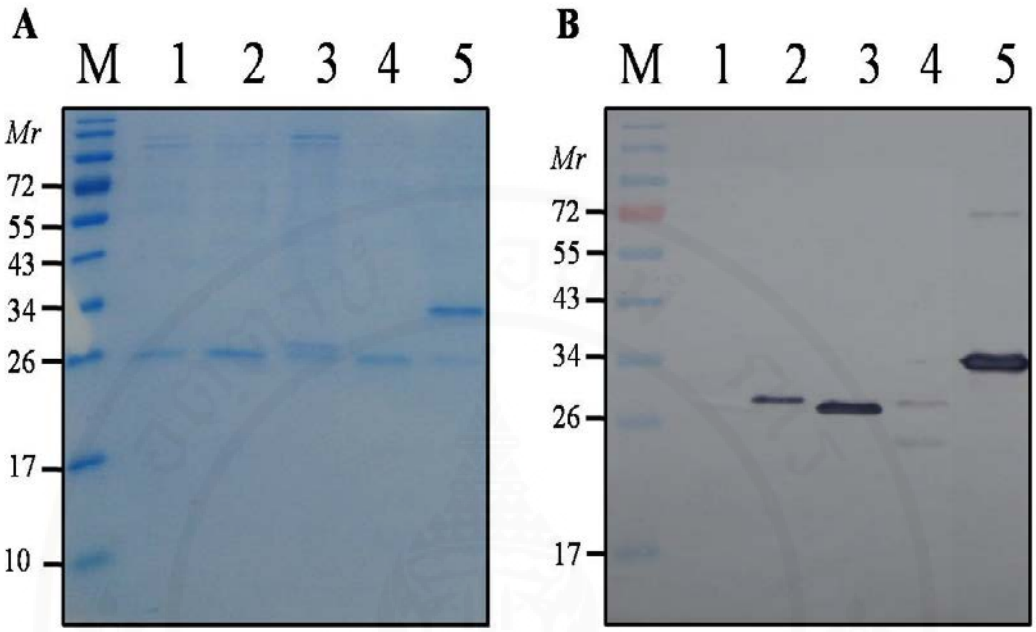

Figure 5.27 CBB stained SDS-PAGE separated purified HuScFv-6xHis purified from transformed BL21 (DE3) *E. coli* clones carrying recombinant pET plasmids with *huscfv26*, *huscfv51*, *huscfv53* and *huscfv99* inserts (**A**).Western blot patterns of the same preparations as detected with anti-His antibody **(B)**.

Lane M, Pre-stained broad range protein standard

Lane 1, Lysate of *E. coli* containing pET plasmids

Lanes 2-5, Purified HuScFv (~26-34 kDa) of clones no. 26, 51, 53 and 99, respectively

Numbers at the left of both blocks are relative molecular masses (*Mr*) of proteins

Copyright by Mahidol University

5.9.2 Determination of binding specificity of HuScFv to the native proteins (H1, N1 and M2) on influenza viruses

Before using purified HuScFv in testing interference of the virus replication cycle, all HuScFv were also determined for binding specificity to the native proteins (H1, N1 and M2) on influenza virion. The purified HuScFv of clones no. 26, 51, 53 and 99 were tested binding activity to the H1N1/2009 virus adsorbed on the hRBC ghost (see method in **section 4.8.1**). The purified lysate of *E. coli* containing pET plasmids and diluents were used as negative controls while the PAb(s) (**section 5.4**) were used as positive antibody controls (**Figure 5.28**). It was found that HuScFv of all clones gave higher OD_{405nm} signal than the purified lysate of BL21 (DE3) containing pET plasmids; implying that HuScFv of all selected clones could bind to the native protein on the virus.

Copyright by Mahidol University

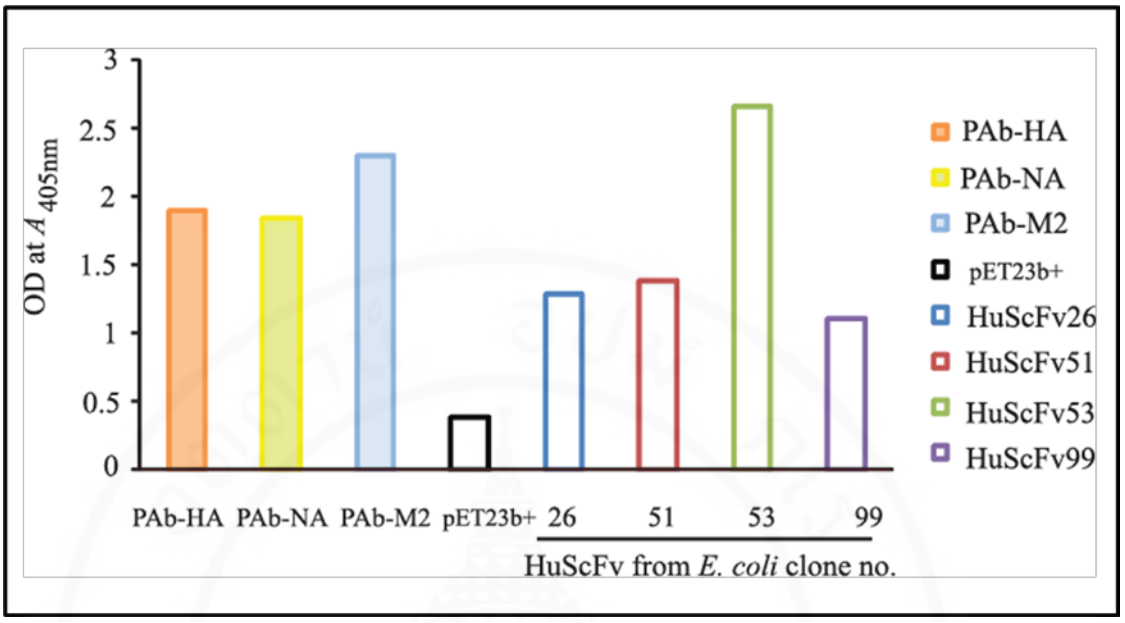

Figure 5.28 Results of indirect ELISA for determining the binding of the HuScFv of clones no. 26, 51, 53 and 99 to the native proteins (H1, N1 and M2) on H1N1/2009 influenza viruses. The results show that HuScFv of all clones gave higher OD_{405nm} than the lysate of BL21 (DE3) containing pET plasmids ($bET23b^{+}$).

PAb-HA, polyclonal antibody to rHA; PAb-NA, polyclonal antibody to rNA; PAb-M2, polyclonal antibody to rM2.

Copyright by Mahidol University

5.10 Determination of HuScFv mediated interference of virus replication cycle

5.10.1 Determination of HuScFv in interference of virus binding and uncoating to the target cells (see method in experimental design I of **Chapter 4.12**)

Influenza viruses were mixed with inhibitors, *i.e*., HuScFv26, HuScFv51, HuScFv53, HuScFv99, HuScFv-NA (received from Assist. Prof. Dr. Potjanee Srimanote), vaccinated serum (1:1,280) or medium alone before adding to the MDCK monolayer. After allowing cellular entry and discarding extracellular viruses, the infected cells were grown in the medium for 15 hours. Thereafter, the cells were washed and subjected to plaque assay. Numbers of virus foci in MDCK cells of all treatments were counted. **Figures 5.29A** and **5.29B** show numbers of virus foci and % inhibition mediated by the inhibitors and controls, respectively. The effectiveness in reducing intracellular virus by increasing order of magnitudes, were HuScFv-NA < HuScFv99 < HuScFv26 < HuScFv51 < HuScFv53. The vaccinated serum control gave ~80% inhibition. The infected cell controls had the highest virus foci (100%) and the least % inhibition.

5.10.2 Determination of HuScFv in interference of virus binding, uncoating, replicating and budding (see method in experimental design II of **Chapter 4.12**)

For experimental design 2, the viruses had been exposed to HuScFv26, HuScFv51, HuScFv53, HuScFv99, HuScFv-NA, vaccinated serum (1:1,280) or medium alone before adding to the cells and the infected cells were cultured in the medium containing the respective inhibitors or medium alone. The numbers of virus foci and % inhibition by the inhibitors and control are shown in **Figure 5.30A** and **5.30B**, respectively. The effectiveness in reducing intracellular virus, in increasing order of magnitude, were HuScFv-NA < HuScFv99 = HuScFv26 < HuScFv53 < HuScFv51. The H1N1/2009 infected cells control [viruses that treated with lysate of BL21 (DE3)] had the highest number of the virus foci or the lowest % inhibition. The

Copyright by Mahidol University

vaccinated serum control gave ~80% inhibition. The appearances of the virus foci in MDCK cells are shown in **Figure 5.31**.

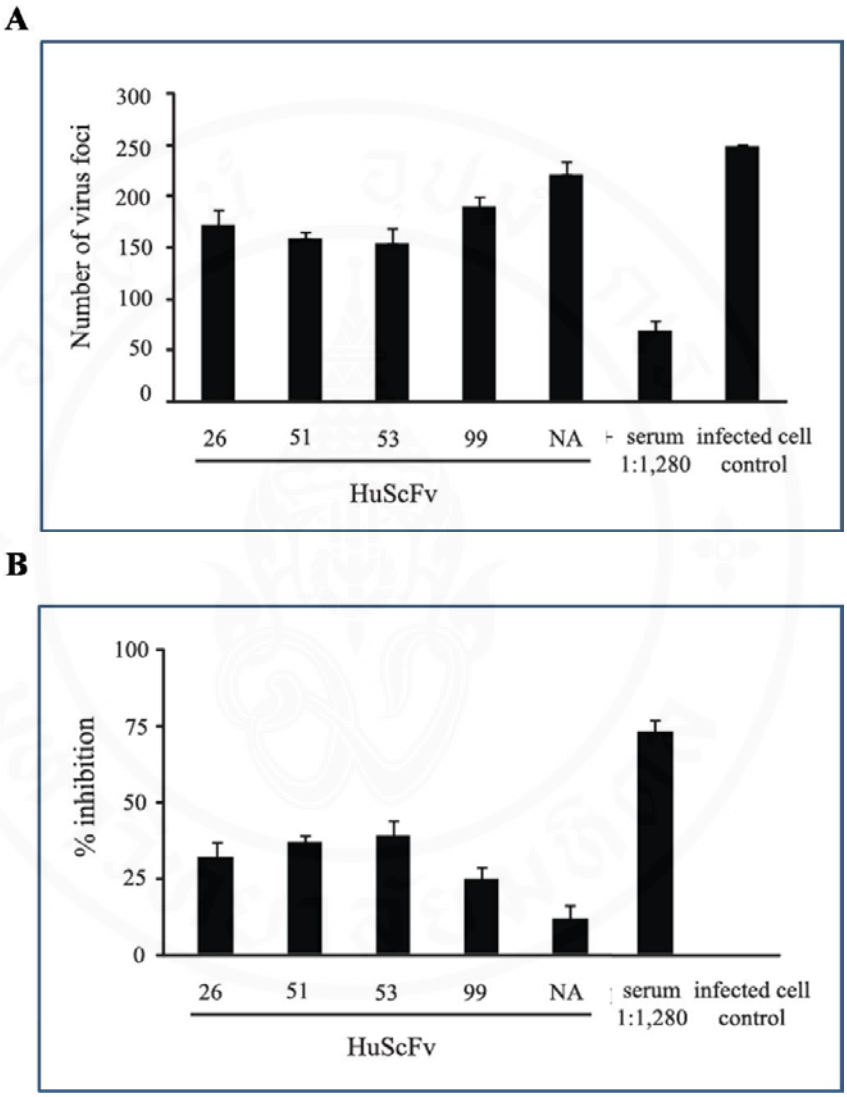

Figure 5.29 Numbers of virus foci (**A**) and percent inhibition of the virus focal formation **(B)** in MDCK cells infected with H1N1/2009 that had been exposed to various inhibitors and controls before adding to the cells and the infected cells were cultured for 15 hours. The virus infected cells exposed to plain medium had the highest number of the virus foci or the lowest % virus replication inhibition. The vaccinated serum control gave ~80% inhibition. The effectiveness in reducing intracellular virus, in increasing order of magnitude, were HuScFv-NA < HuScFv99 < HuScFv26 < HuScFv51 < HuScFv53.

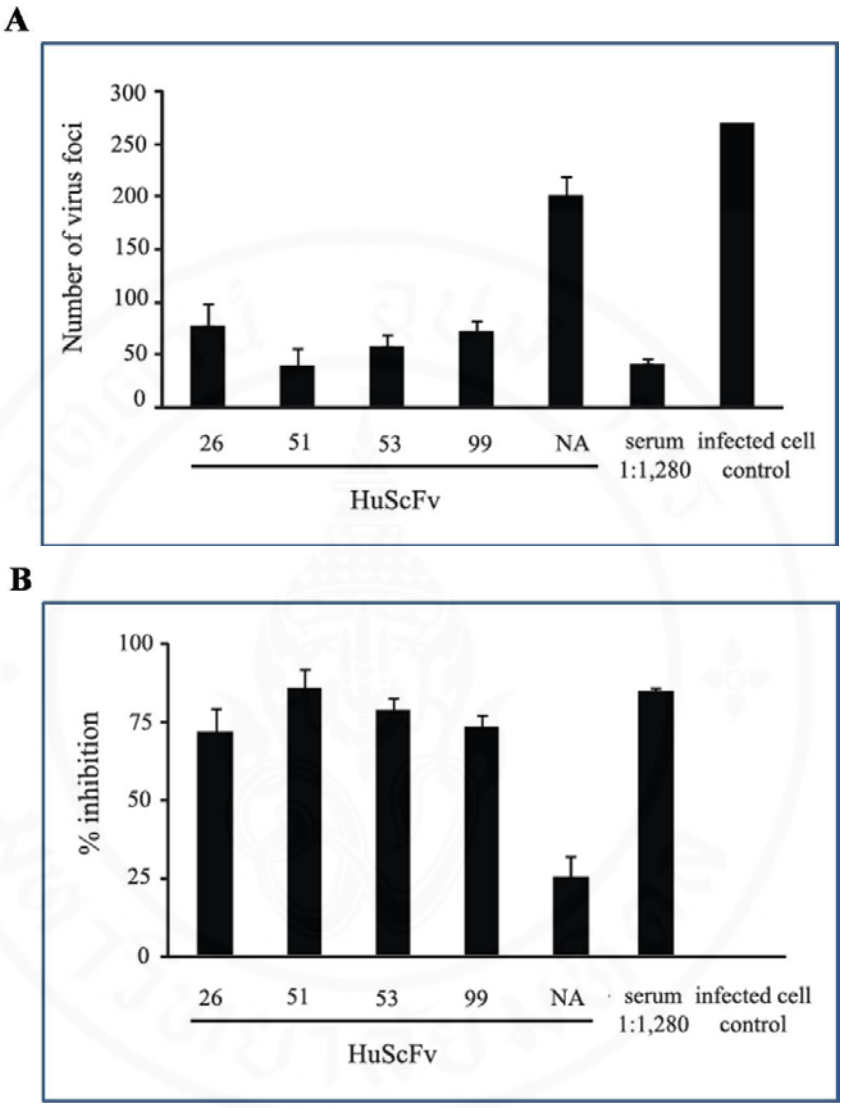

Figure 5.30 Numbers of virus foci (A) and % inhibition of virus replication (B) of experimental design II which the viruses were mixed with the respective inhibitors or control before adding to the cell monolayer. After allowing cellular entry and removing extracellular viruses, the infected cells were cultured in the medium containing inhibitors or controls for 15 hours. The intracellular virus foci were determined. The effectiveness in reducing intracellular virus of the inhibitors, in increasing order of magnitude, were HuScFv-NA < HuScFv99 = HuScFv26 < HuScFv53 < HuScFv51. The H1N1/2009 infected cells controls had the highest number of the virus foci or the lowest % inhibition. The vaccinated serum control gave ~80% inhibition.

Copyright by Mahidol University

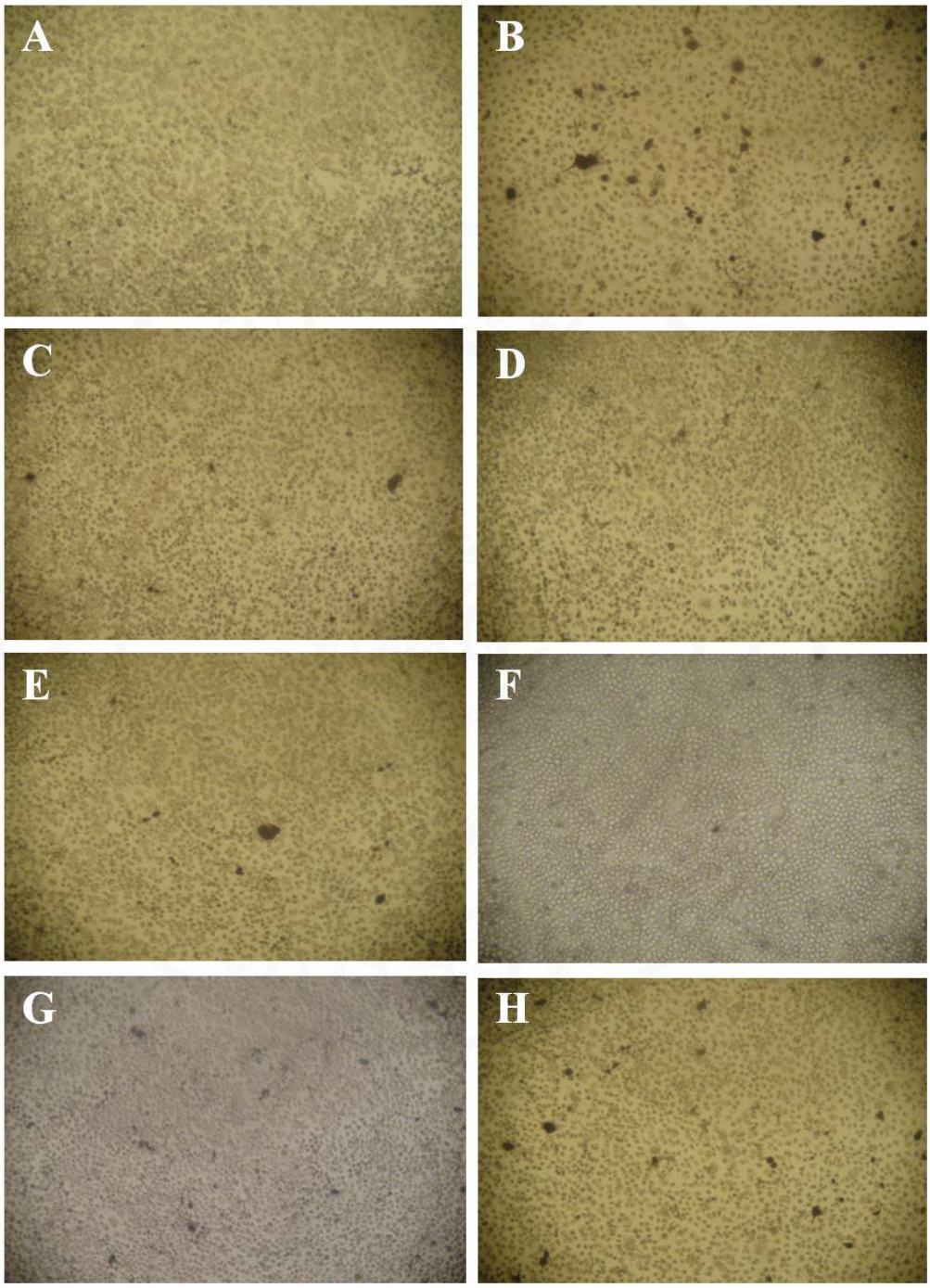

Figure 5.31 Appearances of influenza virus foci in infected MDCK cells treated with HuScFv, purified *E. coli* lysate and vaccinated serum in **Experiment design II**. **A**, Uninfected MDCK cell monolayer; **B**, negative inhibition controls (MDCK cells infected with the viruses); **C**, MDCK cells infected with viruses exposed to vaccinated serum; **D**, **E**, **F, G** and **H**, MDCK cells infected with viruses exposed to HuScFv26, HuScFv51, HuScFv53, HuScFv27, HuScFv99 and HuScFv-NA, respectively.

Copyright by Mahidol University

5.10.3 Determination of HuScFv in interfering of virus release and secondary infection and replication (see method in experimental design III of **Chapter 4.12**)

MDCK cells were infected directly with H1N1/2009. After cellular entry, the extracellular viruses were removed and the infected cells were cultured for 15 hours in the medium containing inhibitors or controls. **Figure 5.32A** and **5.32B** show numbers of virus foci and % inhibition. The effectiveness in reducing intracellular virus, in increasing order of magnitude, were HuScFv-NA < HuScFv99 < HuScFv51 < HuScFv26 < HuScFv 53. In the H1N1/2009 infected cells control had the highest numbers of the virus foci or the lowest % inhibition. The vaccinated serum control gave ~50%. HuScFv-NA had the lowest effect.

Copyright by Mahidol University

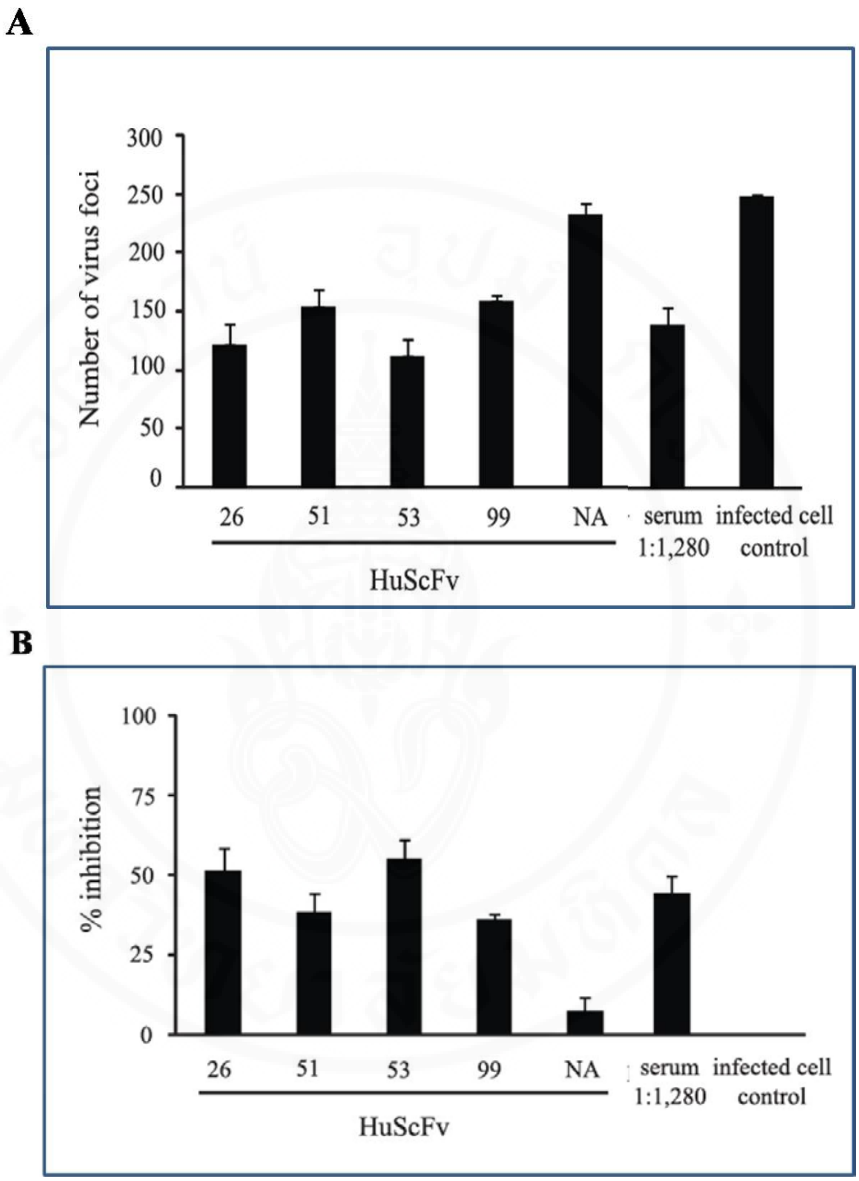

Figure 5.32 Numbers of virus foci (**A**) and % inhibition (**B**) of experiment design III. MDCK cells were infected directly with H1N1/2009. After cellular entry, the extracellular viruses were removed and the infected cells were cultured for 15 hours in the medium containing inhibitors or controls. The effectiveness in reducing intracellular virus, increasing order of magnitude, were HuScFv-NA < HuScFv99 < HuScFv51 < HuScFv26 < HuScFv 53. In the H1N1/2009 infected cells control gave the highest number of the virus foci or the lowest in % inhibition. The vaccinated serum control gave ~50% inhibition. HuScFv-NA had the lowest effect.

Copyright by Mahidol University

5.11 Selection of HuScFv display phage clones that bound to rM2

5.11.1 Results of phage bio-panning with the rM2

The purified soluble rM2 proteins from **section 4.2.3.2** of **Chapter IV** were used as the target antigen in the phage bio-panning (**section 4.5.3** of **Chapter IV**). The antigen bound phages were allowed to infect the HB2151 *E. coli*. Thirty *E. coli* transformants were randomly selected from the selective agar plate. They were verified for the presence of *huscfv* by PCR using the pCANTAB-*R1* and pCANTAB-*R2* primers. Among the 30 screened colonies, 27 clones (90%) revealed the *huscfv* amplicon at size ~1,000 bp (**Figure 5.33**).

5.11.2 Production of soluble HuScFv by the positive *E. coli* clones carrying *huscfv*-phagemids

All of the 27 *huscfv*-positive HB2151 *E. coli* clones were grown under IPTG induction and their cell lysates were analyzed for the presence of the soluble HuScFv by Western blot analysis (methodology in **section 4.7** of **section IV**). There were 17 clones (57%) that could express the soluble HuScFv which appeared as protein bands at *Mr* ~25-27 kDa (**Figure 5.34**).

Copyright by Mahidol University

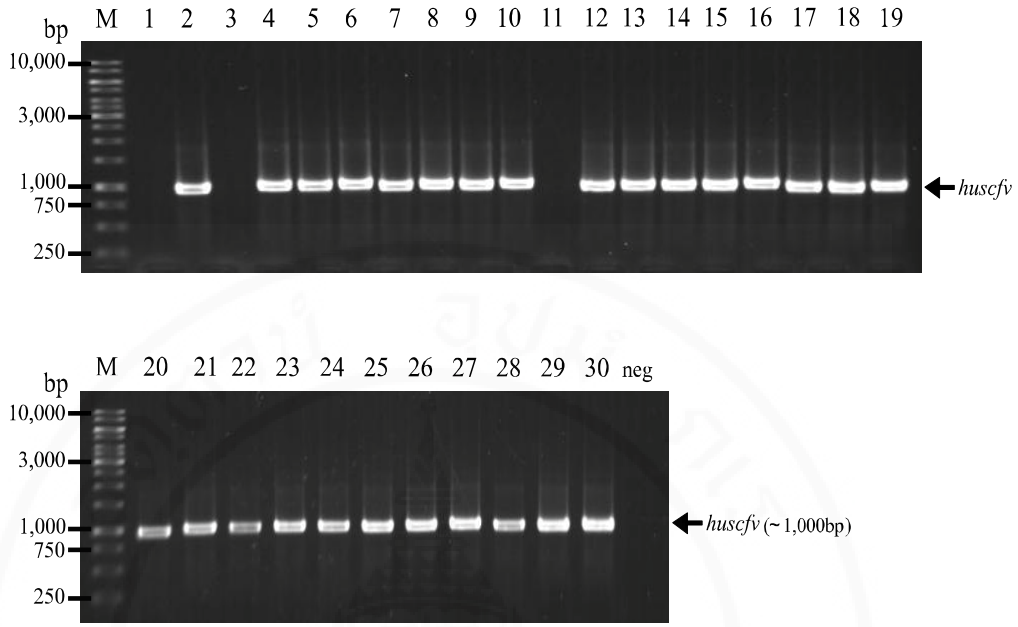

Figure 5.33 Amplicons of *huscfv* in 30 randomly picked phagemid transformed HB2151 *E. coli* clones

Lane M, GeneRuler 1 kb DNA ladder

Lanes 2, 4-10 and 12-30, HB2151 *E. coli* clones that were positive for the *Huscfv*

Lanes 3 and 11, HB2151 *E. coli* clones that were negative for the *huscfv*

Neg, Negative control (no DNA template)

Arrows indicate the location of *huscfv* amplicons (~1,000 bp)

Numbers at the left of both blocks are DNA sizes in bp

Copyright by Mahidol University

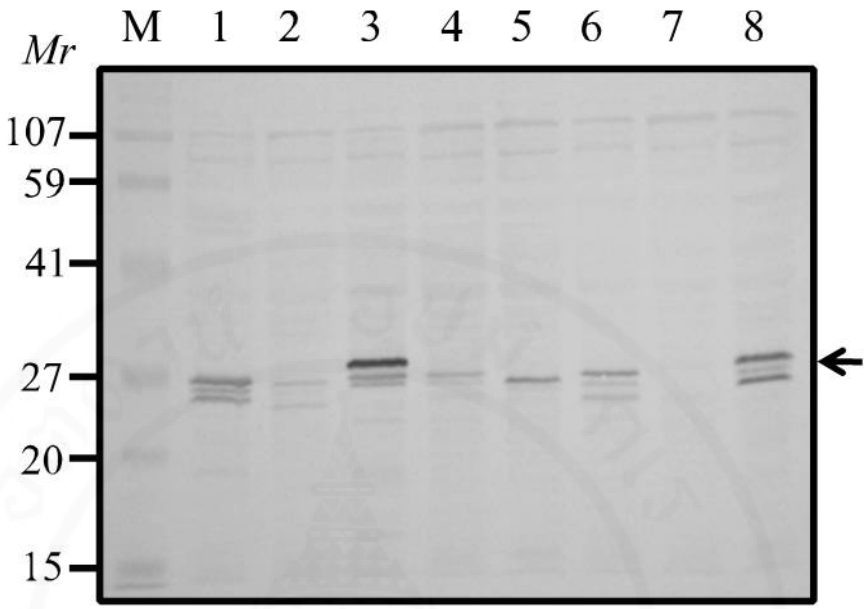

Figure 5.34 Western blot results for detection of HuScFv in lysates of representative *huscfv*-pCANTAB5E-transformed HB2151 *E. coli* colonies

Lane M, Pre-stained broad range protein standard marker

Lanes 1-6 and 8, Reactive bands of HuScFv in lysates of HB2151 *E. coli*

Lane 7, Negative detection of HuScFv in lysate of HB2151 *E. coli*

Arrow indicates location of HuScFv protein (~25-27 kDa) which tends to appear as a protein doublet which the upper band is immature protein with signal peptide and the lower band is mature HuScFv (other faint bands are degraded product of the principal protein)

Copyright by Mahidol University

5.12 Characterization of the M2 specific-HuScFv

5.12.1 Binding specificity of the HuScFv as determined by indirect ELISA

Whole cell lysates of all transformed HB2151 *E. coli* clones that could express HuScFv from **section 5.11** were used in the indirect ELISA for determining the HuScFv binding to the purified rM2 using BSA as an antigen control in the assay. Lysate of HB2151 *E. coli* without *huscfv*-phagemid and diluents were used as negative controls while the mPAb-M2 (**section 5.4**) was used as positive antibody control. HuScFv in lysates of 10/17 *E. coli* clones (no. 2, 5, 9, 13, 14, 19, 20, 23,27 and 29) gave significant binding to the rM2 by indirect ELISA (**Figure 5.35**) while the OD_{405nm} of the negative control was negligible and the OD_{405nm} of the positive control was high.

5.12.2 Restriction fragment length polymorphism (RFLP) of the coding sequences of the HuScFv

The restriction fragment length polymorphism (RFLP) or diversity of the DNA sequences coding for selected 10 HuScFv clones (no. 2, 5, 9, 13, 14, 19, 20, 23, 27 and 29) from **section 5.12** were determined. The *huscfv* sequences of the 10 *E. coli* clones showed 6 different DNA banding patterns after *Mva*I digestion, 14% SDS-PAGE and ethidium bromide staining (**Figure 5.36**). Clones no. 5 and 20 had pattern 2 (lane 2); clones no. 14 and 29 had pattern 3 (lane 3), clones no.13 and 23 had pattern 3 (lane 3), clones no. 13 and 23 had pattern 5 (lane 5) and clones no. 2, 19, 27 had patterns 1, 4 and 6, respectively (lanes 1, 4 and 6).

Copyright by Mahidol University

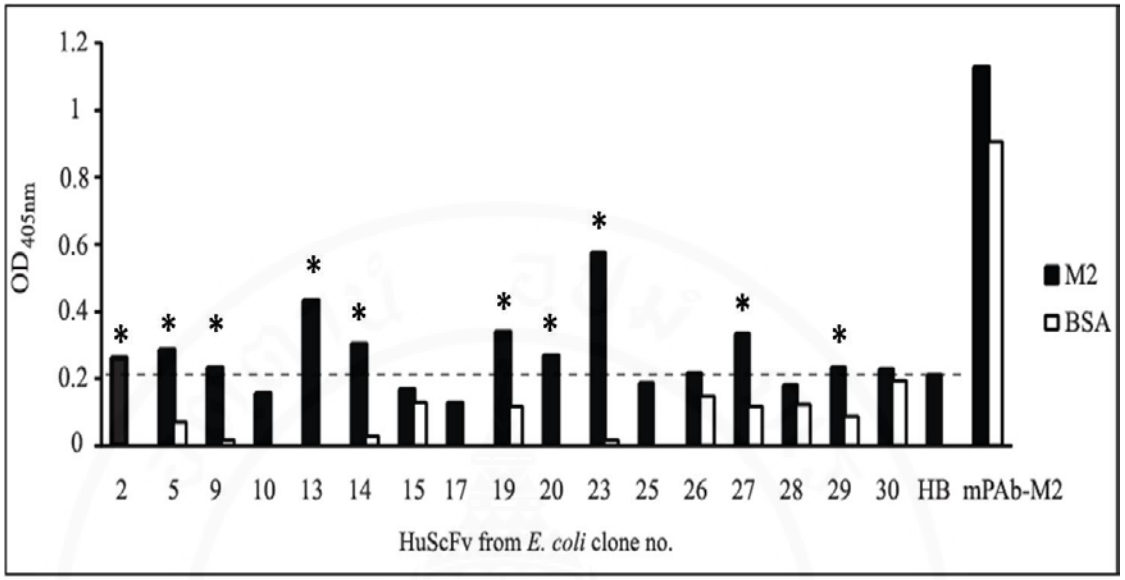

Figure 5.35 Indirect ELISA results showing the binding of HuScFv in lysates of 17 *huscfv* positive *E. coli* clones to rM2 and BSA control. HuScFv of 10 clones (no. 2, 5, 9, 13, 14, 19, 20, 23, 27 and 29) bound specifically to the rM2.

* indicate positive binding and dash line indicate cut off criteria

Copyright by Mahidol University

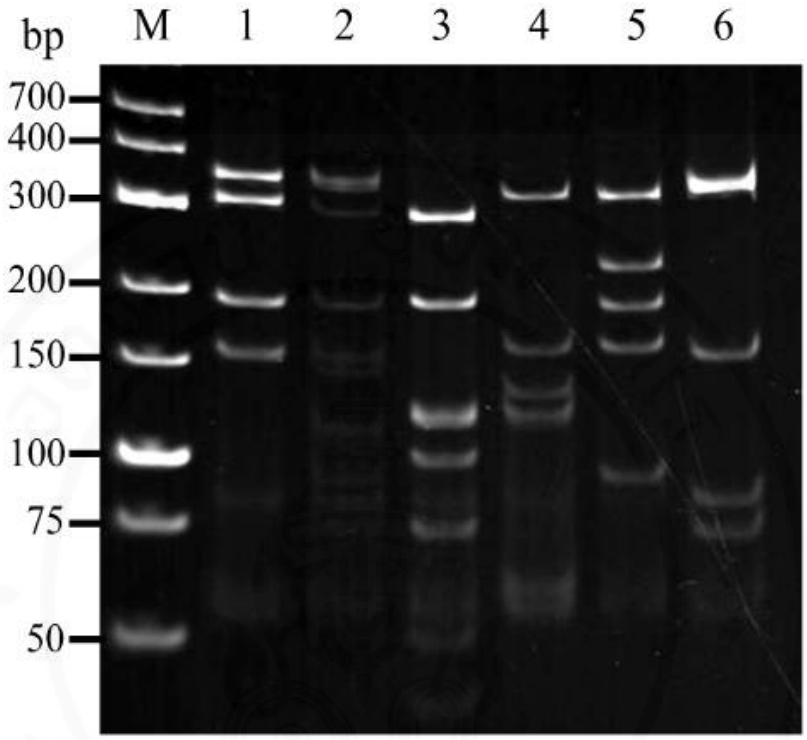

Figure 5.36 RFLP or DNA banding patterns of *huscfv* sequences in 10 HB2151 *E. coli* clones, *i.e.*, no. 2, 5, 9, 13, 14, 19, 20, 23, 27 and 29. The 10 clones revealed 6 different DNA banding patterns.

Lane M, GeneRuler^{TM} low range DNA ladder

Lane 1, DNA banding pattern of *huscfv* of clone no.2

Lane 2, DNA banding pattern of *huscfv* of clones no.5 and 20

Lane 3, DNA banding pattern of *huscfv* of clones no.9 and 14

Lane 4, DNA banding pattern of *huscfv* of clone no.19

Lane 5, DNA banding pattern of *huscfv* of clones no.13 and 23

Lans 6, DNA banding pattern of *huscfv* of clone no. 27

Numbers at the left are DNA sizes in bp

Copyright by Mahidol University

5.12.3 Binding of the HuScFv to recombinant and native M2 as determined by Western blotting and immunofluorescence assay

Whole cell lysates of 6 selected HB2151 *E. coli* clones containing HuScFv, *i.e*., clones no. 2, 5, 14, 19, 23, and 27, that gave 6 different DNA banding patterns were used to test the binding of their HuScFv to the recombinant and native M2 (from homogenate of influenza A/H5N1infected MDCK cells). Western blot results showed that HuScFv of clones no. 2, 19, 23, and 27 (HuScFv2, HuScFv19, HuScFv23 and HuScFv27, respectively) bound to rM2 and nM2 (**Figure 5.37** and **Figure 5.38**, respectively). The HuScFv of these 4 clones also bound to the nM2 in virus infected MDCK cells as tested by immunofluorescence assay (**Figure 5.39**).

5.12.4 Identification of immunoglobulin frameworks (FRs) and complementarity determining regions (CDRs) of HuScFv

The nucleotide sequences of the HuScFv2, 19, 23, and 27 that gave positive binding to the rM2 and nM2 were sequenced. Multiple of the selected HuScFv amino acids were aligned by using ClustalW2 software available on http://www.ebi.ac.uk/Tool/services. The deduced amino acid sequences of all clones were shown to be complete **(Figure 5.40)**, *i.e*., containing full length VH-linker-VL domains. The immunoglobulin frameworks (FRs) and complementarity determining regions (CDRs) of the deduced amino acids of the *huscfv* sequences were predicted using the Immunogenetics Information System server (IMGT/V-QUEST).

Copyright by Mahidol University

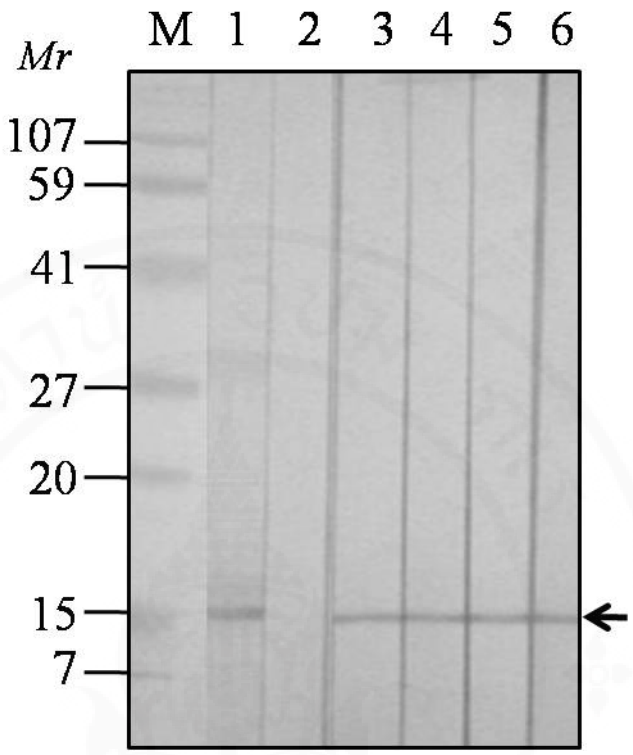

Figure 5.37 Western blot patterns of HuScFv2, 19, 23 and 27 that bound to the rM2 HuScFv5 and 14 did not bind to the rM2 (data not shown).

Lane M, Pre-stained broad range protein standard marker

Lane 1, SDS-PAGE separated rM2 probed with mPAb-M2

Lane 2, SDS-PAGE separated rM2 probed with lysate of HB2151 *E. coli* without HuScFv

Lanes 3-6, SDS-PAGE separated rM2 probed with lysates of *E. coli* clones no. 2, 19, 23 and 27 containing HuScFv2, 19, 23 and 27, respectively

Arrow indicates the location of reactive band of HuScFv bound to rM2

Numbers as the left are relative molecular masses (*Mr*) of proteins

Copyright by Mahidol University

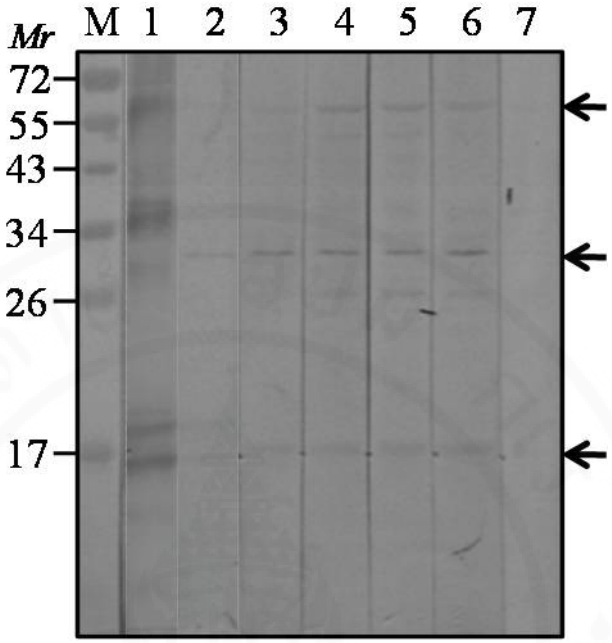

Figure 5.38 Western blot patterns of HuScFv2, 19, 23 and 27 that bound to the nM2

Lane M, Pre-stained broad range protein standard marker

Lane 1, SDS-PAGE separated lysate of influenza virus infected MDCK cells containing nM2 probed with anti-6xHis antibody

Lane 2, SDS-PAGE separated lysate of influenza virus infected MDCK cells containing nM2 probed with PAb-M2

Lanes 3-6, SDS-PAGE separated lysate of influenza virus infected MDCK cells containing nM2 probed with *E. coli* lysates containing HuScFv2, 19, 23 and 27, respectively

Lane 7, SDS-PAGE separated lysate of influenza virus infected MDCK cells containing nM2 probed with lysate of HB2151 *E. coli* without HuScFv

Lower arrow indicated the location of monomeric nM2; middle arrow indicates dimeric nM2 and uppermost arrow indicates tetrameric nM2

Numbers as the left of both blocks are relative molecular masses (*Mr*)

Copyright by Mahidol University

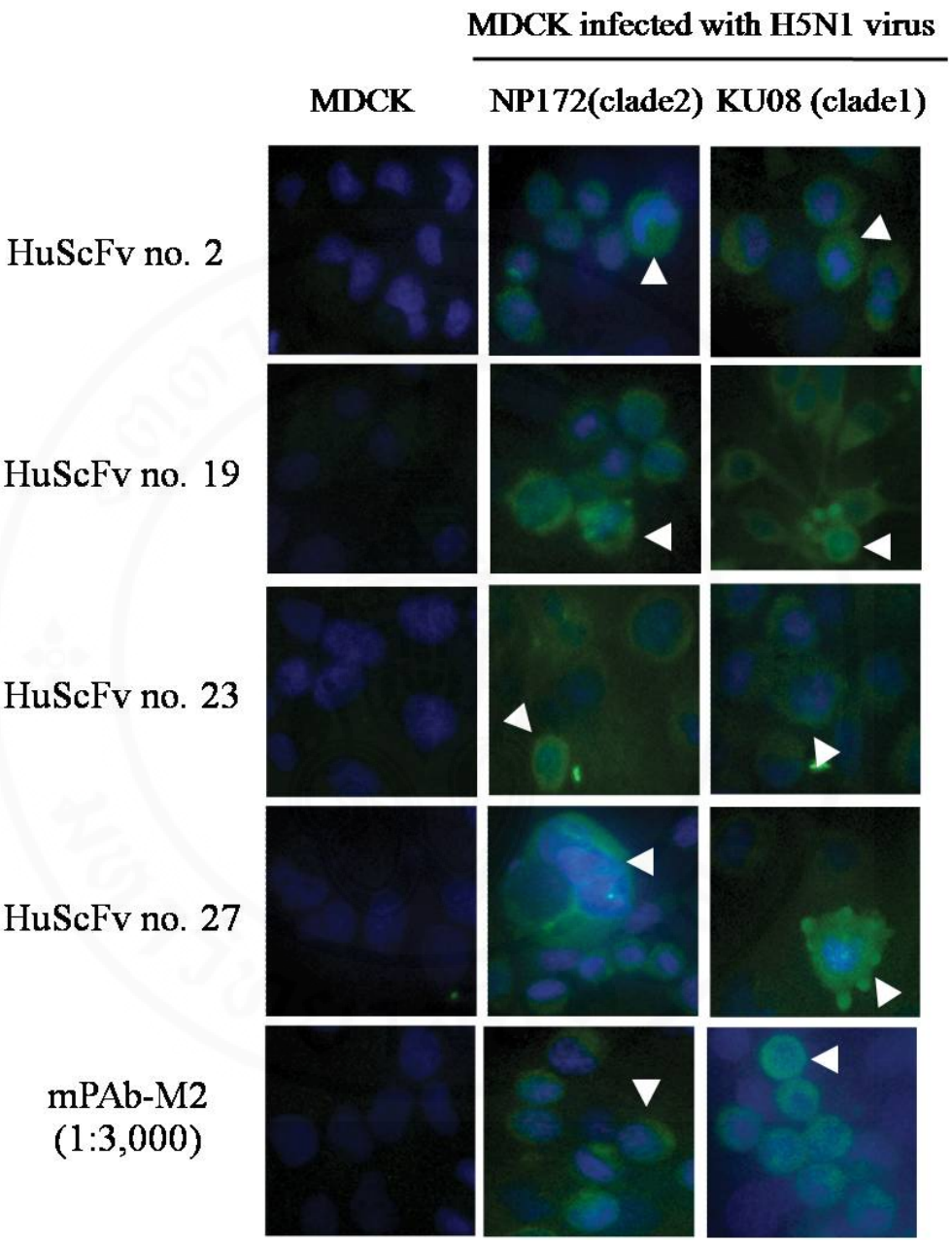

Figure 5.39 Determination of binding activity of M2 specific HuScFv to H5N1 viruses infected MDCK cells by immunofluorescence. Binding of HuScFv2, 19, 23 and 27 and mPAb-M2 (Green, arrow head) in the MDCK cells infected with H5N1 viruses which were amantadine sensitive (NP-172) (blocks of middle column, respectively) and resistant (KU08) (blocks of right column, respectively). Non-infected cells reacted with HuScFv or mPAb-M2 is shown in the respective blocks of the left column.

Copyright by Mahidol University

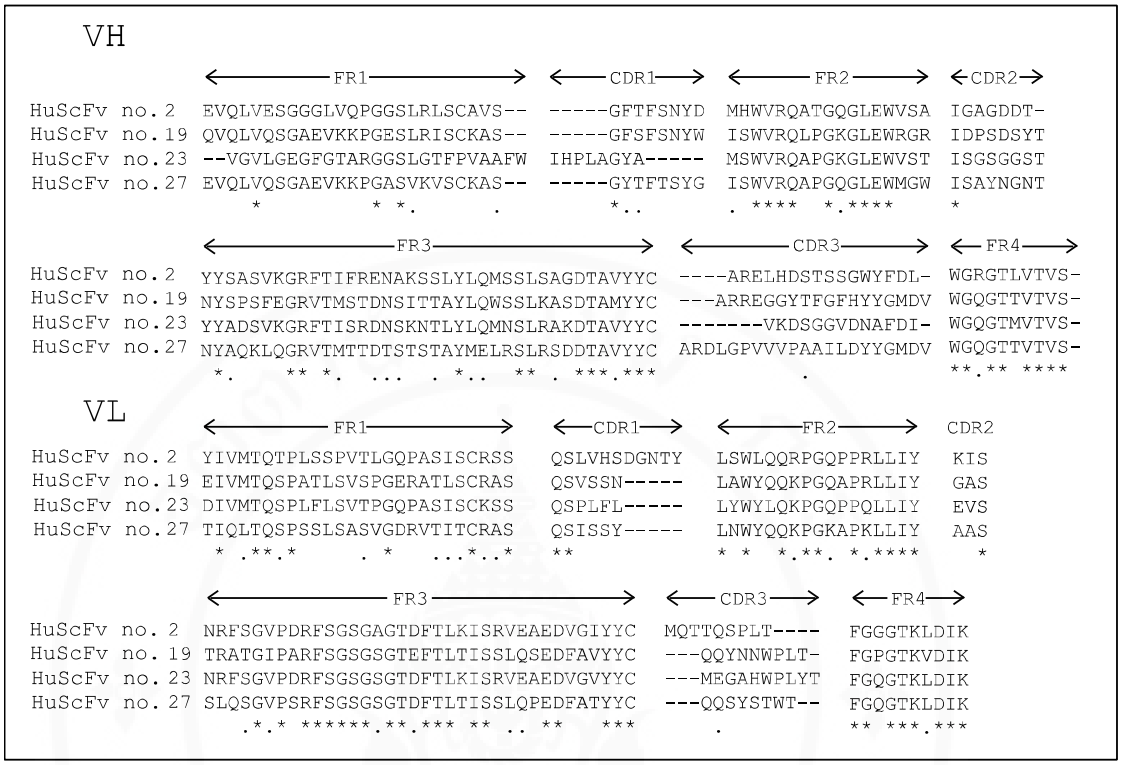

Figure 5.40 Immunoglobulin frameworks (FRs) and complementarity determining regions (CDRs) of heavy (VH) and light (VL) chains HuScFv sequence of clones no. 2, 19, 23 and 27. Three CDRs and four FRs of the HuScFv from the four HB2151 *E. coli* clones were determined by using the IMGT server. Multiple alignments of amino acid sequence diversities in CDRs of VH and VL of the four clones were verified by using ClustalW server.

* indicates identical amino acid

: indicates conservative amino acid substitution

. indicates semi-conservative amino acid substitution

Copyright by Mahidol University

5.13 HuScFv coding sequences in pET plasmid

5.13.1 Large scale expression of the selected HuScFv clones

The HuScFv coding sequences of clones no. 2, 19, 23 and 27 were subcloned from pCANTAB5E phagemid into pET plasmid system to increasing yields of recombinant HuScFv protein. Colony PCR was performed to screen the positive transformed BL21 (DE3) *E. coli* clones that carry the *huscfv* fragments with the expected size at ~1,000 bp (**Figure 5.41**).

According to HuScFv expression condition (**section 4.11** of **Chapter IV**), the expressed HuScFv were predominantly located in the insoluble parts of crude *E. coli* homogenates. Large scale expression and purification of HuScFv-His by using TALON Metal Affinity resin under denaturing condition were performed. **Figure 5.42A** shows CBB stained purified of HuScFv-His from the respective transformed BL21 (DE3) clones after SDS-PAGE separation as well as their respective Western blot patterns (**Figure 5.42B**).

Copyright by Mahidol University

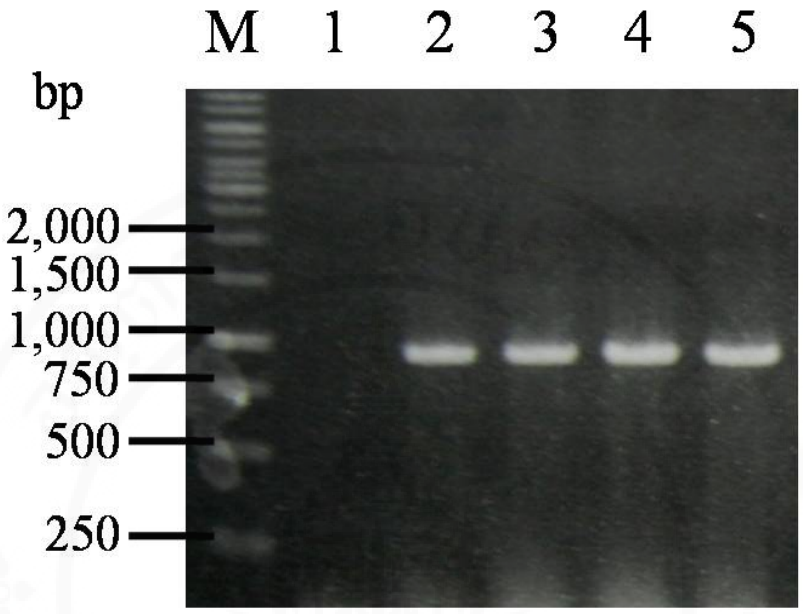

Figure 5.41 Amplicons of *huscfv* of clones no. 2, 19, 23 and 27 after colony PCR for screening of transformed BL21 (DE3) *E. coli* sibling colonies carrying *huscfv*-pET plasmids by using T7 primers and randomly selected colonies of the *E. coli* siblings as DNA templates. Positive clones revealed the *huscfv* DNA amplicons at ~1,000 kb.

Lane M, GeneRuler^{TM} 1 kb DNA ladder marker

Lane 1, Negative internal control (no DNA template)

Lanes 2-5, DNA amplicons of *huscfv* from siblings of *E. coli* clones no. 2, 19, 23 and 27, respectively

Numbers at the left are DNA sizes in bp

Copyright by Mahidol University

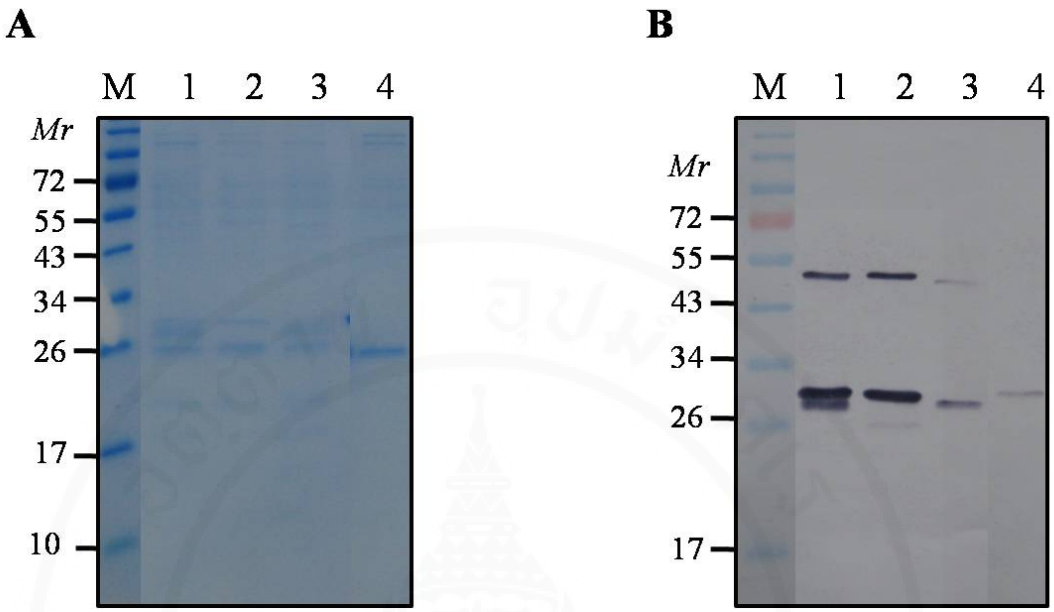

Figure 5.42 CBB stained SDS-PAGE separated HuScFv-6xHis purified from transformed BL21 (DE3) *E. coli* clones carrying recombinant pET plasmids with *huscfv2*, *huscfv19*, *huscfv23* and *huscfv27* inserts **(A).** Western blot patterns of the purified HuScFv-6xHis detected with anti-6xHis antibody **(B)**.

Lane M, Pre-stained broad range protein standard marker

Lane 1, SDS-PAGE separated purified lysate of *E. coli* containing pET plasmids

Lanes 2-5, SDS-PAGE separated purified lysates of siblings of *E. coli* clones no. 2, 19, 23 and 27, respectively

Numbers at the left of both blocks are relative molecular masses (*Mr*) of proteins

Copyright by Mahidol University

5.14 M2 specific-HuScFv mediated interference of influenza virus replication

5.14.1 HuScFv interfered with virus binding and uncoating to the target cells (see method in **experiment design I** of **Chapter 4.12**)

MDCK cells infected with the adamantane sensitive and resistant viruses [A/chicken/Thailand/NP-172/2006 (H5N1) clade 2 and A/dog/Thailand/KU08/2004 (H5N1) clade 1, respectively] were mixed with the test inhibitors, *i.e.*, HuScFv2, HuScFv19, HuScFv23, HuScFv27, control inhibitors rimantadine and PAb-M2) or medium alone (infected control), before adding to MDCK monolayer. After cellular entry and extracellular virus removal, the infected cells were grown for 15 hours.

Numbers of virus foci in MDCK cells were counted. **Figure 5.43A** shows numbers of virus foci in all treatments. The effectiveness of test and control inhibitors in reducing the virus foci in MDCK cells infected with the adamantane sensitive viruses (H5N1/NP172) compared with the infected control, in increasing order of magnitude, were: mPAb-M2 < HuScFv27 < HuScFv2 < rimantadine. The numbers of virus foci in the infected cells treated with HuScFv19 and 23 were not different from the infected cell control.

In MDCK cells infected with the adamantane resistance viruses (H5N1/KU08), the effectiveness in reducing virus foci, in increasing order of magnitude, were rimantadine = PAb-M2 < HuScFv27 < HuScFv19. The virus foci in the groups treated with HuScFv-2 and -23 were not different from infected cell control.

In addition, M1 vRNA in culture supernatants and inside the cells of experimental design I of **Figure 5.44** (cells infected with adamantine sensitive H5N1/NP172) and **Figure 5.45** (cells infected with adamantine resistant H5N1/KU08)] were also quantified by qPCR. Rimantadine was the best in reducing of M1 vRNA in culture supernatants as well as inside the cells of both adamantane sensitive and resistance viruses. In experimental design I of the sensitive virus, HuScFv23 could reduce a little of M1 vRNA in culture supernatant while HuScFv27 and PAb-M2 could reduce M1 mRNA inside the cells. For the resistant virus,

Copyright by Mahidol University

HuScFv19 and rimantadine could reduce M1 RNA both in culture supernatants and inside the cells.

5.14.2 Determination of HuScFv in interference of virus binding, replicating and budding (see method in **experiment design II** of **Chapter 4.12**)

For experiment design 2 which the viruses had been exposed to HuScFv2, HuScFv23, HuScFv19, HuScFv23, HuScFv27, rimantadine, PAb-M2 or medium alone before adding to the cells and the infected cells were cultured in the respective inhibitors or medium alone, the number of virus foci (**Figure 5.43B**) show the adamantane sensitive virus foci were not found in the cells exposed to all inhibitors. Numbers of foci of the amantadine resistant virus treated with the HuScFv, PAb-M2 and rimantadine were markedly reduced compared with the infected cell control. **Figure 5.46** show appearances of the virus foci in MDCK cells

The qPCR results of M1 RNA in culture supernatants and inside the cells were also verified [**Experiment design II** of **Figure 5.44** (H5N1/NP172) and **Experiment design II** of **Figure 5.45** (H5N1/KU08)]. For the sensitive virus, rimantadine show the best in reducing of M1 vRNA both in culture supernatants and inside the cells. The HuScFv of all clones and PAb-M2 could reduce significantly the virus in both culture supernatants and inside the cells in comparison with the infected cells ($p < 0.05$). For the resistant virus the effectiveness of the inhibitors in reducing the virus release were rimantadine = PAb-M2 < HuScFv2 < HuScFv27 < HuScFv23 < HuScFv19 while the reduction of intracellular virus, HuScFv of clones no. 19 and 27 were most effective.

5.14.3 Determination of HuScFv in interference of virus budding (see method in **experiment design III** of **Chapter 4.12)**

Figure 5.43C show numbers of virus foci in MDCK cells infected directly with the viruses and the cells were grown in medium containing inhibitors or medium alone. No foci of the rimantadine sensitive virus were found in the infected cells cultured with HuScFv of clones no. 19 and 23 and rimantadine while only few foci were seen in cells exposed to HuScFv of clones no. 2 and 27 and PAb-M2. The numbers of amantadine-resistant virus foci in infected cells cultured in HuScFv, PAb-

Copyright by Mahidol University

M2 and rimantadine supplemented medium were markedly reduced compared with the infected cell control.

The qPCR results of M1 RNA in culture supernatants and inside the cells were also verified [**Experiment design III** of **Figure 5.44** (H5N1/NP172) and **Experiment design III** of **Figure 5.45** (H5N1/KU08)]. For the sensitive virus, rimantadine show the best in reducing of M1 vRNA both in culture supernatants and inside the cells. The HuScFv of all clones and PAb-M2 could reduce significantly the virus in both culture supernatants and inside the cells in comparison with the infected cells.

In **experiment design III** of drug resistant virus, rimantadine was less effective than the HuScFv 23, HuScFv 27 and mPAb-M2 in reducing the M1 vRNA in the culture supernatants, but equally effective to the HuScFv 2 and HuScFv19. The effectiveness in reducing intracellular virus, in increasing order of magnitude, were HuScFv2 < HuScFv19 < rimantadine < HuScFv27 = mPAb-M2 < HuScFv23.

Copyright by Mahidol University

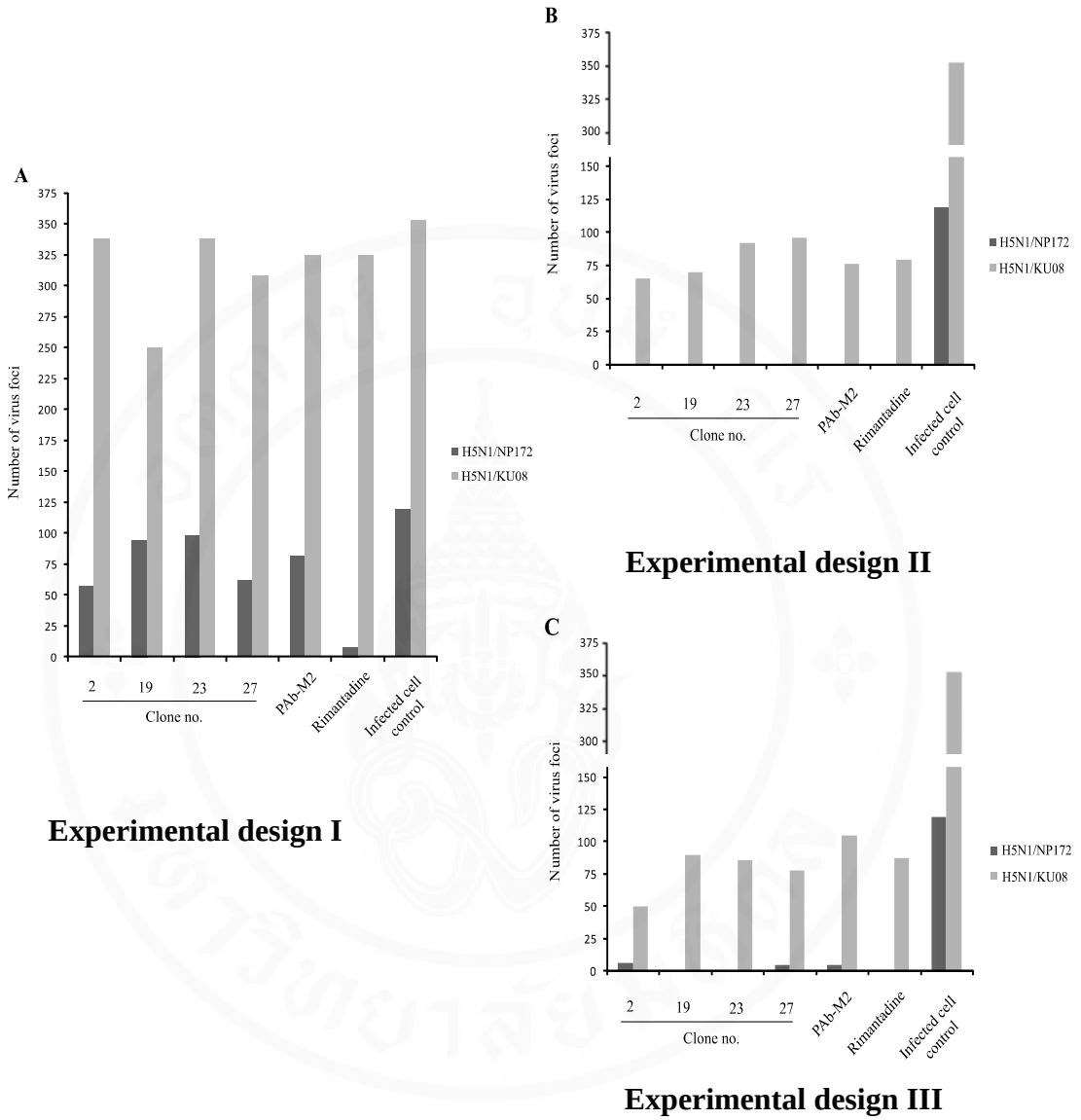

Figure 5.43 Number of virus foci in the MDCK cells infected with adamantane sensitive and resistant viruses

A, Results of experiment design I (viruses were mixed with the test inhibitors or medium alone before adding to MDCK monolayer. After cellular entry and extracellular virus removal, the infected cells were grown in medium alone for 15 hours).

B, Results of experiment design II (viruses had been exposed to inhibitors or medium alone before adding to the cells and the infected cells were cultured in the respective inhibitors or medium alone for 15 hours)

C, Results of experiment design III (MDCK cells infected directly with the viruses and the cells were grown in medium containing inhibitors or medium alone for 15 hours).

Copyright by Mahidol University

Experimental design I: virus exposed to inhibitors/control before adding to cells and cultured in medium alone

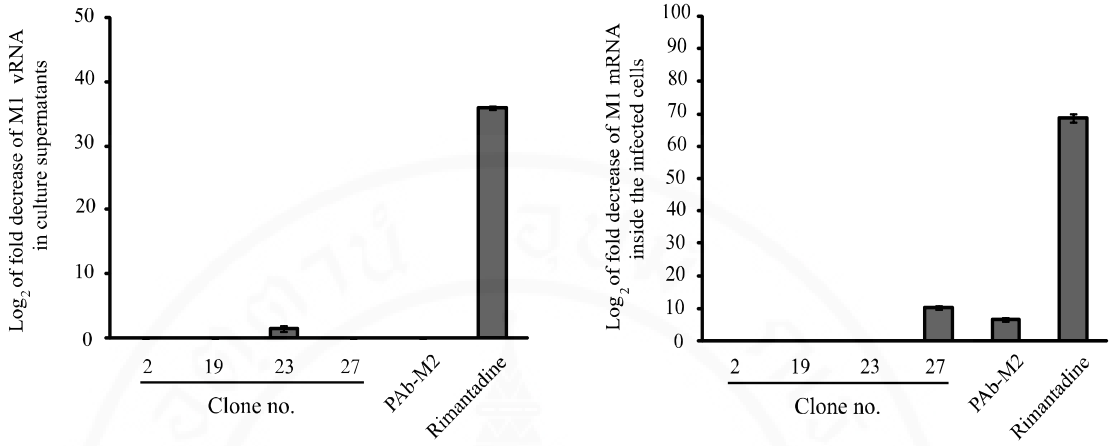

Experiment design II: virus exposed to inhibitors/control before adding to cells and cultured in medium containing inhibitors/medium alone (control)

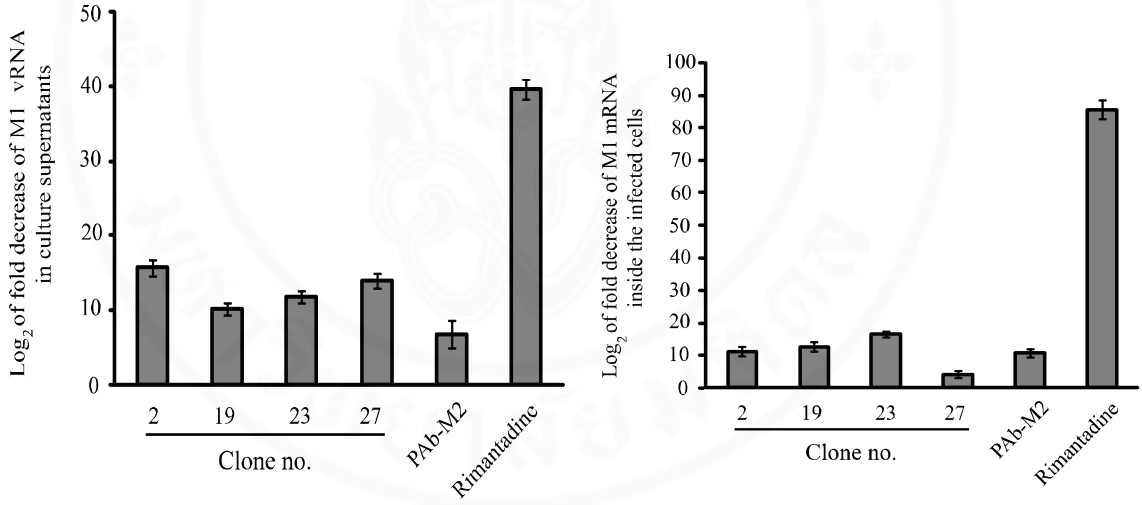

Experiment design III: viruses were added directly to cells; after cellular entry and extracellular virus removal, the infected cells were grown in medium containing inhibitors/control (medium alone)

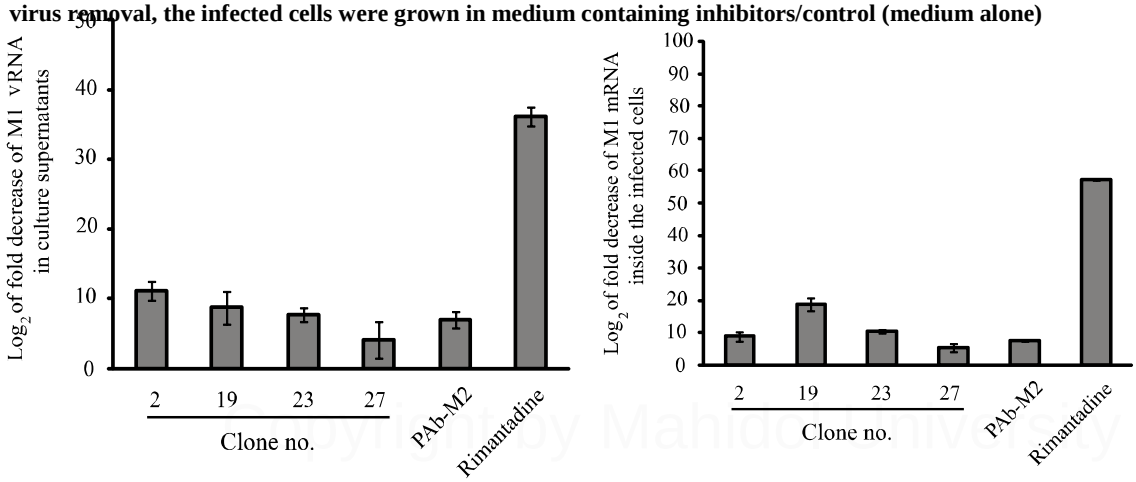

Copyright by Mahidol University

Figure 5.44 (please see legend in the next page)

Figure 5.44 Log_2 of fold decrease in M1 RNA in culture supernatants and inside the cells infected with amantadine sensitive influenza viruses [A/chicken/Thailand/NP172/2006 (clade 2)] treated differently with inhibitors (HuScFv, rimantadine, PAb-M2) in comparison with control (medium alone)

Copyright by Mahidol University

Experimental design I: virus exposed to inhibitors/control before adding to cells and cultured in medium alone

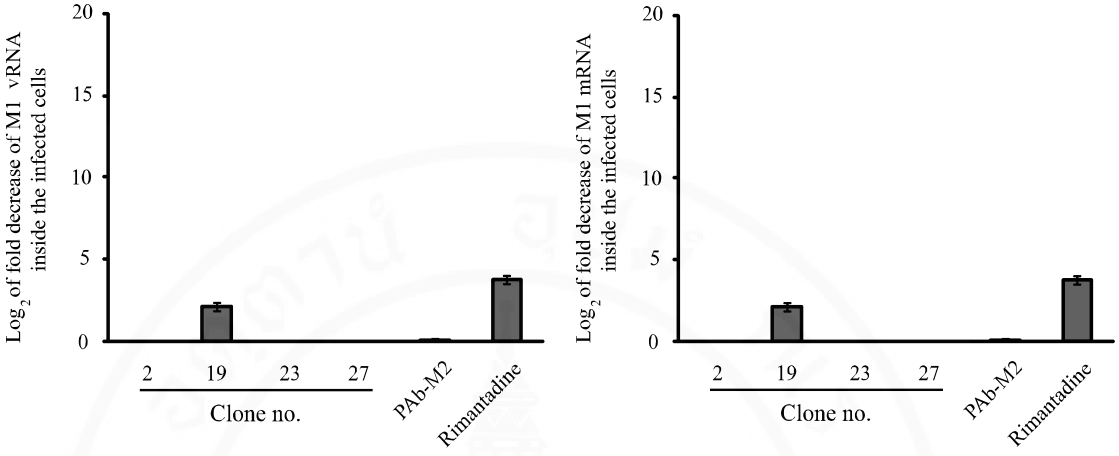

Experiment design II: virus exposed to inhibitors/control before adding to cells and cultured in medium containing inhibitors/medium alone (control)

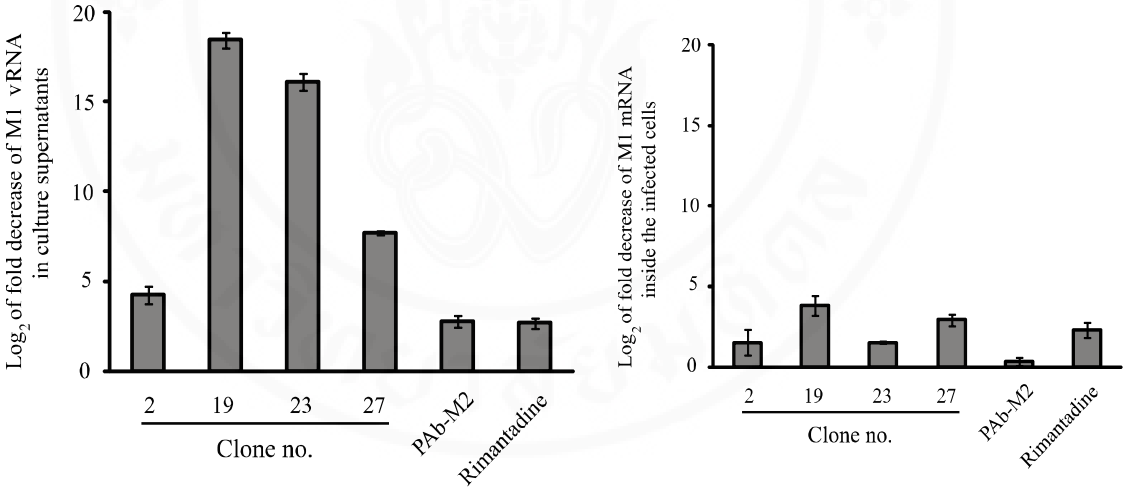

Experiment design III: viruses were added directly to cells; after cellular entry and extracellular virus removal, the infected cells were grown in medium containing inhibitors/control (medium alone)

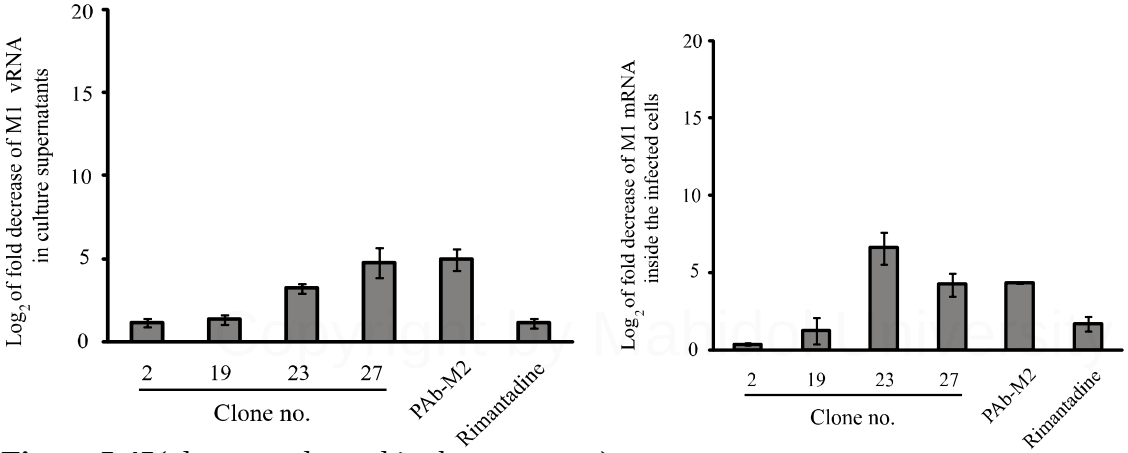

Figure 5.45(please see legend in the next page)

Figure 5.45 Log_2 of fold decrease in RNA in culture supernatants and inside the cells infected with adamatane resistant influenza viruses [A/dog/Thailand/KU08/2004 (clade 1)] treated differently with inhibitors (HuScFv, rimantadine, PAb-M2) in comparison with control (medium alone)

Copyright by Mahidol University

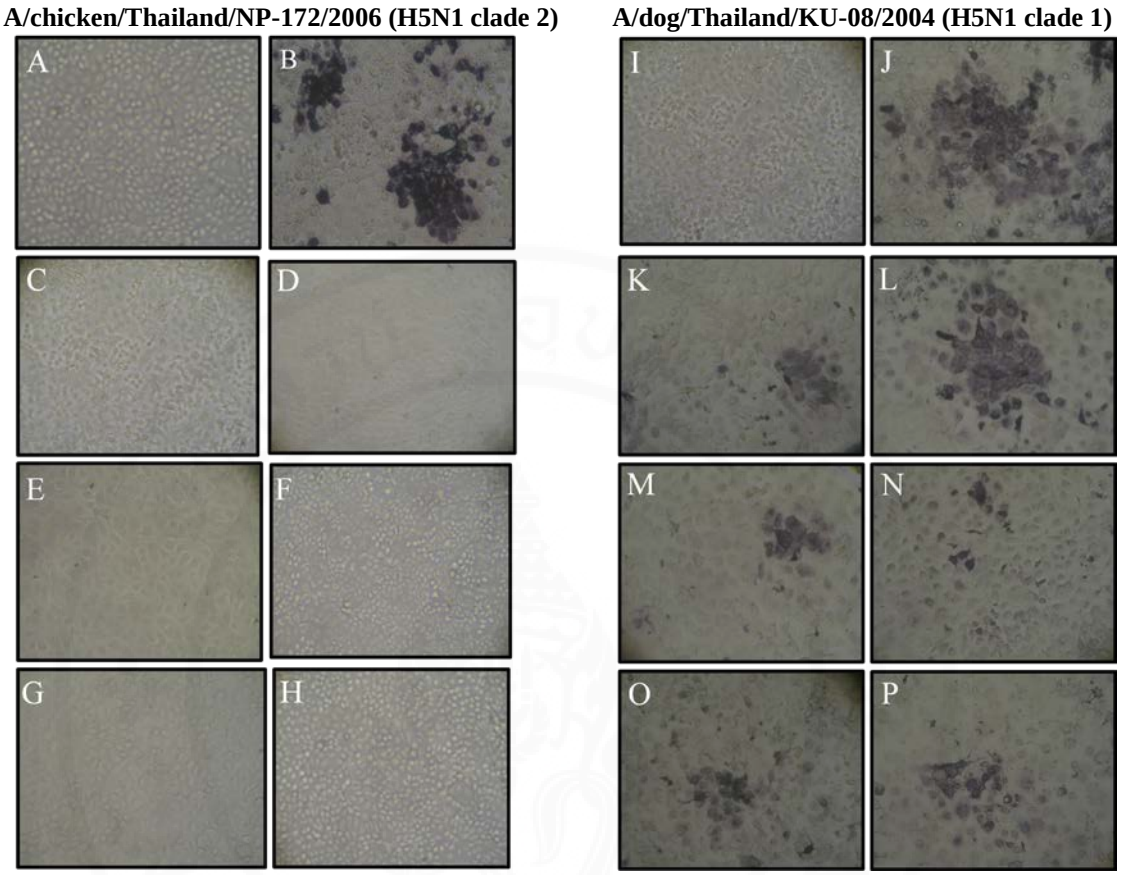

Figure 5.46 Appearances of influenza virus foci in infected MDCK cells treated with HuScFv, PAb to M2 and rimantadine in **Experimental design II**. Adamantane sensitive [A/chicken/Thailand/NP-172/2006 (H5N1 clade 2)] and resistant [A/dog/Thailand/KU-08/2004 (H5N1 clade 1) viruses were incubated with M2 specific-HuScFv, rimantadine, PAb to M2 or medium alone before adding to MDCK cell monolayer. The cells were cultured in the medium containing respective HuScFv, rimantadine, PAb to M2 and medium alone for 15 hours. Extracellular viruses were removed and the cells were washed before subjecting to immune-staining for virus plaques (foci). **A** and **I**: Uninfected MDCK cell monolayer; **B** and **J**: negative inhibition controls (MDCK cells infected with the viruses); **C** and **K**: MDCK cells infected with viruses exposed to PAb to M2; **D** and **L**: MDCK cells infected with rimantadine exposed viruses; **E** and **M**, **F** and **N**, **G** and **O** and **H** and **P**: MDCK cells infected with viruses exposed to HuScFv2, HuScFv19, HuScFv23 and HuScFv27, respectively.

Copyright by Mahidol University

5.15 Phage peptides that bound to HuScFv (mimotopes) and HuScFv epitopes on M2

In order to determine the sequence of the M2 which the HuScFv could bind to, the HuScFv were immobilized in the ELISA wells and allowed to bind with 12-mer peptides displayed phage bio-panning (**section 4.13.1** of **Chapter IV)**. After three rounds of the bio-panning, 10 blue plagues were randomly picked and individual phage genomes were extracted and sequenced. All 10 phage clones that bound to HuScFv2 revealed identical peptide sequence (ELWPPNPHAGPP) designated mimotope type M2-1. There was also one mimotope type, *i.e.*, M19-1 (VQIPLSYGQYYK) of HuScFv19. HuScFv23 had three mimotope types: M23-1(ALWPPNLHAWVP), M23-2 (QYALWPPNLQAGVP) and M23-3 (HSNWDMPPIRLVAS). Two mimotope types were deduced from 10 HuScFv27 bound phage clones: M27-1 (EDVDEIHNQSHP) and M27-2 (ALWPPNLH AWVP). Sequences of all mimotope types were aligned with the monomeric M2 sequences of A/H5N1 of the database, *i.e.*, clade 1: AY651385.1 and clade 2: AB478035.1, in order to locate tentative regions and residues on the monomeric M2 bound by the HuScFv (epitopes) (**Figure 5.47**). The 12 residue phage mimotope peptide of HuScFv of clone no. 2 (M2-1) matched with 39ILWILD44 in transmembrane domain and 63P-TAGVP69 in cytoplasmic domain of M2 of both clades. The mimotope M19-1 matched with 51IYRRLKYG58 of amphipathic helix and 74EEYR77 of cytoplasmic domain. The M23-1 matched with residues 39ILWILD44 of transmembrane helix and 59LK60 of amphipathic helix and 66AGVP69 of cytoplasmic domain; M23-2 matched with 37HLILWILD44 of transmembrane helix, 59LK60 of amphipathic helix and 66AGVP69 of cytoplasmic domain and M23-3 matched with 38LILWILDR45 of transmembrane helix, 59LK60 of amphipathic helix and 67GVPE70 of cytoplasmic domain. The mimotope M27-1 matched with 5TEVE8 and 18RCSDSSDP25 in ectodomain and M27-2: matched with 21DSSDP26 in ectodomain and 37HLILWIL43 in transmembrane helix.

Copyright by Mahidol University

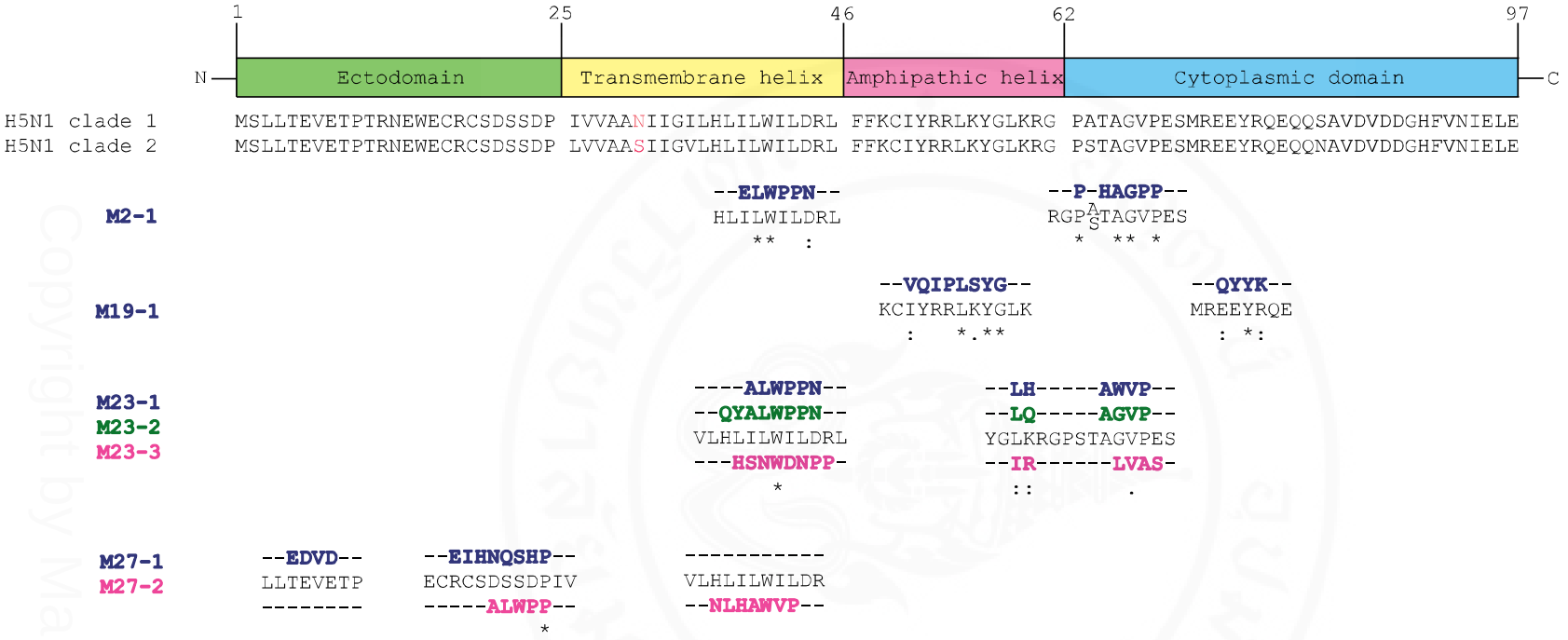

Figure 5.47 Results of the phage peptide sequences matched with residues of A/H5N1 monomeric M2 molecule (epitopes of HuScFv). HuScFv2 mimotope type (M2-1: ELWPPNPHAGPP) matched with amino acid residues in transmembrane helix and cytoplasmic C-terminal of M2 of both viruses; HuScFv19 mimotope type (M19-1: VQIPLSYGQYYK) matched with residues of the M2 amphipathic helix and cytoplasmic C-terminal; HuScFv23 mimotope types (M23-1:ALWPPNLHAWVP, M23-2: QYALWPPNLQAGVP, M23-3: HSNWDNPPIRLVAS) matched with residues in ransmembrane domain, amphipathic helix and cytoplasmic C-terminal; mimotope types of HuScFv27 (M27-: EDVDEIHNQSHP and M27-2: ALWPPNLHANVP) matched with M2 residues in ectodomain and transmembrane helix.

5.16 Determination of the ability of the phage mimotopes in inhibiting the HuScFv binding to the rM2 by using competitive ELISA

Competitive ELISA (see method in **section 4.13.2** of **Chapter IV**) for determining the ability of the phage mimotopes and irrelevant phage mimotope in inhibiting the HuScFv binding to the rM2 are shown in **Figure 5.48**. Binding of the HuScFv clones no. 2, 19, 23, and 27 to the M2 was partially inhibited by the phage mimotope types. The percent inhibition was not 100% for all HuScFv due to binding of the phage peptides to only partial regions of M2. Nevertheless, the results indicated that the mimotopes carried the amino acid residues analogous to the native M2 which verified the mimotope search data.

Copyright by Mahidol University

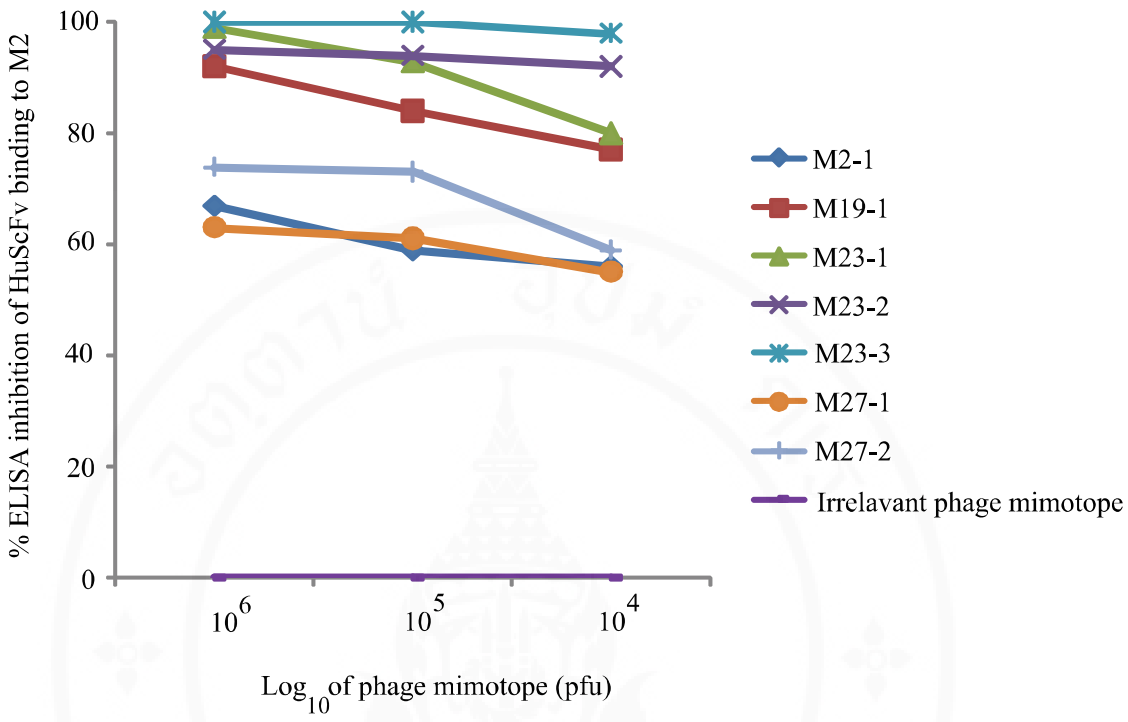

Figure 5.48 Results of competitive ELISA for determining efficiencies of phage mimotopes in blocking the HuScFv binding to rM2. In the assay, individual phage mimotope types, *i.e.*, M2-1: ALWPPNLHAWVP, M19-1: VQIPLSYGQYYK, M23-1: HSNWDMPPIRLVAS, M23-2: QYALWPPNQAGVP, and M23-3: HSNWDMPPIRLVAS, M27-1: EDVDEIHNQSHP and M27-2: ALWPPNLHAWVP at 10^4, 10^5 and 10^6 pfu were mixed with individual HuScFv (5 µg) before adding to the ELISA well containing immobilized rM2 (10 µg). HuScFv mixed with irrelevant phage mimotope [CF-6 (mimotope specific to Can f1): HIWWGPQPWMEP] served as background inhibition controls. The percent ELISA inhibition was calculated. The results indicated that the mimotopes could inhibit the HuScFv binding to rM2; implying that they carried the amino acid residues analogous to the native M2 residues that could be bound by the respective HuScFv.

Copyright by Mahidol University

5.17 Regions and residues of tetrameric M2 ion channel bound by HuScFv as determined by homology modeling and molecular docking

The RDOCK and interactive M2 residues for all HuScFv are shown in **Figure 5.49**. The RDOCK between the HuScFv2 and the tetrameric M2 ion channel was -30.38; the HuScFv2 bound to residues 38LIL-ILDRLF47 of the first monomer, residues 25P---A--II-IL--ILW-LD44 of the third monomer and residues 31NIIGILHLILWIL-RL-F48 of the fourth monomer. The RDOCK between HuScFv19 and the M2 tetramer was also -30.48; the HuScFv19 bound to 25PI---AA-II--L--IL--L--LF48 of the first monomer and 31NI---IL-LILWIL-RLFF49 of the second monomer. The RDOCK between the HuScFv23 and the M2 tetramer was -21.99; the HuScFv23 bound to residues 24DPI-VAA-II--L--L----L44 of the third monomer and 28V--NI--IL-LILWIL-RLFF49 of the fourth monomer. The RDOCK between the HuScFv27 and the M2 tetramer was -27.92; the HuScFv27 bound to residues 25PI-VAA-II--LH-IL--L43 of the third monomer and 31N---LILWIL-LFFK50 of the fourth monomer.

Regions of individual monomers of the tetrameric M2 ion channel template obtained from PDB entry 2LY0 that interacted with the HuScFv2, 19, 23 and 27 were obtained from computerized molecular docking in **Figure 5.50**. The so-obtained structure of this PDB entry contained only six residues of ectodomain, complete transmembrane helix and 3 residues of amphipathic helix but lacks completely the C-terminal residues.

Copyright by Mahidol University

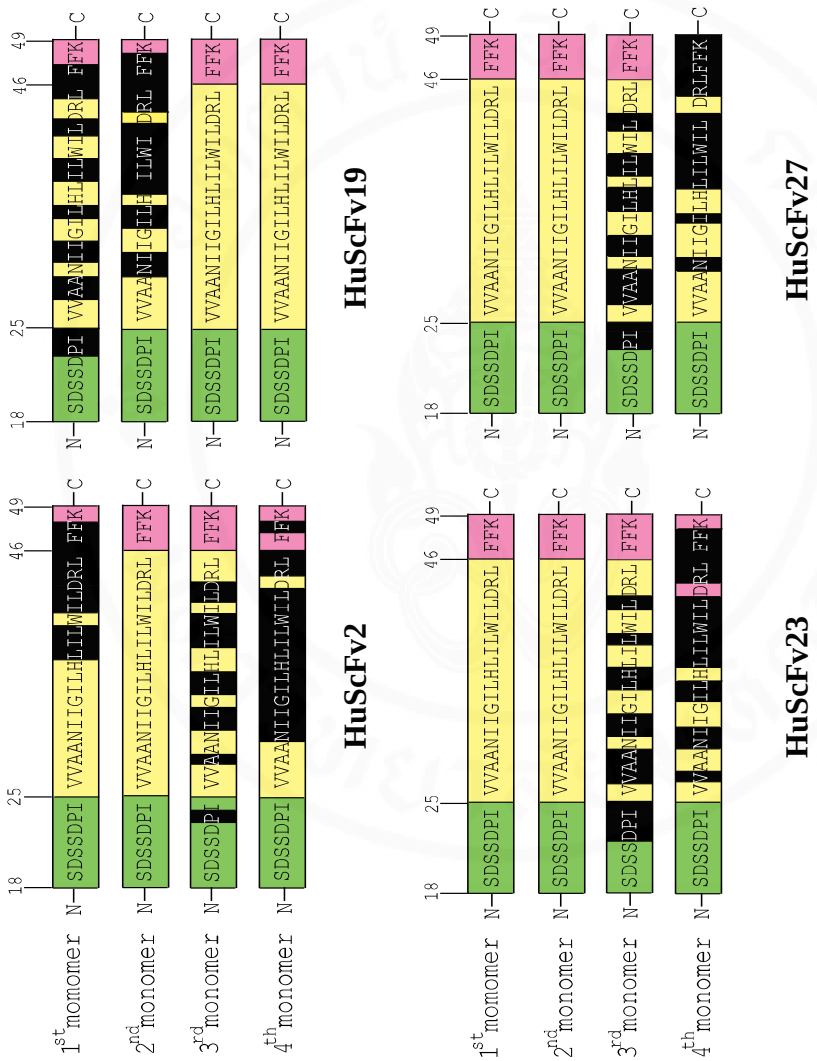

Figure 5.49 Predicted M2 residues (black shades) in individual monomers of the M2 ion channel (tetramer) which were bound by the HuScFv2, 19, 23 and 27

Copyright by Mahidol University

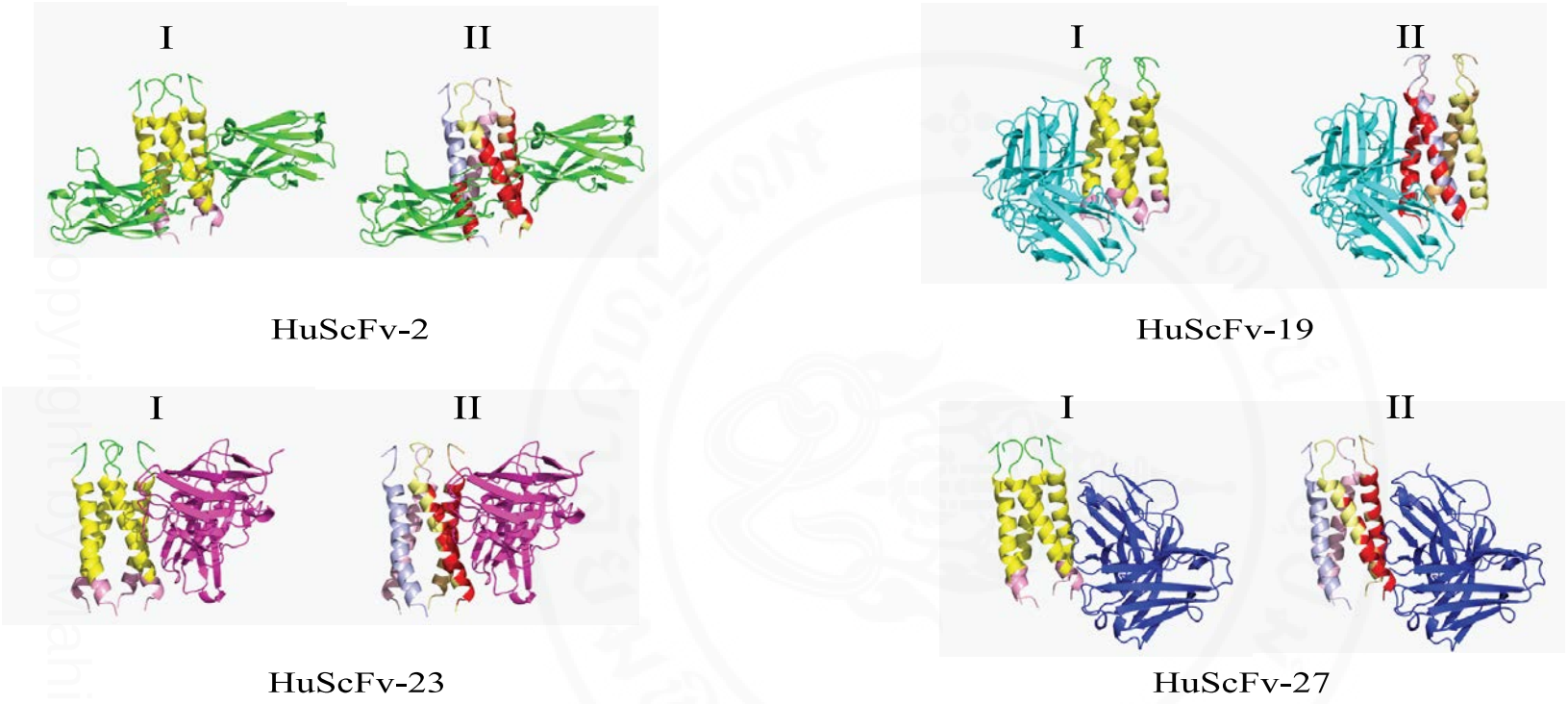

Figure 5.50 Results of molecular docking between the HuScFv with the tetrameric M2 ion channel template which was obtained from PDB entry 2LY0. (I) Interaction of HuScFv2 (green), 19 (cyan), 23 (violet) and 27 (blue) with tetrameric M2 ion channel template. The so-obtained template contained only six residues of ectodomain (green), complete transmembrane helix (yellow) and 3 residues of amphipathic helix (pink) but lacked completely the C-terminal residues. (II) Regions (red shades) of individual M2 monomers (colored in light blue, light pink, light brown and pale yellow for monomers 1-4, respectively) that interacted with the HuScFv.

5.18 Epitopes conservation of M2-specific HuScFv among subtypes and H5N1 clades of type A influenza

Based on M2 sequences of type A influenza deposited in NCBI database (accessed on June, 2013), total unique 1,754 sequences (excluded mixed subtypes and Lab strains) of subtype H5N1, H1N1, H3N2, H7N3, H7N9, and H9N2 which causing human disease were subjected to multiply aligned. **Figure 5.51** illustrates alignments of whole M2 sequences which shown highly conserved as demonstrated in blue shaded (>80% identity) among influenza type A strains. The result implied that the HuScFv should be able to counteract the M2 activities across influenza A virus subtypes and H5N1 clades.

The M2 specific HuScFv binding sites were located at amino acid residue 24 to 50 mapped to transmembrane domain (26-46) and four residues (47-50) of amphipathic helix domain from 97 amino acids length of M2 sequence (from tetrameric M2-HuScFvs docking results, **Figure 5.49**). There are some epitope variants with 11 point mutations in part of transmembrane domain, *i.e*., L26I, V28I, V27A, I32V, S31N, I32V, L36 V, L43I, T, or F, R45H, F48S, and C50S, or F (**Table 5.4**) and two variants at V27A, and S31N were markers of adamantine resistance found in the region of M2-specific HuScFv epitope.

Copyright by Mahidol University

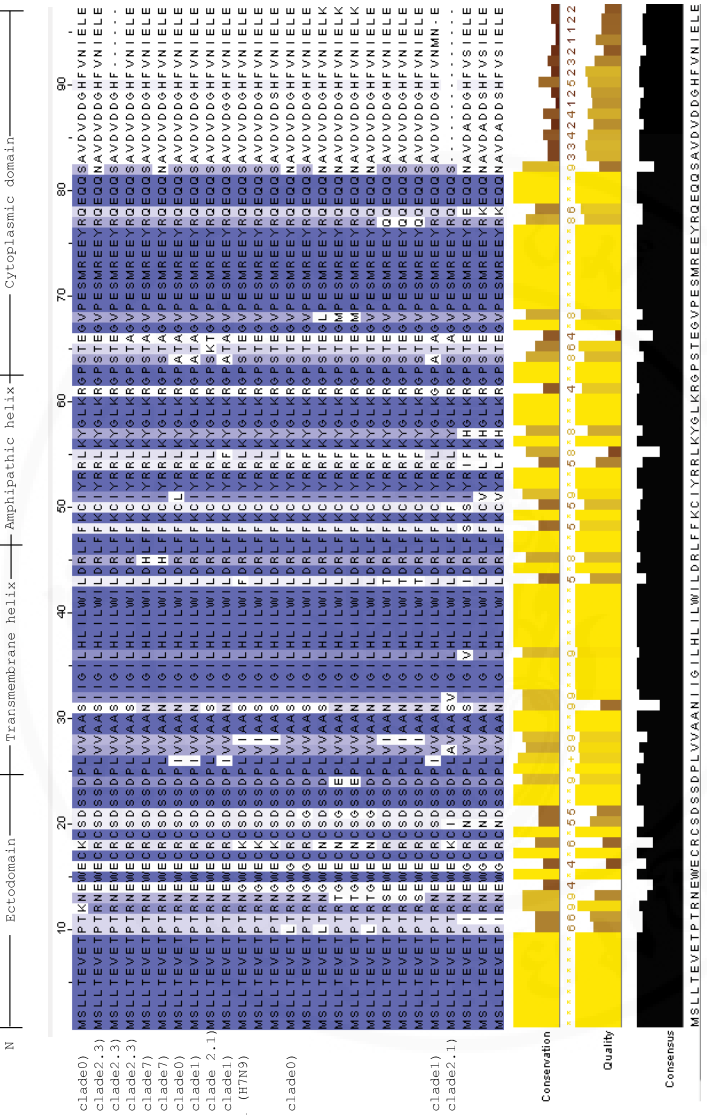

Figure 5.51 Multiple alignments of the M2 amino acid sequences of various influenza A virus subtypes and clades of subtype H5N1. The peptides of M2 proteins which were binding sites of the HuScFv of clones no. 2, 19, 23 and 27 are highly conserved across A subtypesand H5N1 clade

Mahidol University

Table 5.4 Epitope variants of M2 specifc HuScFv among type A influenza

Influenza A virus subtype	Clade	Strain	Transmembrane domain (residue 26 to 46) and amphipathic helix domain (residues 47 to 50)
			24-DPLVVAASIIGILHLILWILDRLFFKC-50*
H5N1	0	A/duck/Vietnam/1/2005	24---I----N--------------------50
H5N1	1	A/Thailand/1(KAN-1)/2004 A/chicken/Thailand/PC-340/2008 A/duck/Thailand/CU-328/07	
H5N1	7	A/chicken/Vietnam/NCVD-093/2008 A/chicken/Shanxi/2/2006	24--------N-------------H------50
H7N3		A/maxico/InDRE7218/2012 A/Canada/rv504/2004	24-----I----------------------50
H7N9		A/northern shoverl/Mississippi/110s145/2011	24-----I--------------F--------50
H7N9		A/Hangzhou/1/2013 A/Zhejiang/DTID-ZJU01/2013	24--------N--------------------50

* indicates M2 wild type of amantadine sensitive strain (Influenza A/duck/Nong-Khai/Thailand/KU-56/2007)

Dash line indicates amino acid identity

Table 5.4 Epitope variants of M2 specifc HuScFv among type A influenza (cont.)

Influenza A virus subtype	Clade	Strain	Transmembrane domain (residue 26 to 46) and amphipathic helix domain (residues 47 to 50)
			24-DPLVVAASIIGILHLILWILDRLFFKC-50*
H5N1	2.1	A/Indonesia/6/2005	24---A----V----------------F-50
H1N1		A/Thailand/CU23/2006	24------------V------I----S-S-50
H3N2		A/Hangzhou/1/2013	24--------N--------------------50
		A/Zhejiang/DTID-ZJU01/2013	
H1N1		A/Thailand/CU-H106/2006	24-----I--N-----------T--------50
		A/Thailand/CU-H2911/2011	
H3N2		A/Indiana/10/2011	

* indicates M2 wild type of amantadine sensitive strain (Influenza A/duck/Nong-Khai/Thailand/KU-56/2007)

Dash line indicates amino acid identity

5.19 Inhibition of M2 mediated LC3-II upreguration by M2 specific-HuScFv

Four clones of M2 specific HuScFv exhibited neutralizing activity (from **section 5.14**) and epitope function at the 60 amino acids at N-terminus of M2 related to anti-autophagy activity.

5.19.1 Determination of LC3-II transcriptional levels of H5N1 /NP172 infected MDCK cells.

Preliminary comparative qPCR results of LC3-II mRNA inside the MDCK cells infected with H5N1/NP172 (MOI 0.5) with and without HuScFv were determined. MDCK cells infected with H5N1/NP172 were used as autophagy negative control which the baseline of fold decrease of LC3-II mRNA was set at 0. Uninfected MDCK cells and infected cells treated with rimantadine were used as autophagy positive controls. The comparative mRNA levels compared to H5N1/NP172 infected cells revealed that rimantadine had the most effect in inhibiting the influenza virus mediated anti-autophagy. HuScFv2 and 27 could up-regulated LC3-II mRNA while HuScfv19, HuScFv23 and pAb-M2 down-regulated LC3-II mRNA. (**Figure 5.52**).

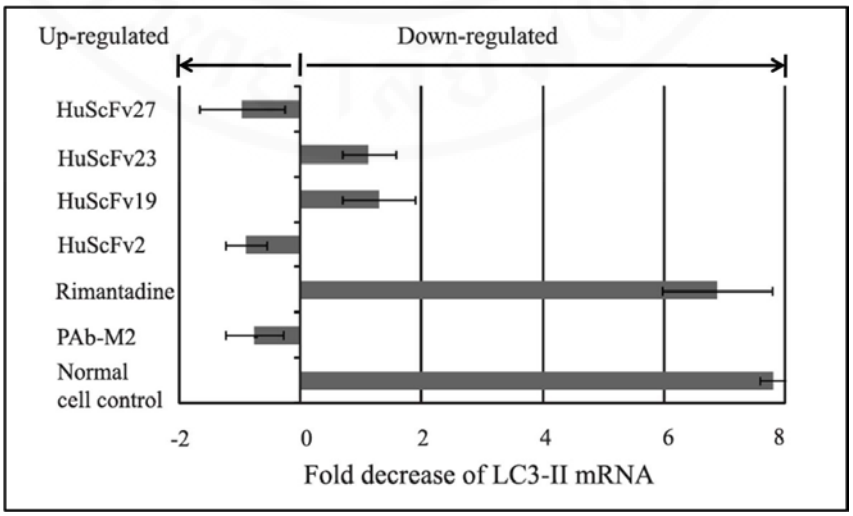

Figure 5.52 Comparative real-time RT-PCR of LC3-II mRNA of H5N1/NP172 (MOI 0.5) infected MDCK cells compared to M2 specific HuScFv2, 19, 23 and 27 treatments. Rimantadine and pAb-M2 were used as positive control and infected cells in medium was used as negative control.

Copyright by Mahidol University

CHAPTER VI
DISCUSSIONS

An unprecedented influenza pandemic caused either by newly re-assorted or highly pathogenic avian influenza viruses (including H5, H7 and H9) that have adapted to more efficient human to human transmission is the current global public health threat (Horimoto and Kawaoka, 1994; Cheung *et al*., 2002; Jia *et al*., 2009; Trifonov *et al*, 2009; Gao *et al*., 2013). This is not only because the world population lack background immunity to the new virus, but also the current seasonal vaccines are not going to be effective against the new pandemic strain. Moreover, the supply of anti-influenza drugs may not be adequate during the pandemic/large epidemic and the virus might resist the currently available anti-influenza agents. Besides, there has been a continuous emergence of the circulating influenza virus variants that are refractory to the influenza treatment (Sheu *et al*., 2011). Extensive research for developing a broad spectrum influenza vaccine which could protect across influenza virus subtypes and a search for new anti-influenza chemicals are ongoing (Saladino *et al*, 2010).

Antibody has been used as therapeutic agents of infectious diseases and intoxication even before the era of antimicrobials (Casadevall, 1996). It is known that antibody is more tolerable to the target mutation than small molecular drugs because of the multiple target contact points created by amino acids in the complementarity determining regions (CDRs) (Davies *et al*., 1996; Kim & Toge, 2004). Antibodies have been used successfully for influenza treatment. For examples, specific monoclonal antibody produced from immune B cells of immunized mice could cure influenza virus infected mice (Smirnov *et al*., 2000; Renegar *et al*., 2004). Humanized- and horse derived $F(ab)'_2$ fragments specific to H5N1 could treat influenza in the mouse model (Lu *et al*., 2006; Hanson *et al*., 2006). Human monoclonal single chain variable antibody fragments (HuScFv) specific to HA of H5N1 virus could rescue mice from lethal infections with homologous and heterologous H5N1 strains (Maneewatch *et al*., 2009). Single domain antibody (V_HH) blocked the M2 ion channel activity and neutralized influenza virus infection in mice (Wei *et al*., 2011). Passively

Copyright by Mahidol University

transferred M2e-specific monoclonal antibody to mice caused acceleration of the lung viral clearance (Treanor *et al*., 1990). Serum of H5N1 convalescing subject could rescue the patient infected with drug resistant H5N1 (Zhou *et al*, 2007). Therefore, influenza therapy by engineered human antibody which could be produced adequately *in vitro* without a prolonged immunization or seeking for the disease convalescing subjects (which the supply is limited) is of interest. The fully human antibodies should be safe and more tolerable also to viral mutation than the small molecule drugs.

Among the 11 proteins of the influenza A viruses, three proteins, namely hemagglutinin (HA), neuraminidase (NA) and matrix protein-2 (M2), are surface exposed on influenza virus envelope and infected cell membrane which are vulnerable targets for immune apparatus including antibodies and cytotoxic lymphocytes (Nayak *et al*, 2010). Recent evidences have shown that during influenza virus infection, cellular membrane has increased permeability (Gonzalez and Carraso, 2003; Wang *et al*., 2010). Thus, therapeutic antibodies especially the small molecular sizes such as single chain antibodies could traverse the cell membrane and become accessible to the intracellular target epitopes.

HuScFv specific to HA, NA and M2 of influenza A virus

Living H1N1-2009 virus adsorbed on the hRBC ghosts were used as panning antigen to select phage clones displaying HuScFv that bound to the functional forms of native HA, NA and M2 from the previously constructed human ScFv (HuScFv) phage display library (Kulkeaw *et al*, 2009). Live, unfixed influenza viruses were used in order to preserve the native/functional epitope configurations of the proteins (Shi *et al*, 1997). The human group O red blood cell ghosts were used for capturing the human influenza virus because the ghosts have α2,6 Gal on the membrane which is the human influenza virus receptor (Hirst, 1948; Nicholls *et al*, 2012) and also the O red cells devoid of interferences from A and B antigens and hemoglobin protein (Dean, 2005).

The HB2151 *E. coli* transfected with phages that bound to H1N1-2009 virus antigen on the hRBC ghosts were selected from the HuScFv phage display library which had been subtracted by panning with the hRBC ghosts without virus for three panning rounds in order to avoid/minimize selection of hRBC ghost bound

Copyright by Mahidol University

phages. The phage transfected bacteria grown on the selective agar plate were screened firstly for the presence of *huscfv* sequences. From the 100 randomly selected phagemid transformed HB2151 *E. coli*, only 34% (34 clones) were positive for the *huscfv* sequences, seen as DNA band at ~ 1,000 bp. Originally, 85% of the phages in the HuScFv display phage library were positive for *huscfv* (Kulkeaw *et al*, 2009). The lower percentage of the *huscfv* carrying *E. coli* clones obtained in this study might be due to a prolonged storage of the phage library (more than 5 years) which some of the clones might have lost the *huscfv* inserts. Among the 34 *huscfv*-phagemid carrying clones, 20 (20%) could express HuScFv seen as protein bands at ~26-35 kDa. The lysates containing HuScFv of these 20 clones were tested for binding to recombinant HA, NA and M2 proteins of influenza virus by indirect ELISA and HuScFv of 8 clones could bind to the target proteins implying that the HuScFv of the other 12 clones bound to the hRBC ghost proteins which were more abundant (Steck, 1974) even though the phage library had been subtracted for three rounds with the hRBC ghosts.

The 8 *huscfv*-phagemid transformed *E. coli* clones could be divided according to the binding specificities of their HuScFv into 4 groups: 1) HuScFv that bound to rHA0, rNA and M2 (clone nos. 2, 10, 26 and 54), HuScFv that bound to rHA0 and rNA (clone no. 53), HuScFv that bound M2 (clone nos. 15 and 51) and HuScFv that bound rHA (clone no. 99). There are many reasons for the multiple protein binding specificities of the HuScFv. First, clustering of native HA, NA and M2 at the budding site of influenza virus from infected cell (Lamb and Rossman, 2011) might have created a unique structure formed by amino acids of individual proteins that have been brought to juxtaposition. Second, similar epitopes might exist on the different influenza virus proteins. Indeed, from multiple alignments of the HA, NA and M2 sequences, a common amino acid sequence with identical, conserved and semi-conserved amino acids were found as the following:

Copyright by Mahidol University

CLUSTAL 2.1 multiple sequence alignment

```
M2   MSLLT-EVET 9   (1-9)
HA   LSSVS-SFER 9   (104-112)
NA   INWLTIGISG 10 (111-120)
       :. ::  ..
```

Nevertheless, the similar epitopes on the three proteins may or may not have similar molecular function in the virus life cycle. Many previous studies have shown that unknown epitopes of these three proteins contributed the same or synergistic function. For examples, membrane pores could be formed by viral glycoproteins (HA and NA) during the entry and infectivity of M2-deficient influenza virus (Watanabe *et al*, 2001). Similar observation was observed for p7 viroporin deficient HCV (Steinmann, 2007; Wozniak *et al*, 2010). The NA protein of influenza A virus is not only required for virion release and spread but also plays a critical role in virion infectivity and HA-mediated membrane fusion (Su *et al*., 2009). M2 is important for virus budding before NA mediated release of the virion (Rossamn and Lamb, 2011).

The HuScFv specific to native M2 derived from phage bio-panning with virus particles adsorbed onto hRBC ghosts did not bind to SDS-PAGE separated rM2 on Western blot membrane (**Figure 5.20**, **Chapter V**) but bound in the indirect ELISA. This might be because the nM2 specific-HuScFv bound to the functional epitopes of correctly folded ectodomain of native M2 formed on the viral target cell (Pietzsch, 2003). The conformation of the native epitope was not preserved in the Western blotting condition. In the ELISA, the refolded rM2 dissolved in PBS and coated onto the surface of the ELISA well may acquire the epitope configuration, *i.e.*, the epitope bound by the nM2 specific-HuScFv was present.

The full length HA (HA0) composed of globular head (HA1) and stem (HA2). After determining the binding specificity by using indirect ELISA and Western blotting, the native HA specific-HuScFv could be divided into two groups depended on the domain of the HA molecule that they bound. HuScFv of clone nos. 2, 10, 26 and 54 (HuScFv2, 10, 26 and 54) reacted to HA1 and HuScFv53 and 99 bound to HA2. The binding specificity of the HuScFv2, 10, 26 and 54 was confirmed by the

Copyright by Mahidol University

finding that they could inhibit hemagglutinin function of the HA1 in the hemagglutination inhibition (HI) assay. HB2151 *E. coli* lysate had background inhibition of the viral hemagglutinin binding to the sialic acid receptor on red blood cells because it contained mannose-specific activity (Rosenthal, 1943; Öhman *et al*, 1982; Vaithilingan *et al*, 2012). However, after normalization of the total proteins in the *E. coli* lysate before testing the HI activity, *E. coli* lysates containing HuScFv2, 10, 26 and 54 could give the HI titers higher than that of the lysate of the original HB2151 *E. coli*.

The amino acid sequences of representative *huscfv*-phagemid transformed *E. coli* clones from each antigen binding groups (clone nos. 26, 51, 53 and 99 for groups 1-4, respectively) were determined before use in the HuScFv mediated-interference of the virus replication cycle. All of the selected HuScFv had different amino acid sequences especially at the CDRs implying that they bound to different epitopes and thus should mediate different mechanisms in interfering the influenza virus replication cycle. Large amounts of the HuScFv of the for clones could be produced after subcloning of the *huscfv* sequences from phagemids to pET plasmids while the antibodies still retained their original antigenic specificities.

Three experimental designs were used in testing efficacy of the HuScFv in interfering with the viral replication cycles. The amounts of viral foci were lowest in experimental design-II (which the HuScFv were mixed with the virus before adding to MDCK cell monolayer as well as adding to the cell culture medium). This should be because the HuScFv could interfere with many processes of the virus infectious cycle including binding to receptor, uncoating, replication and budding. The numbers of viral foci of experimental design-I (HuScFv were mixed with the virus before adding to cells; after incubation, the extracellular fluid was removed and the infected cells were cultured in medium alone without antibody) were highest because the HuScFv could block only at the initial virus adsorption and uncoating. The amount of viral foci in experimental design-III (viruses were allowed to infect cells directly and the infected cells were cultured in the medium containing HuScFv which could block at the steps of virus replication and budding) were moderate (less efficient than experimental design-II but more efficient than experimental design-I).

Copyright by Mahidol University

Vaccinated (immune) serum had the highest efficiency in experimental design-I (blocking at steps of binding and uncoating), because the serum contained polyclonal antibodies specific to HA, NA and M2 which could blocked the binding and uncoating of influenza virus. HuScFv53 (specific to HA and NA) had high efficacy because HuScFv-53 block the virus entry played by HA and NA (Roger *et al*., 1983; Skehel *et al*., 1982; Su *et al*., 2009). HuScFv26 had high efficacy too because it could bind to HA, NA and M2. Although percent of inhibition of HuScFv26 would be lower than HuScFv53 in the experimental design-I, this might be due to different epitope specificity; the epitope of HuScFv26 might not contribute directly to the virus entry and uncoating. The HuScFv51 had high efficacy too because the binding epitope on M2 might involve in virus uncoating. While HuScFv99 (specific to HA) and HuScFv-NA had minimal effect (less than that of HuScFv53 and HuScFv26), this might be because the amino acid epitopes of these HuScFv may not be critical for binding and uncoating.

For comparison of each HuScFv in experimental design-II (blocking virus binding, uncoating as well as replication and budding), vaccinated serum has also the highest efficiency. HuScFv26 (specific to HA, NA and M2) and HuScFv53 (specific to HA and NA) showed high efficacy in these experiment because HuScFv specific to HA and NA might involved in blocking virus binding and uncoating and HuScFv specific to HA, NA and M2 might obstruct virus release from infected cells. HuScFv51 (specific to M2) had high efficacy in inhibition of virus infection too. This may be due to the ability of the eM2 specific-HuScFv to block the ion channel activity and anti-autophagy. HuScFv99 (specific to HA) also gave high efficacy in percent inhibition of virus foci because HuScFv specific to HA might obstruct uncoating of both primary and interfering of viral uncoating of the progeny virion (secondary infection of influenza virus). While HuScFvNA had the lowest efficacy in percent inhibition of virus foci among all HuScFv, these might be because HuScFv specific to NA might only have ability in blocking viral release and budding.

Copyright by Mahidol University

HuScFv53 (specific to HA and NA) and HuScFv26 (specific to HA, NA and M2) had similar efficacy in interference of the influenza virus replication cycle in experimental design-III as they might interfere with the viral release and budding (Su

et al., 2009; Rossman and Lamb, 2011). HuScFv51 (specific to eM2) and HuScFv99 (specific to HA) had lower efficacy in interference of the influenza virus replication cycle than that of HuScFv53 and HuScFv26 because they might interfere only virus entry to the cell. The vaccinated serum had less efficiency than the HuScFv-53 and -26 which might be because of their inability to enter the cells. HuScFv-NA had the lowest efficacy in percent inhibition of virus foci among all HuScFv because HuScFv specific to NA might only have ability in blocking viral release and budding.

From all three experimental designs, HuScFv-NA gave low percent inhibition of virus foci. These might be because HuScFv-NA received from HuScFv phage display library bio-panning with recombinant N1 of H5N1, thus HuScFv-NA may bind N1 of H1N1/2009 in low affinity caused low efficacy in interfering H1N1 replication cycle.

All of the speculative HuScFv mediated mechanisms await experimental clarification by determining the HuScFv epitopic peptides or at least computerized molecular docking.

HuScFv specific to M2 of influenza A virus

Because the HuScFv secreted by *E. coli* clones derived from phage bio-panning with live H1N1-2009 virus adsorbed on hRBC ghosts should react only to the surface exposed portion of the M2, *i.e.*, ectodomain, therefore, the soluble recombinant M2 protein in relatively pure form was used as an antigen in another phage panning for selection of phage clones for production of transformed *E. coli* that could produce HuScFv specific to other M2 domains. The next paragraph gives a brief account on pivotal functions of M2 domains on the influenza virus infectious cycle.

The first known M2 function is the pH dependent selective proton channel activity formed by homotetrameic M2 molecules on the virus surface. The channel is important for vRNP uncoating from endosome into cytoplasm and subsequent replication in nucleus (Helenius, 1992). The ion channel pore is lined by the polar amino acids Val^{27}, Ser^{31}, Gly^{34}, His^{37}, Trp^{41}, Asp^{44} and Arg^{45} of the transmembrane (TM) tetrahelices while the channel integrity is maintained by TM non-polar residues

and the positively charged residues of the TM and the amphipathic helix (Sharma *et al*, 2010). At the high pH, the pore is closed by the TM helices and the constrictive gates mediated by Val^{27} at the N-terminal ion entrance and Trp41 at the C-terminal ion exit (Helenius, 1992; Sharma *et al*, 2010). Under endosomal low pH condition, the highly proton selective His37 senses the acidification at the N-terminal and allows inward flow of H+ through the channel, whereas the gate formed by linking the Trp^{41} indole ring side chain with Asp^{44} and Arg^{45} is open; thus allowing the outward flow of the proton to the C-terminal and release (Achaya *et al*, 2010). Adamantane compounds, including amantadine and its derivative rimantadine, block the ion channel activity of influenza A viruses. Amantadine obstructs the ion channel pore by binding to Ser^{31} and the surrounding Val^{27}, Ala^{30} and Gly^{34} (Stouffeer *et al*, 2008). The rimantadine binds to the gate at a lipid facing pocket of the channel formed by Trp^{41}, Ile^{42}, and Arg^{45} from one TM helix and Leu^{40}, Leu^{43}, and Asp^{44} of the nearby helix (Helenius, 1992). Resistance to the drugs has occurred in > 98% of transmissible A/H1N1, A/H5N1, A/H7N9 and A/H3N2 strains by mutations, most frequently S31N and less so V27A and L26F (Layne *et al*, 2009; Balgi *et al*, 2013). The mutations cause failure of ion channel blocking by amantadine and ineffective fitting of rimantadine into the channel pocket due to the weakness of the TM helix packing (Pielak *et al*, 2009). Several compounds that are potent inhibitors of V27A and L26F mutants have been produced and tested (Balannik *et al*, 2009). However, effective inhibitor of S31N mutant has not been found (Du *et al*, 2012). Therefore, the M2 protein has been attractive target of anti-influenza agents.

In the second part of this study, fully human single chain antibody variable fragments (HuScFv) that bound specifically to recombinant and native M2 of A/H5N1 viruses belonging to different clades were successfully produced using phage display technology. The so-produced small antibodies were tested for their ability to inhibit the virus replication using rimantadine and polyclonal antibodies to full length recombinant M2 (PAb) as positive inhibitors. As expected, rimantadine was highly effective for the drug sensitive virus variant and rather refractory for the resistant mutant. The observed ability of the PAb in reducing the viruses inside the cells and in cell culture supernatant should be due to viral aggregation and steric hindrance of the ion channel activity. The HuScFv derived from all four *E. coli* clones also caused

Copyright by Mahidol University

significant reduction of the amounts of both drug sensitive and resistant A/H5N1 viruses in the infected cells and the culture supernatants in experimental designs-II and -III while these HuScFv(s) had low effect in experimental design-I which the reasons are given below:

In experimental design-I, HuScFv and mPAb-M2 could interact only in the area of eM2 thus amount of virus foci and viral M1 RNA of both infected cells and viral supernatants did not decrease comparing with the infected cell control. Small size of rimantadine drug which can get into the target in the M2 ion channel could decrease amounts of the viral foci and M1 RNA in the H5N1 sensitive strain. HuScFv19, 23, 27 and PAb-M2 caused a decrease of the amount of M1 RNA because they could interact with eM2 (molecular docking revealed that HuScFv19 and 23 bound also to amino acids in eM2).

In experimental design-II, sustained exposure to inhibitors (HuScFv, PAb-M2 and rimantadine) could reduce the virus foci in cells infected both H5N1 sensitive and resistant strains. The amounts of viral M1 RNA of infected cells in all inhibitor treatments were not different significantly. Nevertheless, the viral M1 RNA in supernatants of infected cells with H5N1 resistance strain (viral release) treated with HuScFv were significantly less than infected cells treated with PAb-M2 and rimantadine . This should be due to the ability of the HuScFv to enter the cells and interfered with M2 domains involved in new virion assembly and release. HuScFv19 and 23 gave the most effectiveness in reducing the M1 RNA of adamantane resistant strain as they should interact with the M2 amphipathic helix and cytoplasmic domain which has important role in viral assembly and release (Rossman and Lamb, 2011). HuScFv2 and 27 have lower effect than that of HuScFv19 and 23 because they interact with the M2 ectodomain and transmembrane domains which function in viral uncoating. PAb-M2 has lower effect than that of all HuScFv treatment because they could interfere only ectodomain of M2. Rimantadine has also lower effect than that of all HuScFv treatment because it inhibits only in ion channel function of M2.

In experimental design-III, influenza virus infection increases permeability of membranes of the infected cells. The HuScFv could easily access to the M2 target; thus the HuScFv could reduce the virus foci in cells infected both H5N1 sensitive and

Copyright by Mahidol University

resistant strains. In H5N1 adamantane sensitive strain, the amounts of viral M1 RNA in both infected cells and viral supernatant of rimantadine treatment show the highest reduction while HuScFv and PAb-M2 were not different significantly. In H5N1 adamantane resistant strain, PAb-M2 and HuScFv23 and 27 that interact with transmembrane domain gave high effect in reduction of viral M1 RNA in both infected cells and viral supernatant because they involved in interfering of viral uncoating of the progeny virion (secondary infection). Moreover, HuScFv23 that interact with amphipathic helix domain of M2 also interfere viral assembly and budding, and HuScFv27 that interact with eM2 domain may be help in blocking of viral uncoating (interference of ion channel M2 activity). HuScFv2 and HuScFv19 could interact with only transmembrane domain and amphipathic helix domain, respectively therefore efficacy in reduction of viral M1 RNA were lower than that of HuScFv23 and HuScFv27. Rimantadine has also only one target at transmembrane domain too so the efficacy in reduction of viral M1 RNA were equal with HuScFv2 and HuScFv19

It is known that during various virus infections, such as hepatitis C, human immunodeficiency, polio, toga and influenza, cellular membrane has increased permeability (Carrasco, 1978 & 1995; Gonzalez & Carrasco, 2003; Hout, 2004: Wang *et al*, 2011; Thueng-in *et al*, 2012). Intracellular entry of HuScFv specific to influenza virus protein and co-localization of the antibody with the specific protein target inside the infected cells have been observed by confocal microscopy (data not shown). In this study, the monovalent HuScFv which devoid of virus agglutinating ability were effective in inhibiting the virus replication indicating that the small antibodies could enter the virus infected cells and exerted M2 function interference. Epitopes of the HuScFv identified by means of phage mimotope searching and mimotope inhibition ELISA as well as molecular docking pointed out that the HuScFv of clones no. 2, 23, and 27 bound to the gate area (Trp^{41}) of the M2 ion channel Therefore, the observed ability of the HuScFv of these clones in inhibiting the influenza virus replication was likely to be a consequence of the antibody mediated interference of the ion channel activity leading to failure of the virus uncoating. Moreover, the pH gradient equilibration between the trans-Golgi network and cytosol by the ion channel activity could be interrupted also, causing pre-mature maturation of the virus hemagglutinin

Copyright by Mahidol University

(Sugrue *et al*., 1990). The amphipathic helix and cytoplasmic domain of the influenza virus M2 induces cellular membrane curvature during the virus assembly, increases vRNP packaging by M1-M2 interaction and assists the membrane scission in virus budding process (reference). The finding that peptide epitopes of the HuScFv of clones no. 2, 19 and 23 located in the amphipathic and cytoplasmic domains of the M2 indicated that the antibodies might inhibit the virus replication by interfering with the functions of the amphipathic helix and the cytoplasmic tail. During the infection, the N-terminal 1-60 residues of the influenza virus M2 compromises survival of influenza virus-infected cells by inhibiting the cellular macroautophagy formation (Gannage *et al*, 2009). The finding that many epitopic residues of M2 potentially bound by the HuScFv of all clones also located in the N-terminal portion indicating that the antibodies might as well counteract the M2 function on anti-autophagosome-lysosome fusion.

Multiple alignments of the M2 amino acid sequences of various influenza A subtypes and human pathogenic clades of subtype H5N1 revealed that the HuScFv epitopic peptides are highly conserved among the viruses implying that the HuScFv should be able to counteract the M2 activities across subtypes and H5N1 clades.

There was a trend that HuScFv19 and 23 could down-regulated LC3-II mRNA in the influenza virus infected cells treated with the HuScFv indicating that the HuScFv could rescue the host cells from the M2 mediated anti-autophagy. Nevertheless, demonstration on the reduction in amount of the LC3-II protein and the host proteins involved in the HuScFv mediated inhibition of the anti-autopahgy need further experiments.

Although the speculated molecular mechanisms of the HuScFv produced in this study in interfering with the influenza virus replication await experimental verification, the HuScFv have high potential for developing further as a safe, novel and mutation tolerable pan anti-influenza agent.

Copyright by Mahidol University

CHAPTER VII
CONCLUSIONS

The ultimate goal of this research was to produce human monoclonal single chain variable antibody fragments (HuScFv) specific to influenza type A surface exposed protein (HA, NA, and/or M2) that neutralize bio-functions of the surface exposed proteins for developing further into human anti-influenza agents. The experimental results could be summarized as the followings:

Production of recombinant influenza virus proteins including HA (HA0, HA1 and HA2), M2 and NP

1. Viral RNA from culture supernatant of MDCK cells infected with influenza virus A/Thailand/CU41/2006 (H1N1) and cDNA of HA0-, HA1- and HA2- coding sequences were successfully prepared.
2. The amino acid sequences of HA0, HA1 and HA2 had 100%, 99% and 100% identity, respectively, compared to hemagglutinin sequence of NCBI database, *i.e.*, influenza A virus [A/Thailand/CU41/2006 (H1N1) (accession no.: ABS71664.1)] which was the virus strain used for preparing cDNA template for cloning.
3. Recombinant HA0, HA1 and HA2 and NP were produced from appropraite transformed *E. coli* clones. The recombinant HA0, HA1 and HA2 and NP were found in the insoluble fractions of the respective transformed *E. coli* homogenates. Thus the recombinant proteins were purified under denaturing condition by using buffer containing 8 M urea and Ni-NTA^{TM} affinity resin. Then the purified recombinant proteins were prepared by refolding against PBS.
4. The recombinant M2 were found in both soluble and insoluble fractions of the transformed *E. coli* homogenate; thus the protein was affinity purified under native condition from the soluble *E. coli* fraction.

Copyright© by Mahidol University

HuScFv specific to HA, NA and M2 of influenza A virus

1. H1N1/2009 virus adsorbed-hRBC ghosts were used as target antigen in a single round phage bio-panning to select phage clones displaying HuScFv that could recognize to native conformation of H1, N1 and M2 from a HuScFv phage display library constructed from immunoglobulin genes of Thai blood donors.
2. From 100 randomly selected *huscfv*-phagemid transformed HB2151 *E. coli* colonies, 34 carried *huscfv* genes as determined by colony PCR and 20 clones could produce HuScFv.
3. The HuScFv were tested for binding to rHA0, rHA and rM2 by indirect ELISA and Western blotting. HuScFv from 8 clones could bind to antigens. They were classified into four groups:
    - HuScFv of clone no. 2, 10, 26 and 54 bound to rHA0, rNA and nM2
    - HuScFv of clone no. 53 bound to rHA0 and rNA
    - HuScFv of clone no. 15 and 51 bound to nM2
    - HuScFv of clone 99 bound to rHA
4. HuScFv2, 10, 26 and 54 bound to HA1 while HuScFv53 and 99 bound to HA2.
5. HuScFv2, 10, 26 and 54 (specific to HA) inhibited hemagglutinin activity against H1N1/2009 virus at 4 HAU by using HI assay (HI titers were 1:16, 1:16, 1:16 and 1:32, respectively).
6. HuScFv26 (specific to HA, NA and M2), HuScFv51 (specific to M2), HuScFv53 (specific to HA and NA) and HuScFv99 (specific to HA) had different RFLP (DNA banding patterns) and deduced amino acid sequences.
7. HuScFv26, 51, 53 and 99 were produced in large scale and purified by affinity chromatography under denaturing condition. After refolding against PBS, the purified HuScFv retained binding activity to the target antigen(s) in native conformation of viral particles as determined by indirect ELISA.
8. HuScFv26, 51, 53 and 99 and HuScFv to NA1 (HuScFvN1) interfered with replication cycle of H1N1/2009 (A/Thailand/CU-H106/2009). The replication inhibition in terms of the percentages of virus foci reduction were:
    a) In experimental design I (interference with virus binding and uncoating to the target cells), the percentages of plaque reduction in increasing

Copyright by Mahidol University

order of magnitudes were: HuScFv-N1 < HuScFv99 < HuScFv26 < HuScFv51 < HuScFv53.

b) In experimental design II (interference of virus binding, replicating and budding), the effectiveness in reducing intracellular virus (plaque number) in increasing order of magnitude were HuScFvN1 < HuScFv99 = HuScFv26 < HuScFv53 < HuScFv51.

c) In experimental design III (interference of viral release), the effectiveness in reducing intracellular virus (plaque number) in increasing order of magnitude were HuScFvN1< HuScFv99 < HuScFv51 < HuScFv26 < HuScFv53

From the three experiments, HuScFv of the the experimental design I conferred the lowest effectiveness in reducing intracellular virus while the experimental design II conferred the most.

HuScFv specific to M2 of influenza A virus

1. Soluble form of rM2 was used as target antigen in a single round phage bio-panning to select phage clones displaying HuScFv from the previously constructed HuScFv phage display library.
2. From 30 randomly selected *huscfv*-phagemid-transformed HB2151 *E. coli* colonies, 27 carried *huscfv* genes as determined by colony PCR and 17 clones could produce HuScFv.
3. HuScFv from 10 clones (clone nos. 2, 5, 9, 13, 14, 19, 20, 23, 27 and 29) bound to rM2 by indirect ELISA. The *huscfv* of these 10 clones showed 6 different RFLP patterns.
4. HuScFv2, 19, 23, and 27 which were representatives of individual RFLP patterns bound to both recombinant and native M2 proteins (in homogenate of MDCK cells infected with influenza A/H5N1) as determined by Western blotting. They also reacted with native M2 conformation of M2 protein from virus infected cells as tested by immunofluorescence assay.
5. Amino acid sequences of HuScFv2, 19, 23, and 27 were different especially at CDRs suggesting differences in epitope specificities.

Copyright by Mahidol University

6. HuScFv2, 19, 23, and 27 were produced in large scale and purified by affinity chromatography.
7. M2 specific HuScFv2, 19, 23, and 27 could interfere with replication cycles of both adamantine sensitive and resistant strains of influenza virus when used to treat MDCK infected cells in different experimental designs.
8. By mimotope searching and multiple alignments, conformational epitopes of the HuScFv2, 19, 23, and 27 were revealed:

   Epitope of HuScFv2 located at the residues important for ion channel activity, anti-autophagy and M1 binding.

   Epitope of HuScFv19 located at the M2 amphipathic helix and cytoplasmic tail important for anti-autophagy, virus assembly, morphogenesis and release.

   Epitope of HuScFv23 involved residues important for ion channel activity, anti-autophagy and M1 binding and also amphipathic helix residues for viral budding and release.

   Epitope of HuScFv27 spanned ectodomain, ion channel and anti-autophagy residues.
9. Results of computerized homology modeling and molecular docking conformed to the results of epitope identification by phages.
10. The epitopes of the HuScFv2, 19, 23, and -7 are conserved among influenza A viruses subtypes and H5N1 clades that could infect human.
11. HuScFv19 and 23 could down-regulated LC3-II mRNA accumulation in H5N1/NP172 infected cells at MOI 0.5 indicating that the antibodies might inhibit M2 mediated anti-autophagy mechanism of the influenza virus.
12. The fully human single chain variable antibody fragments that bound specifically to M2 produced in this study have high potential for developing further as a safe, novel and mutation tolerable anti-influenza agent especially against drug resistant influenza virus variants.

Copyright by Mahidol University

REFERENCES

Achaya, R., Carnevale, V., Fiorin, G., Levine, B.G., Polishchuk, A.L., *et al*. (2010). Structure and mechanism of proton transport through the transmembrane tetrameric M2 protein bundle of the influenza A virus. *Proc Natl Acad Sci*, 107(34), 15075-15080.

Air, G.M. & Laver, W.G. (1989). The neuraminidase of influenza virus proteins: structure, function, and genetics. *Proteins*, 6, 341–356.

Balannik, V., Wang, J., Ohigashi, Y., Jing, X. & Magavern, E. (2009). Design and pharmacological characterization of inhibitors of amantadine-resistant mutants of the M2 ion channel of influenza A virus. *Biochemistry*, 48(50), 11872-11882.

Balgi, D.A., Wang, J., Cheng, Y.H.D., Ma, C., Pfeifer, A.T. (2013). Inhibitors of the influenza A virus M2 ion channel discovered using a high-throughput yeast growth restoration assay. *Plos One*, 8(2), e55271.

Beigel, J. & Bray, M. (2008). Current and future antiviral therapy of severe seasonal and avian influenza. *Antiviral Res*, 78(1), 91-102.

Bilsel, P., Castrucci, M.R. & Kawaoka, Y. (1993). Mutations in the cytoplasmic tail of influenza A virus neuraminidase affect incorporation into virions. *J Virol*, 67, 6762–6767.

Blok, J. & Air, G.M. (1982). Sequence variation at the 3’end of the neuraminidase gene from 39 influenza type A viruses. *Virology*, 121, 211–229.

Boulo, S., Akarsu, H., Ruigrok, R.W. & Baudin, F. (2007). Nuclear traffic of influenza virus proteins and ribonucleoprotein complexes. *Virus Res*, 124(1-2): 12-21.

Brankston, G., Gilterman, L., Hirji, Z., Lemieux, C. & Gardam, M. (2007). Transmission of influenza A in human beings. *Lancet Infect Dis*, 7(4), 257-265.

Copyright by Mahidol University

Brekke, O.H. & Sandlie, I. (2003). Therapeutic antibodies for human diseases at the dawn of the twenty-first century. *Nature Rev*, 2, 52-62.

Bush, M.R., Bender, A.C., Subbraroa, K., Subbarao, K., Cox, N.J. & Fitch, W.M. (1999). Predicting the evolution of human influenza A. *Science*, 286, 1921–1925.

Calder, L.J., Wasilewski, S., Berriman, J.A. & Rosenthal, P.B. (2010). Structural organization of a filamentous influenza A virus. *Proc Natl Acad Sci USA*, 107, 10685–10690.

Casadevall, A. (1996). Antibody-based therapies for emerging infectious diseases. *Emerg Infect Dis*, 2(3), 200-208.

Carr, M.C. & Kin, S.P. (1994). Flu virus invasion: halfway there. 266, 234-236.

Carrat, F., Vergu, E., Ferguson, M.N., Lemaitre, M., Cauchemez, S. Leach, S. & Valleron, A.J. (2008). Time lines of infection and disease in human influenza: a review of volunteer challenge studies. *Am. J. Epidemiol.*, 167(7), 775-785.

Carrasco, L. (1978). Membrane leakiness after viral infection and a new approach to the development of antiviral agents. *Nature*, 272, 694-699.

Carrasco, L. (1995). Modification of membrane permeability by animal viruses. *Adv Virus Res*, 45, 61-112.

CDC. (2009). Prevention and control of influenza: Recommendations of the advisory committee on immunization practices (ACIP). *MMWR*, 58(RR-08).

Chen, W., Calvo, A.P., Malide, D., Gibbs, J., Schubert, U., *et al*. (2001). A novel influenza A virus mitochondrial protein that induces cell death. *Nat Med*, 7(12), 1306-1312.

Cheung, C.Y., Poon, L.L., Lau, A.S., Luk, W., Lau, Y.L., *et al*. (2002). Induction of proinflammatory cytokines in human macrophages by influenza A (H5N1) viruses: a mechanism for the unusual severity of human disease?. *Lancet*, 360(9348), 1831-1837.

Chotpitayasunondh, T., Lochindarat, S., Srisan, P., Chunsuthiwat, S., Sawanpanyalert, P., *et al*. (2004). Cases of influenza A (H5N1)-Thailand. *MMWR*, 5, 100-103.

Copyright by Mahidol University

Cox, N.J., Neumann, G., Donis, R.O. & Kawaoka, Y. (2010). Orthomyxoviruses: influenza. Topley and Wilson's Microbiology and Microbial Infections, 1, 639-698.

Das, K., Aramini, M.J., Ma, L., Krug, R.M. & Arnold, E. (2010). Structure of influenza A proteins and an insight into anti viral drug targets. *Nat Struct Mol Biol*, 17, 530-538.

Davies, E.L., Smith, J.S., Birkett, C.R., Manser, J.M., Anderson, D.D. & Young, J.R. (1995). Selection of specific phage-display antibodies using libraries derived from chicken immunoglobulin genes. *J Immunol Methods*, 186, 125-135.

Dean L. (2005). Blood Groups and Red Cell Antigens. Bethesda (MD): National Center for Biotechnology Information (US), Chapter 5, The ABO blood group. Available from: http://www.ncbi.nlm.nih.gov/books/NBK2267/

Devies, R.D. & Cohen, H.G. (1996). Interactions of protein antigents with antibodies. *Proc Natl Acad Sci USA*, 93(1), 7-12.

Demicheli, V., Jefferson, T., Rivetti, D. & Deeks, J. (2000). Prevention and early treatment of influenza in healthy adults. *Vaccine*, 18(1-12), 957-1030.

Du, J., Cross, A.T. & Zhou, H.X. (2012). Recent progress in structure-based anti-influenza drug design. *Drug Discovery Today*, 17, 1111-1120.

Eccles, R. (2005). Understanding the symptoms of the common cold and influenza. *Lancet Infect Dis*, 5(11), 718-725.

Fiore, E.A., Fry, A., Shay, D., Gubareva, L., Bresee, S.J. & Uyeki, M.T. (2011). Antiviral agents for the treatment and chemoprophylaxis of influenza. *MMWR*, 60(RR01), 1-24.

Fowlkes, A., Dasgupta, S., Chao, E., Lemmings, J., Goodin, K., *et al*. (2012). Estimating influenza incidence and rates of influenza-like illness in the outpatient setting. *Respi Viruses*, [Epub ahead of print].

Garcia-Sastre, A. & Palese, P. (1995). The cytoplasmic tail of the neuraminidase protein of influenza A virus does not play an important role in the packaging of this protein into viral envelopes. *Virus Res*, 37, 37–47.

Copyright by Mahidol University

Garten, J.R., Davis, T.C., Russell, A.C., Shi, B., Lindstrom, S., *et al*. (2009). Antigenic and genetic characteristics of swine-origin 2009 A (H1N1) influenza viruses circulating in humans. *Science*, 325, 197-201.

Gannage, M., Dormann, D., Albrecht, R., Dengjel, J., Torossi, T., *et al*. (2009). Matrix protein 2 of influenza A virus blocks autophagosome fusion with lysomes. *Cell*, 6, 367-380.

Gao, H.N., Lu, H.Z., Cao, B., Du, B., Shang, H., *et al*. (2013). Clinical findings in 111 cases of influenza A (H7N9) virus infection. *N Engl Med*, [Epub ahead of print].

Goldsby, R.A., Kindt, T.J. & Osborne, B.A. (2000). Organisation and expression of immunoglobulin genes. In: Kuby Immunology. 4th ed. *WH Freeman and Company*, 115-147.

Gonzalez, M.E. & Carrasco, L. (2003). Viroporins**.** *FEBS Lett*, 552, 28-34.

Hagen, M., Chung, T.Y., Butcher, A. & Krystal, M. (1994). Recombinant influenza virus polymerase: requirement of both 5′ and 3′ viral ends for endonuclease activity. *J Virol*, 68, 1509–1515.

Hanson, J.B., Boon,CM.A., Lim, PC.A., Webb, A., Ooi, E.E. & Webby, J.R. (2000). Passive immunoprophylaxis and therapy with humanized monoclonal antibody specific for influenza A H5 hemagglutinin in mice. *Respiratory Research*, 7, 126.

Hayden, F.G. (1996). Amantadine and rimantadine – clinical aspects. In: Richman, D.D. (ed.), Antiviral Drug Resistance. *New York: John Wiley & Sons Ltd.*, 59–77.

Hayden, F.G., Atmar, R.L., Schilling, M., Johnson, C., Poretz, D., *et al*. (1999). Use of the selective oral neuraminidase inhibitor oseltamivir to prevent influenza. *N Engl J Med*, 341, 1336–1343.

Helenius, A. (1992). Unpacking the incoming influenza virus. *Cell*, 69, 577-578.

Hinshaw, V.S., Webster, R.G., Naeve, C.W. & Murphy, B.R. (1983). Altered tissue tropism of human-avian reassortant influenza viruses. *Virology*, 128, 260–263.

Copyright by Mahidol University

Hirst, G.K. (1948). The nature of the virus receptors of red cells; evidence on the chemical nature of the virus receptors of red cells and of the existence of a closely analogous substance in normal serum. *J Exp Med*, 87, 301-314.

Homma, M. & Otuchi, M. (1973). Trypsin action on the growth of Sendai virus in tissue culture cells. III. Structural difference of Sendai viruses grown in eggs and tissue culture cells. *J Virol*, 12, 1457-1465.

Horimoto, T. & Kawaoka, Y. (1994). Reververse genetics provides direct evidence for a correlation ofhemagglutinin cleavability and virulence of an avian influenza A virus. *J Virol*, 68(5), 3120-3128.

Hout, SD. (2004). A multifunctional protein that enhances the pathogenesis of human immunodeficiency virus type 1. *Curr HIV Res*, 2, 255-270.

Hu, Y., Lu, S., Song, Z., Wang, W., Hao, P., *et al*., (2013). Association between asverse clinical outcome in human disease caused by novel influenza A H7N9 virus and sustained viral shedding and emergene of antiviral resistance. *Lancet*, 6736(13), 61125-61133.

Ito, T., Gorman, O.T., Kawaoka, Y., Bean, W.J. & Webster, R.G. (1991). Evolutionary analysis of the influenza A virus M gene with comparison of the M1 and M2 proteins. *J Virol*, 65, 5491-5498.

Jefferson, T., Jones, M.A., Doshi, P., Del Mar, C.B., Henegham, C.J., *et al*, (2012). Neuraminidase inhibitors for preventing and treating influenza in healthy adults and children (Review). The Cochrane library, 10, 1-224.

Jia, N., de Vlas, S.J., Liu, Y.X., Zhang, J.S., Zhan, L., *et al*. (2009). Serological reports of human infections of H7 and H9 avian influenza viruses in northern China. *J Clin Virol*, 44(3), 225-229.

Kash, J.C., Tumpey, T.M., Proll, S.C., Carter, V., Perwitasari, O., *et al*. (2006). Genomic analysis of increased host immune and cell death responses induced by 1918 influenza virus. *Nature*, 443(7111), 578-581.

Kelly, M.L., Cook, J.A., Brown-Augsburger, P., Heinz, B.A., Smith, M.C. & Pinto, L.H. (2003). Demonstrating the intrinsic ion channel activity of virally encoded proteins. *FEBS Lett*, 552(1), 61-67.

Copyright by Mahidol University

Kim, R. & Toge, T. (2004). Changes in therapy for solid tumors: potential for overcoming drug resistance in vivo with molecular targeting agent. *Surg Today*, 34, 293-303.

Kobasa, D., Jones, S.M., Shinya, K., Kash, J.C., Copps, J., *et al*. (2007). Aberrant innate immune response in lethal infection of macaques with the 1918 influenza virus. *Nature*, 445(7125), 319-323.

Korteweg, C. & Gu, J. (2001). Pathology, molecular biology and pathogenesis of avian influenza A (H5N1) infection in human. *Am. J. Pathol.*, 172(5), 1155-1170.

Krung, R.M. & Lamp, R.A. (1996). Orthomyxoviridae: The viruses and their replication. Fields Virology. 3rd edition. Knipe DM, Howley PM. eds. *Philadelphia: Lippincott Williams & Wilkins*, 1353-1445.

Kulkeaw, K., Sakolvaree, Y., Srimanote, P., Tongtawe, P., Maneewatch. S., *et al*. (2009). Human monoclonal ScFv neutralize lethal Thai cobra, *Naja kaothia*, neurotoxin. *J Proteomics*, 72, 270-282.

Lamb, R.A. & Krug, R.M. (2001). Orthomyxoviridae: the viruses and their replication. In: Fundamental Virology. *Lippincott Williams & Wilkins, Philadelphia*, 1487-1531.

Lamb, A.R., Zebedee, L.S. & Richard, D.C. (1985). Influenza virus M2 protein is an integral membrane protein expressed on the infected-cell surface. *Cell*, 40(3), 627-633.

Lambert, C.L. & Fauci, S.A. (2010). Influenza vaccines for future. *N Engl J med*, 363, 2036-2044.

Lackenby, A., Hungnes, O., Dudman S.G., Meijer, A., Paget, W.J., Hay, A.J. & Zambon, M.C. (2008). Emergence of resistance to oseltamivir among influenza A (H1N1) viruses in Europe. *Euro Surveill*, 13(5), 8026.

Layne, E. (1957). Spectrophotometric and turbidimetric method for measuring proteins. *Method in enzymology*, 3, 447-455.

Layne, P.S., Monto, S.A. & Taubenberger, K.S. (2009). Pandemic influenza: an inconvenient mutation. *Science*, 323(5921), 1560-1561.

Copyright by Mahidol University

Lentz, M.R., Webster, R.G. & Air, G.M. (1987). Site-directed mutation of the active site of influenza neuraminidase and implications for the catalytic mechanism. *Biochemistry*, 26, 5351–5358.

Lu, J., Guo, Z., Pan, X, Wang, G., Zhang D., *et al*. (2006). Passive immunotherapy for influenza A h%N1 virus infection with equine hyperimmune globulin F(ab')2 in mice. *Respiratory Research*, 7(1), 43.

Luke, T.C., Kilbane, E.M., Jackson, J.L., & Hoffman, S.L. (2006). Meta-analysis: convalescent blood products for Spanish influenza pneumonia: a future H5N1 treatment?. *Ann Intern Med*, 145(8), 599-609.

Maneewatch, S., Thanongsaksrikul, J., Songserm, T., Thueng-In, K., Kulkeaw, K., *et al*. (2009). Human single-chain antibodies that neutralize homologous and heterologous strains and clades of influenza A virus. *Antiviral therapy*, 14, 221-223.

Matrosovich, N.M., Matrosovich, Y.T., Gray, T., Roberts, A.N., Klenk, D.H. (2004). Neuraminidase is important for the initiation of influenza virus infection in human airway epithelium. *J Virol*, 78, 12665-12667.

Mazur, I., Anhlan, D., Mitzer, D., Wixler, L., Schubert, U. & Ludwig, S. (2008). The pro-apoptotic influenza A virus protein PB1-F2 regulates viral polymerase activity by interaction with the PB1 protein. *Cell Microbiol*, 10(5), 1140-1152.

Makela, M.J., Pauksens, K., Rostila, T., Fleming, D.M., Man, C.Y., *et al*. (2000). Clinical efficacy and safety of the orally inhaled neuraminidase inhibitor zanamivir in the treatment of influenza: a randomized, double-blind, placebo-controlled European study. *J Infect*, 40, 42–48.

McCafferty, J., Griffiths, A.D., Winter, G. & Chiswell, D.J. (1990). Phage antibodies: filamentous phage displaying antibody variable domains. *Nature*, 348, 552-554.

Mitamura, K. & Sukaya, N. (2006). Diagnosis and treatment of influenza clinical investigation on viral shedding in children with influenza. *Uirusu*, 56(1), 109-116.

Copyright by Mahidol University

Mitzner, D., Dudek, S.E., Studtrucker, N., Anhlan, D., Mazur, I, *et al*. (2009). Phosphorylation of the influenza A virus protein PB1-F2 by PKC is crucial for apoptosis promoting functions in monocytes. *Cell Microbiol*, 11(11), 1502-1516.

Moscona, A. (2005). Neuraminidase inhibitors for influenza. *N Engl J Med*, 353, 1363-1373.

Nayak, P.D., Balogun, A.R., Yamada, H., Zhou, H.Z. & Barman, S. (2009). Influenza virus morphogenesis and budding. *Virus Res*, 143(2), 147-161.

Nelson, A.L. & Reichert, J.M. (2009). Development trends for therapeutic antibody fragments. *Nature Biotech*, 27, 331-337.

Nemeroff, M.E., Barabino, S.M., Li, Y., Keller, W. & Krug, R.M. (1998). Influenza virus NS1 protein interacts with the cellular 30 kDa subunit of CPSF and inhibits 3′ end formation of cellular pre-mRNAs. *Mol Cell*, 1, 991–1000.

Newcomb, L.L., Kuo, R.L., Ye, Q., Jiang, Y., Tao, J.Y. & Krug, M.R. (2009). Interaction of the influenza a virus nucleocapsid protein with the viral RNA polymerase potentiates unprimed viral RNA replication. *J Virol*, 83, 29–36.

Neumann, G., Hughes, T.M. & Kawaoka, Y. (2000). Influenza A virus NS2 protein mediates vRNP nuclear export through NES-independent interaction with hCRM1. *EMBO J*, 19, 6751–6758.

Nielsen, U.B., Adams, G.P., Weiner, L.M. & Marks, J.D. Targeting of bivalent anti-ErbB2 diabody antibody fragments to tumor cells is independent of the intrinsic antibody affinity. *Cancer Res*, 60(22), 6434-6440.

Nicholls, M.J., Lai, J. & Garcia, JM. (2012). Investigating the interaction between influenza and sialic acid: making and breaking the link. M. von Itzstein (ed.), *Influenza Virus Sialidase-A Drug Discovery Target*, Milestones in Drug Therapy, 38-45.

Nicholls, S.J., Chan, R.W., Russell, R.J., Air, G.M. & Peiris, J.S. (2008). Evolving complexities of influenza virus and its receptor. *Trends Microbiol*, 16(4), 149-157.

Copyright by Mahidol University

Nieva, L.J., Madan, V. & Carrasco, L. (2012). Viroporines: structure and biological functions. *Nature Review*, 10, 563-574.

O'Neill, R.E., Talon, J. & Palese, P. (1998). The influenza virus NEP (NS2 protein) mediates the nuclear export of viral ribonucleoproteins. *EMBO J*, 17, 288–296.

Öhman, L., Magesson, KE. & Stendahl O. (1982). The mannose-specific lectin activity of *Escheichia coli* type I fimbriae assayed by agglutination of glycolipid-containning liposomes, erythrocytes, and yeast cells and hydrophobic interaction chromatography. *FEMS Microbiology Letters*, 149-153.

Pielak, M.R., Schnell, R.J. & Chou, J.J. (2009). Mechanism of drug inhibition and drug resistance of influenza A M2 channel. *Proc Natl Acad Sci*, 18, 7379-7384.

Pietzsch, J. (2003). The importance of *protein folding*. Horizon Symposia, http://www.nature.com/horizon/proteinfolding/background/importance.html 26.

Pinto, L.H., Holsinger, L.J. & Lamb, R.A. (1992). Influenza virus M2 protein has ion channel activity. *Cell*, 69, 517–528.

Plotch, S.J., Bouloy, M., Ulmanen, I. & Krug, R.M. (1981). A unique cap (m7GpppXm)-dependent influenza virion endonuclease cleaves capped RNAs to generate the primers that initiate viral RNA transcription. *Cell*, 23, 847–858.

Plotkin, J.B. & Dushoff, J. (2003). Codon bias and frequency-dependent selection on the hemagglutinin epitopes of influenza A virus. *Proc Natl Acad Sci USA*, 100, 7152–7157.

Reed, L.J., Muench, H. (1938). A simple method of estimating fifty percent endpoints. *The American Journal of Hygiene*. 27, 493-497.

Renegar, B.K., Small, A.P., Boykins, G.L. & Wright, F.P. (2004). Role of IgA versus IgG in the control of influenza viral infection in the murine respiratory tract. *J Immunol*, 173, 1978-1986.

Riechmann, L., Clark, M., Waldmann, H. & Winter, G. (1988). Reshaping human antibodies for therapy. *Nature*, 333(6162), 323-327.

Copyright by Mahidol University

Roger, N.G. & Paulson, C.J. (1983). Receptor determinants of human and animal influenza virus isolates: differences in receptor specificity of the H3 hemagglutinin based on species of origin. *Virology*, 127, 361-373.

Rossman, S.J. & Lamb, A.R. (2011). Influenza virus assembly and budding. *Virology*, 411, 229-236.

Rosenthal, L. (1943). Agglutination properties of *Escherichia coli*. *J Bacteriol*, 45(6), 545-550.

Rust, M.J., Lakadamyali, M., Zhang, F. & Zhuang, X. (2004). Assembly of endocytic machinery around individual influenza viruses during viral entry. *Nat Struct Mol Biol*, 11, 567-573.

Saladino, R., Barontini, M., Crucianelli, M, Nencioni, M., Sgarbanti, R. & Palamara, A.T. (2010). Current advances in anti-influenza therapy. *Curr Med Chem*, 17(10), 2101-2140.

Samji, T. (2009). Influenza A: Understanding the viral life cycle. *Yale J Biol Med*, 82(4), 153-159.

Sharma, M., Yi, M., Dong, H., Qin, H., Peterson, E., *et al*. (2010). Insight into the mechanism of the influenza A proton channel from a structure in a structure in a lipid bilayer. *Science*, 330(6003): 509-512.

Scholtissek, C., Hinshaw, V.S. & Olsen, C.W. (1998). Influenza in pigs and their roles as the intermediate host. In: Nicholson KG, Webster RG, Hey AJ (Eds.). Textbook of Influenza. *Blackwell Science, Oxford*, 137-145.

Schimitz, N., Kurrer, M. & Bachmann, M. (2005). Interleukin-1 is responsible for acute lung immunopathology but increases survival of respiratory influenza virus infection. *J Virol*, 70(10), 6441-6448.

Scheiffele, P., Rieteld, A., Wilk, T. & Simons, K. (1999). Influenza viruses select ordered lipid domains during budding from the plasma membrane. *J. Biol. Chem.* 274, 2038-2044.

Schnell, J.R. & Chou, J.J. (2008). Structure and mechanism of the M2 proton channel of influenza A virus. *Nature*, 451, 591-595.

Sheu, T.G., Fry, A.M., Garten, R.J., Deyde, V.M., Shwe, T., *et al*. (2011). Dual resistance to adamantanes and oseltamivir among seasonal influenza A(H1N1) viruses: 2008-2010. *J Infect Dis*, 203(1), 13-17.

Copyright by Mahidol University

Sheu, G.T., Deyde, M.V., Okomo-Adhiambo, M., Garten, R.J., Xu, X., *et al*. (2011). Surveillance for neuraminidase inhibitor resistance among human influenza A and B viruses circulating worldwide from 2004 to 2008. *Antimicrob Agents Chemother*, 52, 3284–3292.

Shi, S.R., Cote, R.J. & Taylor, C.R. (1997). Antigen retrieval immunohistochamistry: past, present and future. *J Histochem Cytochem*, 45(3), 327-343.

Shimizu, K., Iguchi, A., Gomyou, R. & Ono, Y. (1999). Influenza virus inhibits cleavage of the HSP70 pre-mRNAs at the polyadenylation site. *Virology*, 254, 213–219.

Shin, J.H., Sung, J.H., Park, S.J., Lee, J.H., Lee, D.Y., *et al*. (2003). Species identification and strain differentiation of dermatophyte fungi using polymerase chain reaction amplification and restriction enzyme analysis. *J Am Acad Dermatol*, 48(6), 857-865.

Shinya, K., Ebina, M., Yamada, D., Ono, M., Kasai, N. & Kawaoka, Y. (2006). Avian flu: influenza virus receptors in the human airway. *Nature*, 440(7083), 435-436.

Skehel, J.J., Bayley, P.M., Brown, E.B.**,** Martin, S.R.,Waterfield, M.D., *et al*. (1982). Changes in the conformation of influenza virus hemagglutinin at the pH optimum of virus-mediated membrane fusion. *Proc Natl Acad Sci USA*, 79, 968–972.

Smirnov, Y.A., Lipatov, A.S., Gitelman, A.K., Claas, E.C., Osterhaus, A.D. (2000). Prevention and treatment of bronchopneumonia in mice caused by mouse-adapted variant of avain H5N2 influenza A virus using monoclonal antibody against conserved conserved epitope in the HA stem region. *Arch Virol*, 145(8), 1733-1741.

Steck, L.T. (1974). The organization of proteins in the human red blood cell membrane. *J Cell Biol*, 62(1), 1-19.

Steinmann, E. (2007). Hepatitis C virus p7 protein is crucial for assembly and release of infectious virions. *Plos Pathog*, 3, (962-971)

Stoscheck, C.M. (1990). Quantitation of protein. *Method in enzymology*, 182, 50-69.

Stouffer, L.A., Acharya, R., Salom, A., Levine, S.A., Costanzo, L., *et al*,. (2008). Structural basis for the function and inhibition of an influenza virus proton channel. *Nature*, 451, 596-599.

Su, B., Wurtzer, S., Rameix-Welti, M.E., Dwyer, D., van der Werf, S., *et al*. (2009). Enhancement of the influenza A hemagglutinin (HA)-mediated cell-cell fusion and virus entry by the viral neuraminidase (NA). *Plos One*, 4(12), e8495.

Sheu, G.T., Fry, M.A., Garten, R.J., *et al*,. (2011). Dual resistance to adamantanes and oseltamivir among seasonal influenza A (H1N1) viruses: 2008-2010. *J Infect Dis*, 203(1): 13-17.

Sugrue, R.J., Bahadur, G., Zambon, C.M., Hall-Smith, M., Douglas, R.A. & Hay, J.A. (1990). Specific structural alteration of the influenza haemagglutinin by amantadine. *EMBO J*, 9, 3469–3476.

Sui, J., Hwang, W.C., Perez, S., Wei, G., Aird, D., *et al*. (2009). Structural and functional bases for broad-spectrum neutralization of avian and human influenza A viruses. *Nat Struct Mol Biol*, 16(3), 265-273.

Tellier, R. (2006). Review of aerosol transmission of influenza A virus. *Emerging Infect. Dis*, 12(11), 1657-1662.

Kim, R. & Toge, T. (2004). Changes in therapy for solid tumors: potential for overcoming drug resistance in vivo with molecular targeting agents. *Surg Today*, 34, 293-303.

Thanongsaksrikul, J., Srimanote, P., Maneewatch, S., Choowongkomon, K., Tapchaisri, P., *et al.* (2010). A V_HH that neutralizes the zinc metalloproteinase activity of botulinum neurotoxin type A. *J Biol Chem*, 28, 9657–9666.

Thueng-in, K., Thanongsaksrikul, J., Srimanote, P., Bangphoomi, K., Pougpair, O., *et al*. (2012). Cell penetrable humanized-VH-VHH that inhibit RNA dependent RNA polymerase (NS5B) of HCV. *Plos One*, 7(11), e49254.

Treanor, J.J., Tierney, E.L., Zebedee, S.L., Lamb, R.A. & Murphy, B.R. (1990). Passively transferred monoclonal antibody to the M2 protein inhibits influenza A virus replication in mice. *J Virol*, 64, 1375-1377.

Copyright by Mahidol University

Trifonov, V., Khiabanian, H. & Rabadan, R. (2009). Geographic dependence, surveillance, and origins of the 2009 influenza A (H1N1). *N Engl J Med*, 361(2): 115-119.

Ulmanen, I., Broni, B.A. & Krug, R.M. (1981). The role of two of the influenza virus core P proteins in recognizing cap 1 structures (m7GpppNm) on RNAs and in initiating viral RNA transcription. *Proc Natl Acad Sci USA*, 78: 7355–7359.

Van Riel, D., Munster, V.J., de Wit, E., Rimmelzwaan, F.G., Fouchier, M.R., *et al*. (2006). H5N1 virus attachment to lower respiratory tract. *Science*, 312(5772), 399.

Van Riel, D., Munster, V.J., de Wit, E., Rimmelzwaan, F.G., Fouchier, M.R., *et al*. (2007). Human and avian influenza viruses target different cells in the lower respiratory tract of humans and other mammals. *Am. J. Pathol.*, 171(4), 1215-1223.

Van Voris, L.P. & Newell, P.M. (1992). Antivirals for the chemoprophylaxis and treatment of influenza. *Semin Respir Infect*, 7, 61–70.

Vaithilingan, A., Teixei, E.J., Miller, J.P., Heron, T.B. & Huston, D.C. (2012). *Entamoeba histolytica* cell surface calreticulin binds human C1q and functions in amebic phagocytosis of host cells. *Infect Immun*, 80(6), 2008-2018.

Wang, J., Qiu, J. X., Soto, C. & DeGrado, W.F. (2011). Structural and dynamic mechanisms for the function and inhibition of the M2 proton channel from influenza A virus. *Curr. Opin. Struct. Biol*, 21, 68-80.

Watanabe, T., Watanabe, S., Ito, H., Kida, H. & Kawaoka, Y. (2001). Influenza A virus can undergo multiple cycles of replication without M2 ion channel activity. *J. Virol.*, 75, 5656-5662.

Webster, R.G., Layer, W.G., Air, G.M. & Schild, G.C. (1982). Molecular mechanisms of variation in influenza viruses. *Natur*e, 296, 115-121.

Webster, R.G. (1998). Influenza: an emerging disease. *Emerg Infect Dis*, 4, 436-441.

Wei, G., Meng, W., Guo, H., Liu, J., *et al*. (2011). Potent neutralization of influenza A virus by single domain antibody blocking M2 ion channel protein. *Plos one*, 6(12), e28309.

Whittaker, G.R., Kann, M. & Helenius, A. (2000). Viral entry into the nucleus. *Annu. Rev. Cell Dev. Biol*. 16, 627-651.

Winter, G., Griffiths, A.D., Hawkins, R.E. & Hoogenboom, H.R. (1994). Making antibodies by phage display technology. *Annu Rev Immunol*, 12, 433-455.

Winther, B., Gwaltney, J., Mygind, N. & Hendley, J. (1998). Viral-induced rhinitis. *Am J Rhinol*, 12(1), 17-20.

Wozniak, L.A., Griffin, S., Rowlands, D., *et al*. (2010). Intracellular proton conductance of the hepatitis C virus p7 protein and its contribution to infectious virus production. *Plos Pathog*, 6(9), e1001087.

World Health Organization: WHO Manual on Animal Influenza Diagnosis and Surveillance. Department of Communicable Disease Surveillance and Response; 2002. www.who.int/vaccine_research/diseases/influenza/WHO_manual_on_animal-diagnosis_and_surveillance_2002_5.pdf.

Youthao, S., Jaroensutasinee, M., & Jaroensutasinee, K. (2008). Analysis of influenza cases and seasonal index in Thailand. *Int J Biol Life Sci*, 2, 113-116.

Yeun, K.Y., Chan, P.K., Peiris, M., Tsang, D.N., Que, T.L. *et al*. (1998). Clinical features and rapid viral diagnosis of human disease associated with avian influenza A H5N1 virus. *Lancet*, 351, 467-471.

Zebedee, L.S. & Lamb, A.R. (1988). Influenza A virus M2 protein: Monoclonal antibody restriction of virus growth and detection of M2 in virion. *J. Virol.*, 62(8), 2762-2772.

Zhang, J., Pekosz, A. & Lamb, R.A. (2000). Influenza virus assembly and lipid raft microdomains: a role for the cytoplasmic tails of the spike glycoproteins. *J. Virol.* 74(10). 4634-4644.

Zhou, B., Zhong, N. & Guan, Y. (2007). Treatment with convalescent plasma for influenza A (H5N1) infection. *N Engl J Med*, 357, 1450-1451.

Copyright by Mahidol University

APPENDICES

Copyright by Mahidol University

APPENDIX A

Reagents for DNA manipulation and electrophoresis

1. Tris-EDTA buffer

The buffer was prepared by dissolving Tris (USB, USA) 1.21 g and EDTA (USB, Cleveland, USA) 0.29 g in 700 ml of DW. After completely dissolving, pH of the solution was adjusted to 8.0 with HCl (Merk, Darmstadt, Germany). The volume was made up to 1 liter with DW.

2. Sodium acetate solution (3 M, pH 5.2)

Sodium acetate 40.8 g was dissolved in 50 ml of DW. After dissolving, pH of the solution was adjusted to 5.2 with glacial acetic acid (Merk, Darmstadt, Germany). The volume was made up to 100 ml with DW.

3. TBE buffer (5x)

The following ingredients were dissolved in 700 ml of DW:

Tris-base	52.0	g
Boric acid (USB, Cleveland, USA)	27.5	g
EDTA.2H_2O (USB, Cleveland, USA)	4.65	g

The pH of the solution was adjusted to 8.3 with concentrate HCl before the volume was made to 1,000 ml with DW. This buffer was sterilized by autoclaving.

4. Ethidium bromide solution

To prepare stock ethidium bromide solution, a tablet of ethidium bromide (USB, Corporation, USA) was dissolved in 1 ml of DW to make 10 mg/ml concentration. Fifty microliters of the stock solution was then added to 100 ml of 1x TAE to make 0.5 µg/ml working concentration. The solution was protected from light.

Copyright by Mahidol University

5. DNA loading dye (10x)

DNA loading dye stock was prepared by dissolving 0.25 g each of bromophenol blue (Bio-Rad, USA) and xylene cyanol (USB, Cleveland, USA) in 50 ml of glycerol. The volume of the preparation was adjusted to 100 ml with DW.

6. TAE buffer (50x)

The buffer was prepared by dissolving the following ingredients in 700 ml of DW:

Tris-base	242.0	g
EDTA.2H_2O	18.16	g
Glacial acetic acid	57.1	ml

The buffer pH was adjusted to 8.3 with glacial acetic. The volume was made up to 1,000 ml with DW and the solution was sterilized by autoclaving. To prepare 1x TAE working solution, 20 ml of the 50x TAE buffer were added to 980 ml of DW and mixed.

7. Agarose gel preparation (1%)

Agarose (USB Corparation, USA) 0.3 g was dissolved in 30 ml of 1x TAE buffer by heating. Melted agarose solution was poured into a gel casting apparatus and allowed to solidify at 25 ºC for minutes.

Copyright by Mahidol University

APPENDIX B

Bacterial media

1. Luria-Bertani (LB) broth

The medium was prepared by dissolving 10 g of casein enzyme hydrolysate, type-I (Hymedia®, Munbai, India), 5 g of yeast extract powder (Hymedia®, Munbai, India), and 5 g of NaCl (UNIVAR, NSW, Australia) in 1,000 ml of DW. After mixing the mixture, the broth was sterilized by autoclaving and kept at 25 ºC.

2. LB-Ampicillin (LB-A) broth

The LB broth was prepared as described in (**1**). After autoclaving and cooling down, ampicillin (General Drug House, Thailand) was added to the final concentration of 100 µg/ml. The broth was kept at 4 ºC.

3. LB-Ampicillin and Kanamycin (LB-AK) broth

The LB broth was prepared as described in (**1**). After autoclaving and cooling down, ampicillin and kanamycin (General Drug House, Thailand) were added to the final concentration of 100 µg/ml and 25 µg/ml, respectively. The broth was kept at 4 ºC.

4. LB-Ampicillin-Glucose (LB-AG) broth

The LB broth was prepared as described in (**1**). After autoclaving and cooling down, 55.6 ml of 2 M glucose solution and ampicillin was added to final concentration of 100 µg/ml. The broth was kept at 4 ºC.

Copyright by Mahidol University

5. LB agar

One liter of LB medium was prepared as described in (**1**). Bacto agar powder (Hymedia) 17 g was added and dissolved by heating. After autoclaving and cooling down, the preparation was poured into 100-mm petridishes (25 ml/plate). The plate was stored at 4 ºC until use. Before using, surface of the agar was dried at 37 ºC for 1 hour.

6. LB-A agar

LB agar was prepared as described in (**4**). After autoclaving and cooling down, ampicillin was added to the final concentration of 100 µg/ml. Homogeneous melted agar was poured into 100-mm petridishes (25 ml/plate). The plate was stored at 4 ºC until use. Before using, surface of the agar was dried at 37 ºC for 1 hour.

7. LB-AK agar

LB agar was prepared as described in (**4**). After autoclaving and cooling down, ampicillin and kanamycin were added to the final concentration of 100 µg/ml and 25 µg/ml, respectively. Homogeneous melted agar was poured into 100-mm petridishes (25 ml/plate). The plate was stored at 4 ºC until use. Before using, surface of the agar was dried at 37 ºC for 1 hour.

8. LB-AG agar

LB agar was prepared as described in (**4**). After autoclaving and cooling down, 55.6 ml of 2 M glucose solution and ampicillin was added to the final concentration of 100 µg/ml. The broth was kept at 4 ºC. Homogeneous melted agar was poured into 100-mm petridishes (25 ml/plate). The plate was stored at 4 ºC until use. Before using, surface of the agar was dried at 37 ºC for 1 hour.

9. 2x Yeast extract and Tryptone (2xYT) broth

The medium was prepared by dissolving 17 g of casein enzyme hydrolysate, type-I, 10 g of yeast extract powder, and 5 g of NaCl in 1,000 ml of DW. After mixing the mixture, the broth was sterilized by autoclaving and kept at 25 ºC.

10. 2xYT-Ampicillin (2xYT-A) broth

The 2xYT broth was prepared as described in (**7**). After autoclaving and cooling down, ampicillin was added to the final concentration of 100 µg/ml. The broth was kept at 4 ºC.

11. 2xYT-Ampicillin-Glucose (2xYT-AG) broth

The 2x YT broth was prepared as described in (**7**). After autoclaving and cooling down, 55.6 ml of 2 M glucose solution and ampicillin was added to the final concentration of 100 µg/ml. The broth was kept at 4 ºC.

12. 2xYT agar

One liter of 2x YT medium was prepared as described in (**7**). Bacto agar powder 17 g was added and dissolved by heating. After autoclaving and cooling down, the preparation was poured into 100-mm petridishes (25 ml/plate). The plate was stored at 4 ºC until use. Before using, surface of the agar was dried at 37 ºC for 1 hour.

13. 2xYT-A agar

2xYT agar was prepared as described in (**10**). After autoclaving and cooling down, ampicillin was added to the final concentration of 100 µg/ml. Homogeneous melted agar was poured into 100-mm petridishes (25 ml/plate). The plate was stored at 4 ºC until use. Before using, surface of the agar was dried at 37 ºC for 1 hour.

14. 2xYT-AG agar

LB agar was prepared as described in (**10**). After autoclaving and cooling down, 55.6 ml of 2 M glucose solution and ampicillin was added to the final concentration of 100 µg/ml. The broth was kept at 4 ºC. Homogeneous melted agar was poured into 100-mm petridishes (25 ml/plate). The plate was stored at 4 ºC until use. Before using, surface of the agar was dried at 37 ºC for 1 hour.

Copyright by Mahidol University

APPENDIX C

Reagents for plasmid preparation and bacterial transformation

1. Magnesium chloride solution (0.1 M)

$MgCl_2$ (Sigma, St. Louis, USA) 0.95 g was dissolved in 100 ml of DW. The mixture was sterilized by filtering through a sterile 0.2 µm membrane. The solution was kept at 4 ºC.

2. Calcium chloride solution (0.1)

$CaCl_2$ (Sigma, St. Louis, USA) 1.1 g was dissolved in 100 ml of DW. After completely dissolving, the preparation was sterilized by filtering through a sterile 0.2 µm membrane. The solution was kept at 4 ºC.

3. Reagents for mini-scale plasmid extraction from *E. coli*

3.1 Solution-I (50 mM glucose, 10mM EDTA, 25 mMTris-HCl, pH 8.0)

The solution was prepared by dissolving the following ingredients in 80 ml DW:

Glucose	0.9	g
Tris	0.33	g
EDTA	0.37	g

After completely dissolved, the pH was adjusted to 8.0 with 1 M HCl or 1 N NaOH. The solution was sterilized by autoclaving and then stored at 25 ºC.

Copyright by Mahidol University

3.2 Solution-II (0.2 M NaOH, 1% SDS)

The solution was freshly prepared by mixing the following ingredients together:

NaOH (5N) (Merck, Germany)	0.2	ml
SDS (10%) (USB, Cleveland, USA)	0.5	ml
DW	4.3	ml

3.3 Solution-III (3 M potassium acetate, pH 5.2)

2.44 g of potassium acetate (Univar, NSW, Australia) was dissolved in 70 ml DW. The pH of the solution was adjusted to 5.2 with glacial acetic acid. The volume was made up to 100 ml with DW before autoclaving. The solution was stored at 25 ºC.

3.4 Glycerol (80%)

Eighty microliters of Glycerol (Univar, NSW, Australia) was mixed with 20 ml of DW. After thoroughly mixing, the solution was sterilized by autoclaving.

Copyright by Mahidol University

APPENDIX D

Reagents for recombinant protein purification

1. Affinity chromatography by Ni-NTA™ bead (denaturing purification condition)

1.1 Lysis buffer C (8 M Urea, 100 mM NaH_2PO_4, 0.5 M NaCl, 100 mMTris-HCl pH 6.3)

100 mM NaH_2PO_4	7 g
0.5 mMNaCl	29.2 g
100 mMTris	12 g
8 M Urea	480.5g

All ingredients were dissolved in 800 ml of UDW. After completely dissolving, the pH of the solution was adjusted to 8.0 with NaOH. The final volume was made to 1,000 ml with UDW. The solution was filtered through a filter paper Whatman™ grade no.1.

1.2 Washing buffer Buffer B (8 M Urea, 100 mM NaH_2PO_4, 0.5 M NaCl, 10 mMTris-HCl pH 8.0)

100 mM NaH_2PO_4	7 g
0.5 mMNaCl	29.2 g
10 mMTris	1.2g
8 M Urea	480.5g

All ingredients were dissolved in 800 ml of UDW. After completely dissolving, the pH of the solution was adjusted to 8.0 with NaOH. The final volume was made to 1,000 ml with UDW. The solution was filtered through a filter paper Whatman™ grade no.1

Copyright by Mahidol University

1.3 Imidazole (3 M)

Imidazole (USB) (20.4 g) was dissolved in 70 ml of buffer C. After dissolving, the volume was made up to 100 ml with buffer C. The solution was kept as stock at 4 °C.

2. Affinity chromatography by TALON™ resin (denaturing condition)

2.1 Extraction/wash buffer pH 7.0

50 mM Na_2HPO_4	7.098 g
280 mMNaCl	17.532 g
8 M urea	480.48 g

All ingredients were added to 700 ml of UDW to dissolve the urea. The pH of the solution was adjusted to 7.0 with 1 M HCl or 1 N NaOH and the volume was brought up to 1,000 ml with UDW. The solution was filtered through a filter paper Whatman™ grade no.1.

2.2 Elution buffer pH 7.0

45 mM Na_2HPO_4	6.3882 g
270 mMNaCl	15.7788 g
8 M urea	480.48 g
150 mM imidazole	10.212 g

All ingredients were added to 700 ml of UDW to dissolve the urea. The pH of the solution was adjusted to 7.0 with 1 M HCl or 1 N NaOH and the volume was brought up to 1,000 ml with UDW.The solution was filtered through a filter paper Whatman™ grade no.1.

Copyright by Mahidol University

APPENDIX E

Reagents for Sodium Dodecyl Sulfate-Polyacrylamide Gel Electrophoresis (SDS-PAGE) and Colloidal Coomassie Brilliant Blue G-250 stain

1. Reducing SDS-PAGE sample buffer (6x)

This buffer was prepared as a 6x solution by combining the following ingredients:

SDS	0.6	mg
Bromophenol blue	0.5	mg
Tris-HCl (0.5 M, pH 8.8)	3.75	ml
Glycerol (USB Corporation, OH, USA)	4.6	ml
β-mercaptoethanol	1.5	ml

The volume of the preparation was made to 10 ml by adding UDW. The complete sample buffer was kept in a 1 ml-aliquot at -20 °C until use.

For SDS-PAGE, five parts of the sample was diluted with one part of 6x sample buffer and heated at 100 °C for 5 minutes before loading into the casted SDS-PAGE gel.

2. Tris-HCl solution (1.5 M, pH 8.8)

To prepare this solution, 18.15 g of Tris-base (Affymetrix, Inc., OH, USA) were dissolved in 50 ml of UDW, and then the pH was adjusted to 8.8 with 1 N HCl. The volume was brought up to 100 ml with UDW. The solution was sterile by autoclaving and stored at 4 °C until use.

Copyright by Mahidol University

3. Tris-HCl (0.5 M, pH 6.8)

To prepare the solution, 6.05 g of Tris-base were dissolved in 50 ml of UDW, then pH was adjusted to 6.8 with 1 N HCl. The volume was brought up to 100 ml with UDW. The solution was sterile by autoclaving and stored at 4 °C until use.

4. Sodium dodecyl sulfate solution (SDS, 10%)

The solution was prepared by dissolving 10 g of SDS (USB Corporation, OH, USA) in 100 ml of UDW. The solution was filtered through a filter paper Whatman™ grade no.1 membrane (GE Healthcare Life Sciences, United Kingdom).

5. Ammonium persulfate solution (10%)

The solution was freshly prepared by dissolving 50 mg of ammonium persulfate (UNIVAR, Australia) in 0.5 ml of UDW.

6. Polyacrylamide resolving gel (12%)

The following solutions were combined with 3.4 ml of UDW

Tris-HCl, pH 8.8 (1.5 M)	2.5	ml
SDS solution (10%)	0.1	ml
Stock polyacrylamide solution 30% (Bio-Rad Laboratories, Hercules, CA)	4.0	ml

The preparation was degassed under a vacuum for at least 5 minutes. Gel polymerization was initiated by adding 50 µl of 10% ammonium persulfate and 5 µl of TEMED (Bio-Rad Laboratories, Hercules, CA). The preparation was poured into the gel casting apparatus, over-layered with UDW and allowed to polymerize at 25 °C for at least 30 minutes.

7. Polyacrylamide stacking gel (4%)

The following solutions were combined with 3.05 ml of UDW:

Tris-HCl, pH 6.8 (0.5 M)	1.25	ml
SDS solution (10%)	0.05	ml
Stock polyacrylamide solution 30% (Bio-Rad Laboratories, Hercules, CA)	0.65	ml

Copyright by Mahidol University

The preparation was degassed under a vacuum for at least 5 minutes. Gel polymerization was initiated by adding 25 µl of 10% ammonium persulfate and 5 µl of TEMED (Bio-Rad Laboratories, Hercules, CA). The preparation was gently layered onto the polymerized 12% resolving gel in the gel casting apparatus, a comb was properly placed and the gel was allowed to polymerize at 25 °C for at least 30 minutes before use.

8. SDS electrophoresis running buffer (Tris-glycine buffer)

The buffer contained the following ingredients:

Tris	30.3	g
Glycine	144	g
SDS	10	g

The reagents were dissolved in UDW and the volume was made up to 1 liters with UDW. The buffer could be stored at 25 °C for up to 3 months.

9. Collidal Coomassie Brilliant Blue G-250 (CBB) Staining

9.1 Fixing solution

The solution was freshly prepared by mixing 500 µl of 85% *o*-phosphoric acid with 20 ml UDW. The 5 ml of methanol was added and mixed.

9.2 Staining solution

The solution consisted of 10 ml of 20% $(NH_4)_2SO_4$, 500 µl of 85% *o*-phosphoric acid, and 0.025 g of Coomassie Brilliant Blue G250 in 10 ml DW. Then 5 ml of methanol was added and mixed.

9.3 Neutralization solution

The solution was prepared by dissolving 6 g of Tris-base in 250 ml of deionized distilled water. The pH was adjusted to 6.5 with *o*-phosphoric acid and the final volume was brought up to 500 ml with deionized distilled water.

Copyright by Mahidol University

9.4 Washing solution

The solution was prepared by adding 125 ml of methanol in 375 ml of deionized distilled water.

9.5 Stabilizing solution

The solution was prepared by dissolving 100 g of ammonium sulfate in 250 ml of deionized distilled water. The final volume was brought up to 500 ml with deionized distilled water

Copyright by Mahidol University

APPENDIX F

Reagents for Western blotting

1. Transfer buffer [25mM Tris, 192 mM glycine and 20% (*v/v*) methanol]

To prepare 1 liter of transfer buffer, 3.03 g of Tris-base (Hydroxymethylaminomethane) and 14.4 g of Glycine was dissolved in 800 ml of UDW. Finally 200 ml (20% v/v) of methanol was added.

2. Blocking solution (5% skimmed milk or 3% BSA in PBS)

The solution was prepared by dissolving 5 g of skim milk (HYMEDIA®, India) or 3 g of BSA (SIGMA-ALDRICH, Inc., Germany) in 100 ml of PBS, pH 7.4.

3. Washing buffer or diluents solution (0.05% Tween-20 in TBS, pH 7.4; TBS-T)

Tris-base 1.21 g and 8.77 g of sodium chloride were dissolved in 500 ml of UDW. The pH was adjusted to 7.4 with HCl. The total volume was brought up to 1,000 ml. TBS-T solution was prepared by adding 0.5 ml Tween-20.

4. Equilibrating buffer (0.15 M Tris-HCl, pH 9.6)

To prepare Tris buffer, 18.15 g of Tris-base were dissolved in 700 ml of UDW. After dissolving, the pH of the solution was adjusted to 9.6 with 1 N HCl and the volume was made up to 1 liter with UDW.

5. Substrate solution

Commercial BCIP/NBT substrate solution was purchased from Kirkegaard & Perry Laboratory (KPL), USA. To prepare this solution, one part of concentrate substrate was diluted with three part of diluent (0.15 M Tris-HCl, pH 9.6). This substrate should be prepared freshly and protected from the light.

Copyright by Mahidol University

APPENDIX G

Reagents for indirect ELISA

1. Coating buffer (0.05 M carbonate-bicarbonate buffer, pH 9.6)

The buffer was prepared by dissolving 2.1 g of $NaHCO_3$ in 400 ml of DW. After completely dissolving, the pH of the solution was adjusted to 9.6 with 0.05 Na_2CO_3 (0.53 g in 100 ml of UDW). The volume was made up to 500 ml with DW.

2. Diluent (0.2% BSA and 0.2% gelatin in PBS)

This buffer was prepared by dissolving 0.2g of gelatin (Sigma) in 100 ml of PBS with heating (50-60 °C) for completely dissolved. After cooling, the preparation was added with 0.2 g of BSA**.** The solution was filtered through a sterile 0.2 µm filter membrane and stored at 4 °C until use.

3. Phosphate buffered saline (PBS, 0.01 M, pH 7.4)

The buffer was prepared by mixing the following ingredients in 900 ml of DW:

NaCl	8	g
KCl	0.2	g
Na_2HO_4	1.44	g
KH_2PO_4	0.24	g

The solution was adjusted to pH 7.4 with NaOH or HCl, and DW was added to 1 liter. The solution was sterilized by autoclaving.

4. PBS-T buffer (0.05% Tween-20 in PBS)

The solution was prepared by mixing 0.5 ml of Tween-20 (Sigma) with 1 liter of PBS, pH 7.4.

Copyright by Mahidol University

APPENDIX H

Reagent for restriction fragment length polymorphism (RFLP)

1. TBE buffer (5x)

The buffer was prepared by dissolving 52.0 g of in Tris-base, 27.5 g of boric acid (USB) and 4.65 g of EDTA in 700 ml of UDW. The pH of the solution was adjusted to 8.3 with concentrate HCl and then the volume was made to 1,000 ml with UDW. This buffer was sterilized by autoclaving. For 1x working solution, 200 ml of the stock were added to 800 ml of UDW.

2. Polyacrylamide gel for RFLP (14% acrylamide gel containing 0.5% glycerol)

The following solutions were combined with 3.73 ml of DW:

Glycerol	0.06	ml
TBE buffer (5x)	2.4	ml
Stock acrylamide solution (30%) (Bio-Rad)	5.6	ml

The preparation was degassed under a vacuum for at least 5 minutes. Gel polymerization was initiated by adding 200 µl of 10% ammonium persulfate (freshly prepared) and 10 µl of TEMED (Sigma). The preparation was poured into the gel casting apparatus, over-layered with DW and allowed to polymerize at 25 °C for at least 30 minutes before use.

Copyright by Mahidol University

APPENDIX I

Reagents for mimotope searching

1. Tris buffered saline (0.05 M Tris-HCl, 150 mM NaCl, pH 7.5; 1x TBS or TBS)

Tris (16.0757 g) and NaCl (8.77 g) were dissolved in 900 ml of DW. After dissolving, pH of the solution was adjusted to 7.5 with 1 N HCl. The volume was brought to 1 liter with DW and sterilized by autoclaving.

2. Washing solution (0.1% TBST)

The solution was prepared by adding 1.0 ml of Tween-20 to 1 liter of TBS, pH 7.5 and mixed well.

3. Elution buffer (0.1% BSA in 0.1 M glycine-HCl, pH 2.2)

The buffer was prepared by dissolving 0.75 g of glycine in 70 ml of UDW. The pH of the solution was adjusted to 2.2 with concentrate HCl, and then the volume was made up to 100 ml with DW. Ten milligrams of BSA were dissolved in 10 ml of the solution before use.

4. Neutralizing buffer (2 M Tris)

The buffer was prepared by dissolving 24.22 g of Tris-base in 70 ml of UDW. The volume of the solution was adjusted to 100 ml with UDW.

Copyright by Mahidol University

APPENDIX J

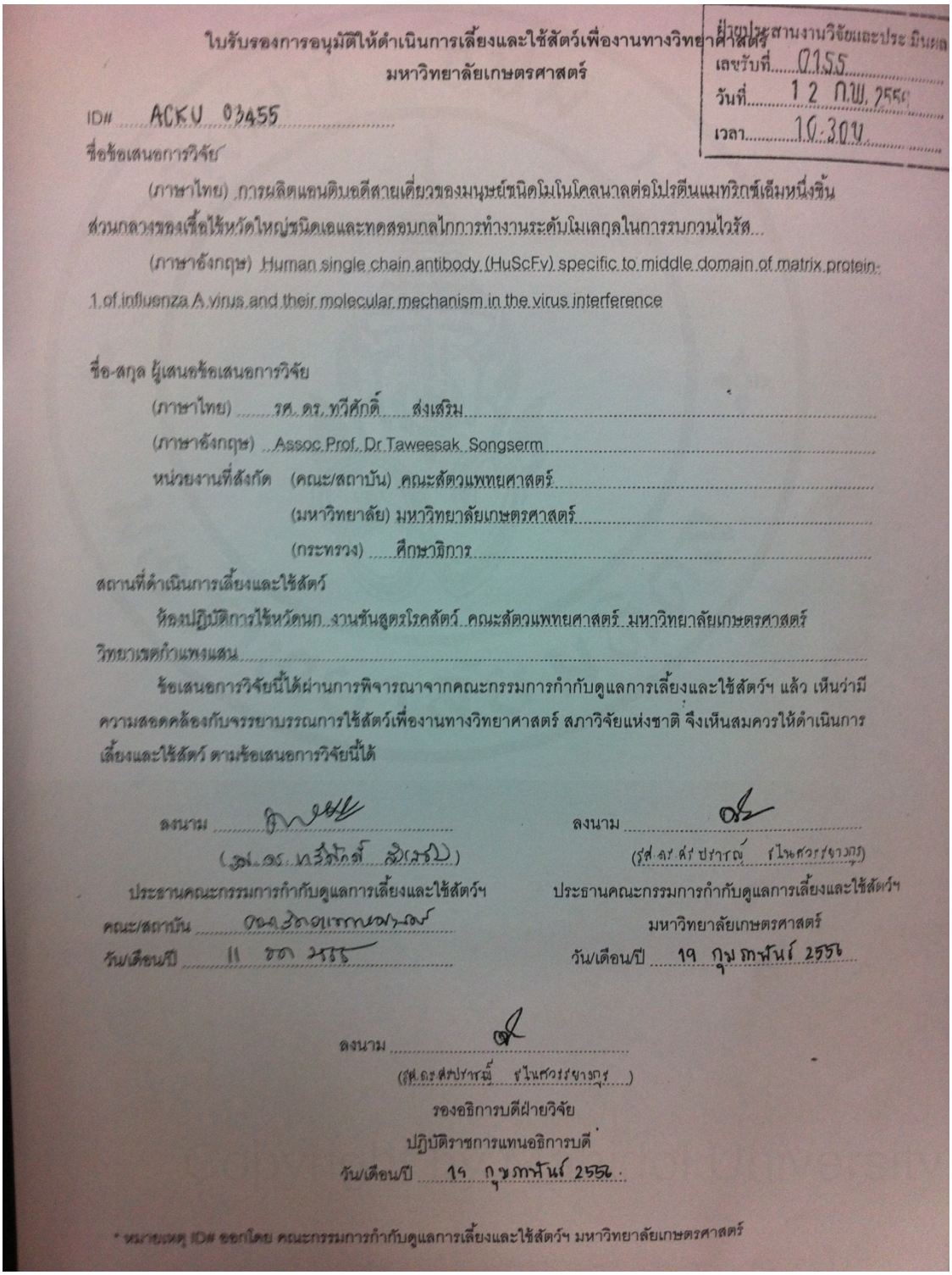

ใบรับรองการอนุมัติให้ดำเนินการเลี้ยงและใช้สัตว์เพื่องานทางวิทยาศาสตร์
มหาวิทยาลัยเกษตรศาสตร์

ฝ่ายประสานงานวิจัยและประเมินผล
เลขรับที่ 0155
วันที่ 12 กพ. 2556
เวลา 10:30น.

ID# ACKU 03455

ชื่อข้อเสนอการวิจัย

(ภาษาไทย) การผลิตแอนติบอดีสายเดี่ยวของมนุษย์ชนิดโมโนโคลนาลต่อโปรตีนแมทริกซ์เอ็มหนึ่งชิ้นส่วนกลางของเชื้อไข้หวัดใหญ่ชนิดเอและทดสอบกลไกการทำงานระดับโมเลกุลในการรบกวนไวรัส

(ภาษาอังกฤษ) Human single chain antibody (HuScFv) specific to middle domain of matrix protein-1 of influenza A virus and their molecular mechanism in the virus interference

ชื่อ-สกุล ผู้เสนอข้อเสนอการวิจัย

(ภาษาไทย) รศ. ดร. ทวีศักดิ์ ส่งเสริม

(ภาษาอังกฤษ) Assoc Prof. Dr Taweesak Songserm

หน่วยงานที่สังกัด (คณะ/สถาบัน) คณะสัตวแพทยศาสตร์

(มหาวิทยาลัย) มหาวิทยาลัยเกษตรศาสตร์

(กระทรวง) ศึกษาธิการ

สถานที่ดำเนินการเลี้ยงและใช้สัตว์

ห้องปฏิบัติการไร้เชื้อนก งานชันสูตรโรคสัตว์ คณะสัตวแพทยศาสตร์ มหาวิทยาลัยเกษตรศาสตร์ วิทยาเขตกำแพงแสน

ข้อเสนอการวิจัยนี้ได้ผ่านการพิจารณาจากคณะกรรมการกำกับดูแลการเลี้ยงและใช้สัตว์ฯ แล้ว เห็นว่ามีความสอดคล้องกับจรรยาบรรณการใช้สัตว์เพื่องานทางวิทยาศาสตร์ สภาวิจัยแห่งชาติ จึงเห็นสมควรให้ดำเนินการเลี้ยงและใช้สัตว์ ตามข้อเสนอการวิจัยนี้ได้

ลงนาม .....
(รศ. ดร. ทวีศักดิ์ ส่งเสริม)
ประธานคณะกรรมการกำกับดูแลการเลี้ยงและใช้สัตว์ฯ
คณะ/สถาบัน คณะสัตวแพทยศาสตร์
วัน/เดือน/ปี 11 ธค 2555

ลงนาม .....
(รศ.ดร.ศรปราณี ชไนศวรรยางกูร)
ประธานคณะกรรมการกำกับดูแลการเลี้ยงและใช้สัตว์ฯ
มหาวิทยาลัยเกษตรศาสตร์
วัน/เดือน/ปี 19 กุมภาพันธ์ 2556

ลงนาม .....
(รศ.ดร.ศรปราณี ชไนศวรรยางกูร)
รองอธิการบดีฝ่ายวิจัย
ปฏิบัติราชการแทนอธิการบดี
วัน/เดือน/ปี 19 กุมภาพันธ์ 2556

* หมายเหตุ ID# ออกโดย คณะกรรมการกำกับดูแลการเลี้ยงและใช้สัตว์ฯ มหาวิทยาลัยเกษตรศาสตร์

BIOGRAPHY

NAME	Tippawan Pissawong
DATE OF BIRTH	5 February 1986
PLACE OF BIRTH	Bangkok, Thailand
INSTITUTIONS ATTENDED	Mahidol University, 2005-2008 Bachelor of Science First Class Honours (Medical Technology) Mahidol University, 2008-2012 Doctor of Philosophy (Immunology)
RESEARCH GRANTS	Commission on Higher Education Congress (CHE Congress)
HOME ADDRESS	11 Soi Tiwanon 50/2, Tiwanon Road, Muang District, Nonthaburi 11000, Thailand. Tel. 084-5525847 E-mail: tpw029@gmail.com

PUBLICATION

1. Pissawong, T., Maneewatch, S., Thueng-In, K., Srimanote, P., Dong-Din-On, F., Thanongsaksrikul, J., Songserm, T., Tongtawe, P., Bangphoomi, K. & Chaicumpa, W. (2013) Human monoclonal ScFv that bind to different functional domains of M2 and inhibit H5N1 influenza virus replication. *Virol J*, 10, 148

2. Piacham, T., Nantasenamat, C., Suksrichavalit, T., Puttipanyalears, C., Pissawong, T., Maneewas, S., Isarankura-Na-Ayudhya, C. & Prachayasittikul, V. (2009). Synthesis and Theoretical Study of Molecularly Imprinted Nanospheres for Recognition of Tocopherols. *Molecules*, 14, 2985-3002.

Copyright by Mahidol University

PRESENTATIONS

ORAL PRESENTATIONS

1. Human ScFv to M2 protein that interferes influenza virus cycle. Graduate research forum 2012 international conference in medicine and public health to commemorate the 150th anniversary of birth of Queen Sri Savaridira on 18-19 September 2012. (**The first prize for best oral presentation award**)

2. Human ScFv to M2 protein that interferes influenza virus cycle. Joint Intenational Tropical Medicine Meeting 2012 (JITMM2012) on 12-14 December 2012. (**The consolidation prize for oral presentation**)

POSTER PRESENTATIONS

1. Human monoclonal antibodies specific to native hemagglutinin of A/H1N1 influenza virus. CHE-USDC II on 27-29 September 2009.

2. Human monoclonal antibodies that bind specifically to- and interfere with- the bio-functions of influenza virus surface exposed proteins: hemagglutinin-1 and M2 protein. Molecular Medicine Conference (MMC2012) on 19-22 December 2012.

Copyright by Mahidol University